The Purification and Identification of Interactors to Elucidate Novel Connections in the HEK 293 Cell Line

Brett Hawley

Biochemistry, Microbiology and Immunology
Faculty of Medicine
University of Ottawa

ABSTRACT

The field of proteomics studies the structure and function of proteins in a large scale and high throughput manner. My work in the field of proteomics focuses on identifying interactions between proteins and discovering novel interactions. The identification of these interactions provides new information on metabolic and disease pathways and the working proteome of a cell. Cells are lysed and purified using antibody based affinity purification followed by digestion and identification using an HPLC coupled to a mass spectrometer. In my studies, I looked at the interaction networks of several AD related genes (Apolipoprotein E, Clusterin variant 1 and 2, Low-density lipoprotein receptor, Phosphatidylinositol binding clathrin assembly protein, Alpha-synuclein and Platelet-activating factor receptor) and an endosomal recycling pathway involved in cholesterol metabolism (Eps15 homology domain 1,2 and 4, Proprotein convertase subtilisin/kexin type 9 and Low-density lipoprotein receptor). Several novel and existing interactors were identified and these interactions were validated using co-immunopurification, which could be the basis for future research.

ACKNOWLEDGEMENTS

I would like to take this opportunity to thank my supervisor, Dr. Daniel Figeys, for his support and guidance throughout my studies in his lab. It was a great experience to work in his lab and I am very thankful I was given the chance to learn and work under him. I would also like to thank the members of my lab for all their assistance in learning new techniques and equipment in the lab. In particular, I would like to thank Hu Zhou, Rui Chen, and Zhibin Ning. They provided me with a lot of assistance in working with and operating the HPLC and mass spectrometers and discussed results and troubleshooting numerous times.

TABLE OF CONTENTS

LIST OF FIGURES

LIST OF TABLES

LIST OF APPENDICES

LIST OF ABREVIATIONS

αsAPP..... Alpha-secretase cleaved amyloid precursor protein

βsAPP..... Beta-secretase cleaved amyloid precursor protein

µg ..... microgram

Aβ..... amyloid Beta peptide

AD..... Alzheimer's Disease

AICD..... amyloid intracellular domain

AP-2 ..... adaptor protein 2

AP-MS ..... affinity purification mass spectrometry

APP ..... amyloid precursor protein

APOE ..... apolipoprotein E

ATP ..... adenosine triphosphate

BACE-1..... Beta secretase

BiNGO ..... Biological Networks Gene Ontology tool

BLAST..... basic local alignment search tool

cDNA ..... complementary deoxyribonucleic acid

CHAPS..... 3-[(3-Cholamidopropyl)dimethylammonio]-1 propanesulfonate

CLINT1..... clathrin interactor 1

CLU1..... clusterin variant 1

CLU2..... clusterin variant 2

CLTC ..... clathrin, heavy chain

DAVID..... Database for Annotation, Visualization and Integrated Discovery

DMEM ..... Dulbecco's Modified Eagle Medium

DNA ..... deoxyribonucleic acid

DTT ..... dithiothreitol

EHD1-4 ..... Eps15 homology domain containing protein 1-4

ER ..... endoplasmic reticulum

ERC ..... endocytic recycling compartment

ESI ..... electrospray ionization

FAD ..... Familial (early-onset) Alzheimer's Disease

FASP ..... filter-assisted sample preparation

FBS ..... fetal bovine serum

GFP ..... green fluorescent protein

GPC ..... glycerophosphocholines

GPCR ..... G-protein coupled receptor

GWAS ..... genome wide association study

HEK 293 ..... human embryonic kidney 293 cells

HPLC ..... high performance liquid chromatography

HPRD ..... Human Protein Reference Database

IAA ..... indole-3-acetic acid

IPA ..... Ingenuity Pathway Analysis

LC ..... liquid chromatography

LC-MS/MS ..... liquid chromatography coupled to mass spectrometry

LDLR ..... low-density lipoprotein receptor

LOAD ..... Late-onset Alzheimer's Disease

LTQ ..... linear trap quadrapole

m/z ..... mass to charge ratio

mg ..... milligram

mM ..... milliMolar concentration

MS ..... mass spectrometry

NP-40 ..... Nonidet P-40 (octylphenoxypolyethoxyethanol)

ORF ..... open reading frame

PAF ..... platelet activating factor

PAFR ..... platelet activating factor receptor

pCMV-entry ..... vector used to transfect gene of interest into human cell line

PCSK9 ..... proprotein convertase subtilisin/kexin type 9

PICALM ..... phosphatidylinositol binding clathrin assembly protein

RNA ..... ribonucleic acid

SAINT ..... significance analysis of interactome

SDS ..... sodium dodecyl sulphate

SDS-PAGE ..... sodium dodecyl sulphate polyacrylamide gel electrophoresis

SILAC ..... stable isotope labeling with amino acids in culture

SNAP91 ..... synaptosomal-associated protein, 91kDa homolog

SNCA ..... Alpha synuclein

SNCB ..... Beta synuclein

SNP ..... single-nucleotide polymorphisms

TBS ..... tris-buffered saline

TOM ..... translocase of the outer membrane

v/v ..... volume concentration

VDAC ..... voltage dependent anion channel

VLDL ..... very low density lipoprotein

w/v ..... mass concentration

WB ..... western blot

XRCC..... X-ray repair complementing defective repair in Chinese hamster cells

CHAPTER 1. INTRODUCTION

I. Interactome Proteomics Through Affinity Purification-Mass Spectrometry

Mass Spectrometry based Proteomics

Proteomics refers to the large-scale ("omics") determination of cellular function at the protein level ("prote"); including identification, localization, modification(s) and quantitation (4).Various methods and techniques are involved in the field of proteomics, but due to the high complexity of the protein makeup of a cell, mass spectrometry has become one of the most popular techniques (76). Even low abundant proteins can now be detected and studied by mass spectrometry because of its high sensitivity (57), and there is a greater understanding of organisms and cellular pathways.

Mass spectrometry involves the detection of ions in the gas phase and the measurement of the ions mass to charge (*m/z*) ratios. This analysis takes place when samples are delivered to a mass spectrometer, which consists of an ion source, a mass analyzer and a detector (4). A common setup for the delivery of peptides and proteins to the mass spectrometer involves a high performance liquid chromatographer (HPLC) coupled to a mass spectrometer by electrospray ionization (ESI). An HPLC separates a mixture of compounds by using a stationary phase contained inside a column. In this project, the HPLC separates peptides using a reverse phase column so the peptides can more easily be detected and identified by the mass spectrometer. In reverse phase chromatography, a non-polar substance (ie. C18 carbon chain beads) is the stationary phase and a mixture of an aqueous buffer and organic solvent (ie. water and acetonitrile) is the mobile phase. Peptides are eluted from the column as the gradient changes and the ratio of acetonitrile to water increases. Following the HPLC, the peptides move to the ion

source, where ions that exist in the solution are moved into the gas phase prior to their mass spectrometry analysis. ESI is one commonly used technique and is the one used in this project (26, 60). ESI is beneficial when working with peptides dissolved in solution and when using chromatography to separate the sample because it readily transfers ions from the solution phase to the gas phase (215). A 2-6 kV potential difference is applied between the tip of the column and the entrance of the mass spectrometer, which directs the charged droplets/molecules toward the mass spectrometer (245). Sample travels through the column and the shape of the tip and the potential difference applied produces a Taylor cone when it reaches the tip of the column and then produces a spray of charged droplets. The small charged droplets shrink as the solvent evaporates until it reaches the point when charge density becomes too high and as a result the droplet explodes into smaller droplets. The droplets continuously become smaller and smaller until desolvated charged molecules are produced (190, 217). Next, the ions enter the mass spectrometer at the mass analyzer, where they are placed in a vacuum and separated based on *m/z* ratios and travel to the detector where the number of ions at each *m/z* is counted. Figure 1-1 illustrates HPLC-ESI coupled to a mass spectrometer.

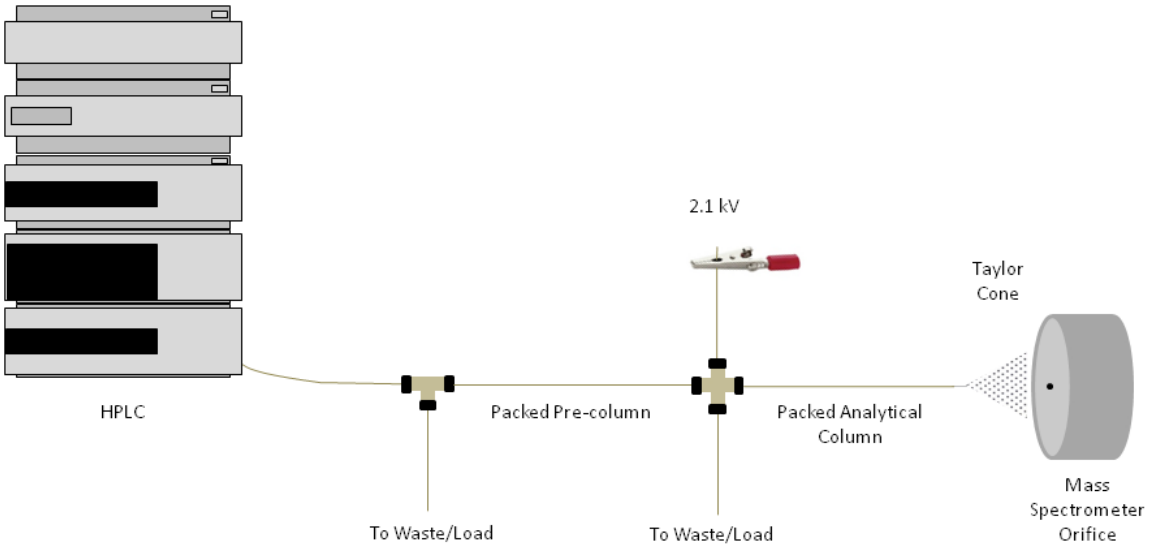
2.1 kV
Taylor
Cone
HPLC
Packed Pre-column
Packed Analytical
Column
Mass
Spectrometer
Orifice
To Waste/Load
To Waste/Load

Figure 1-1: LC-MS/MS Configuration. Representation of the HPLC-MS/MS system used in the separation and analysis of digested peptides. The HPLC combines the digested sample with a mixture of acetonitrile (5% (v/v)), and formic acid (0.1% (v/v)), and loads the mixture onto the packed precolumn at a 3 µL/min flow rate. Following a 10 minute wash step with 0.1% (v/v) formic acid, the flow path is changed and an increasing acetonitrile gradient is applied (5-80%(v/v)) to allow the eluent peptides to load onto the analytical column for electrospray ionization and mass spectrometry analysis. A Taylor cone is formed in the electrospray ionization process after a 2.1 kV potential difference is applied between the analytical column and the entrance to the mass spectromter.

There are four basic types of mass analyzers, the quadrupole, ion trap, time-of-flight and Fourier transform ion cyclotron analyzers. The ion trap was utilized in this project. A quadrupole analyzer is composed of four parallel electric rods which generate complex electric fields between them (56). The ions travel through the electric fields where only ions within a narrow *m/z* range are able to pass through without colliding with one of the rods. The frequency and potential between the rods changes over the course of the analysis to allow ions in a different *m/z* range to pass through the quadrupole to the detector (233). An ion trap is able to select for ions of a specific *m/z* by changing the electric potential within the trap. The ions become encased within the trap and are ejected to the detector by changing the amplitude and potentials within the trap (232). A linear ion trap (LTQ, Thermo Scientific, Lafayette, CO) and an Orbitrap (LTQ-Orbitrap, Thermo Scientific, Lafayette, CO) were used in this experiment. The linear ion trap has a similar structure to a triple quadrupole instrument, except each section has a discrete DC potential, which allows the three quadrupoles to work together to trap ions within the center quadrupole before they are ejected to the detector (201). Linear ion traps are well suited for protein identification because of their fast scan rates and the ability to perform collision induced dissociation and tandem mass spectrometry (245). An Orbitrap uses a static electrostatic field to trap ions around an axial electrode and *m/z* values are detected by measuring the frequency of harmonic ion oscillations along its axis (89). It features high mass resolution (up to 150,000), large ion capacity, high mass accuracy, broad *m/z* range and the ability to calculate *m/z* without a detector (232, 89). When an Orbitrap is coupled to a LTQ linear ion trap, it increases the speed and sensitivity of the analysis because both analyzers can work in parallel (245). Mass spectrometry has become central tool for the study of proteins. It has enabled researchers the

ability to detect thousands of proteins, many of them not known before (239). Researchers are as close as they ever have been to mapping the protein makeup of a cell, increasing the understanding of the entirety of a cell's biological functions.

Identification of Protein-Protein Interactions

Most cellular processes are not performed by a single protein, but instead require several proteins compiled into multi-subunit complexes by protein-protein interactions (7). These protein complexes can be small or large and usually interact with other complexes in the cell; forming vast networks of biological function and disease (231). Moreover, studies and technological developments have been completed in order to identify and define protein-protein interactions in the cell. In yeast, the two hybrid system has helped characterize the interactome by identifying thousands of interactions (94) (reviewed in (169)). Purification of a protein of interest using an epitope tag has become one of the more popular and important methods in identifying interactions. By cloning a protein tag, such as FLAG (24, 38) or TAP (187), to a protein of interest, efficient purification is possible whilst keeping interactions intact. The sample of purified proteins can be digested and the components of the purification can be identified using mass spectrometry. Affinity purification/mass spectrometry (AP-MS) was first used in the identification of the proteins of the U1 small ribonucleoprotein complex in yeast. Twenty subunits of the complex were identified by mass spectrometry following separation by SDS-PAGE gels and tryptic in-gel digestion. AP-MS is now used for large-scale analysis of interaction networks (66) as well as the identification of novel interactions of a multiprotein complexes (42).

A variety of different protein tags have been developed and used in molecular biology. The tags range in size from a few amino acids (FLAG, V5, etc.) to several hundred amino acids (Maltose-binding protein); they can contain multiple cleavable tags (TAP), and can be C- or N-terminally tagged to the protein of interest (55). Different tags and their location are chosen based on the expression of the recombinant protein and the efficiency of the purification. In this project, the FLAG tag was chosen as the protein tag. The FLAG tag is an eight amino acid peptide (DYKDDDDK), which is small and minimizes the effect on recombinant protein expression, binds strongly to FLAG antibody, and can be eluted efficiently by competitive elution with synthetic FLAG peptides (24). Three FLAG antibodies exist and are used, M1, M2 and M5. M1 is calcium independent, and does not bind as strongly as M2. M5 has the highest binding affinity for the FLAG peptide but requires a methionine to precede the FLAG tag. The M2 antibody is calcium independent, does not require any preceding amino acids and is generally used more than the other two antibodies. M2 was used in this project (55). Briefly, agarose beads containing the FLAG antibody are introduced into sample containing the FLAG-tagged bait and given time to allow for binding to occur. The beads are extensively washed to remove any contaminants and unspecific binding proteins. Following the wash, the FLAG tagged bait and bound interaction partners are eluted by competitive elution. The purified sample is digested by trypsin and the bait protein and interactors are identified by a mass spectrometer. Because of the competitive elution and the high efficiency of the FLAG binding, the purification results in few background contaminants; making the identification of the proteins by mass spectrometry more effective. It may not be able to isolate complexes as efficiently as a tag which uses multiple steps and/or tags such as TAP, but because the FLAG tag purifies in a single step, it does provide the potential to isolate weaker protein-protein interactions (55).

The FLAG tag and its purification has been utilized in many studies from small scale to large scale studies and for the identification of novel interactors and for the confirmation of theoretical interactors (36, 132, 193, 203). A large scale study by Ho et al. looked at the interactions of 725 proteins in yeast and was able to identify 3617 interactions (about 25% of the yeast proteome) (87). A more appropriate study in a human cell line by Ewing et al. looked at 338 proteins and identified 24,540 probable protein-protein interactions and was further validated to form a dataset of 6463 interactions between 2235 proteins (58). The two studies used FLAG affinity purification, SDS-PAGE, in-gel digestion, and were analyzed by LC-MS/MS.

II. The Interactome of Several Alzheimer's disease Related Genes

i. Literature Review

Pathology of Alzheimer's Disease

Alzheimer's disease (AD) is affecting an increasing number people every year. The disease has taken hold of 35 million people worldwide. Moreover, the risk of disease increases with age, 5% of Canadians over the age of 65 will be affected by AD, and 25% at an age of 80 (25). Therefore, the incidence of AD is expected to grow even more as the baby-boomer population moves further into the risk factor age (179).

AD is defined as a deterioration of the brain and memory and the progressing loss of cognitive function leading to dementia and death. Pathologically it is characterized by an accumulation of misfolded proteins in the brain, which leads to the formation of plaques and oxidative and inflammatory damage and dysfunction (50).

AD is separated into two main fields of study, the study of early-onset familial Alzheimer's disease (FAD) and sporadic Alzheimer's disease or Late-onset Alzheimer's disease (LOAD) (213). FAD is caused by dominant mutations that are genetically passed. The mutations associated with FAD are found in the genes for amyloid precursor protein (APP) or in presenilin-1 or presenilin-2. The mutations cause an increase in the amount of β -amyloid peptide, or an increase in the proportion of the longer, 42 amino acid long β -amyloid peptide. The longer form of the peptide has a tendency to aggregate into plaques and cause inflammation in the cell (95). The FAD form of the disease is better understood, but it represents less than 10% of the total number of individuals with AD (209). LOAD represents the majority of cases, these cases generally arise later in life and the cause and pathology of the disease is less understood. LOAD

involves an accumulation of misfolding proteins, such as β -amyloid peptide and tau, and an inflammatory response in the brain (213).

The most common misfolded protein in the study of AD is the β -amyloid peptide (Aβ). It is the major constituent of the neuritic plaques found in the brain. It is produced by the proteolytic cleavage of APP. APP is a transmembrane protein known for its iron trafficking properties, effects on synaptic plasticity and regulation of early development events (51, 74, 126, 77). APP can be cleaved by α-secretase, β-secretase and γ-secretase. Following cleavage by β-secretase and γ-secretase, the Aβ peptide is produced; it is 40-42 amino acids in length and is a normal secreted product of the cell. (Figure 1-2) When there is an imbalance in the brain between production and clearance of Aβ, the peptides accumulate and aggregate into larger insoluble plaques, causing a number of possible effects such as: inflammation, oxidatitive stress, and synaptic and neuronal dysfunction (75).

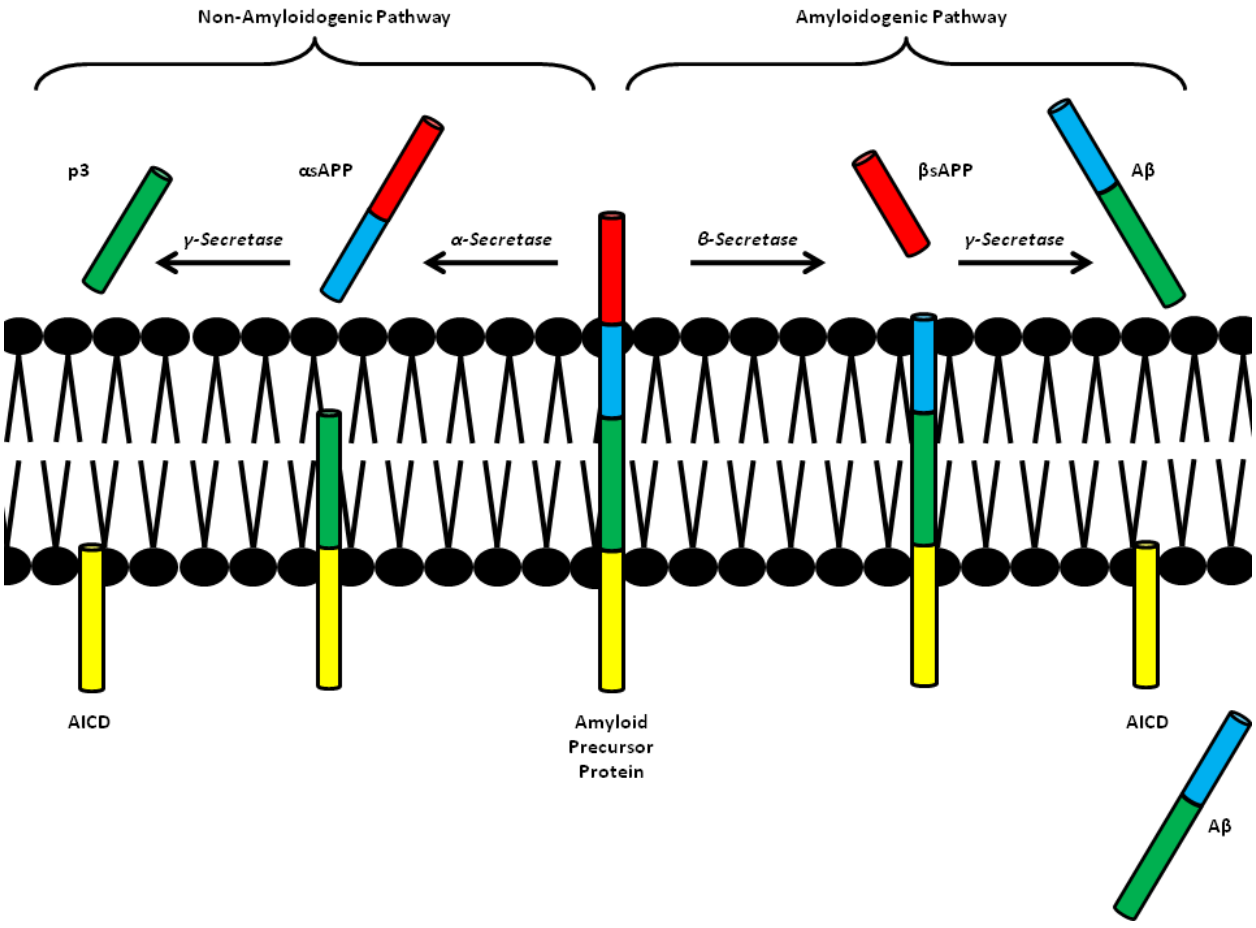
Non-Amyloidogenic Pathway
Amyloidogenic Pathway
p3
αsAPP
βsAPP
Aβ
γ-Secretase
α-Secretase
β-Secretase
γ-Secretase
AICD
Amyloid
Precursor
Protein
AICD
Aβ

Figure 1-2: The Alternate Pathways in the Processing of Amyloid Precursor Protein. The APP protein begins to be processed by being cleaved either by α-secretase or β-secretase (or BACE-1). When APP is cleaved by α-secretase followed by γ-secretase, the amyloid intracellular domain (AICD), extracellular p3, and α-secretase cleaved APP(αsAPP) are produced in a non-amyloidogenic pathway. When APP is cleaved by β-secretase followed by γ-secretase, the amyloid intracellular domain (AICD), amyloid Beta, and β-secretase cleaved APP (βsAPP) are produced in an amyloidogenic pathway (179).

Another protein found almost as commonly as Aβ in the brains of AD affected patients is the hyperphosphorylated tau protein. Tau is commonly produced in cells to promote microtubule stability and assembly, and it is functionally regulated by phosphorylation (179). When Tau becomes abnormally hyperphosphorylated it disrupts the assembly of the microtubules and therefore impairs axonal transport and synaptic function in neurons. Following hyperphosphorylation the tau also becomes highly susceptible to aggregating into insoluble tau tangles, which further impairs axonal and synaptic function (91).

The presence of plaques and tangles in diseased brains has assisted in classifying AD and is a major risk factor in the disease however the role of the plaques and tangles in the progression and pathology of the disease is still debated. One interesting hypothesis suggests that three key steps are needed for the appearance of clinical symptoms of AD: 1) an initiating injury, 2) an inflammatory response and 3) a change in the cellular make up of the brain (85). (Figure 1-3) In this hypothesis, Aβ plaques and Tau tangles are the result of an injury and an inflammatory response, but further propagate the disease because the protein deposits stimulate more inflammation. Hundreds of possible hypothesis have been studied and published, yet there is still no certainty or agreement on the cause of the disease (85).

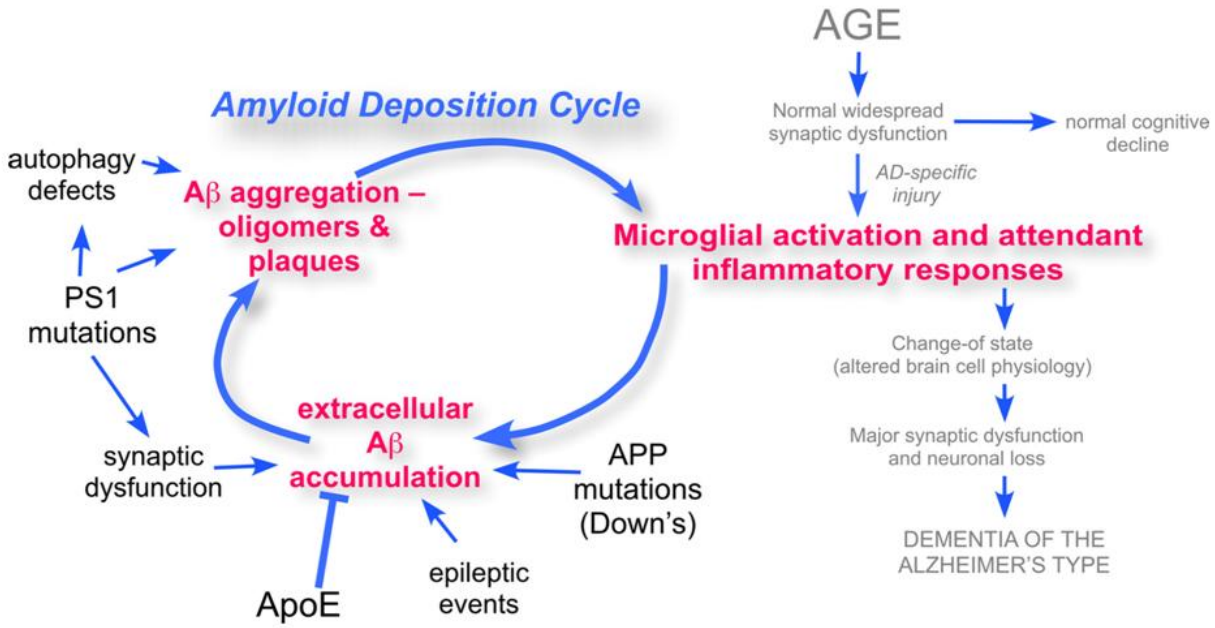
AGE
Amyloid Deposition Cycle
Normal widespread synaptic dysfunction
normal cognitive decline
AD-specific injury
autophagy defects
Aβ aggregation – oligomers & plaques
Microglial activation and attendant inflammatory responses
PS1 mutations
Change-of state (altered brain cell physiology)
extracellular Aβ accumulation
synaptic dysfunction
APP mutations (Down's)
Major synaptic dysfunction and neuronal loss
DEMENTIA OF THE ALZHEIMER'S TYPE
ApoE
epileptic events

Figure 1-3: A Three Step Process to the Appearance of Clinical Symptoms of Alzheimer's Disease. This hypothesized pathway for the emergence of dementia in AD presents age as the dominant risk factor. The first step is an initiating AD-specific injury which triggers the second step: an inflammatory response causing an increasing amount of stress on the cell's of the brain. The inflammation results in a continuous but distinct cycle of amyloid Beta deposition and further inflammatory responses. The final step occurs when the brain cell physiology has become altered and brain function begins to deteriorate (85). Figure used with permission from Dr. Karl Herrup.

Mitochondrial dysfunction is evident in all stages of AD and may be a key player in the pathogenesis of the disease. Mitochondrial damage can lead to many problems in the cell; the most major being the release of oxidizing free radicals (125). The free radicals cause oxidative stress and damage in the cell and this damage may precede pathological changes of AD (214). Damaged mitochondrial may also release cytochrome c, Omi/HtrA2 and Smac/Diablo, which can all lead to apoptosis (146). Some of this toxicity and dysfunction is caused by Aβ plaques, which is a mitochondrial toxin. Aβ inhibits enzymes of the mitochondria in the brain and as a result impairs electron transport, ATP production, oxygen consumption and membrane potential. Without the cells major power plant for energy the cells begins to die and move through apoptosis. Several pieces of evidence of changes in the mitochondria in the early stages of AD have been studied such as: a decrease in the number if mitochondria in vulnerable neurons, a decrease in brain glucose metabolism, and reduced activity of both TCA cycle enzymes and cytochrome c oxidase (8).

The most widely known and studied protein with regards to AD is apolipoprotein E (APOE). The APOE ε4 allele was associated with LOAD in 1993 after first finding a relation between chromosome 19 and AD and an interaction between APOE and Aβ (43, 219). ε4 is one of three different alleles for APOE, the other two being ε2 and ε3. ε3 is the most common and is found in 77% of the general population, while ε2 is the least common (8%) and also conveys protection against LOAD. The ε4 allele is found in 15% of people on average but that percentage increases to 40% when a population of only AD patients is examined instead (27). The proteins produced by the three alleles only differ by one amino acid, but the one small difference seems to have a large impact on how the protein interacts and functions in the body (197). The substitution results in different binding preferences at both the N- and C-terminal for lipids and

lipoproteins, which may be due to the formation of unique salt bridges in each of the isoforms, changing the 3-dimensional structure of APOE (48, 49, 137). Changes between APOE3 and APOE4 are seen in the cells ability to complete synaptic repair and plasticity, cholesterol transport, Aβ clearance and production and tau tangle formation (27). Studies have shown these changes between the different APOE isoforms, yet no confirmation has been made on which change(s) causes the onset and progression of AD (98, 111, 218, 236). In this project, the interactions of APOE3 will be investigated, which may be able to be compared to APOE4 in the future. By studying the APOE3 form it provides the ability to find interactions in the non-risk form of the protein, and discover what may be affected if different forms of the protein are present instead.

Genome-wide Association Studies Highlighted New Genes Associated with AD

Genome-wide association studies (GWAS), which assays thousands to hundreds of thousands single nucleotide polymorphisms in the search of genetic variants and heritability of disease, has made many novel discoveries over the last few years. The studies have given new insights into the complexity of diseases such as AD and other neurodegenerative diseases (139). As stated above, the discovery of a genetic relation between APOE and AD in two GWAS in 1993 was one of the most important discoveries with regard to AD in the last 20 years (43, 219). More recent GWAS have found other interesting genes associated with AD risk. Clusterin (CLU), phosphatidylinositol binding clathrin assembly protein (PICALM), low-density lipoprotein receptor (LDLR) and alpha-synuclein (SNCA) genes have all been identified to have a significant association with a risk for AD (78, 116, 117, 241, 83, 145). These four proteins and APOE were chosen to be studied to identify interactors in this project.

Two recent GWAS found CLU and PICALM genes to have a significant association with a risk for AD (78, 116). These two studies have also been replicated and confirmed by other researchers (102, 103). In the study by Jun et al. they also found that presence of the APOE ε4 allele greatly influenced the presence of the CLU and PICALM single nucleotide polymorphisms (SNPs). The CLU SNPs were only present in patients without the APOE ε4 allele and that PICALM SNPs were strongly associated with the presence of the APOE ε4 allele (102). This finding suggests that there may be some association between PICALM and APOE. Based on the research, CLU and PICALM are unlikely to be major risk factors in the development of AD, but with further research and characterization, they could provide insight into the mechanisms of the cause and progression of the disease. CLU and PICALM were both chosen for further study in my project in hopes of understanding and building connections between them and AD.

Clusterin, also known as apolipoprotein J, is a chaperone protein involved in several cell processes such as apoptosis, protein aggregation and proliferation. It is normally secreted in the cell but under stressful conditions and with different isoforms can be found in the cytoplasm or nucleus (164). Along with GWAS, CLU had already been associated with AD (149). In the paper an increase in CLU expression was seen in the hippocampus of patients with AD. CLU mainly functions as a chaperone molecule and this is shown in its similarity with other chaperone molecules like the heat shock proteins and its molten globule domain. The molten globule domain allows CLU to form interactions with high affinity and low specificity, which is typical of proteins engaging in protein aggregation and cell clearance (164). Three variants of CLU exist; variant 1 and 2 were looked at in this project because they are the variants found when the cell becomes stressed and both are known to cause cell death. Variant 1 is the truncated, non-glycosylated nuclear form and variant 2 which remains in the cytoplasm. The 3rd variant is the

secreted form and has been studied much more extensively (124, 185). The first 2 variants are known to cause apoptosis in the cell by interacting with DNA binding subunits and signaling cell death (242). Variant 1 and variant 2 may represent the form that is predominantly expressed following stressful conditions such as the conditions following a neuronal injury and the inflammatory response (124).

PICALM is an assembly protein involved in clathrin-mediated endocytosis, an important process in synaptic transmission, the regulation of receptors on the plasma membrane and the uptake of substances required by the cell. PICALM is responsible for the recruitment of clathrin, adapter protein 2 (AP-2) to the site of endocytosis by binding both of them to its C-terminus and binding phosphatidyllinositol-4,5-biphosphate on the plasma membrane with its N-terminus (62). The two proteins are recruited to the membrane in order for a clathrin coated pit to be formed on the cytoplasmic side of the plasma membrane. The pit pinches off into a clathrin coated vesicle containing within it a portion of both the cytoplasmic and extracellular space within it. The newly formed vesicle merges with either endosomes, lysosomes, Golgi apparatus or is shuttled back to the plasma membrane (150). Fluctuations in the levels of PICALM, due to either overexpression or degradation, will negatively affect the cell and can halt endocytosis. A study by Baig et al. showed that PICALM is predominantly found in endothelial cells of the brain and that its expression was increased in the frontal cortex of AD brains (9). Endocytosis is involved in the production of Aβ peptide because the processing of the internalized amyloid precursor protein (APP) within endosomes results in the production of Aβ peptide and its secretion out of the cell. Because of the connection between PICALM and Aβ (115), and the results of GWAS done on PICALM, it was chosen for this study to find interactors.

The low-density lipoprotein receptor (LDLR), the receptor that binds to APOE and is responsible for the uptake of lipoproteins and cholesterol into the cell, is another protein that may have a major role in AD. LDLR is a cell-surface glycoprotein and binds to circulating lipoproteins particles so that they can enter the cell by endocytosis via clathrin-coated pits. After the LDLR-lipoprotein complex enters the cell it is shuttled to the endosomes so that the lipoprotein dissociates from the LDLR and the lipoprotein may be processed. Following release of the lipoprotein, LDLR is recycled back to the cell-surface so that it may complete the cycle again (97), Mutations to LDLR that cause loss-of-function can cause familial hypercholestemia, which is characterized by an elevated cholesterol and LDL concentration in plasma and low levels in the cytoplasm (97). As stated earlier, one of the major characteristics of AD is the accumulation of Aβ protein deposits. Cholesterol regulates the generation and clearance of Aβ, and drugs that lower cholesterol levels are being considered as potential therapies for AD treatment (178). The exact connection and mechanisms between cholesterol and the production and trafficking of Aβ and APP remains unknown and requires further investigation (142). One study that follows the expression and localization of LDLR in models of AD suggested that the levels of cholesterol and other lipids change in AD patients because Aβ over production causes a disruption in microtubule trafficking which in turn decreases the cycling of LDLR back to the cell surface (2). While another study shows that LDLR overexpression in the brains of transgenic mice causes a decrease in APOE, reduced Aβ aggregation and improved Aβ clearance. The paper also suggested LDLR as a therapeutic target because the results were so strong (108). GWAS studies have also suggested that the LDLR gene may be associated with an increased risk for AD (117). Because of the strong connection between cholesterol, APOE, and the recent GWAS

paper studying the connection between LDLR and AD, it was chosen for this study to look for interactors.

Lewy bodies are hallmarks in the detection and characterization of Parkinson's disease. Lewy bodies are insoluble protein aggregates consisting mostly of α-synuclein (SNCA), and are usually found in parts of the brain containing the most damage (200). Along with Parkinson's disease, Lewy bodies are also frequently found in the brain of individuals diagnosed with AD. The cause or mechanism of the formation of Lewy bodies in AD is not yet known, but there are several speculations (131). One of the main speculations is that there is an overlap in the pathology of the two diseases. A 25% proportion of AD patients develops a form of Parkinson's disease and develops Lewy body inclusion containing the SNCA peptide (131, 221). This means that there could possibly be an interaction between SNCA and the some of the proteins involved in AD pathology, Aβ, APP, or presenilin-1 and presenilin-2 (221). GWAS between SNCA variants and AD have been performed with mixed results (83, 145, 170, 241). One paper concluded that a SNCA polymorphism provided a protective effect against AD in individuals carrying the APOE3 variant (241). Another study could not replicate the experiment and conclude any protective effect (83) and a third report associated SNCA with LOAD in women independently of APOE (145).

ii. Hypothesis

The study of protein-protein interactions provides a means to characterize and visualize proteins within the makeup of a cell. The manner in which a protein is related to other proteins and pathways is imperative information to researchers and to the study of disease. We hypothesize that interactions play a key role in the function of proteins involved in AD and that mutations in these proteins affect their interactions and the molecular processes involved in AD. The characterization of the interactome of wild-type and mutated proteins in AD will help better understand the molecular processes involved in AD. Here we performed the first step in this study by a combination of different techniques to establish the interactome of some of the wild-type and truncated isoform of some proteins associated with AD. Six genes, APOE, CLU1, CLU2, LDLR, PICALM, SNCA, were purified by antibody coupled agarose beads and analyzed by mass spectrometry. The resulting data was used to reveal known and novel protein-protein interactions for each of the genes.

III. The Purification and Analysis of the Platelet Activating Factor Receptor

i. Literature Review

Platelet-activating factor lipids (PAF, 1-0-alkyl-2-acetl-sn-glycero-3-phosphocholine) are a class of glycerophosphocholines (GPC) identified by an alkyl-ether at sn-1 position, an acetyl at sn-2 position and phosphocholine at the sn-3 position (92). Many species exist naturally, due to the heterogeneity of the sn-1 chain length and degree of unsaturation. The lipids are produced via 3 different pathways. The remodeling and de novo pathways form PAF members enzymatically and the nonenzymatic oxidation pathway forms PAF-like lipids with longer sn-2 chains. (Figure 1-4) PAF was originally recognized for its ability to induce platelet aggregation and secretion during inflammation (18), and has now been shown to be involved in fertility (114) and long-term potentiation in neurons (35, 104) at normal physiological conditions. When PAF levels become elevated, it exerts toxic effects through downstream signaling in the cell (13, 22, 104, 194). Concentrations of PAF above 100 nM in the brain have been shown to be critical to the cell and result in the production apoptotic bodies (22). The accumulation of PAF is believed to signal caspase activation, which triggers endoplasmic reticulum(ER) stress in the cells. The ER stress signals the activation of a caspase, and subsequently cell death (237).

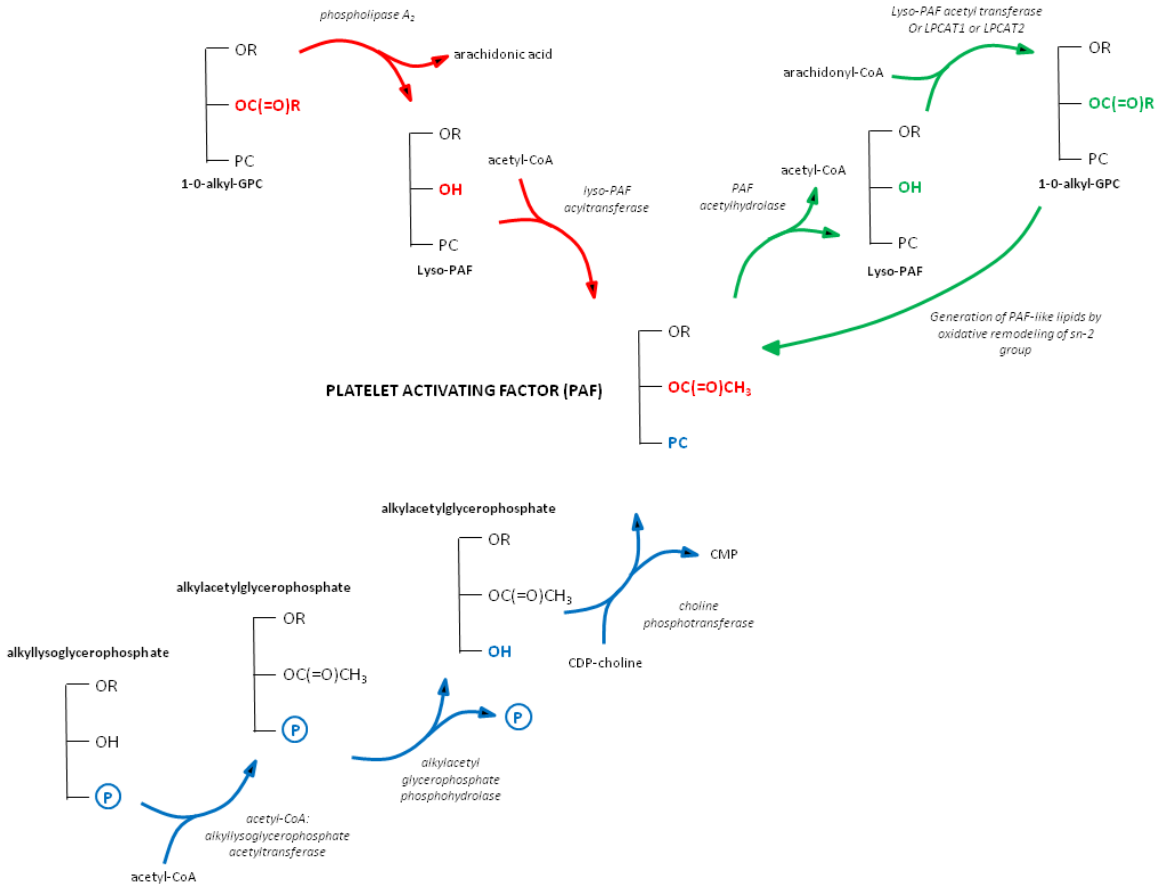
phospholipase A2
arachidonic acid
OR
OC(=O)R
PC
1-0-alkyl-GPC
OR
OH
PC
Lyso-PAF
acetyl-CoA
lyso-PAF acyltransferase
Lyso-PAF acetyl transferase
Or LPCAT1 or LPCAT2
arachidonyl-CoA
OR
OC(=O)R
PC
1-0-alkyl-GPC
acetyl-CoA
PAF acetylhydrolase
OR
OH
PC
Lyso-PAF
Generation of PAF-like lipids by oxidative remodeling of sn-2 group
PLATELET ACTIVATING FACTOR (PAF)
OR
OC(=O)CH3
PC
alkylacetylglycerophosphate
OR
OC(=O)CH3
OH
CMP
choline phosphotransferase
CDP-choline
alkylacetylglycerophosphate
OR
OC(=O)CH3
P
alkyllysoglycerophosphate
OR
OH
P
acetyl-CoA: alkyllysoglycerophosphate acetyltransferase
acetyl-CoA
alkylacetyl glycerophosphate phosphohydrolase
P

Figure 1-4: The Three Pathways in PAF Synthesis. Platelet activating factor (PAF) is produced by three different pathways. The remodeling (red) and de novo pathways (blue) produce PAF species enzymatically, and the oxidation pathway (green) forms PAF-like lipids. The remodelling and oxidation pathways both form PAF and PAF-like lipids starting with 1-alkyl-2-arachidonyl-glycerophosphocholine and the de novo pathway forms PAF starting with alkylsoglycerophosphate. The most common form of PAF produced is the 1-O-hexadecyl-2-acetyl-sn-glycero-3-phosphocholine or PC (O-16:0/2:0) (194).

High levels of PAF have been found to be involved in the neurodegeneration of the brain in AD patients. Aβ plaques can activate cytosolic phospholipase A2, which through the remodeling pathway leads to the synthesis of PAF and elevated levels (14). One species of PAF containing a palmitic acid (16:0) at the sn-1 position (PC (O-16:0/2:0)) was elevated in human neurons following exposure to Aβ. Those elevated levels activated signaling pathways resulting in the hyperphosphorylation of tau and neuronal death (195).

PAF has been studied more extensively with regard to stroke rather than AD. Stroke refers to the sudden loss of brain function due to a loss in blood flow to the brain. Caused either by a blood clot in the case of ischemic stroke or due to a rupture of blood vessels in the brain in the case of hemorrhagic stroke (47). Some neurons die immediately due to the sudden loss of oxygen and ATP because of the restricted blood flow. The area surrounding these neurons, known as the ischemic penumbra, maintains cell function and integrity just above the cell's threshold level for a short time after the infarction, but eventually begins necrosis and die (82). Changes in the levels of platelet-activating factors (PAF) and the mRNA of its receptor PAF receptor (PTAFR or PAFR) have been detected immediately after an ischemic stroke (17). There is a sudden increase in the levels of PAF and a decrease in the levels of PAFR. The changes last for approximately 2 days and then return back to normal, but it is during that time that the cells of the penumbra area die. Some recent research has shown that the PAF lipids may be responsible for the cell death, but the mechanism by which this occurs has not been worked out yet (194, 196). The variation in the levels of PAFR and the interaction between PAFR and PAF may be a major factor in this process.

PAFR is a G protein-coupled receptor (GPCR) with seven trans-membrane helices. It is widely distributed in the body including cells of the kidneys, liver, and brain (93). GPCRs make

up the large known group of membrane bound protein and mediate many cellular responses.(191) After being activated by an external stimulus, the receptor stimulates downstream signaling via G-proteins, which further activate other effector cells (240). The receptors are involved in the transmission of cellular signals, such as ones from hormones and neurotransmitters (165). Five families of GPCRs exist based on the sequence and structure of the receptor (191). PAFR belongs to the rhodopsin (class A) family, (12) which plays a larger part in cell growth and differentiation (113).

Most of the study of PAF receptor has been in regard to inflammation and the immune system, and has provided a wealth of information to work with when looking at PAFR and its effects in the central nervous system. The structure of the PAFR is highly conserved between different organisms; guinea pig, human, and rat species showed a 74% overall conservation with 81% conserved in the seven transmembrane spanning regions (92). The human PAFR gene generates four main forms of PAFR, the expression of the four forms is driven by alternative splicing. Transcripts 1 and 2 are the most commonly studied forms of PAFR. Transcript 1 is found ubiquitously, and more importantly is the form that is present in the brain, transcript 2 is still present in areas including heart and kidneys and has also been detected as two other variants in porcine tissue (243). The variants all code for the same protein, but are driven by different promoters and/or different untranslated regions (93).

The binding between extracellular PAF and PAFR and the resulting downstream effects has been the biggest focus of AD research regarding. The PAFR recognizes PAF based on its sn-2 and sn-3 groups and the longer length sn-2 chains exhibit the highest affinity for PAFR (177). The sn-1 carbon chain length and degree of unsaturation effects the downstream signaling of the receptor and may activate completely different pathways (194). The two most common forms of

PAF are PC (O-16:0/2:0) and the PC (O-18:0/2:0). PC (O-18:0/2:0) and PC (O-16:0/2:0) are both able to bind PAFR and trigger apoptosis in neuronal cells. But the pathways they signal to cause apoptosis are different (194). One other major difference between the two is how they interact with the PAFR. In the absence of the PAFR, PC (O-16:0/2:0) triggers apoptosis in a caspase 3/7 dependent pathway. PAFR has the ability to promote neuronal survival when activated by PC (O-16:0/2:0). During a stroke levels of PAFR decrease and PAF levels increase (163, 249) and these neuroprotective effects of PAFR cannot be utilized, allowing the PAF lipids to trigger apoptosis in the neurons (249). PC (O-18:0/2:0) signals apoptosis through a non-caspase 3/7 pathway in the absence of the PAFR, and in the presence of PAFR, it signals cell death through a caspase 3/7 pathway, the same as PC (O-16:0/2:0). (Figure 1-5) PAFR is not able to promote survival in the presence of PC (O-18:0/2:0). The changing levels of PC (O-16:0/2:0) and PC (O-18:0/2:0) become very important, and PAF no longer becomes a general term when studying its toxic effects (196).

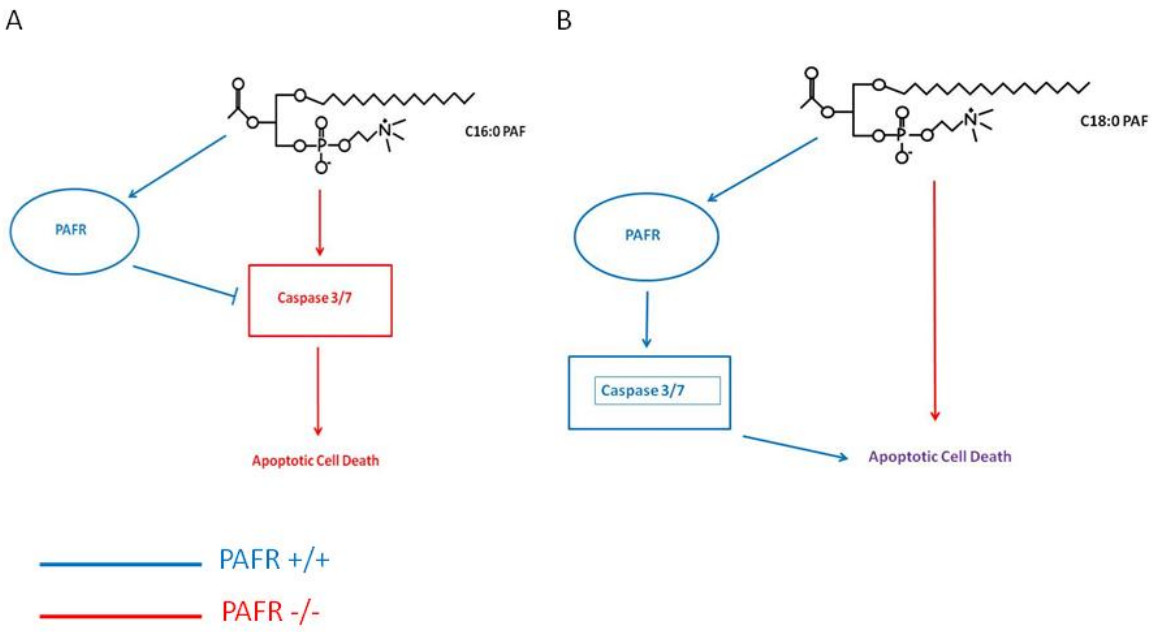
A
C16:0 PAF
PAFR
Caspase 3/7
Apoptotic Cell Death
B
C18:0 PAF
PAFR
Caspase 3/7
Apoptotic Cell Death
PAFR +/+
PAFR -/-

Figure 1-5: Effects of platelet-activating factor (PAF) on the cell is dependent on the presence of the PAF receptor and whether PC (O-16:0/2:0) or PC (O-18:0/2:0) is present. **(A)** Effect of PC (O-16:0/2:0) in the presence and absence of the PAF Receptor. Without the PAF receptor, PAF will induce apoptosis by activating caspase 3 and 7 dependent pathway. If PAF receptor is present at the membrane it will bind to the PC (O-16:0/2:0) and block the ability of PAF to activate caspase 3 and 7. **(B)** Effect of PC (O-18:0/2:0) in the presence and absence of the PAF Receptor. Without the PAF receptor, PAF will induce apoptosis non caspase 3 and 7 pathway. If PAF receptor is present at the membrane it will bind to the PC (O-18:0/2:0) and also induce apoptosis, but this time by activating a caspase 3 and 7 dependent pathway.

When PAF is able to interact with its receptor, it activates many signalling pathways. It is able to activate phospholipid turnover using the Phospholipase C, A2, and D, and phosphatidylinositol 3-kinase pathways. PAFR also has the ability to activate several protein kinases including protein kinase C, and mitogen activated protein kinase (32, 92, 186, 189, 210, 230). (Figure 1-6) These signaling pathways become regulated by internalization, desensitization, and down-regulation of gene-expression (31). These pathways have been studied very well already with regard to PAFR and other G protein-coupled receptors, and hopefully new signaling pathways and mechanisms will be discovered with regard to how it affects the brain following stroke or a neurodegenerative disease.

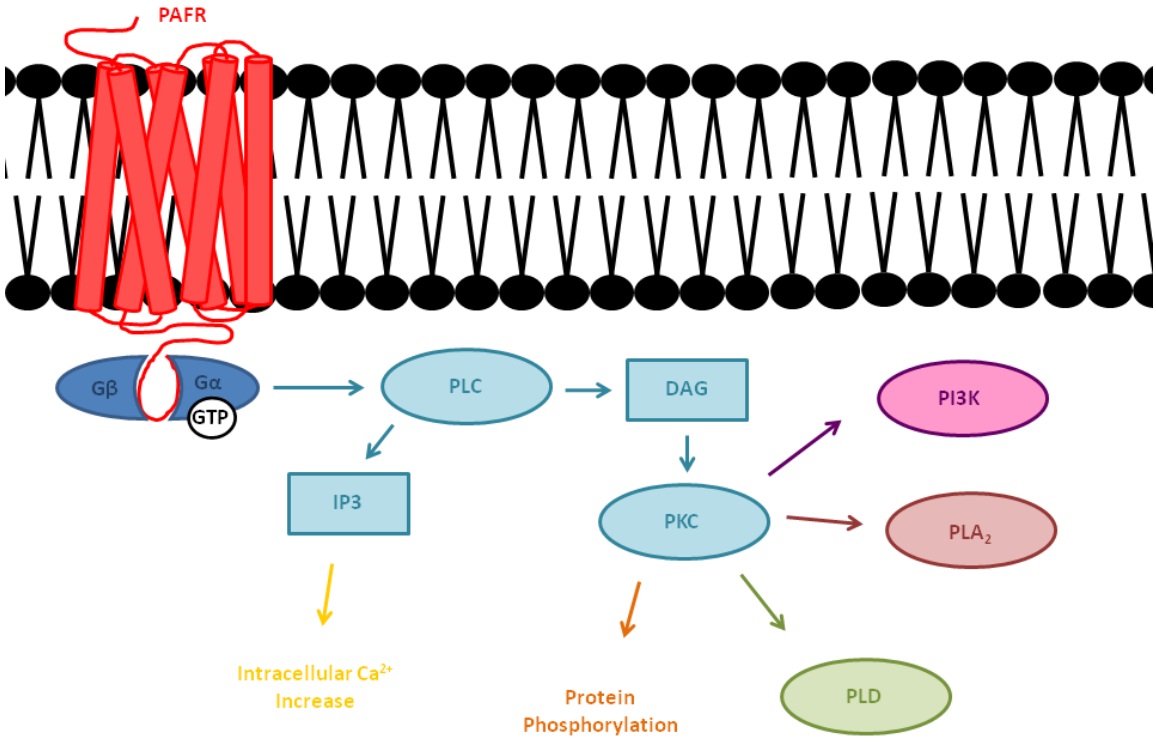
PAFR
Gβ
Gα
GTP
PLC
DAG
PI3K
IP3
PKC
PLA2
Intracellular Ca2+
Increase
Protein
Phosphorylation
PLD

Figure 1-6: The Signaling Pathways of the Activated PAFR. The most well-known and studied downstream signaling molecules linked to the platelet-activating factor receptor are presented in this schematic. Some steps are not shown and are represented by arrows. DAG: diacylglycerol; Gβ: G-protein beta subunit; Gα: G-protein alpha subunit; GTP: guanosine triphosphate; IP3:inositol (1,4,5)-triphosphate; PAFR: platelet activating factor receptor; PI3K: phosphoinositide 3-kinase; PKC: protein kinase C; PLA_2:phospholipase A_2; PLC: phospholipase C; PLD: phospholipase D (34).

Hypothesis

PAFR has been shown to mediate the apoptosis of neuronal cells in models of stroke and AD. By studying the interactome of PAFR and how these interactions vary depending on ligands present will help to better understand the relation between PAFR and apoptosis in the brain. Briefly, this will be done by purifying the protein and detecting interactors by mass spectrometry. I hypothesize that along with known interactors such as PC (O-16:0/2:0), the PAF receptor will interact with other effector proteins in neuronal protection pathways. We also hypothesize that disruptions in the PAFR interactors will lead to apoptosis, or other cell problems such as hypertrophy or increased cell proliferation. Any preferences the PAF receptor has towards certain PAF species, and the changes in downstream effector proteins between different PAF species could also be investigated.

IV. Purification and Comparison of Eh Domain Protein 1-4 in Association with Low-Density Lipoprotein Receptor and Proprotein convertase subtilisin/kexin type 9

i. Literature Review

Low-Density Lipoprotein Receptor (LDLR) is a membrane bound protein which binds to circulating lipoproteins particles so that they can enter the cell by clathrin-mediated endocytosis. It contains one transmembrane domain and is known to be a receptor for Apolipoprotein E (APOE) (97). The LDLR mediates the levels of LDL and cholesterol by removing it from the blood through endocytosis (67). After the LDLR-lipoprotein complex enters the cell it is shuttled to the endosome where the lipoprotein dissociates from the LDLR and can be processed in the cell. Following release of the lipoprotein, LDLR is recycled back to the cell-surface through the endocytic recycling compartment (ERC) so that it may complete the cycle again (150). It has a crucial role in the cell and changes to the expression of LDLR or its recycling can cause major changes to plasma cholesterol levels.

Elevated cholesterol levels increase the levels Amyloid Beta (Aβ) and are known as a risk factor for LOAD (226). Genetic (71, 109) studies (71, 118) and LDLR expression studies (3, 109, 154) have also shown the connection between LDLR and LOAD. And studies have shown the connection between AD and LDLR's ligand, APOE, already (27).

Proprotein convertase subtilisin/kexin type 9 (PCSK9) is another protein known to bind to LDLR. PCSK9 is most dominantly produced in the liver and intestines, but is produced in other tissues as well. It is a secreted glycoprotein which is self-cleaved into a pro and catalytic domain before exiting the cell (40). After secretion, PCSK9 binds to LDLR, and is internalized by endocytosis but it has been proposed that instead of moving to the ERC, LDLR is shuttled to the lysosome and degraded (161). Gain-of-function mutations in PCSK9 are genetically linked to

autosomal dominant hypercholestemia (1). Without LDLR present at the membrane to internalize cholesterol and lipoproteins, lipid levels in the plasma increase leading to an increased risk to coronary heart disease (40). Many variants of PCSK9 have been identified and studied. Single point mutations to different domains of PCSK9 have produced gain of function or loss of function mutants, many of them are naturally occurring (46). The mechanism by which PCSK9 shuttles LDLR to the lysosome for degradation is still unknown, but there are several theories (222). One theory involves a connection between LDLR, PCSK9 and a group of regulatory proteins known as C-terminal Eps15 homology domain (EHD) proteins (159).

EHD proteins are known to regulate the internalization of receptors such as LDLR (158). Research on the EHD proteins is at an early stage and a lot is still unknown and unconfirmed. There are four isoforms of the protein, each with a slightly different function in the cell. The sequence of the proteins is highly conserved, and is the reason why each protein has a similar structure and function (158). Each plays a different part in the shuttling of internalized membrane proteins either to the lysosome, endosomes, and back to the membrane or cell body depending on the objective of the internalization (157). If receptors are moved to the endosome, they move through the endosomal recycling compartment for slow recycling back to the membrane, while if they are shuttled to the lysosome they will be degraded by the enzymes contained within. Some receptors use a fast recycling process, such as the transferrin receptor; instead of moving to the endosomal recycling compartment, the receptor exits the endosome before it matures and is shuttled back to the membrane (73, 147). A small amount of internalized receptors are shuttled through the retrograde transport system to the trans-Golgi network for sorting, proteolytic processing or recycling back to the golgi network (20). Different EHD

proteins are involved in each of the endocytic transport pathways; hence the proteins associated with each EHD should also differ when purified. (Figure 1-7)

EHD1 is the most extensively studied and characterized EHD protein. It regulates the recycling of transferrin receptor and receptors that are internalized by clathrin-mediated endocytosis. One of the receptors which have been suggested to be involved with EHD1 is LDLR. In EHD1 knockout cells, the levels of LDL-derived cholesterol decreased. No increase in levels was seen after incubating the cells with supplemental LDL, making the proposition that EHD effects LDLR and the internalization of LDL more confident (159). Since EHD1 has already been shown to regulate the recycling of similar receptors which are also internalized by clathrin mediated endocytosis (101), it has been hypothesized that EHD1 regulates LDLR internalization (29, 129, 156). EHD1 also interacts with proteins involved in retrograde transport to the Golgi and specific internalization pathways in specialized cells like neurons (70, 244). EHD1 knockout mice showed no distinguishable changes from normal mice, but mouse embryonic fibroblast cells with EHD1 expression knockdown showed impaired recycling of some membrane integrins, impaired cell migration and larger focal adhesions (65, 101, 183).

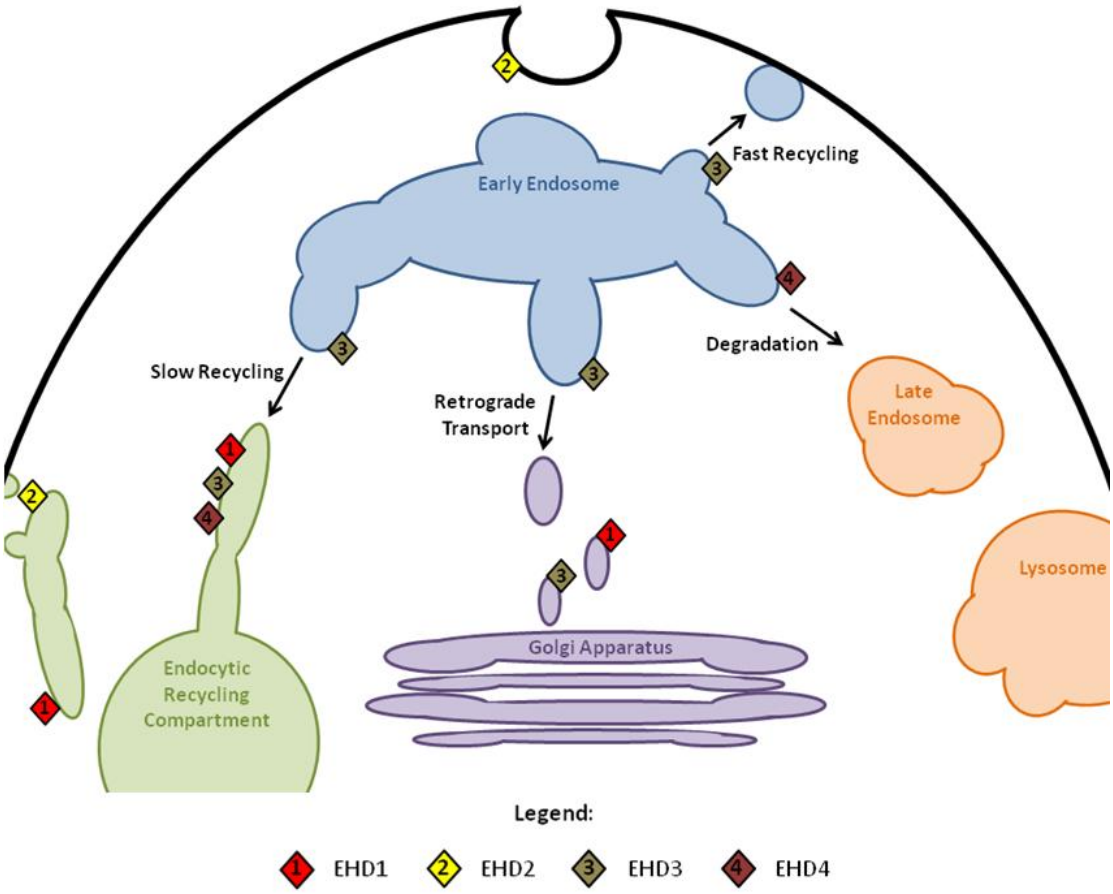
Early Endosome
Fast Recycling
Slow Recycling
Degradation
Retrograde
Transport
Late
Endosome
Lysosome
Golgi Apparatus
Endocytic
Recycling
Compartment
Legend:
EHD1
EHD2
EHD3
EHD4

Figure 1-7: The Role of EHD Protein Isoforms in Endocytic Transport. After receptors are internalized by endocytosis, they move through one of four pathways starting with the early endosome. Some receptors move directly back to the membrane from the early endosome with the help of EHD3.(160) EHD4 is involved in the shuttling of receptors to the lysosome, where they are degraded. Retrograde transport moves receptors from the early endosome to the Golgi by EHD1 and EHD3. Receptors, such as LDLR, can also be recycled back to the membrane by moving through the endocytic recycling compartment. All four EHD proteins are necessary for this slower recycling pathway. Along with the 4 EHD proteins, several Ras-related proteins (Rab) and Rabenosyn proteins are involved in endocytic transport (158, 244).

EHD2 is the farthest homolog from EHD1, and its precise function is still unknown. It does have some known interacting partners and has been linked to receptor internalization. It is thought to have some similar functions to EHD1, but EHD2 knockdown cells had even smaller effects to the recycling of some receptors (65, 65, 158).

One of the known interactors of EHD1 and the closest homolog to EHD1 is EHD3. Like EHD1 it is involved in endosomal recycling and Golgi retrograde transport, but its role is not as redundant as the other EHDs as knockout EHD3 cells showed a more detrimental phenotype (160).

The fourth homolog, EHD4, plays an earlier role in the endocytic transport and is found consistently in the early endosome, transporting receptors to the endosomal recycling compartment or the lysosome. Like the other three, there is redundancy in the function of EHD4 compared to the others and this is apparent in EHD4 knockout mice, which show no severe phenotypes (206).

The changes between the 4 homologs are so small because of their redundancies and similarities. One of the best ways to identify changes is to identify associated proteins and interaction partners. The changes can also be seen when each of the homologs is transfected into cells along with LDLR or PCSK9. Some interactions are known for each homolog from immunopurification and yeast two hybrid assays (158), and can be used to test and validate the findings.

ii. Hypothesis

Recent studies have shown that based on function and localization there is a relation between PCSK9, LDLR, and the EHD proteins (159, 161, 222). These proteins are all involved in the recycling of the LDLR, which has a direct effect on cellular LDL and cholesterol levels. However, the mechanistic relationship between PCSK9, LDLR and EHD remain elusive and limited information is available on the protein-protein interactions of EHDs. Here, we hypothesize that EHD proteins are involved in the recycling and regulation of the LDLR through their roles in the endocytic pathway and therefore can potentially impact the regulation of the LDLR by PCSK9. In order better understand the relations and interactions between these proteins, we studied the interactomes of EHD proteins in the presence/absence of PCSK9 and LDLR. Briefly, this was done by transfecting cells with an EHD protein alone or with either PCSK9 or LDLR. Biological purifications were done on individual samples followed by analysis using high performance liquid chromatography and mass spectrometry. This analysis was done to identify interaction partners of EHD proteins and to test whether individual EHD proteins have different or overlapping interactors and whether the interactors change when LDLR and PCSK9 are present. The outcome from this study will improve our mechanistic understanding of LDLR recycling and endocytic transport.

V. Summary

Proteomics is a useful and essential tool in the identification of protein-protein interactions. Single proteins do not perform most cellular processes, sets of multi-subunit protein complexes bound by protein-protein interactions are critical to the function of most proteins (7). Proteomic tools, such as mass spectrometry, are commonly used to identify protein-protein interactions and is frequently incorporated into experiments and published in scientific journals (245). Through technical advances in the past decade, mass spectrometry have become more accessible, easier to operate, and higher throughput. Large databases, for example the Human Protein Reference Database (106), have been created to compile the results and are useful in mapping and comparing identified protein interactors. Identifying interactions has become an effective way to understand the pathology behind complex diseases, particularly neurodegenerative diseases depicted by protein aggregation and plagues (127).

This thesis portrays the use of affinity purification-mass spectrometry (AP-MS) to identify protein interaction networks. Three different projects were completed for this thesis. Each project employed the use of the exact same purification method (Figure 1-8) using the same affinity tag (FLAG). The projects differed slightly in the fact that a different lysate preparation method, a different digestion method, or a different mass spectrometer was used. Each project was also related by their involvement in AD. Chapter 3 and 4, Section I describe the interactions identified for several proteins that have been identified as AD risk factors by genome wide association studies. Chapter 3 and 4, Section II describe the study of PAFR and the purification of membrane proteins with several transmembrane domains. PAFR can cause detrimental effects to the cell depending on the extracellular binding of PAF. The levels of PAF change in the brains of AD patients (195). Lastly, the third project contained in Chapter 3 and 4, Section III describe

the study of the changes in protein-protein interactions between EHD proteins, LDLR, and PCSK9. Together these proteins have a major role in the maintenance of cholesterol levels in cells and throughout the body (46, 158). Cholesterol levels are linked to the levels of Aβ and are a risk factor for LOAD (226). Taken together, the three projects show the value of using a method such AP-MS to identify protein-protein interactions and result in the production of a large database of interaction data that can be used for the basis of other related projects.

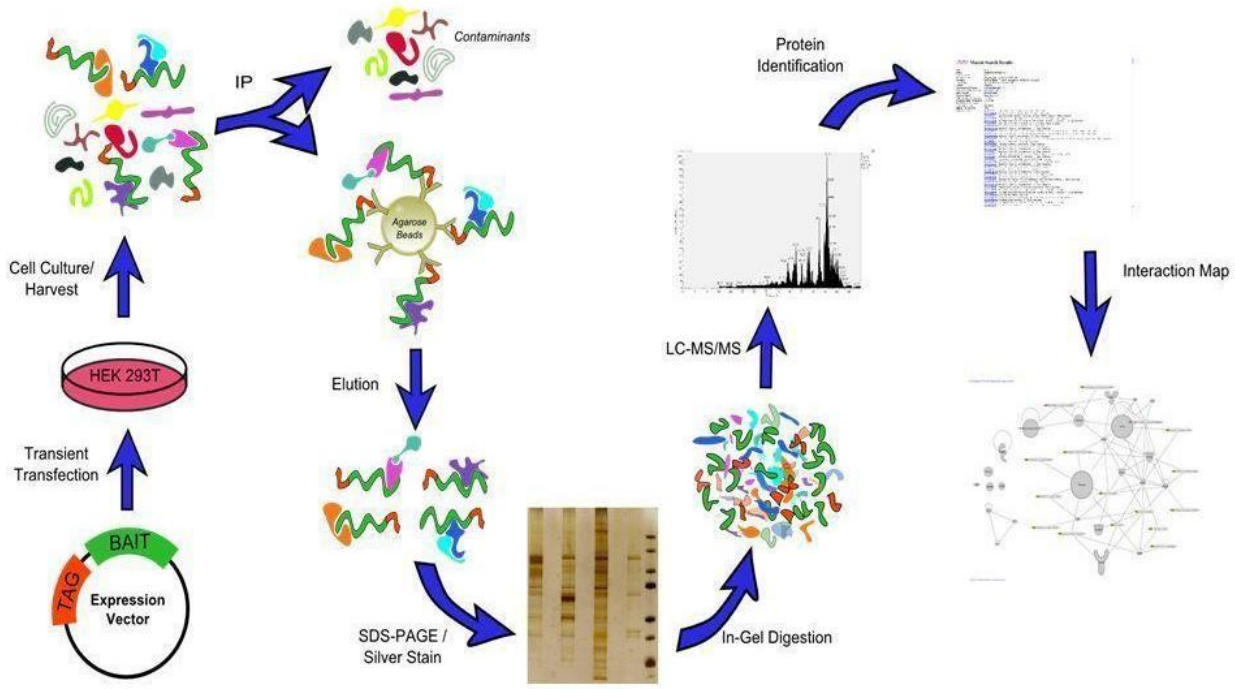
Contaminants
IP
Agarose Beads
Cell Culture/ Harvest
HEK 293T
Transient Transfection
BAIT
TAG
Expression Vector
Elution
SDS-PAGE / Silver Stain
In-Gel Digestion
LC-MS/MS
Protein Identification
Interaction Map

Figure 1-8: Experimental protocol for the transfection, immunopurification, digestion and analysis of interacting proteins bound to a bait protein. HEK 293T cells at 70% confluency are transiently transfected with a FLAG-tagged expression vector containing a gene of interest. The cells are grown for 24 hours before being harvested. The harvested cells are lysed using a modified RIPA buffer and immunopurified with FLAG coupled agarose beads. The bound protein is washed 5-6 times and competitively eluted using FLAG peptide. The eluted protein is loaded and run on precast gels and silver-stained. Following the staining, protein bands are excised and the proteins are extracted from the gel pieces and digested. The digested peptides are analyzed by LC-MS/MS and the resulting file is searched through a protein database in order to identify proteins. Network maps and tables can be created after proteins have been identified.

CHAPTER 2. METHODS

Gateway Vectors and Cloning

Full-length cDNA clone and the empty vector control for the purification of PAFR were purchased from openbiosystems (Thermo Scientific, Lafayette, CO).The cDNA clone purchased was for the gene, platelet activating factor receptor (5176867). The clone was contained in the pCMV-SPORT6 vector, which is a basic expression vector in the gateway cloning system. The vector does not contain any tag or reporter regions, therefore in order to express the gene with a tag it needs to be cloned into another vector. The gateway cloning system uses the lambda recombination system in order to transfer heterologous DNA sequences between vectors. Using a BP reaction, the gene is swapped into a donor vector called pDONR221 (Life Technologies Inc. Burlington, ON), which is catalyzed by the BP Clonase enzyme mix (Life Technologies Inc. Burlington, ON). A BP reaction is a reaction between a PCR product flanked by attB sites and a donor vector containing attP sites (234). The other vector formed during the catalysis contains a gene which prevents its growth in bacteria, and thus allows for its negative selection. The pDONR221 vector now contains our gene of interest and is now called an entry clone. The platelet activating factor receptor gene needs to be cloned into a destination vector that contains an expression tag before it is transfected into a cell line. Using a LR reaction, the gene is swapped into the expression vector called 3XFLAG (generously provided by the laboratory of Dr. Mike Tyers), which is catalyzed by the LR Clonase enzyme mix (Life Technologies Inc. Burlington, ON). An LR reaction is a reaction between an entry clone containg attL sites and an expression vector containing attR sites (234). The vector contains an N-terminal triple FLAG tag

for easy antibody detection and purification of the protein coded for in the open reading frame. Here again the vector formed as a byproduct is negatively selected and the new vector, 3XFLAG, now contains the gene of interest, platelet activating factor receptor gene (72). Following each recombination, the vectors were digested using the BsrGI enzyme for 90 minutes at 37°C. The digested DNA is loaded on a 1% agarose gel containing ethidium bromide and then exposed to UV light in order to illuminate the DNA. The digestion and gel exposure was done in order to check for the successful completion of the gateway recombination.

Bacterial Transformation of cDNA baits from Origene

Full-length cDNA clones of the baits and the empty vector control for all three projects were purchased through Origene (OriGene Technologies Inc. Rockville, MD). The cDNA clones purchased were for the genes: apolipoprotein E (RC200395), Clusterin variant 1 (RC211875), clusterin variant 2 (RC203941), low-density lipoprotein receptor (RC200006), phosphatidylinositol binding clathrin assembly protein (RC213791), alpha synuclein (RC210606), platelet activating factor receptor (RC228830), EHD1 (RC211158), EHD2 (RC204848), EHD3 (RC214168) and EHD4 (RC202486). The empty vector (PS100001) was also purchased from Origene and used as a negative control. The PCSK9-V5 contruct was cloned into a derivative of the mammalian expression vector pIRES2-EGFP (enhanced GFP) (CLONTECH) by the lab of Nabil G. Seideh and given to this lab.(204)(204, 204) The accuracy of the cDNA was assessed using a restriction digest where EcoRI and EcoRV are mixed with the cDNA for 90 minutes at 37°C. The digested DNA was visualized on a 1% agarose gel and exposed to ethidium bromide and UV light. The vector contains a C-terminal MYC/DDK tag,

DDK is another term for the FLAG tag so this vector can easily be used for antibody detection and purification using the ANTI-FLAG antibody. The digested DNA is visualized under UV light on a 1% agarose gel with ethidium bromide. The construct from Origene and the platelet activating factor receptor gene in 3XFLAG were individually transformed into Mach1 competent cells by incubating on ice for 30 minutes followed by a short heat shock and growth in LB media. The transformed cells were grown at 37°C for 16-18 hours on LB agar plates containing kanamycin. Single, isolated colonies were picked and added to LB media containing 50 ug/ml of kanamycin and grown again for 16-18 hours. The DNA was extracted from the bacteria using the midi-prep kit from Sigma Aldrich (Sigma-Aldrich Canada Ltd. Oakville, ON) and the maxi prep kit from Qiagen (QIAGEN Inc. Toronto, ON).

Cell Culture

HEK 293T cells are used in all the experiments. They are maintained in Dulbecco's Modified Eagle Medium (DMEM) supplemented with 10% (v/v) fetal bovine serum (FBS) and 1% (v/v) anti-mycotic antibiotic reagent at 37°C in a 5% CO_2 humidified incubator. Transfection of the HEK 293 cells was performed at 35% confluency and the cells were washed twice with 5 mL of PBS prior to transfection. Then the media was replaced with a media containing no FBS or antibiotic. PEI reagent (Polysciences Inc. Warrington, PA) at a concentration of 4.6 ug/mL in media is mixed with DNA in the media at a concentration of 1.8 ug/mL. 3 hours after the transfection, the cell media was replaced with fresh media containing FBS and no antibiotic. All of the cultures were verified by microscopy prior to harvesting. 48 hours after transfection, cells were harvested by washing twice with 5 mL of PBS and scrapping the cells off the plate after adding another 5 mL of PBS buffer. The cells were then centrifuged, aspirated and snap frozen with liquid nitrogen.

Immunopurification

Harvested cells were thawed and mRIPA lysis buffer (50 mM Tris-Cl pH 7.5, 100 mM NaCl, 5mM EDTA, 0.4% (v/v) NP-40, and one complete mini EDTA-free tablet (Hoffmann-La Roche Limited, Mississauga, ON)) was added to the pellet. Lysis occurred by rapidly switching between ice and hand thawing until the pellet was resuspended in the lysis buffer and broken up further by passing the lysates through a 21 gauge needle 10 times. The lysate was spun twice at 7000 rpm at 4°C and the supernantant was collected (23, 110). The amount of protein in each sample was assessed by detergent compatible protein assay (Bio-Rad Laboratories (Canada) Ltd. Mississauga, ON). 1 mg of protein is used per immunopurification. 60 µL of FLAG-agarose bead slurry is used to purify 1 mg of protein from the lysate in a total volume of 500 µL of mRIPA lysis buffer, the beads are left to nuate with the lysate overnight at 4°C. The following day, the beads were spun down and washed three times with 50 mM Tris-Cl, 100 mM NaCl, pH 7.5 and then twice with 100 mM Tris-Cl, 150 mM NaCl, pH 7.5. The protein complex was eluted from the beads with a competitive elution by nuating the beads in 200 ng/ul FLAG peptide for 30 minutes at 4°C. The elution was aliquoted into multiple tubes and dried for storage at -20 °C.

Membrane Isolation

In order to study plasma membrane associated proteins more effectively, the membrane can be isolated before any purification or digestion. Briefly, cells were harvested as described above, except they were not snap frozen in liquid nitrogen. The cell pellets were homogenized in 20 mM Tris-Cl, 250 mM sucrose, 1 mM EDTA, pH 7.4, and one complete mini EDTA-free tablet (Hoffmann-La Roche Limited, Mississauga, ON) using an 18 gauge needle, and ball-

bearing homogenizer. The lysate was cleared by spinning at 2,000 g for 10 minutes at 11,000 g for 20 minutes. The pellet was homogenized further in 20 mM Tris-Cl, 1 mM EDTA, pH 7.4, and one complete mini EDTA-free tablet with a glass homogenizer. An interface was created between the lysate and 20 mM Tris-Cl, 1.12 M sucrose, pH 7.4 by spinning at 100,000 g for 60 minutes. The interface was washed using 200 mM Na_2CO_3, pH 12.4 and 20 mM Tris-Cl, 4 M Urea, pH 7.4 followed by centrifugation at 541,000 g for 30 minutes at 4 °C. The pellet was resuspended in 100 mM Tris-Cl, pH 7.5 for further studying (251).

Western Blot Analysis

Protein samples were added to 6 X SDS sample loading buffer and boiled for 5 minutes at 95 °C. The 6X SDS sample loading buffer was composed of 30% (v/v) glycerol, 10% (w/v) SDS, 0.6 M DTT, 0.012% (w/v) bromophenol blue, 10% (v/v) β mercaptoethanol in 0.5 M Tris-Cl containing 0.4% (w/v) SDS pH6.8. The samples were loaded on NuPage 4-12% Bis-tris precast gels (Life Technologies Inc. Burlington, ON) or onto 10% Bis-acrylamide stacked gels and ran for 1 hour and 20 minutes at 160 volts. The proteins from the gels were transferred onto a nitrocellulose membrane using the XCell II Blot Module (Life Technologies Inc. Burlington, ON). The membrane was blocked overnight at 4 °C in TBS-Tween (150 mM NaCl, 10 mM Tris-HCl pH 7.6 and 0.05% (v/v) Tween 20) + 5% (w/v) milk and washed 3 times for 5 minutes each time in TBS-T. Antibodies were added at a 1:10 000 (v/v) dilution in TBS-Tween + 5% (w/v) milk for 1 hour at room temperature and washed 3 times for 10 minutes each time in TBS-T. Secondary antibodies (if needed) were added at a 1:5000 (v/v) dilution in TBS-Tween + 5% (w/v) milk for 1 hour at room temperature and washed 3 times for 10 minutes each time in TBS-

T. The membrane was incubated for 5 minutes in Immobilon Western Chemiluminescent HRP substrate (EMD Millipore Corporation, Billerica, MA) and then exposed to film in a dark room.

SDS-PAGE and Silver Staining

Immunopurified and cell lysate samples are added to alkaline protein loading buffer and boiled for 5 minutes at 95 °C. The alkaline protein buffer contains 50 mM Tris-Cl pH 8, 2% (w/v) sodium dodecyl sulfate (SDS), 100 mM DTT, 10% (v/v) glycerol and 1% (w/v) bromophenol blue. The samples were loaded and run on NuPage 4-12% Bis-tris precast gels (Life Technologies Inc. Burlington, ON) and then silver stained. The gel was run for 90 minutes at 160 V, and placed in a fixing solution of 50% (v/v) methanol and 2.5% (v/v) acetic acid for 30 minutes on a shaker at room temperature. This solution renders the proteins inside the gel insoluble so they remain inside the gel and any contaminants are washed away. The gel was washed twice in water for about 1 minute each time to remove the methanol and acetic acid. And then the gel was washed in water for 2 to 24 hours on a shaker at room temperature. After washing, the gel was incubated with 0.02% (w/v) sodium thiosulfate for 1 minute. The sodium thiosulfate enhances the staining by reducing background staining by preventing free silver's reduction to metallic silver and by providing sulfide ions, which accelerates and enhances development (180). The gel was washed again 2 times in water for 30 seconds each time. Next the gel was incubated in 0.1% (w/v) silver nitrate for 30 minutes at room temperature while shaking. The silver ions impregnate the gel and complex with the protein in the gel. The gel was washed 2 more times in water for 30 seconds each before developing. Developing occurs by shaking in 0.01% (v/v) formaldehyde and 2% (w/v) sodium carbonate for 5-10 minutes and the

solution may need to be replaced if it becomes very dark. The formaldehyde reduces the silver ions into metallic silver which is now visible and the sodium carbonate increases the pH of the solution to about 12 so this reduction can occur. When the gel staining was satisfactory, the gel was placed in 1% (v/v) acetic acid, which acidifies the pH and prevents anymore reduction from happening (180).

In-Gel Separation and Digestion

After the gels have been silver stained, they are cut into sections and cubes and are separated into 8-20 tubes per lane depending on the number of dark bands visible in the lane. Gel fragments/cubes are first washed in 50 mM ammonium bicarbonate, then centrifuged and the liquid removed and discarded. The gel pieces are shrunk in 50% (v/v) acetonitrile, 25 mM ammonium bicarbonate for 15 minutes, and following incubation the liquid is discarded and gel pieces dried in the speed vacuum. The gel fragments are swollen and cysteine bridges are broken in 50 mM ammonium bicarbonate, 10 mM DTT for 15 minutes at 56 °C. After the liquid is cooled it is removed and 100 mM iodoacetamide, 50 mM Ammonium bicarbonate is added and incubated for 15 minutes in a dark place. The liquid is removed and the gel pieces are washed in 50 mM ammonium bicarbonate. Gel pieces are shrunk again in 50% (v/v) acetonitrile, 25 mM ammonium bicarbonate for 15 minutes and following incubation the liquid is discarded and gel pieces dried in the speed vacuum. Trypsin in 50 mM ammonium bicarbonate (enzyme to protein ratio 1:100) is added to the gel pieces and incubated at 37 °C for at least 3 hours. After incubation the liquid is removed and added to clean, labeled tubes, and 25 mM ammonium bicarbonate is added and incubated for 20 minutes. After incubation the liquid is removed again

and added to the labeled tubes from before, and 5% (v/v) formic acid, 50% (v/v) acetonitrile is added and incubated for 20 minutes. After incubation the liquid is removed again and added to the pooled samples in the labeled tubes from before. The tubes are dried down in the speed vacuum and stored at -20 °C until samples are ready to be analyzed by the mass spectrometer (208).

In-solution Digestion

In-solution digestion can also be done to digest proteins. It increases the digestion efficiency, reduces sample loss and contamination, but it does not allow the sample/purification to be visualized and separated before digestion and it does not use strong detergents such as SDS (239). As well the enrichment method was adapted as follows: following the elution of the protein complex from the beads, 80 uL of eluted protein was placed into a 2 mL tube. Then, 130 µL of 13.3 M urea in 50 mM Tris-Cl, 100 mM NaCl, pH 7.5 (to a final concentration of 8 M urea) and 0.7 µL of 3 M DTT in the same buffer (to a final concentration of 10 mM DTT) were added to the eluate. The sample was heated for 1 hour at 37°C to denature the protein and to facilitate the reduction of cysteine bridges by DTT. Then, 44 µL of 0.1 M iodoacetamide in 50 mM Tris-Cl, 100 mM NaCl, pH 7.5 (to a final concentration of 20 mM iodoacetamide) was added to the sample in a dark place at room temperature for 30 minutes to facilitate the alkylation of cysteines by iodoacetamide. In order for trypsin to digest effectively, the urea concentration will need to be lowered. The concentration of urea was reduced to 1.0 M by adding 1.70 mL of 100 mM Tris-Cl pH 8.0 to the sample to facilitate the digestion of proteins. Then, 1 ug of trypsin enzyme in 50 µL of 50 mM ammonium bicarbonate was added to the tube and

incubated at 37°C for 4 hours to overnight. Following the digestion, the sample was acidified by adding 80 uL of 10% (v/v) trifluoroacetic acid and the peptides were enriched using a desalting column (235).

Filter-Assisted Sample Preparation/Digestion

Filter-assisted sample preparation/digestion (FASP) (239) is similar to in-solution digestion and in-gel digestion, it has high digestion efficiency and does not allow the sample to be visualized and separated before digestion. FASP does utilize the strong detergent SDS, which allows for better solubilization of the total lysate. Briefly, dried protein (30 ug to 200 ug) obtained above by immunopurification or cell lysate were solubilized in 2% (w/v) SDS, 100 mM Tris-Cl, 100 mM DTT at pH 7.6. The solubilized samples are loaded onto Microcon YM-30 filter units (EMD Millipore Corporation, Billerica, MA) using 200 uL of 8 M Urea in 0.1 M Tris-Cl at pH 8.5, and spun down at 14,000 x g for 15 minutes. Another 250 uL of 8 M Urea in 0.1 M Tris-Cl at pH 8.5 was added and the tube was spun down again at 14,000 x g for 15 minutes and the flow-through was discarded. 100 uL of 0.05 M iodoacetamide in 8 M Urea in 0.1 M Tris-Cl at pH 8.5 was added, mixed for 1 minute and incubated in the dark for 20 minutes to facilitate the alkylation of cysteines. The tube was spun down again at 14,000 x g for 15 minutes, and twice washed with 200 uL of 8 M Urea in 0.1 M Tris-Cl at pH 8.5 and centrifuged at 14,000 x g for 15 minutes. The urea was removed by twice washing with 100 uL of 0.05 M ammonium bicarbonate and centrifugating at 14,000 x g for 10 minutes. 60 uL of 0.05 M ammonium bicarbonate with trypsin (enzyme to protein ratio 1:100) was added and mixed for 1 minute followed by incubation at 37 °C for at least 3 hours. The filter units are transferred to new

collection tubes and centrifuged at 14,000 x g for 10 minutes at 4 °C. 100 uL of 0.5 M sodium chloride is added to the filter units and it is spun down again at 14,000 x g for 10 minutes at 4 °C. The sample is acidified with 30 uL of 5% (v/v) formic acid and is ready for desalting (239).

Desalting

1 cc C18 Sep-PAK cartridges are used for desalting the digested peptides from the filter-assisted sample preparation/digestion and the in-solution digestion (Waters Limited, Mississauga, ON). The tubes are activated by adding 1 mL of acetonitrile to the cartridge and allowing it to flow through the filter by gravity. The filter is washed twice with 1 mL of 0.1 % (v/v) formic acid. The acidified and digested peptide sample is added next to the cartridge and allowed to flow by gravity completely. The filter is washed again twice with 750 uL of formic acid, and the desalted peptides are eluted with 1 mL of 80% (v/v) acetonitrile. The eluted peptides are dried down in the speed vacuum at 50 °C, and can be stored at -20 °C until ready for HPLC-MS/MS.

HPLC-MS/MS

The digested peptides were separated by reversed phase chromatography using a configuration consisting of micro pre-column and column coupled to a mass spectrometer. (Figure 1-1) The pre-columns are home-made by first polymerizing a frit consisting of potassium silicate on one end of a capillary tube (200 µm inner diameter and 360 µm outer diameter). Briefly, one end of the capillary tube is dipped in a mixture of potassium silicate (KASIL 1, PQ

Corporation, Valley Forge, PA) and formamide at a ratio of 11 to 2. The two substances need to be mixed very quickly and vortexed immediately to prevent polymerization. The liquid fills the capillary tube by capillary action to a length of 0.5 cm. The capillary tube containing the frit is left in a vertical position overnight at room temperature so the silica can completely solidify. The analytical columns are packed in-house using a tip from New Objective (New Objective, Inc. Woburn, MA). Both the capillary pre-column and the capillary analytical column were packed in-house using 5 µM Reprosil-Pur 200 C18-AQ beads (Dr. Maisch GmbH, Ammerbuch, Germany) to a length of 5-10 cm were washed using an 1100 or 1200 micro high-performance liquid chromatography system (HPLC)(Agilent Technologies, Santa Clara, Ca) at a flow rate 20 µL/min and 150-250 bar for the pre-column and a flow rate of 3 µL/min and 150-250 bar for the analytical column. The pre-column and analytical column were inspected by microscopy and if adequate were installed on the HPLC. All samples were solubilized in 0.5% (v/v) formic acid and installed into a 96 well plate for injection into the HPLC. The peptide mixtures were automatically injected onto the pre-column at a 3 µL/min flow rate and then rinsed for 10 minutes with 0.1% (v/v) formic acid at a 3µL/min flow rate. Then the flow path was automatically reduced and the flow path was changed to allow the eluent from the pre-column to be directed to the analytical column. The peptides were eluted using an acetonitrile gradient of 5% to 80% acetonitrile (v/v) with 0.1% (v/v) formic acid. Depending on the amount of separation desired, the length of time of the gradient varied from 75 to 300 minutes. Eluted peptides flow through the analytical column at 200 nL/min flow rate following flow-splitting (250).

Mass Spectrometry

The ionized peptides are loaded onto either a Thermo Scientific LTQ or LTQ Orbitrap XL (Thermo Electron, Waltham, MA). The spray voltage was set to 2.1 kV and the temperature of heated capillary was 200 °C. The instrument method consisted of one full MS scan from 400 to 1800 *m/z* followed by data-dependent MS/MS scan of the ten most intense ions, a dynamic exclusion repeat count of 2 and a repeat duration of 90 s. All data was recorded with Xcalibur software (ThermoFisher Scientific, San Jose, CA) and saved as .RAW files so that they can be used for data analysis (250).

Database Searching and Data Analysis

Raw files are produced by the mass spectrometer for each sample analyzed. The raw files were converted into .mgf files and searched against a protein sequence database (RefSeq_Human version 4) using the Mascot software (Matrix Science Inc. Boston, MA). The search criteria for the analysis done on the LTQ Orbitrap XL were: limited to tryptic digested peptides with a maximum of 2 missed cleavages, a peptide tolerance of 20 ppm, MS/MS tolerance of 0.6 Da and peptide charges of +2 and +3. As well, fixed modification was set for carboxymethylion on cysteines and variable modification was set to oxidation of methionine. The search results were further refined by only accepting peptides with a mascot score >30, a p-value of 0.01 and only accepting proteins with a least one bold red peptide match (a bold red peptide match is the highest scoring match for a particular query). The searches performed following analysis with the LTQ mass spectrometer were identical with the exception that 2 Da mass tolerance instead of 20 ppm was used for the peptide tolerance.

Data was further analyzed and organized using Prohits (Samuel Lunenfeld Research Institute, Toronto, ON) (133). Prohits is an open-source software that allows the organization of the data based on bait, experiment, samples or a user-defined organization; it also allows for further refining by adding or removing restrictions to the Mascot search results, and by adding common experiment and bio filters to the results. Analysis can also be done with SAINT (significance analysis of interactome)(39); a helpful program embedded into Prohits. SAINT is a computational tool that assigns confidence scores to the mass spectrometry data in order to predict which interactions are in fact true. It normalizes spectral counts to the length of proteins and to the total number of spectra and compares each purification with the controls as well as with the other purifications. The probabilities calculated from SAINT are used to select which interactors to pursue in validation experiments.

Three programs were used to visualize and perform functional annotation analysis. Ingenuity Pathway Analysis (Ingenuity Systems, Redwood City, Ca) is a program used to analyze, model and understand complex biological interactions. Results of Mascot database searches or SAINT are inputted into the software and analyzed using known protein-protein interaction data to determine the most significant interaction networks, pathways and functions (184, 212). Cytoscape (205) is a software platform also used for visualization and integration of pathways into existing profiles and data. Cytoscape was used in this project because it facilitates the use of a plugin is known as BiNGO, Biological Networks Gene Ontology tool. BiNGO determines which set of genes or proteins are statistically overexpressed in a dataset and matches that set to a Gene Ontology (GO) annotation (134). DAVID (Database for Annotation, Visualization and Integrated Discovery) (90) is a set of computational and functional analysis tools that was also used to interpret datasets. The only tool from DAVID that

was used was the functional annotation tool. It is very similar to BiNGO; it groups genes or proteins into statistically relevant groupings according GO annotation. The difference between them is that the groupings are not as broad as the ones available with BiNGO. More specific groupings or classes of proteins can be compared using DAVID over BiNGO.

Co-immunopurification Validation Experiments

To test the validity of the immunopurification and mass spectrometry data, co-immunopurification experiments were performed. As previously described, an immunopurification was done using FLAG-coupled agarose beads in order to purify the FLAG tagged protein in each sample. The eluted proteins are loaded onto a gel after adding 20 µL alkaline protein loading buffer and boiling for 5 minutes at 95 °C. The alkaline protein buffer contains 50 mM Tris-HCl pH 8, 2% (w/v) sodium dodecyl sulfate (SDS), 100 mM DTT, 10% (v/v) glycerol and 1% (w/v) bromophenol blue. The samples were loaded on NuPage 4-12% Bis-tris precast gels (Life Technologies Inc. Burlington, ON). The gel was run at 160 V for 1 hour and 20 minutes. After the gel was finished running, the proteins were transferred to a nitrocellulose membrane using the wet transfer apparatus, XCell II Blot Module (Life Technologies Inc. Burlington, ON). Following the transfer, the membrane was blocked in 5% (w/v) milk in TBS-T (150 mM NaCl, 10 mM Tris-HCl pH 7.6 and 0.05% (v/v)Tween 20) for 1 hour or overnight at 4°C. The membrane was washed three times for 5 minutes each time in TBS-T. Primary antibodies were added at a 1:10 000 (v/v) dilution in TBS-T + 5% (w/v) milk for 1 hour at room temperature and washed three times for 10 minutes each time in TBS-T. The primary antibodies used were purchased from Abcam (Abcam, Cambridge, MA) and Cell

signaling (Cell Signaling Technology, Inc. Danvers, MA). Anti-VDAC (D73D12) was ordered from Cell signaling and anti-CLTC (ab21679), anti-TOMM40 (ab99485) and anti-CLINT1 (ab86046) was ordered from Abcam. Secondary antibody, Anti-Rabbit IgG Horseradish peroxidase linked whole antibody (NA934V)(GE Healthcare Life Sciences, Baie d'Urfe, QC), was added at a 1:5000 (v/v) dilution in TBS-T + 5% (w/v) milk for 1 hour at room temperature and washed three times for 10 minutes each time in TBS-T. The membrane was incubated for 5 minutes in Immobilon Western Chemiluminescent HRP substrate (EMD Millipore Corporation, Billerica, MA) and then exposed to film in a dark room.

CHAPER 3. RESULTS

I. The Interactome of Several Alzheimer's disease Related Genes

Quality control of the different constructs

A systematic approach for quality control of the different constructs of interest was performed. First, all the pCMV-Entry plasmids (Origene, OriGene Technologies Inc. Rockville, MD) were tested by DNA restriction digestion using EcoRI and EcoRV for consistency versus the predicted profile. The DNA restriction digest confirmed that all of the DNA constructs were of the correct size. (Figure 3-1) Small scale transfections of the vectors into HEK 293T cells were then performed and cell lysates were then tested by western blot to determine if the protein is produced and is responsive to the FLAG antibody. (Figure 3-2) Finally, the western blots were used to assess whether the plasmids were transfected in the cells at approximately the same efficiency of protein translation. All of the constructs used in this project passed all of our quality control tests.

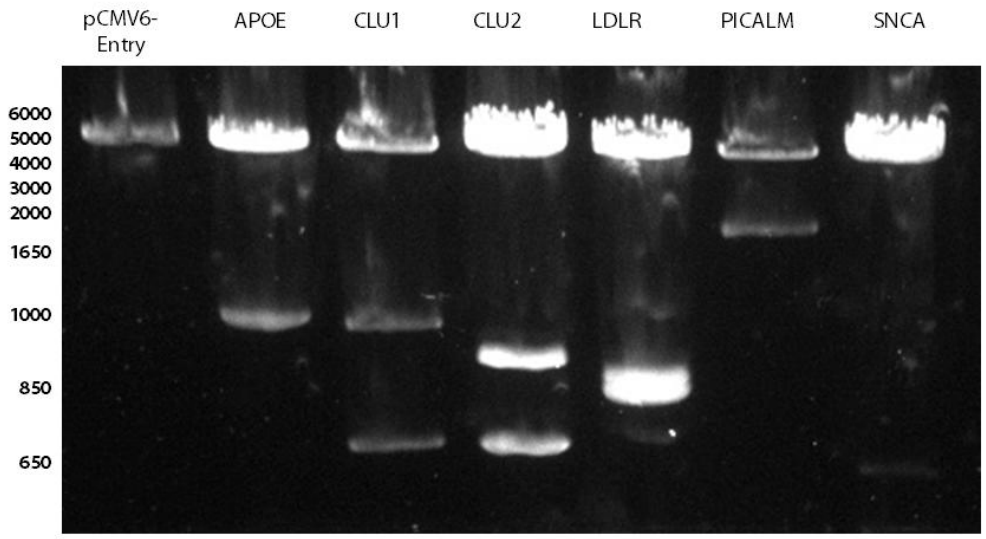
pCMV6-
Entry
APOE
CLU1
CLU2
LDLR
PICALM
SNCA
6000
5000
4000
3000
2000
1650
1000
850
650

Figure 3-1: Restriction digest of AD-related clones in pCMV6 expression vector. Each clone was digested by EcoRV and EcoRI restriction endonucleases. The endonucleases cut the expression vector at the multiple cloning sites at the 3' and 5' end resulting in a 4900 bp fragment. The sizes of the fragments were compared to a molecular weight standard to infer that the correct gene was contained in the clone. The DNA was digested for 1 hour and 30 minutes at 37°C. The digestion was analyzed on a 1% agarose gel pre-stained with 0.01 ug/ml of ethidium bromide and examined under UV light. Expected sizes of inserts: APOE:954 bp; CLU1:973 and 599 bp; CLU2:817 and 599 bp; LDLR:804,774 and 718 bp; PICALM:1959 bp; SNCA:423 bp.

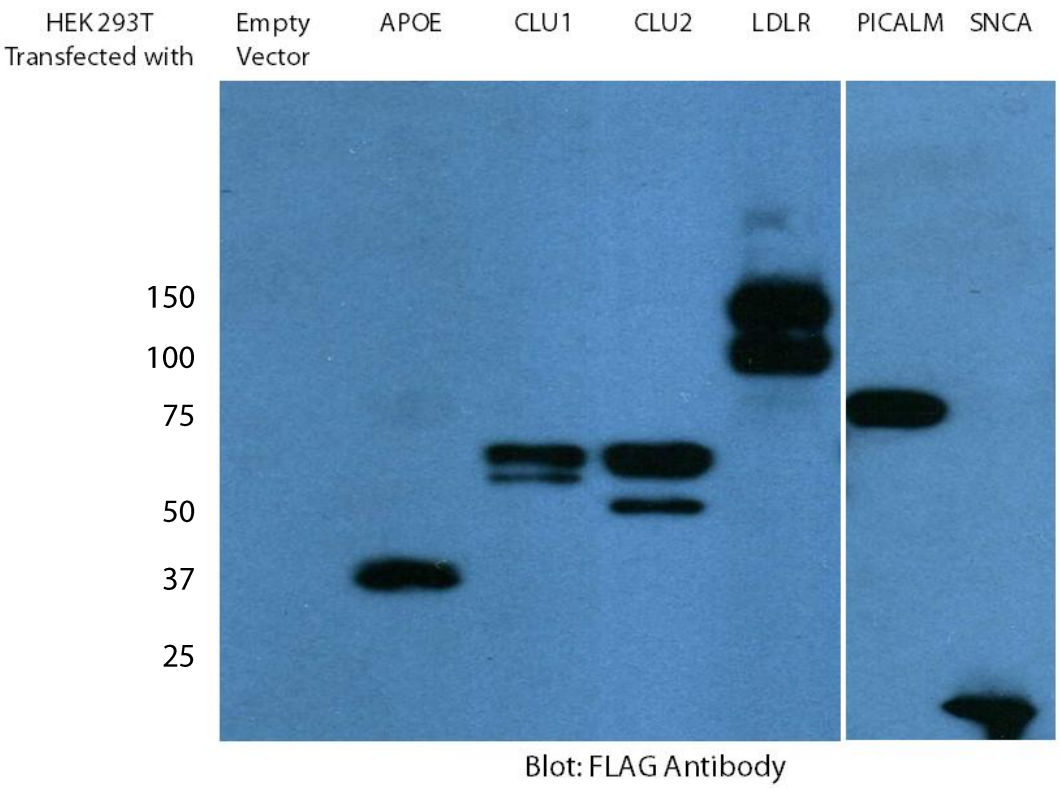
HEK 293T
Transfected with
Empty
Vector
APOE
CLU1
CLU2
LDLR
PICALM
SNCA
150
100
75
50
37
25
Blot: FLAG Antibody

Figure 3-2: Western blot (WB) validation of expression of FLAG-tagged recombinant proteins. HEK 293T cells were transfected with one of six tagged AD genes studied (APOE, CLU1, CLU2, LDLR, PICALM and SNCA) or the negative control, which is the empty vector (pCMV-Entry). 10 ug of the cell lysate from each transfection was separated by SDS-PAGE, and transferred to nitrocellulose membranes for WB analysis against the FLAG antibody. Expected sizes of proteins: APOE:34.2 kDa; CLU1:57.7 kDa; CLU2:50 kDa; LDLR:93 and 120 kDa; PICALM:70.6 kDa; SNCA:14.3 kDa.

Immunopurification and Optimization

The next step in our approach was the optimization of the immunopurification protocol. The optimization is performed in order to enhance the recovery of the bait protein and capture its interacting partners while minimizing non-specific interactions. Briefly, the construct transfected into 293T cells expresses the FLAG-tagged bait protein, which then associates with endogenous proteins to form complexes. Immunopurifications were performed to pull down the bait protein (FLAG tagged protein) along with its binding partners. The interaction networks for a specific bait provides a wealth of information from which function, localization, complexes, and any of its regulators or activators can be inferred (231). The optimization of the protocol is critical to minimize false positive and false negative interactors (36). For example, extensive washing of the enrichment beads following an immunopurification can lead to the loss of most interactors. Similarly, if the beads are not sufficiently washed, the number of false positive interactors will overshadow the real interactors. Moreover, the amount of cell lysate and FLAG coupled agarose beads and their ratio also influences the outcome of the immunopurifications and therefore needs tweaking for optimal results. The optimization of our immunopurification protocol was performed using an SDS-PAGE gel followed by silver staining. The amount of protein and complexity of the immunopurification was evaluated based on the intensity of the staining. This was contrasted against negative control immunopurifications performed by transfecting into cells tagged construct containing no recombinant gene. Efficient purification and washes would result in few protein bands in the negative control and many distinct protein bands in the immunopurification of the bait protein. To achieve optimal results, eighty five immunopurifications were done and silver stained on SDS-PAGE gels before any proteins were

digested and analyzed by mass spectrometry. Some of the gels that were produced after optimization and were digested and analyzed are shown in figure 3-3. The composition of the lysis buffer, wash buffer(s) and elution buffer as well as the number of washes, length of wash times, length of elution time, amount of beads, cell lysate volume and cell lysate concentration were altered in order to optimize the protocol. Successful IP's were obtained from using 1 mg of total cell lysate in 500 µL of cell lysis buffer (50 mM Tris-Cl pH 7.5, 100 mM NaCl, 5mM EDTA, 0.4% (v/v) NP-40, one complete mini EDTA-free tablet (Hoffmann-La Roche Limited, Mississauga, ON)) and 60 µL of FLAG-coupled agarose 50% bead slurry (Sigma-Aldrich Canada Ltd. Oakville, ON). The washing procedure was most successful when the beads were washed three times in a weaker salt buffer (50 mM Tris-Cl, 100 mM NaCl, pH 7.5) and washed another two times in a stronger salt buffer (100 mM Tris-Cl, 150 mM NaCl, pH 7.5). The elution worked best when eluted in 200 ng/uL FLAG peptide dissolved in the weaker salt buffer for 30 minutes at 4°C. Using this optimized protocol provided the most contrast between the immunopurification of the bait protein and the negative control, and was very easily reproducible.

Interactome Mapping Using Optimized Immunopurification Protocol

The optimized immunopurification protocol was used to systematically purify the bait proteins expressed in HEK 293T cells. Each bait was analyzed at least three times using this protocol. Briefly, the proteins in complex with the bait proteins were immunopurified and were separated by SDS-PAGE gel electrophoresis followed by visualization by silver staining. As well, 10% (v/v) of the purified protein complex was used for western blot analysis to test the efficiency and specificity of the immunopurification. After silver staining, gel bands were

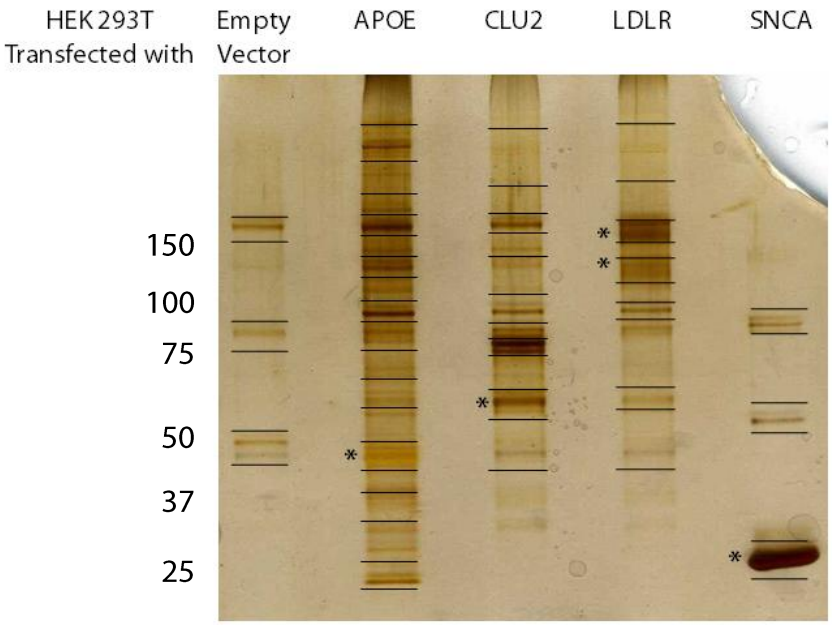
HEK 293T
Transfected with
Empty
Vector
APOE
CLU2
LDLR
SNCA
150
100
75
50
37
25
IP: FLAG
Silver Stain

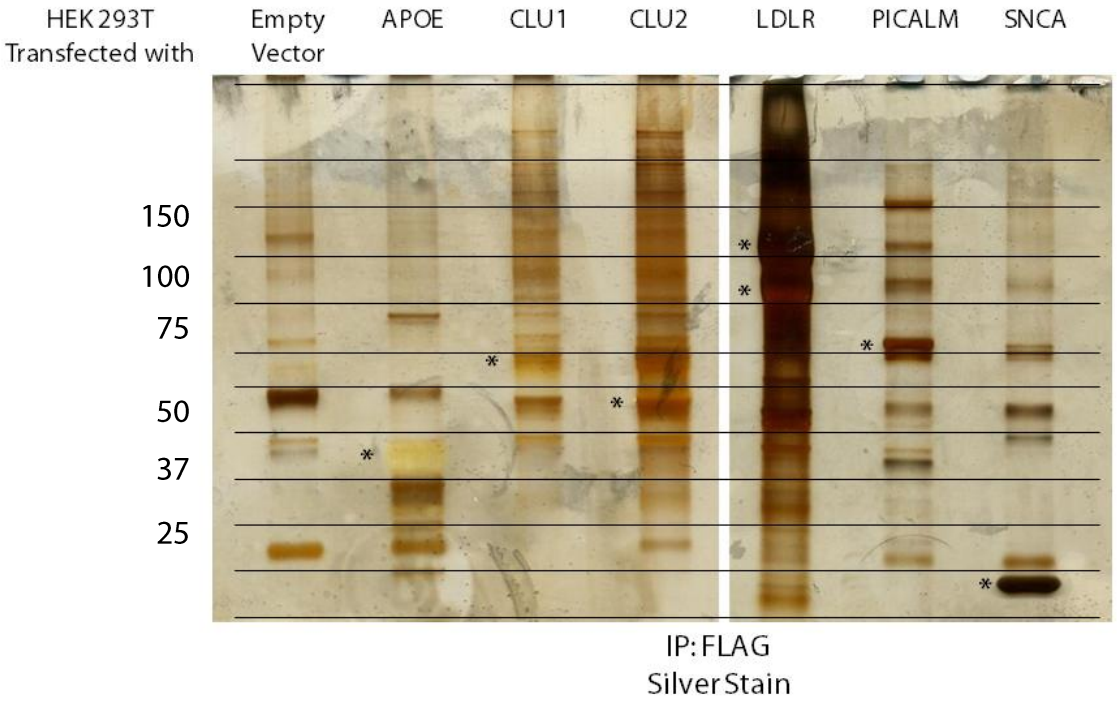
HEK 293T
Transfected with
Empty
Vector
APOE
CLU1
CLU2
LDLR
PICALM
SNCA
150
100
75
50
37
25
IP: FLAG
Silver Stain

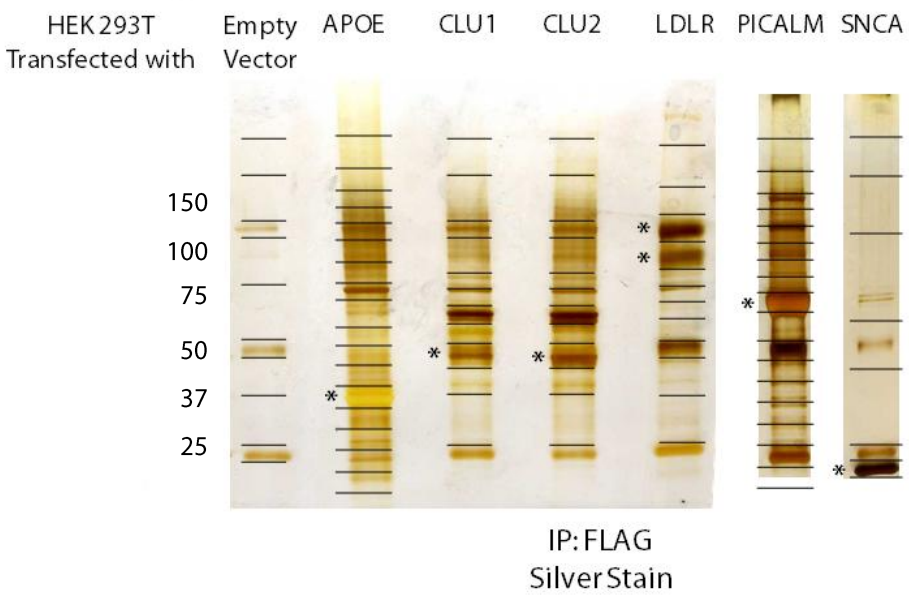
HEK 293T
Transfected with
Empty Vector
APOE
CLU1
CLU2
LDLR
PICALM
SNCA
150
100
75
50
37
25
IP: FLAG
Silver Stain

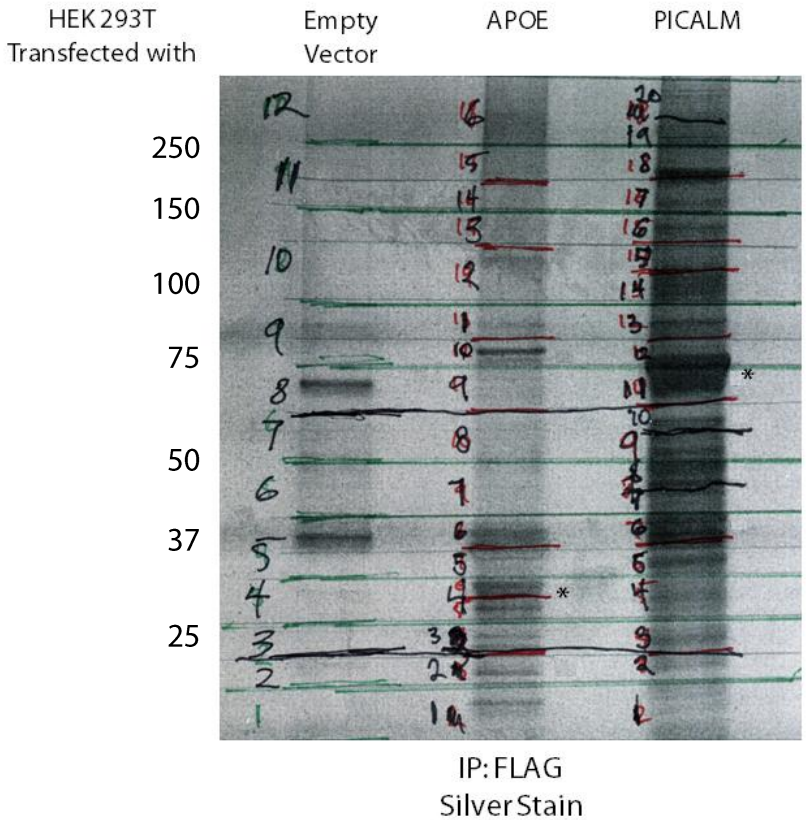
HEK 293T
Transfected with
Empty Vector
APOE
PICALM
250
150
100
75
50
37
25
IP: FLAG
Silver Stain

Figure 3-3: Example of silver-stained gels obtained from the optimized immunopurification of the FLAG-tagged bait proteins and their interaction partners from HEK 293T cells. All of the gels above were ones that had been optimized and were believed to be the best result. Each was digested with trypsin using the in-gel digestion protocol and the resulting peptides were analyzed by mass spectrometry. The lines over top of the gel show where the cuts were made to increase the efficiency of the digestion and sequester protein of similar molecular weight together. (*) was added beside bands of the bait protein. Expected sizes of bait proteins: APOE:34.2 kDa; CLU1:57.7 kDa; CLU2:50 kDa; LDLR:93 and 120 kDa; PICALM:70.6 kDa; SNCA:14.3 kDa.

excised from the gel and digested with trypsin. The resulting peptides were then analyzed by mass spectrometry. (Figure 3-4)

In total, 239 protein bands were analyzed by HPLC-ESI-MS/MS generating 2.7 million MS/MS spectra. MS/MS spectra of peptides contain information related to the amino acid sequence of the peptide. Although, part or complete sequence information can be manually extracted from individual MS/MS, it would be prohibitive to attempt to manually annotate all of the generated MS/MS spectra. Instead, we used a software called Mascot which performs protein sequence database searches using the information in the MS/MS spectra and returns the most probable peptide sequences. As well, this software computes the most probable full length proteins based on the unique peptides identified from the MS/MS spectra. All of the mass spectrometer results obtained for the protein gel bands were analyzed using the Mascot software and were converted into protein matches. Mascot assigns a score to each protein match based on a probabilistic model that calculates the probability that a certain spectra produced by a peptide was produced by the actual peptide or could have just been produced by chance. A higher score represents a higher probability of a protein match (172). Prohits, a mass spectrometry data management and analysis tool (133), was used to organize the protein matches into tables and remove common contaminants such as keratin, albumin and ribosomal proteins. Prohits has also been used to refine the list of protein matches to the matches which received a mascot score higher than 30, contained a unique peptide sequence match and within the 0.01 p-value threshold. Each bait was purified, stained and digested 3 times and the resulting peptide sequence data combined together for comparison.

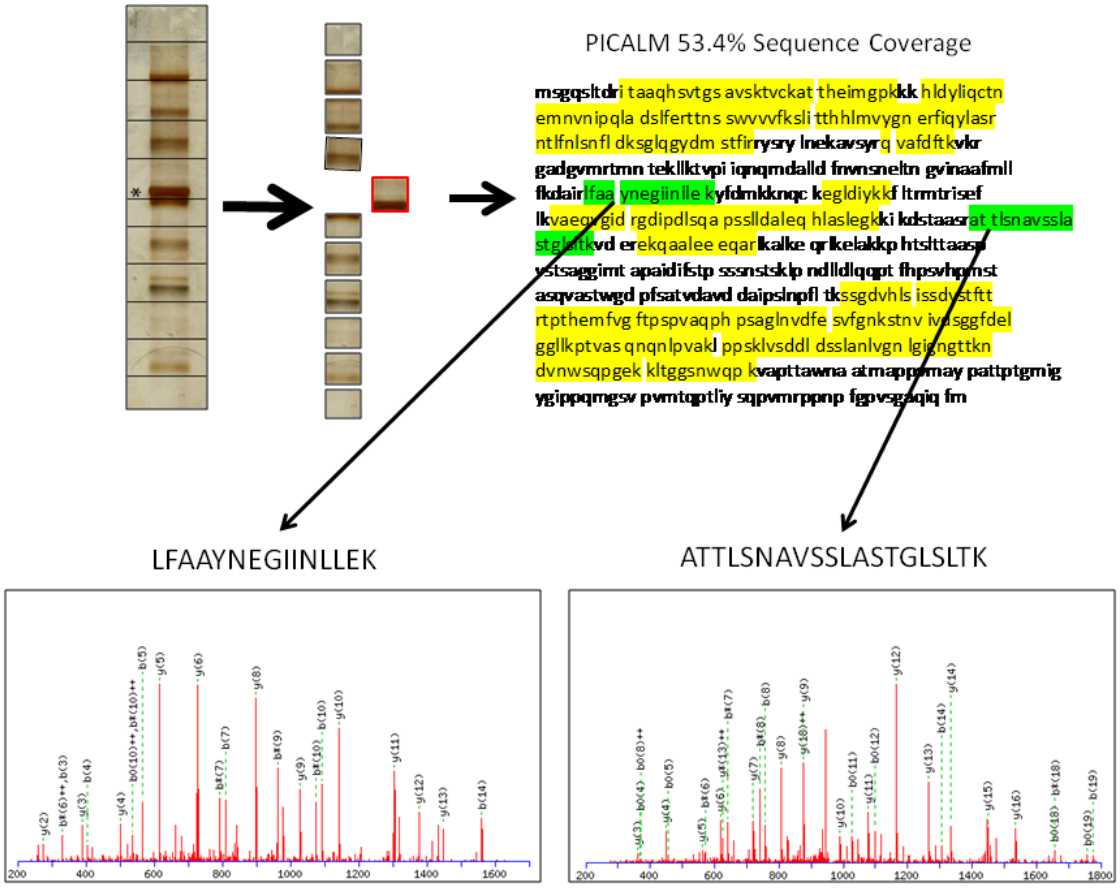
PICALM 53.4% Sequence Coverage
msgqsltdri taaqhsvtgs avsktvckat theimgpkkk hldyliqctn
emnvnipqla dslferttns swvvvfksli tthhlmvygn erfiqylasr
ntlfnlsnfl dksglqgydm stfirrysry lnekavsyrq vafdftkvkr
gadgvmrtmn teklltvpi iqnqmdalld fnvnsneltn gvinaafmll
fkdairlfaa ynegiinlle kyfdmkknqc kegldiykkf ltrmtrisef
lkvaeqvgid rgdipdlsqa pssllaleq hlaslegkki kdstaasrat tlsnavssla
stglsltkvd erekqaalee eqarlkalke qrlkelakkp htslttaasl
vstsaggimt apaidifstp sssnstsklp ndlldlqqpt fhpsvhqmst
asqvastwgd pfsatvdavd daipslnpfl tkssgdvhls issdvstftt
rtpthemfvg ftpspvaqph psaglnvdfe svfgnkstnv ivasggfdel
ggllkptvas qnqnlpvakl ppsklvsddl dsslanlvgn lgingttkn
dvnwsqpgek kltggsnwqp kvapttawna atmapppmay pattptgmig
ygippqmgsv pvmtqptliy sqpvmrppnp fgpvsgaqiq fm
LFAAYNEGIINLLEK
ATTLSNAVSSLASTGLSLTK

Figure 3-4: Illustration of the Transition from In-gel digestion to MS/MS Sequencing Results. Gel lanes are cut into 8-20 pieces depending on the intensity of the staining. The lane below was loaded with immunopurified sample from HEK 293T cells transfected with PICALM-FLAG. The lane was cut into 11 pieces, enzymatically digested by typsin and analyzed by LC-MS/MS. The sequence coverage for PICALM taken from the gel piece outlined in red is shown by the amino acids highlighted in yellow and green. Two annotated MS/MS spectra are shown for the two peptides highlighted in green.

Table 3-1: The results of the in-gel digestion of cells transfected with the 6 tagged AD genes studied (APOE, CLU1, CLU2, LDLR, PICALM and SNCA) and cells transfected with the negative control, which is the empty vector (pCMV-Entry). Hit Gene Name: the name of the gene matched to the peptides by Mascot; Hit Protein ID: protein identifier from GI database; Hit Score: Mascot probability score associated with the protein match; Peptide Number: total number of peptide sequences matched to the protein; Unique Peptide Number: number of unique peptide sequences matched to the protein; Coverage: the percentage of amino acids matched to protein. Rows highlighted in red are bait proteins; rows highlighted in green are known interactors; rows highlighted in yellow are suspected interactors. This table is a summary of the top 50 MS results found for each bait; Appendix 3-1 presents all of the results.

EMPTY

Hit Gene Name	Hit Protein ID	Hit Score	Peptide Number	Unique Peptide Number	Coverage (%)
ATP1A1	21361181	1797	114	28	34
SSBP1	4507231	187	50	3	27.7
IRS4	4504733	907	48	17	18.6
KIF11	13699824	1219	46	23	22.3
HSPA5	16507237	780	34	13	29.5
ATP2A2	4502285	649	29	12	15.1
BASP1	30795231	113	29	2	12.3
ATP2B1	48255945	490	28	9	10.7
ATP2B4	48255957	488	27	4	9.9
HSP90B1	4507677	556	26	11	15.1
MAP2	87578396	437	25	9	7.2
IGF2R	119964726	488	24	10	4.6
SLC1A5	5032093	463	24	7	22
HIST1H2AG	4504239	67	24	1	14.6
ATP1A3	22748667	320	21	6	10.3
MARCKSL1	13491174	154	21	2	14.4
MARCKS	153070260	196	20	4	19.6
TFRC	189458817	454	19	9	14.2
MAP1B	153945728	249	19	4	2.9
PRMT5	20070220	541	18	10	19.2
SLC3A2	61744477	394	18	7	14.7
DDX21	50659095	309	18	8	12.4
CANX	10716563	160	18	3	6.2
LOC728026	113420837	83	18	1	11.9
CKAP4	19920317	455	17	9	21.6
NCL	55956788	158	17	3	5.6
AHSG	156523970	63	17	1	3.3

HNRNPK	14165435	173	16	3	9.5
MTDH	223555917	395	15	7	15.3
RPN1	4506675	389	15	9	17.3
RPN2	35493916	315	15	6	15.5
YBX1	34098946	168	15	2	11.1
BSG	38372919	265	14	6	27.3
VAMP3	4759300	257	14	4	40
BCAP31	32171186	200	14	4	13
GAPDH	7669492	157	14	3	13.7
SCAMP3	16445419	335	13	5	22.8
RAB7A	34147513	264	13	5	31.9
RAB1A	4758988	254	13	5	32.2
SRPRB	284795266	211	13	4	19.9
FLNA	116063573	165	13	3	2.5
HIST2H4A	4504301	137	13	3	29.1
DSG2	116534898	312	12	5	7.6
DDOST	20070197	285	12	5	13.2
RAB5C	41393545	281	12	5	31
VDAC1	4507879	274	12	4	25.4
GNAI3	5729850	270	11	6	18.4
FLOT2	94538362	268	11	6	15.4
RAB14	19923483	252	11	4	32.1

APOE

Hit Gene Name	Hit Protein ID	Hit Score	Peptide Number	Unique Peptide Number	Coverage (%)
APOE	4557325	1258	603	21	64
VDAC1	4507879	773	157	13	58
VDAC2	42476281	433	93	6	26.9
UBR5	15147337	1026	47	22	10.3
CANX	10716563	672	41	14	24.5
VDAC3	25188179	251	39	3	12.4
HSPA8	5729877	635	28	13	24
NCL	55956788	455	22	10	13.9
CSE1L	29029559	559	21	10	12.4
YBX1	34098946	621	20	10	40.7
XRCC6	4503841	573	18	11	23
HSPA1B	167466173	516	18	8	19.2
HSPA5	16507237	280	17	5	10.6
PRMT5	20070220	389	15	8	13.7
PABPC1	46367787	362	13	8	14.5
PPM1B	4505995	376	13	8	24

ATP5A1	4757810	338	13	6	13.4
PGRMC1	5729875	394	13	6	34.4
RAB1B	13569962	235	12	5	29.9
IMMT	154354962	356	12	7	9.8
UQCRC2	50592988	312	12	6	20.1
NSF	156564401	329	11	8	12.2
HADHA	20127408	325	11	7	10.4
CYP51A1	4503243	318	11	6	15.3
CSDA	224586882	283	11	1	15.9
RAB1A	4758988	227	11	1	26.8
RAB7A	34147513	340	11	6	41.5
HYOU1	5453832	373	11	7	8
BSG	38372919	296	11	5	14.3
XRCC5	10863945	311	10	6	7.9
POR	127139033	266	10	6	9
RAB10	256222019	183	10	2	20.5
PLIN3	255958282	329	9	6	18.9
PHB2	6005854	299	9	6	20.4
BCAP31	32171186	248	9	4	21.1
COX5B	17017988	84	9	2	9.3
MTDH	223555917	245	8	5	10.3
LMAN1	5031873	154	8	4	7.8
ATP5B	32189394	238	8	5	12.7
PHB	4505773	216	8	5	19.1
RAB11B	190358517	228	8	4	19.7
RAB5C	41393545	225	8	5	27.8
SPCS2	162417971	250	8	4	24.8
COX5A	190885499	77	8	1	10
RPS27A	4506713	49	8	1	10.3
CKAP4	19920317	218	8	5	9.6
UQCRC1	46593007	271	8	5	12.5
HIST1H1C	4885375	86	8	2	11.3
TOMM40	5174723	223	4	3	18.3

CLU1

Hit Gene Name	Hit Protein ID	Hit Score	Peptide Number	Unique Peptide Number	Coverage (%)
CLU	42716297	975	57	18	32.3
HSPA8	5729877	1238	56	22	37.9
KIF11	13699824	1457	53	28	27.4
CANX	10716563	805	40	16	29.2
HSPA1B	167466173	882	34	12	27.6

PRKDC	13654237	781	24	14	4.5
ATP5A1	4757810	701	23	12	26
TCP1	57863257	994	22	13	31.7
HSP90AB1	20149594	572	20	11	16.3
HSP90AA1	154146191	507	18	3	14.5
HSPD1	31542947	585	16	10	23.4
HSPA5	16507237	461	15	6	15.3
RPN1	4506675	389	14	7	14.3
AIFM1	4757732	477	13	9	16.6
AMBP	4502067	103	13	1	6.5
CSE1L	29029559	320	11	7	7.5
PRMT5	20070220	373	11	6	13.8
PHGDH	23308577	342	11	6	14.8
BAG2	4757834	270	11	6	28.9
GCN1L1	54607053	328	10	8	3.7
GNB2L1	5174447	415	10	8	28.7
TFRC	189458817	419	10	7	10.8
MAGED2	19387846	258	10	4	9.2
DDX5	4758138	56	10	1	2
ATP5B	32189394	349	9	6	14.9
PCNA	4505641	342	9	5	25.3
SLC25A5	156071459	287	9	6	18.8
MCM7	33469968	311	9	6	9.7
HSPA1L	124256496	223	9	1	7.3
MCM3	6631095	353	8	6	10.5
NUP93	208609990	278	8	6	9.4
SLC25A6	156071462	244	8	1	18.1
PPM1B	4505995	213	8	4	12.1
CCT8	48762932	202	8	4	7.7
RAB5C	41393545	211	8	4	21.3
XPOT	8051636	248	7	5	6.2
NPEPPS	158937236	243	7	4	4.8
MTHFD1	222136639	223	7	4	5.5
EMD	4557553	292	7	4	22
PSMD2	25777602	160	7	4	4.7
HSPA9	24234688	334	7	6	11.6
PABPC1	46367787	204	7	5	8.5
CCT6A	4502643	128	7	3	5.3
PSMC1	24430151	202	7	4	12
RAB18	10880989	207	7	4	25.2
RAB10	256222019	163	7	3	17
EPRS	62241042	179	6	3	2.8
XRCC5	10863945	87	1	1	1.9

XRCC6	4503841	138	4	3	5.7

CLU2

Hit Gene Name	Hit Protein ID	Hit Score	Peptide Number	Unique Peptide Number	Coverage (%)
KIF11	13699824	1958	74	37	36.1
HSPA8	5729877	1008	57	20	33.7
CLU	42716297	471	56	9	18.2
PRKDC	113430845	1656	48	35	10.8
CANX	10716563	761	36	14	24.8
HSPA1B	167466173	670	36	10	22.6
PRMT5	20070220	547	26	11	20.7
WDR77	13129110	386	24	7	29.5
HSP90AB1	20149594	650	19	13	18.8
HSPA5	16507237	357	19	5	13.9
DYNC1H1	33350932	591	18	13	3.3
CSE1L	29029559	511	18	11	11.5
TCP1	57863257	680	17	10	23.2
GANAB	38202257	338	15	8	8.4
PHGDH	23308577	447	13	8	19.9
PPM1B	4505995	362	12	7	19.6
FLNA	116063573	183	12	4	2.3
HIST1H1C	4885375	139	12	3	10.3
MCM7	33469968	392	11	9	14
CAD	18105007	328	11	7	4.4
HNRNPM	14141152	184	11	5	6.7
SLC25A5	156071459	277	10	6	17.1
HSP90AA1	154146191	231	10	5	7.9
HNRNPU	14141161	95	10	1	1.9
NUP205	57634534	321	9	7	3.8
MTHFD1	222136639	346	9	6	7.6
ATP5A1	4757810	321	9	5	11
HNRNPK	14165435	259	9	5	12.5
PRKCSH	48255889	212	9	5	9.7
YBX1	34098946	128	9	2	14.5
GCN1L1	54607053	226	8	6	3
CCT8	48762932	265	8	6	13
CCT3	58761484	262	8	6	12.6
CCT7	5453607	259	8	7	13.3
CCT4	38455427	230	8	6	11.9
RUVBL1	4506753	317	8	5	14.9
NCL	55956788	149	8	4	5.4

NUP93	208609990	320	7	5	7.8
GNE	4885285	239	7	5	8.4
IRAK1	68800243	238	7	5	7.2
RPN1	4506675	307	7	5	13.3
RARS	15149476	217	7	4	7.6
RUVBL2	5730023	179	7	4	8
RNF219	88759348	195	7	5	7.2
ATP2A2	4502285	159	6	3	5.4
PANK4	8922665	258	6	4	7.6
IGF2R	119964726	175	6	4	1.8
XRCC6	4503841	131	5	3	6.1
XRCC5	10863945	121	3	2	3.6

LDLR

Hit Gene Name	Hit Protein ID	Hit Score	Peptide Number	Unique Peptide Number	Coverage (%)
LDLR	4504975	616	291	10	13.1
KIF11	13699824	1771	122	36	33.3
CANX	10716563	1093	63	19	29.4
HSP90AB1	20149594	478	49	10	20
CSE1L	29029559	1158	44	22	25.2
HSP90AA1	153792590	325	43	2	8.7
LOC731751	113430845	1118	29	21	6.2
TFRC	189458817	644	23	12	17.6
GCN1L1	54607053	535	21	12	5.7
XPO1	4507943	465	19	10	9.3
TNPO1	23510381	518	18	11	14.3
HSPA1B	167466173	487	18	10	18.9
NSF	156564401	501	15	12	17.7
HSPD1	31542947	502	14	7	17.5
PRMT5	20070220	156	14	3	6
KPNB1	19923142	397	13	8	9.6
HSPA8	5729877	345	13	4	13.2
CNBP	4827071	253	12	4	28.2
IPO8	53759103	351	12	7	7.1
ENO1	4503571	154	12	3	13.1
ATP5A1	4757810	390	11	6	13.6
SRPRB	284795266	369	11	7	31
PRDX1	4505591	256	11	6	27.1
ENO3	301897469	103	11	1	10.1
ATP1A1	21361181	463	10	6	8.3
SEC63	6005872	272	10	5	8

CYP51A1	4503243	309	10	6	14.3
RAB5C	41393545	280	10	5	27.8
RAB10	256222019	240	10	5	32
MTHFD1	222136639	386	9	7	7.7
IPO7	5453998	347	9	6	7.1
TNPO2	48675813	252	9	1	5.9
POR	127139033	295	9	6	11.8
CCT3	58761484	276	9	6	12.8
CCT4	38455427	235	9	4	9.5
PHGDH	23308577	306	9	6	13.3
RUVBL2	5730023	226	9	5	12.5
PHB2	6005854	251	9	5	15.7
RAB1A	4758988	172	9	2	24.4
APOB	105990532	198	8	5	1.3
MCM3	6631095	286	8	7	10
STAT3	21618338	243	8	4	7.7
TELO2	225545550	234	8	5	5.6
MCM7	33469922	242	8	4	8.7
CCT7	5453607	210	8	5	9.2
DDOST	20070197	204	8	4	9.2
GNB2L1	5174447	198	8	5	14.2
PGRMC1	5729875	194	8	3	22.1
HSPA5	16507237	335	7	5	11.8

PICALM

Hit Gene Name	Hit Protein ID	Hit Score	Peptide Number	Unique Peptide Number	Coverage (%)
PICALM	56788366	1604	124	26	53.4
CLTC	4758012	2081	93	38	25.1
KIF11	13699824	2018	87	39	36.9
HSPA8	5729877	1015	41	17	37.9
HSPA1B	167466173	1203	39	20	40.2
HSPA5	16507237	904	28	13	29.8
HSPA9	24234688	632	19	11	21.4
HSPA1L	124256496	534	19	1	17.2
PRMT5	20070220	571	17	10	17
HSP90AA1	154146191	453	17	9	13.9
HSP90AB1	20149594	387	17	4	13.1
HSPA4	38327039	507	16	8	11.4
HSPH1	42544159	439	14	8	11.2
RNH1	21361547	404	14	8	20.2
HSPD1	31542947	460	14	6	16.4

IGF2R	119964726	294	13	7	3
NCL	55956788	313	13	8	10.4
YWHAQ	5803227	361	13	7	22
WDR77	13129110	374	12	6	19
CSE1L	29029559	369	12	8	9.5
CLINT1	7661968	400	11	7	14.4
HSPA6	34419635	297	11	1	8.2
PIK3C2A	157671929	324	10	6	4.6
KCTD5	9506651	279	10	6	32.5
ENO1	4503571	363	9	5	17.7
YBX1	34098946	332	9	6	31.5
YWHAG	21464101	252	9	2	19
ATP5B	32189394	346	9	6	14.7
PPM1B	4505995	301	8	5	14.6
FASN	41872631	275	8	6	2.9
COPA	148536853	249	8	6	4.6
YWHAZ	4507953	209	8	2	16.3
CCT8	48762932	250	8	5	10.9
GPS1	47078238	204	8	4	9.3
PSMD3	25777612	207	8	4	8.6
PSMD2	25777602	295	8	5	7.6
HSPA4L	31541941	239	8	5	7.2
PRKDC	13654237	265	8	6	1.5
AP2A1	19913414	258	7	5	5.9
AP2M1	14917109	142	7	4	7.8
SCAMP3	16445419	199	7	3	13
STX12	28933465	193	7	4	17
PSMC6	195539395	210	7	4	12.2
CANX	10716563	204	7	4	8.4
MTHFD1	222136639	227	7	4	5.1
EIF3A	4503509	246	7	5	4.3
POTEE	134133226	182	6	1	4.8
EPRS	62241042	152	6	3	2.6
AP2B1	4557469	227	6	5	6

SNCA

Hit Gene Name	Hit Protein ID	Hit Score	Peptide Number	Unique Peptide Number	Coverage (%)
SNCA	4507109	873	97	12	62.1
HSPA8	5729877	738	32	16	28.9
HSPA5	16507237	727	27	12	29.8
HSPA1B	167466173	473	18	8	18.7

SNCB	4507111	209	12	1	16.4
HSPA9	24234688	339	9	6	13.7
HNRNPM	14141152	189	8	5	6.2
HIST2H4A	4504301	103	5	2	17.5
HBA2	4504345	102	3	2	19
HNRNPH1	5031753	140	3	3	9.6
DCD	16751921	96	3	2	20
HBB	4504349	53	2	1	6.8
KCTD5	9506651	79	2	1	6.8
DDX5	4758138	65	2	2	3.1
DSG1	119703744	69	2	2	3.3
HRNR	57864582	87	2	2	1.3
LYZ	4557894	50	2	1	8.1
LRRC15	288541295	49	2	1	1.7
NPAT	155969714	34	2	1	0.6
SHROOM3	203098098	35	2	1	0.5
HNRNPU	14141161	75	1	1	1.9
CSTA	4885165	76	1	1	18.4
RPS27A	4506713	50	1	1	10.3
CALML5	223278387	77	1	1	15.8
PGRMC1	5729875	58	1	1	10.3
CDC7	4502715	50	1	1	1.6
PEG10	94421475	65	1	1	1.3
OR2T35	49226830	40	1	1	2.5
ADCY2	115387102	34	1	1	0.5
HSPA6	34419635	64	1	1	2.5
NUS1	20270243	37	1	1	4.4
308387374	308387374	32	1	1	1.1
SAMD14	28557802	35	1	1	1.8
ZMYM2	4508011	35	1	1	0.9
LSM1	7657313	33	1	1	6
NALCN	24119274	31	1	1	2.1

All of the bait proteins were successfully purified using this strategy. The proteins found by mascot were organized into tables and the tables were ordered according to the number of peptides identified per protein. The bait proteins, except clusterin variant 2, had the most peptides identified in each respective immunopurification. This was an expected result, as each Western blot for the immunopurifications successfully showed expression of a FLAG-tagged protein at the correct molecular weight, and the darkest stained band of each lane of the silver stained gel was at the correct molecular weight.

Filtering of the results using SAINT

Prohits and the SAINT algorithm (39) has been used to further filter and analyze the interactomes. First, Prohits was used to filter the interactome by requiring each protein identified to have at least one unique peptide match, with a Mascot score of at least 30 and a significance threshold lower than 0.01. Then, the SAINT algorithm (39) was used to evaluate the significance of the protein in the interactome. SAINT is used to convert label-free mass spectrometry data into probabilities that an interactor found is in fact a true one. Firstly, SAINT models the spectral counts of each bait-prey relationship into true and false interactions based on a Poisson distribution. The probability of a true interaction is calculated using Bayes rule and is done on each individual replicate. The final probability (SAINT score) is computed by taking an average of the probabilities from each replicate (39). Using SAINT, all of the generated interactomes from the bait proteins are compared to the negative controls in order to compute interaction probabilities. SAINT provides a score between 0 and 1 and is proportional to the probability that the interaction exists (39). Table 3-2 presents the SAINT scores for each immunopurification, with a cutoff score of 0.200. Some of the known interactors (eg. CLTC, AP2A1, SNCB) were

above the cutoff score while others (eg. XRCC5, SNAP91) were below the cutoff score and not shown in Table 3-2. This computational tool/algorithm has only been available since December 2010, and was bridged with Prohits in August 2011. There are still some tweaks needed to the program in the opinion of this researcher. Some proteins found in the control and multiple purifications still have high SAINT scores. If a protein is found with a similar amount of peptide matches for multiple samples or if it is found in the control it should be negated as an interactor, and be thought of as a contaminant or background. There are some circumstances which need to be considered where this is not true, but for the majority of cases it is. SAINT is thus used as a device for further investigation. It allows us to see the most likely interactors so that they can be validated and further studied.

Table 3-2: SAINT probability scores for the results of the MS analysis of in-gel digested HEK 293T cells transfected with the 6 tagged AD genes studied (APOE, CLU1, CLU2, LDLR, PICALM and SNCA) and cells transfected with the negative control, which is the empty vector (pCMV-Entry). Gene Name: the gene name matched to the peptides by Mascot; Hit protein ID: protein identifier from GI database; SAINT Score: the confidence score of true interaction calculated by the SAINT algorithm. Rows highlighted in red are bait proteins; rows highlighted in green are known interactors; rows highlighted in yellow are suspected interactors. Only interactors with a score >0.200 are shown.

Apolipoprotein E

Gene Name	Hit Protein ID	SAINT Score
APOE	4557325	1
VDAC1	4507879	0.542
VDAC2	42476281	0.528
RAB7A	34147513	0.464
BCAP31	32171186	0.44
YBX1	34098946	0.41
RAB1B	13569962	0.408
SPCS2	162417971	0.404
PHB	4505773	0.386
CANX	10716563	0.38
PHB2	6005854	0.38
COX2	251831110	0.374
PGRMC1	5729875	0.368
CSDA	224586882	0.36
RPS27A	4506713	0.358
C1QBP	4502491	0.354
BSG	38372919	0.352
COX4I1	4502981	0.35
TMED10	98986464	0.334
COX4NB	5174615	0.332
RAB10	256222019	0.33
RAB1A	4758988	0.328
TMX1	151101292	0.328
RAB11B	190358517	0.326
VDAC3	25188179	0.318
PGRMC2	291621647	0.316
TOMM22	9910382	0.312

RAB5C	41393545	0.31
C15orf24	9910346	0.31
RAB6B	96975097	0.304
CYB5B	83921614	0.302
VAPB	4759302	0.298
RDH14	10190746	0.296
XRCC6	4503841	0.294
TOMM40	5174723	0.292
RAB2A	4506365	0.278
RAB14	19923483	0.276
TMED9	39725636	0.276
NAPA	47933379	0.274
RAB5A	19923262	0.268
CYC1	21359867	0.26
UQCRC2	50592988	0.258
TMEM111	8923857	0.256
PLIN3	255958282	0.248
CHCHD2	7705851	0.242
TMEM109	13129092	0.236
UBR5	15147337	0.234
SEC62	4507525	0.234
JAGN1	190014601	0.232
SPCS3	11345462	0.21
VAMP3	4759300	0.208
C19orf63	45580696	0.204

Clusterin V1

Gene Name	Hit Protein ID	SAINT Score
CLU	NM_001831.3	1
TCP1	57863257	0.774
SLC25A5	156071459	0.514
HSPA8	5729877	0.506
BAG2	4757834	0.504
RPS27A	4506713	0.452
CANX	10716563	0.446
ATP5A1	4757810	0.398
RAB1A	4758988	0.382
HSP90AA1	154146191	0.37
AIFM1	4757732	0.352
UBL4A	7657667	0.34
RAB10	256222019	0.334

CCT6A	4502643	0.326
YBX1	34098946	0.316
PHGDH	23308577	0.302
EMD	4557553	0.298
MCM7	33469968	0.296
RAB5C	41393545	0.294
RPN1	4506675	0.294
RAB18	10880989	0.29
MAGED2	19387846	0.288
SLC25A6	156071462	0.286
HNRNPK	14165435	0.284
PSMA6	23110944	0.28
RUVBL2	5730023	0.276
RAB14	19923483	0.27
TIMM50	48526509	0.27
PRDX1	4505591	0.248
ATP5B	32189394	0.244
PGRMC1	5729875	0.236
MCM3	6631095	0.236
RUVBL1	4506753	0.234
SLC25A3	4505775	0.226
HSP90AB1	20149594	0.224
PSMC1	24430151	0.222
NUP93	208609990	0.216
RAB7A	34147513	0.214
ATP1A1	21361181	0.214
XPOT	8051636	0.2

Clusterin V2

Gene Name	Hit Protein ID	SAINT Score
CLU	NM_001831.3	1
WDR77	13129110	0.904
PRKCSH	48255889	0.874
PRMT5	20070220	0.772
TCP1	57863257	0.746
SLC25A5	156071459	0.548
HSPA8	5729877	0.53
CANX	10716563	0.466
PPM1B	4505995	0.464
PSMD13	157502193	0.344
YBX1	34098946	0.33

HNRNPK	14165435	0.33
GANAB	38202257	0.308
RUVBL1	4506753	0.302
DNAJA1	4504511	0.298
MAGED2	19387846	0.296
CCT5	24307939	0.286
SLC25A6	156071462	0.28
MCM7	33469968	0.278
HLA-C	52630342	0.27
CAD	18105007	0.25
LOC731751	XM_001129414.2	0.248
SSR4	5454090	0.24
PPP6C	4506029	0.238
IGBP1	4557663	0.232
RPN1	4506675	0.224
RUVBL2	5730023	0.224
PHGDH	23308577	0.222
SLC1A5	223468564	0.22
MRI1	23943880	0.218
ATP1A1	21361181	0.216
GNE	4885285	0.214
ARF4	4502205	0.208
SFXN4	47458811	0.202

Low Density Lipoprotein Receptor

Gene Name	Hit Protein ID	SAINT Score
LDLR	4504975	0.978
CNBP	4827071	0.6
CANX	10716563	0.456
RAB10	256222019	0.382
CSE1L	29029559	0.328
RAB14	19923483	0.29
SPCS2	162417971	0.288
ARL6IP1	24308007	0.282
TFRC	189458817	0.264
CFL1	5031635	0.262
RAB7A	34147513	0.258
TMEM109	13129092	0.258
RAB1A	4758988	0.256
SLC3A2	61744477	0.254
FHL1	21361122	0.252

RAB3D	4759000	0.252
PRDX1	4505591	0.25
RAB8A	16933567	0.25
PGRMC1	5729875	0.248
LASP1	5453710	0.248
ARF4	4502205	0.246
ATP5O	4502303	0.242
PHB	4505773	0.238
SRPRB	284795266	0.238
CSRP2	4503101	0.234
VAPB	4759302	0.228
CNBP	187608732	0.224
TNPO1	23510381	0.22
RAB5B	4506371	0.214
RAB2A	4506365	0.206
ATP1A1	21361181	0.202
RAB18	10880989	0.202

PICALM

Gene Name	Hit Protein ID	SAINT Score
PICALM	56788366	1
CLTC	4758012	0.996
CLTB	4502901	0.594
HSPA1B	167466173	0.586
HSPA1L	124256496	0.522
HSPA5	16507237	0.488
HSPA8	5729877	0.466
BAG2	4757834	0.462
HSPA4	38327039	0.446
YWHAG	21464101	0.446
HSPA9	24234688	0.41
CLINT1	7661968	0.406
HSPA6	34419635	0.398
HSPH1	42544159	0.39
RNH1	21361547	0.386
CLTA	4502899	0.37
YWHAQ	5803227	0.368
WDR77	13129110	0.354
YWHAZ	4507953	0.352
HSP90AA1	154146191	0.318
YBX1	34098946	0.318

P2A1	19913414	0.316
S100A7A	28827815	0.258
NACA	5031931	0.254
HSPA4L	31541941	0.238
STX12	28933465	0.236
GAPDH	7669492	0.218

Alpha-Synuclein

Gene Name	Hit Protein ID	SAINT Score
SNCA	4507109	1
SNCB	4507111	0.536
HSPA5	16507237	0.444
HSPA8	5729877	0.376
DCD	16751921	0.33
HIST2H4A	4504301	0.23

Comparison with the Human Protein Reference Database (HPRD)

The Human Protein Reference Database (HPRD) (106, 171) was used to find the previously known interactors for every bait protein. The bait protein APOE was investigated using the database. APOE is known to directly interact with several lipoprotein receptors, such as LDLR, Low density lipoprotein receptor-related protein 1 and 8 and the VLDL receptor, as well as megalin and Aβ. These interactions were found by bioaffinity assays but not by immunopurification and mass spectrometry (112, 218, 223, 238). None of those known interactors were picked up by the immunopurification followed by LC-MS. APOE is endogenously (171) expressed in kidney cells and should therefore also be expressed in the human embryonic kidney cell line used (HEK 293T) (19). The problem here might have been due to the FLAG tag that might have disrupted proper folding of the protein, or it might have blocked the interaction (36). The tag was added to the C-terminal end of the protein, which happens to be the major lipid binding region: amino acids 244-272 of the 317 amino acid protein and it is also the region which binds Aβ (27). There is also cooperativity between the N-terminal and C-terminal binding domains so the tag could affect N-terminal binding as well (173). The proteins that were found had high Mascot scores and a large number of unique and total peptides found. The number one interactor found was the voltage-dependent anion channel 1(VDAC1), it was identified with 13 unique peptides and 157 total peptides. Voltage-dependent anion channel 2 and voltage-dependent anion channel 3 (VDAC2 and VDAC3) were found with 6 and 3 unique peptide matches, respectively. These proteins are highly conserved channels responsible for the movement of ions across the mitochondrial outer membrane (15). Currently, there is no known interaction between APOE and VDAC1, VDAC2 or VDAC3. Another interesting protein identified was translocase of outer mitochondrial membrane 40 homolog (TOMM40 or TOM40). TOMM40 is also an outer mitochondrial membrane protein. It is an essential protein, responsible

for the movement of proteins across the outer mitochondrial membrane (15). It is the core protein in the complex of proteins known as translocase of the mitochondrial membrane (TOM) (246). Genetically, TOMM40 is separated by only 2 kb on chromosome 19 from APOE, and has been previously studied as a possible risk gene for LOAD (192).

CLU variant 1 and 2 are very similar and only differ slightly in size. Variant 1 is the nuclear isoform, it is ~49 kDa and has an open reading frame (ORF) of 1350 bp. Variant 2 is the cytoplasmic isoform or precursor isoform, it is ~57 kDa and has an ORF of 1506 bp. The cytoplasmic form has also been shown to splice into the variant 2 form following radiation or cell stress (124). A third variant exists, which is the secreted form. The secreted form is the most common, it is cleaved into α and β peptides, both of which being 40 kDa. The final protein weighs ~60 kDa after the two units are linked by five disulfide bridges and is N-glycosylated (164). The secreted form is mainly thought of as a molecular chaperone that can bind to a wide array of ligands including Aβ and important lipids (164). The known interactors of the cytoplasmic and nuclear form are not as well-known as the secreted form. The known interactors of the nuclear form of CLU are the X-ray repair complementing defective repair in Chinese hamster cells 6/thyroid autoantigen 70kD (Ku antigen) (XRCC6) and X-ray repair complementing defective repair in Chinese hamster cells 5/thyroid autoantigen 80kD (XRCC5) (124). XRCC5 and XRCC6 form a complex together in the nucleus, which is involved in DNA repair of nonhomologous ends. The binding between the XRCC6/XRCC5 complex to CLU1 is thought to possibly block the ability of the complex to bind to DNA and perform the repair (124). Both of these proteins were purified and detected by mass spectrometry and both of the proteins were found in both the CLU1 and CLU2 purification. The expected result would be for it to be found in just the CLU1 purification but the cytoplasmic and nuclear isoforms are very

similar and the stress from the transient transfection may have caused some of the cytoplasmic isoform to be shuttled to the nucleus. CLU1 is also known to interact with Bcl-2 family proteins, which are checkpoint proteins involved in regulating the permeability of the outer mitochondrial membrane (122). One of the top interactors found for CLU1 was Bcl2-associated athanogene 2 (BAG2), it is not a known interactor of CLU1, but it is associated with a known interactor (Bcl2). XRCC7 or PRKDC is a DNA-activated protein kinase, which is part of the DNA repair complex with XRCC5 and XRCC6. It is not a known interactor of either of the CLU variants, but is associated based on the interaction with the rest of the complex (59). In the CLU1 and CLU2 immunopurification, 35 and 14 unique peptides were identified respectively, making it one of the number one protein matches found in the experiment. The expected result was for PRKDC to be found only in the CLU1 purification, and just as before with XRCC5 and XRCC6 it was found in both the CLU1 and CLU2 purification.

Low-density lipoprotein receptor is a widely studied protein because of its direct interaction with APOE and the implication it has on cholesterol levels in the bloodstream (64). This glycoprotein localizes to the plasma membrane and is responsible for the removal of LDL and VLDL from the bloodstream by internalizing the lipoprotein for further processing.(2) According to HPRD (106), the known interactors include: APOE, ApoB-100, Proprotein convertase PC9, HSPA5 and Platelet factor 4. APOB and HSPA5 were both found in this immunopurification. Apolipoprotein B-100 was found solely in the LDLR immunopurification and was found with 5 unique peptides. ApoB-100 is a major component of LDL particles and is responsible for the recognition of the LDL particle by LDLR (64). HSPA5 is a heat shock protein involved in the retention of LDLR at the ER during stressful conditions (100), but this protein was also found in all of the other purifications. HSPA5 is responsible for the retention of

several proteins at the ER during stress (119), and is a common background contaminant from the FLAG IP procedure (36). The SAINT algorithm did not find HSPA5 or APOB to be significant interactors and are not visible in Table 3-2. There was no known or suspected interactor found with a high number of peptides; most of the top 20 proteins matches were also found in other immunopurifications. The reason behind this may be that because LDLR is a trans-membrane protein and the interactions may have been lost during lysis and the immunipurification process due to conformational changes after removal from membrane (138).

PICALM plays an important role in clathrin-mediated endocytosis and has been studied extensively in the past few years because of many GWAS's, which have associated PICALM mutants with AD (44, 78, 102, 103). Endocytosis is vital to the uptake of nutrients, neurotransmitters, receptors and the removal of apoptotic cells (9, 229). One interesting connection between AD and PICALM exists in the fact that the amyloid precursor protein (APP) is processed following endocyctosis (9). Since PICALM affects the amount of endocytosis occurring in the cell it may be a factor in Aβ levels in the cell (151). PICALM is involved in clathrin-mediated endocytosis of the plasma membrane, it was expected to purify with adaptor proteins, clathrin, and plasma membrane related proteins (224). The known interactors for PICALM according HPRD (106) include clathrin, adaptor related protein complex 2, phospholipase c and caspase 3 and 8. In this immunopurification, several known interactors were found. They include Clathrin heavy chain, Clathrin light chain A and B and Adaptor related protein complex 2 alpha 1 subunit. Clathrin heavy chain was the number 1 hit with a Mascot score of 2081, 93 peptides matches with 38 of them being unique peptide matches. Along with the known interactors found, many possible novel interactors may have been identified. Adaptor related protein complex 2 alpha 1 subunit (AP2A1) was previously identified by

coimmunopurification and colocalization as an interactor, but no other forms of AP2 or AP1 were found to co-immunoprecipitate or colocalize in the paper (224). AP2A1 was identified as well as the alpha 2, beta 1 and AP1G1 and AP2M1 forms, all with at least 3 unique peptide matches. Clathrin interactor 1 (CLINT1) was found with 7 unique peptides, it is responsible for stimulating clathrin assembly and vesicle transport within the cell (152). Synaptosomal-associated protein, 91kDa homolog (SNAP91) or assembly protein, 180kDa only had one unique peptide match but has been previously shown to interact with several of the adaptor complex proteins and clathrin, and promotes the assembly of clathrin to the membrane and is thus very similar to PICALM based on function (228). Phosphatidylinositol-4-phosphate 3-kinase C2 domain-containing alpha polypeptide (PIK3C2A) has a role in clathrin vesicle formation and protein trafficking and may interact with CLINT1, clathrin heavy chain or SNAP91 (61). It was found with 6 unique peptides, and may be a possible interactor. Coated vesicle-associated kinase of 104 kDa (CVAK104 or SCYL2) is another related protein found. It may play a role in clathrin mediated endocytosis and transport and is known to co-immunoprecipitate with AP1 and Clathrin (21, 54). It may be another protein that PICALM recruits to the site of endocytosis. Many known and expected interactors were found in this immunopurification and exemplify the success and effectiveness of the affinity purification paired with HPLC and mass spectrometry.

Alpha-synuclein, the major constituent of Lewy bodies and studied in regard to both AD and Parkinson's disease was also purified and analyzed. The known interactors for SNCA include Aβ, beta-synuclein (SNCB), parkin, calmodulin1 and several adaptor and transport proteins (106). When visualizing the immunopurificaion on a silver stained SDS-PAGE gel, the lane for SNCA was always very clean and contained very few stained bands (usually less than 7) and resembled the empty vector control. These clean purifications resulted in only 38 proteins

being matched to the mass spectrometry data. Each time there was a very dark band at a weight of 20 kDa representing the SNCA protein. SNCA is a very small protein/peptide at 140 amino acids (68), which leaves the number of amino acids on the protein available for binding to a minimum. Only one known interactor was found in SNCA immunopurifications, SNCB. One unique peptide match was identified for SNCB; many peptide matches were shared between SNCA and SNCB because of the high sequence similarity (62%) between them. Calmodulin-like 5 (CALML5) was also matched and identified using one unique peptide, it is 51% identical to calmodulin1 and differs in length by only 3 amino acids. CALM1 is the closest homolog to CALML5 according to Basic Local Alignment Search Tool (BLAST) (http://blast.ncbi.nlm.nih.gov). The unique peptide matched 80% with calmodulin1 and was the number two match according to BLAST. No other known interactors or related proteins were found. In order to find more interactors, the stringency of the washing steps may need to be decreased so any associated proteins are not washed away before the elution step.

pCMV6-SPORT6 containing no genes in the open reading frame was transfected into the cells and used as a negative control for the experiments. If any proteins were matched from the purification of the empty vector they were most likely contaminants or background proteins which have affinity towards the agarose beads used in the purifications (36). These mostly consisted of heat shock proteins, keratin, ATPases, and signal proteins. 10 control immunopurifications were done in order to have a good base to compare to the other immunopurifications and improve the validity of the results. When visualizing the silver stained gels, the empty vector control helped with the optimization of the immunopurifications. The desired result was an empty vector lane which contained only 2 bands (the immunoglobin from the agarose beads) and the sample lanes containing as many bands as possible.

Bioinformatic analysis using the Ingenuity Pathway Analysis software:

IPA is software used to analyze, visualize and comprehend complex biological systems using the software's large knowledge base (184, 212). Mass spectrometry or SAINT data is imported into IPA. The software interprets each gene ID and completes a core analysis to investigate cellular processes, disease pathways, network analysis, downstream effect analysis and transcription factor analysis. Following analysis, the user is able to view and build possible networks and pathways, compare different datasets and find novel biological interactions for further validation. Figure 3-5 and 3-6 shows two possible pathways for PICALM and APOE incorporating existing and novel interactions found through these purifications and existing interactions from IPA's extensive database.

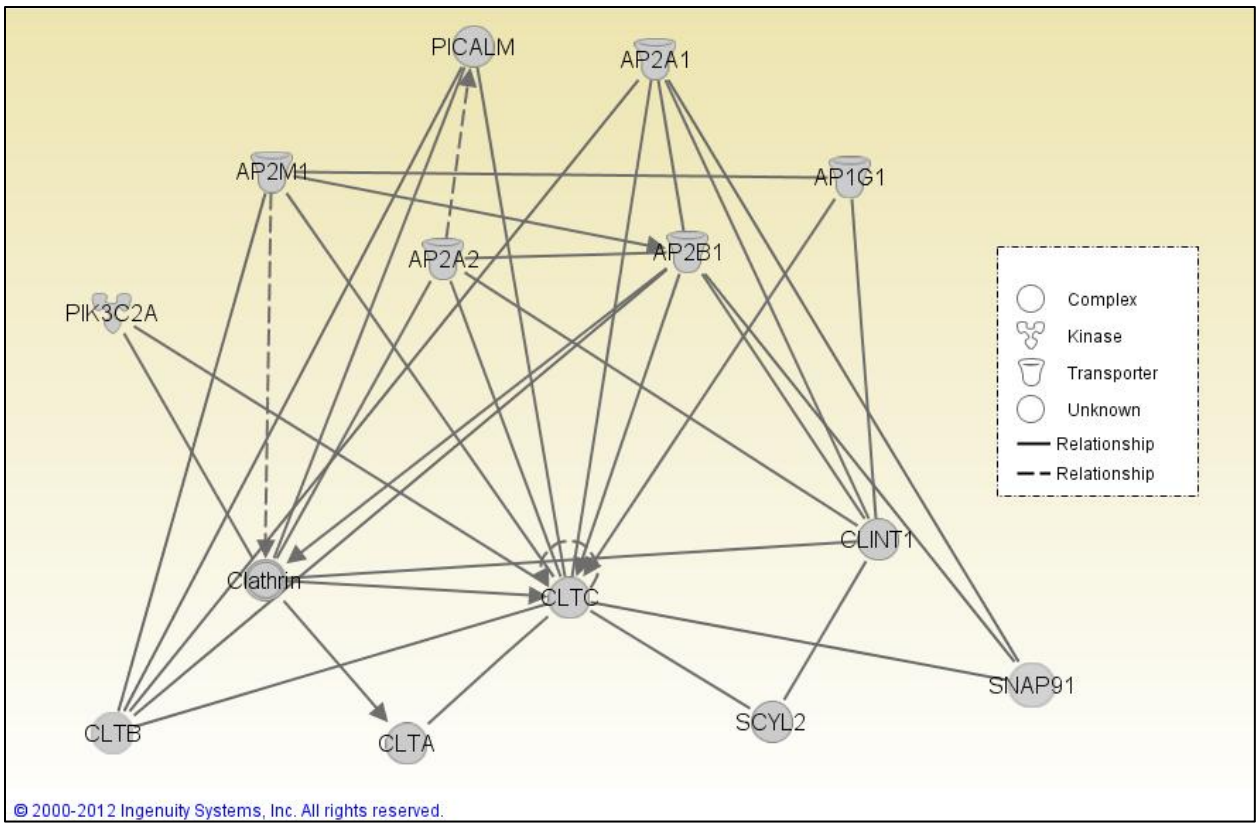
PICALM
AP2A1
AP2M1
AP1G1
AP2A2
AP2B1
PIK3C2A
Complex
Kinase
Transporter
Unknown
Relationship
Relationship
CLINT1
Clathrin
CLTC
SNAP91
CLTB
CLTA
SCYL2
© 2000-2012 Ingenuity Systems, Inc. All rights reserved.

Figure 3-5: PICALM recruits clathrin, adaptor proteins and cargo proteins to the site of endocyctosis during the early stages of the clathrin-coated vesicle cycle. Ingenuity Pathway Analysis (184, 212) was used to visualize protein-protein interactions associated with the AP-MS of PICALM. All of the proteins in the pathway were identified by the immunopurification of PICALM. The shape of each node corresponds to the protein molecular function according to Ingenuity knowledge base.

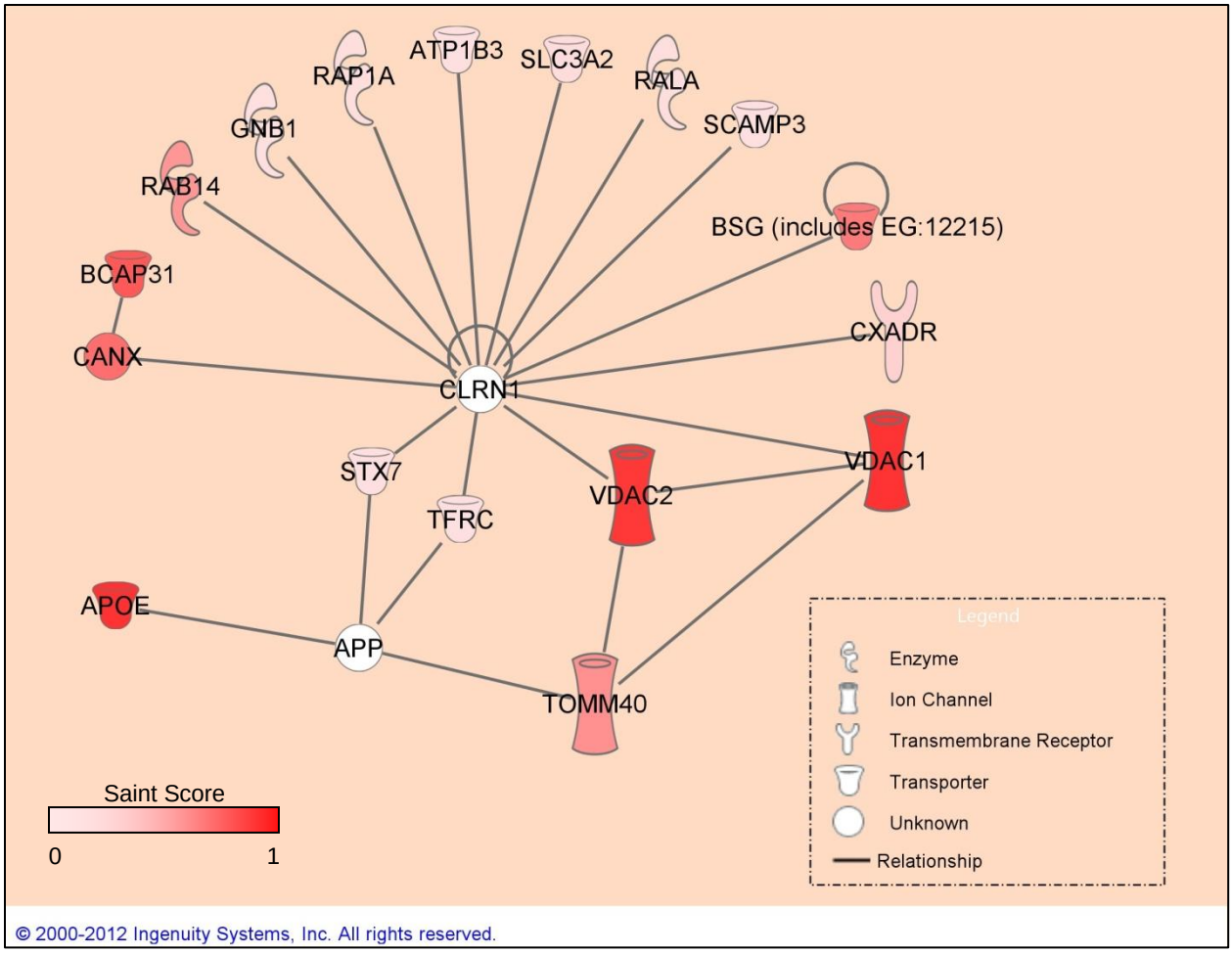

Figure 3-6: The predicted interactors of APOE based on a model where APOE is a factor in mitochondrial dysfunction and subsequent cell stress. Ingenuity Pathway Analysis (184, 212) was used to visualize protein-protein interactions associated with the AP-MS of APOE. Each red shaded protein was identified by the immunopurification of APOE, and the two white proteins are known interactors and were added to connect the pathway. The intensity of the colour of each node represents the SAINT probability score associated with the interactor. The shape of each node corresponds to the protein molecular function according to Ingenuity knowledge base. The interactions represented by a solid line indicates a direct interaction and a dashed line represents an indirect interaction.

Following analysis, several interactors were chosen for validation via co-immunopurification. CLTC (PICALM), CLINT1 (PICALM), VDAC (APOE) and TOMM40 (APOE) were chosen for further validation. CLTC was chosen because it is a known interactor of PICALM (224) and had the highest SAINT probability score (0.996). CLINT1 was chosen because it was suspected to interact with PICALM based on function and localization of both of the proteins, but no interaction between the two has been shown as of yet (151, 152). The CLINT1 was identified by 7 unique peptides and a 0.406 SAINT probability score was calculated for the interaction between CLINT1 and PICALM. Validation of the interaction between VDAC and APOE was selected because VDAC was identified with 13 unique peptide matches and 157 total peptide matches. The interaction between the two is not known, but a high SAINT score (0.542), the presence of a peptide aggregation motif on both proteins (225) and a shared involvement in Aβ aggregation and toxicity (140) hints at the possibility. TOMM40 was picked for validation because it has been found to be a risk factor for AD and is related to APOE by the regulatory elements that control the transcription of both APOE and TOMM40 (16, 176, 207). TOMM40 was also identified with 3 unique peptides and had a high SAINT score(0.292). Briefly, the immunopurifications of empty vector control, APOE or PICALM were completed as described above and loaded onto SDS-PAGE gels. The gels were transferred to a nitrocellulose membrane and exposed to one of the four antibodies, respectively. This is an essential step in the verification of the interaction. All four proteins tested by co-immunopurification were successfully probed by the antibody of the suspected interactor. Figure 3-7 shows the results of the four co-immunopurification experiments.

Loading control experiments were attempted using an antibody for actin, but it proved to be unsuccessful because the amount of actin differed between different purifications because actin interacts/associates differently with each protein. (Figure 3-8) Actin was also tested on the cell lysates before the purifications were completed to ensure that an equal amount of protein was used. (Figure 3-9)

A

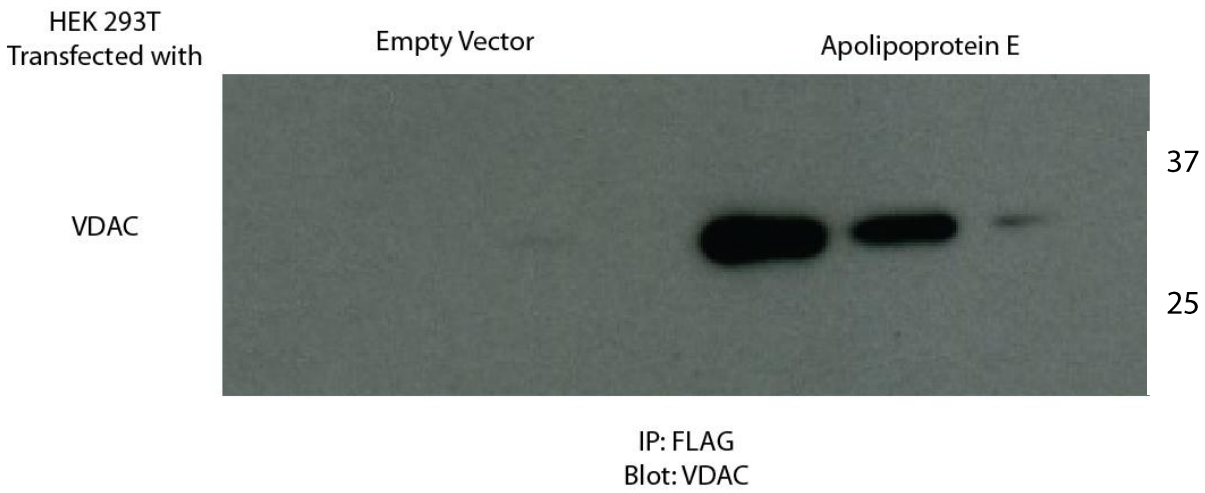
HEK 293T
Transfected with
Empty Vector
Apolipoprotein E
VDAC
37
25
IP: FLAG
Blot: VDAC

B

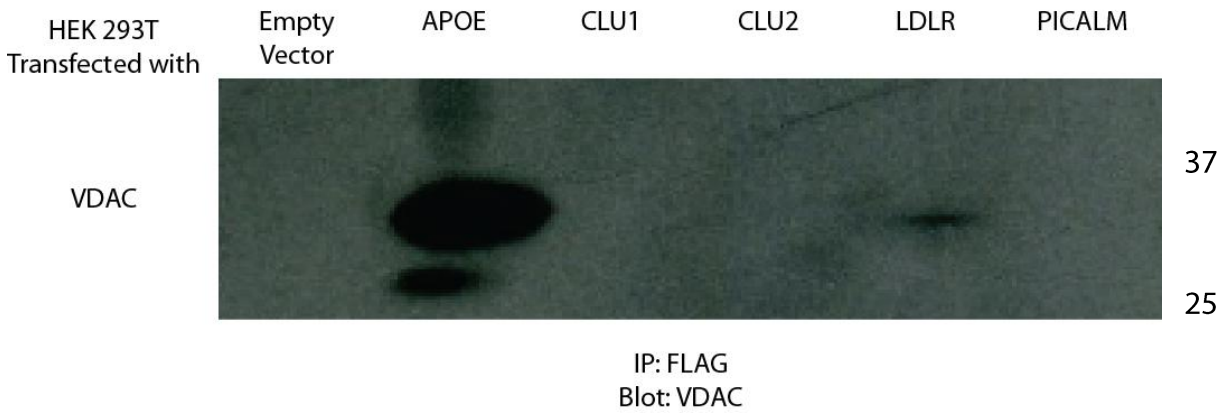
HEK 293T
Transfected with
Empty Vector
APOE
CLU1
CLU2
LDLR
PICALM
VDAC
37
25
IP: FLAG
Blot: VDAC

C

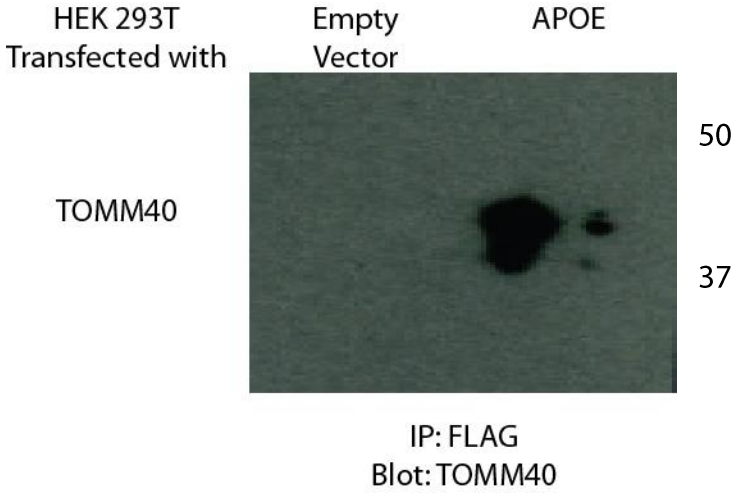
HEK 293T
Transfected with
Empty
Vector
APOE
TOMM40
50
37
IP: FLAG
Blot: TOMM40

D

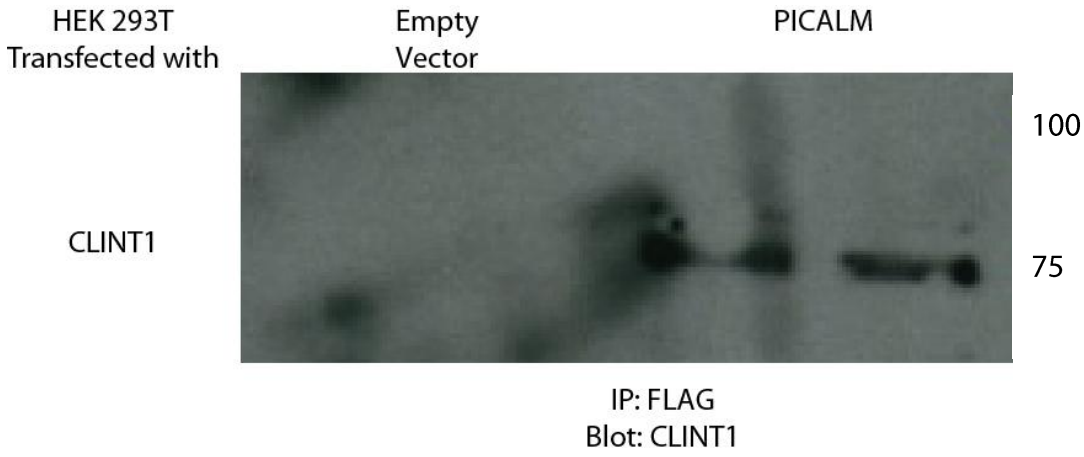
HEK 293T
Transfected with
Empty
Vector
PICALM
CLINT1
100
75
IP: FLAG
Blot: CLINT1

E

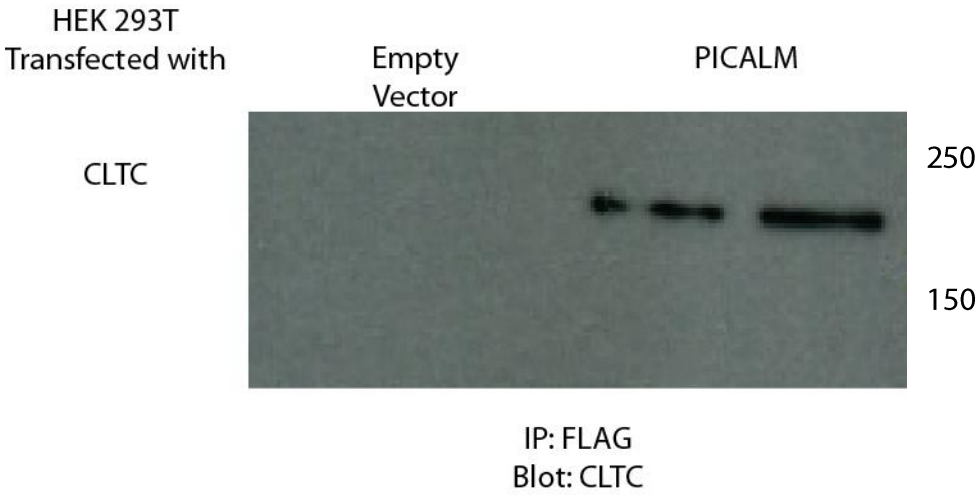
HEK 293T
Transfected with
Empty
Vector
PICALM
CLTC
250
150
IP: FLAG
Blot: CLTC

Figure 3-7: Co-immunopurification validation of interactors identified by mass spectrometry analysis. HEK 293T cells were transfected with one of six tagged AD genes studied (APOE, CLU1, CLU2, LDLR, PICALM and SNCA) or the negative control, which is the empty vector (pCMV-Entry). The cell lysates were immunopurified, separated by SDS-PAGE, and transferred to nitrocellulose membranes for Western blot (WB) analysis against the antibodies of the predicted interactors. (A) In triplicate, cells were transfected with empty vector or APOE, were immunopurified and tested for the expression of VDAC. (B) Cells were transfected with the empty vector and each of the six tagged AD genes, immunopurified and tested for the expression of VDAC (C) Cells were transfected with empty vector or APOE, immunopurified and tested for the expression of TOMM40. (D) In duplicate, cells were transfected with empty vector or PICALM, immunopurified and tested for the expression of CLINT1. (E) In duplicate, cells were transfected with empty vector or PICALM, immunopurified and tested for the expression of CLTC. Expected sizes of validated proteins: VDAC:30 kDa; CLINT1:70 kDa; CLTC:190 kDa; TOMM40:38 kDa.

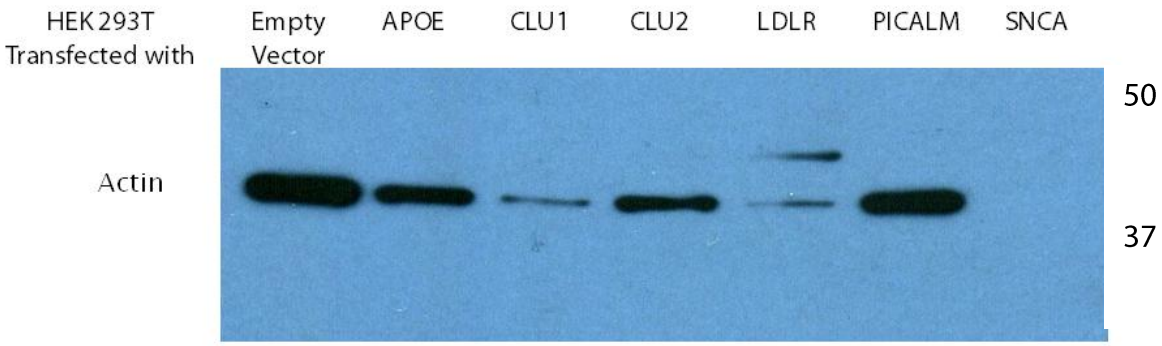
HEK 293T
Transfected with
Empty
Vector
APOE
CLU1
CLU2
LDLR
PICALM
SNCA
Actin
50
37

Figure 3-8: Western blot (WB) testing for actin following immunopurificationof FLAG-tagged recombinant proteins. HEK 293T cells were transfected with one of six tagged AD genes studied (APOE, CLU1, CLU2, LDLR, PICALM and SNCA) or the negative control, which is the empty vector (pCMV-Entry). The lysates were immunopurified using FLAG-coupled agarose beads and 5% of the elution was seperated by SDS-PAGE, and transferred to nitrocellulose membranes for WB analysis against the Actin antibody. Following immunopurification, the amount of actin varies between each gene studied.

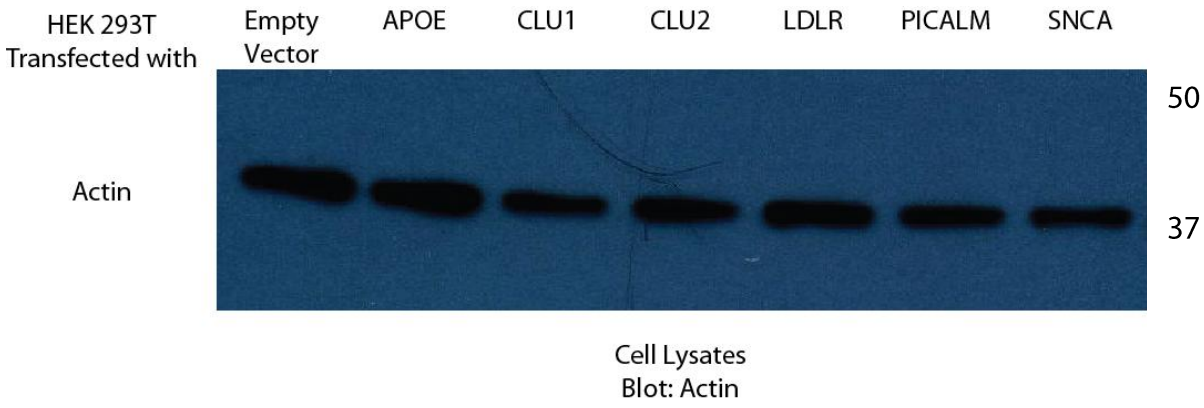
HEK 293T
Transfected with
Empty Vector
APOE
CLU1
CLU2
LDLR
PICALM
SNCA
Actin
50
37
Cell Lysates
Blot: Actin

Figure 3-9: Loading control used to ensure equal quantity of protein used in each immunopurification experiment. HEK 293T cells were transfected with one of six tagged AD genes studied (APOE, CLU1, CLU2, LDLR, PICALM and SNCA) or the negative control, which is the empty vector (pCMV-Entry). 30 ug of each cell lysate is loaded and separated by SDS-PAGE electrophoresis, transferred to a nitrocellulose membrane and exposed to anti-actin.

The Purification and Analysis of the Platelet Activating Factor Receptor

Vector Preparation and Transfection

In order to prepare a tagged recombinant platelet activating factor receptor (PAFR) protein, the PAFR was purchased in a Gateway compatible vector and shuttled into a Gateway destination vector containing the FLAG tag. Each shuttle reaction was verified by a restriction digest using the BsrGI restriction enzyme, which cuts at the *att* sites of the gateway vectors. The *att* sites flank the outside of the gene and BsrGI rarely digests to regions other than the *att* sites (234). The results of the restriction digests done on gateway vectors are shown below in figure 3-10. The PAFR tagged vectors were transfected into HEK 293T cells using PEI and harvested 48 hours later. The cell lysates were tested for PAFR expression using the FLAG antibody, and figure 3-11 shows some of the results. The PAFR protein seems to aggregate at the top of the gel, and was not able to enter the gel and segregate to the expected and appropriate molecular weight. Many adjustments were made to improve the expression including changing the gel ingredients and percentage of acrylamide, using a pre-cast gradient gel instead of a lab-made gel, changing the loading buffer, changing the lysis buffer and altering the concentration of protein. After all the changes, not much improvement was made to the PAFR expression. The PAFR gene in the expression vector was sequenced as well to verify that the correct gene was being transfected. Instead of continuing to troubleshoot, a different construct was purchased from Origene. The construct was ready-to-use in an expression vector containing the DDK tag, which has exactly the same sequence as the FLAG tag. The construct was also tested by restriction digest to ensure the gene and vector are the correct size. The restriction digest was done using EcoRI and EcoRV. The results of the restriction digest are shown in figure 3-12.

A.

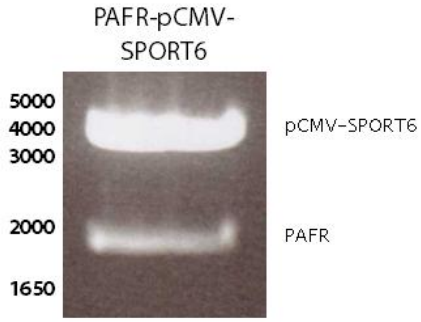
PAFR-pCMV-
SPORT6
5000
4000
3000
2000
1650
pCMV-SPORT6
PAFR

B.

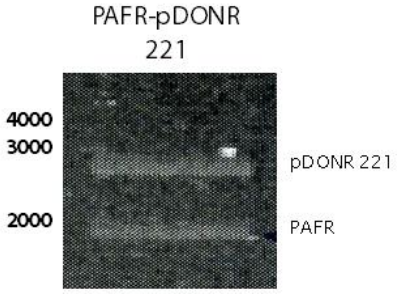
PAFR-pDONR
221
4000
3000
2000
pDONR 221
PAFR

C.

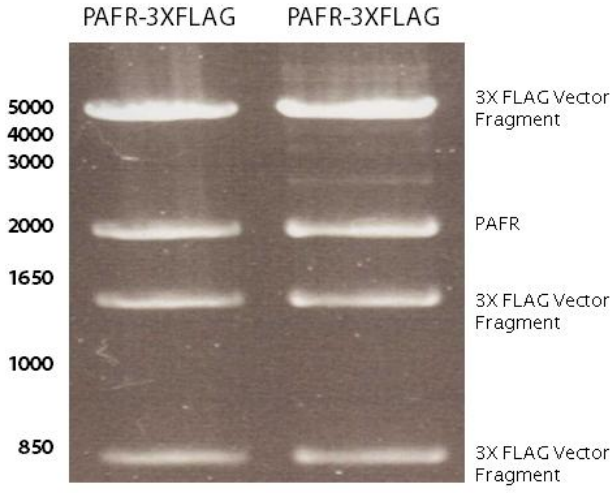
PAFR-3XFLAG
PAFR-3XFLAG
5000
4000
3000
2000
1650
1000
850
3X FLAG Vector
Fragment
PAFR
3X FLAG Vector
Fragment
3X FLAG Vector
Fragment

Figure 3-10: Restriction digest of PAFR in gateway expression vectors. Each recombinant vector was digested by BsRGI restriction endonuclease, which cuts at the attL and attB sites of gateway vectors. The sizes of the fragments were compared to a molecular weight standard to infer that PAFR (1822 bp) was contained in the correct vector. The DNA was digested for 1 hour and 30 minutes at 37°C. The digestion was analyzed on a 1% agarose gel pre-stained with 0.01 ug/ml of ethidium bromide and examined under UV light. (A) The digestion of PAFR in pCMV-SPORT6 expression vector. Expected Sizes: 4396 and 1822 bp. (B) The digestion of PAFR in pDONR 221 entry vector. Expected Sizes: 2388 and 1822 bp. (C) The digestion of PAFR in 3X-FLAG expression vector. Expected Sizes: 4.2, 1.8, 1.3 and 0.65 Kb.

A.

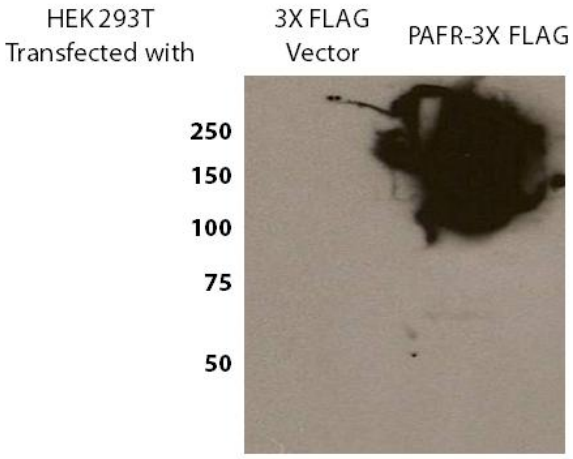
HEK 293T
Transfected with
3X FLAG
Vector
PAFR-3X FLAG
250
150
100
75
50

B.

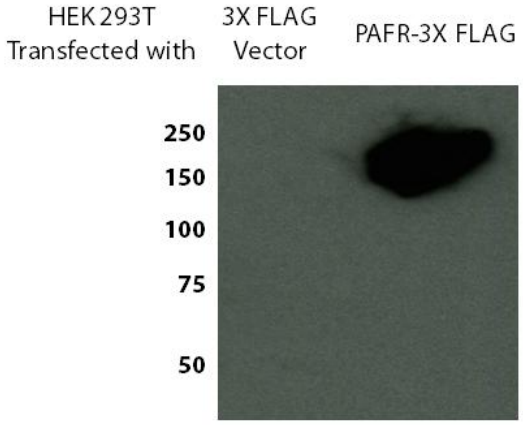
HEK 293T
Transfected with
3X FLAG
Vector
PAFR-3X FLAG
250
150
100
75
50

Figure 3-11: Western blot (WB) validation of expression of FLAG-tagged PAFR in 3X FLAG expression vector. HEK 293T cells were transfected with PAFR-3XFLAG or the negative control, which is the empty vector (3XFLAG-Entry). Varying amounts of the cell lysate were separated by SDS-PAGE, and transferred to nitrocellulose membranes for WB analysis against the FLAG antibody. (A) 1.5 ug/uL of protein was loaded in a buffer containing 2% (w/v) SDS. An aggregated clump of protein appears at the top of the gel. (B) 0.75 ug/uL of protein was loaded in a buffer containing 2% (w/v) SDS. An aggregated clump of protein also appears at the top of the gel. Expected size of PAFR: 39 kDa.

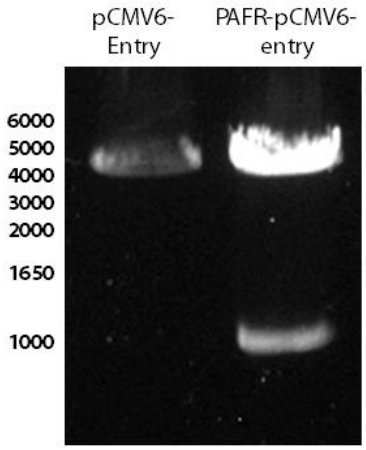
pCMV6-
Entry
PAFR-pCMV6-
entry
6000
5000
4000
3000
2000
1650
1000

Figure 3-12: Restriction digest of PAFR in pCMV6 entry vector. The recombinant vector was digested by EcoRI and RcoRV restriction endonucleases, The endonucleases cut the expression vector at the multiple cloning sites at the 3' and 5' end resulting in a 4900 bp fragment. The other fragment represents the PAFR gene (1029 bp). The DNA was digested for 1 hour and 30 minutes at 37°C. The digestion was analyzed on a 1% agarose gel pre-stained with 0.01 ug/ml of ethidium bromide and examined under UV light. Expected size of fragments: 4900 and 1029 bp.

The construct from Origene still required some troubleshooting, but after some optimization of the concentration and loading buffer strength, expression was successfully visible. Figure 3-13 shows the results of several PAFR lysates expression testing using different concentrations and lysis buffers. An interesting finding from the western blots was that a band is seen in each blot at ~75 kDa. The band may represent a modification to PAFR such as forming a dimer, glycosylation or some other post translational modification. No tests were done to test these possibilities, but a paper by Jonathan A. Javitch has shown that G-protein coupled receptors commonly form dimers (96).

A.

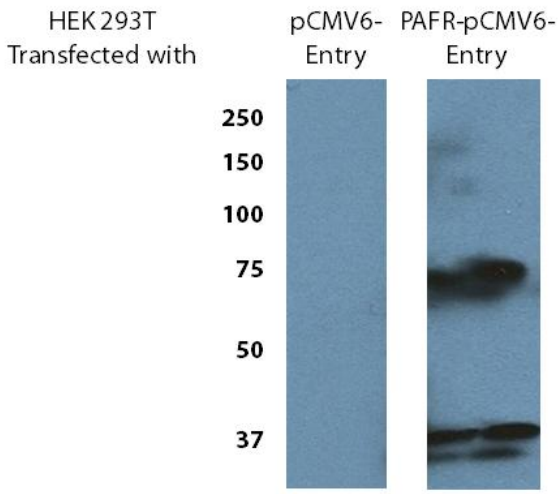
HEK 293T
Transfected with
pCMV6-
Entry
PAFR-pCMV6-
Entry
250
150
100
75
50
37

B.

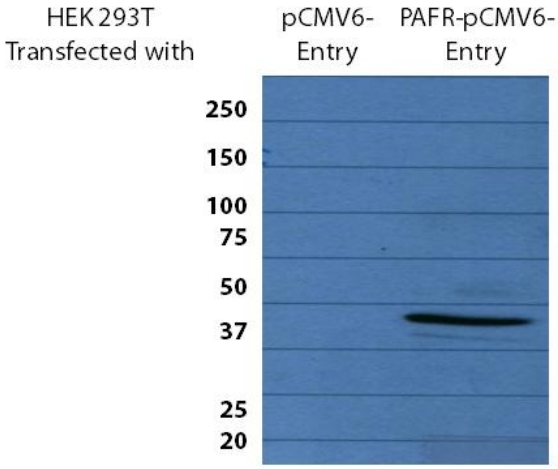
HEK 293T
Transfected with
pCMV6-
Entry
PAFR-pCMV6-
Entry
250
150
100
75
50
37
25
20

Figure 3-13: Western blot (WB) validation of expression of FLAG-tagged PAFR in pCMV6 entry. HEK 293T cells were transfected with PAFR-pCMV6-entry or the negative control, which is the empty vector (pCMV6-Entry). Varying amounts of the cell lysate were separated by SDS-PAGE, and transferred to nitrocellulose membranes for WB analysis against the FLAG antibody. (A) 0.5 ug/uL of protein was loaded in a buffer containing 2% (w/v) SDS. A band at the correct molecular weight (~39 kDa) appears as well as a band at ~75 kDa. (C) 0.25 ug/uL of protein was loaded in a buffer containing 10% (w/v) SDS. All protein resolved to the correct molecular weight (~39 kDa).

Immunopurifications of PAFR

PAFR was successfully transfected and expressed in HEK 293T cells. Looking at past research, only one publication has successfully transfected and expressed PAFR (22, 166). Previous members in this lab had also attempted PAFR transfection and expression without success. The next step was to purify PAFR using FLAG-coupled agarose beads and uncover any interactors. More problems and issues with the immunopurifications were found. The eluted proteins were run on an SDS-PAGE gel and silver stained and compared to a control purification of cells that were transfected with the same vector as PAFR except that it contained no genes. The PAFR lane and control lane appeared to be exactly the same according to the silver stain. The immunopurifications may not have been successful or PAFR may not have been entering the gel. 10% of the eluted proteins were reserved for western blots and were tested for the FLAG tag. The FLAG tag was present in the purification according to the western blots; some problem was occurring in which PAFR was not visible on the silver stained gel. (Figure 3-14A) Even if the protein is present in the western blot, not enough was purified to be visible on the silver stained gel and continue with digestion and mass spectrometry analysis. It is imperative when doing immunopurifications that the most prominent protein found is the bait protein. It cannot be concluded that the proteins present on the gel are actually interactors and not background contamination.

The first attempt to fix the problem was done by scaling up the purifications. Instead of using 1 mg of PAFR in 1 mL of lysis buffer with 60 uL of agarose beads, 3 tubes of the same amounts were used and the eluted proteins were combined into one tube once the purification was completed. The same was done for the empty vector control transfected cells. This proved to

be unsuccessful; there was no difference between PAFR and control in the silver stain gel. The second attempt involved using more protein and more beads in a larger volume and keeping the same ratio as before. This also proved to be unsuccessful. Other changes were made to protein concentrations as it worked well to improve the results of the expression testing earlier, but the immunopurification was still unsuccessful. The PAFR protein may not have been able to separate from the membrane and stronger detergents were needed in the lysis buffer. Three non-ionic detergents, Nonidet P40 substitute (NP-40), Triton X-100, and Tween 20, were experimented with and the immunopurifications were repeated. (Figure 3-14B) Non-ionic detertgents helps stabilize proteins in their native conformations and prevent aggregation. They are effective in the solubilization of membrane proteins especially when used in 2-dimensional electrophoresis (37). NP-40, or octyl phenoxylpolyethoxylethanol, is a commonly used detergent in the lysis of cells (79, 84, 198). An increased concentration of NP-40 (2.5% v/v) was used in the buffer because NP-40 has been successfully used in the purification of other G-protein coupled receptors (45) and a lower concentration was successful used in the immunopurification APOE, LDLR, CLU1, CLU2, PICALM and SNCA. Triton X-100, a polyethylene oxide surfactant, was used in the lysis buffer because it is an effective and commonly used detergent in the analysis of membrane fractions (11, 199). Tween-20, also known as polyethylene glycol sorbitan monolaurate, is a milder surfactant effective in the separation of membrane bound proteins (41, 86, 199). Other commonly used detergents in the extraction of membrane bound proteins such as CHAPS (3-[(3-cholamidopropyl)dimethylammonio]-1-propanesulfonate) and SDS (Sodium dodecyl sulfate) were not used because of the effect it would have on the ability of the FLAG antibody to bind to FLAG-tagged proteins (23). Success was found with a lysis buffer

containing a higher concentration NP-40 at 2.5%. The results comparing the different buffers are shown in figure 3-14.

A

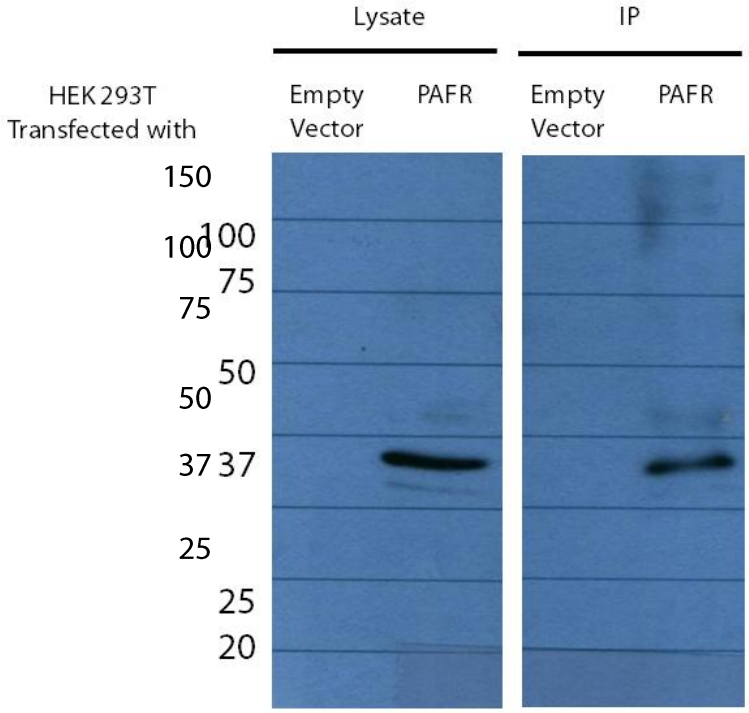
Lysate
IP
HEK 293T
Transfected with
Empty Vector
PAFR
Empty Vector
PAFR
150
100
100
75
75
50
50
37
37
25
25
20

B

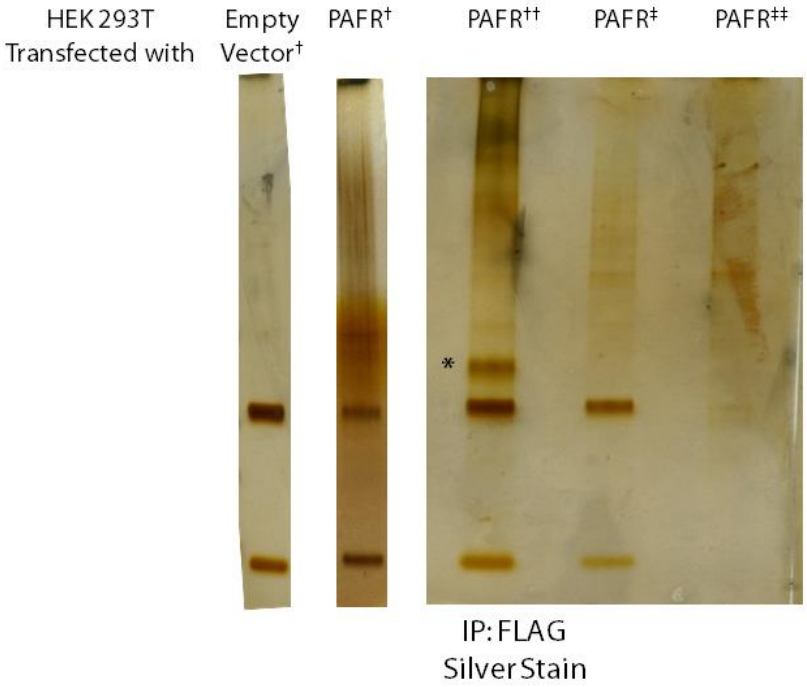
HEK 293T
Transfected with
Empty Vector†
PAFR†
PAFR††
PAFR‡
PAFR‡‡
*
IP: FLAG
Silver Stain

Figure 3-14: Comparison of different lysis bufferes in the immunopurification of FLAG-tagged PAFR in HEK 293T cells. (A) HEK 293T cells were transfected with PAFR-pCMV6-entry or the negative control, which is the empty vector (pCMV6-Entry). 2.5 ug at 0.25 ug/uL of protein was loaded in a buffer containing 10% (w/v) SDS for the lysate. The IP lanes contain 10% of the FLAG IP elution. PAFR resolved to the correct molecular weight (~39 kDa). (B)All of the immunopurifications of PAFR in this gel were performed in exactly the same way, except a different lysis buffer was used in each one. (*) was added beside bands of the bait protein. Lysis buffers were composed of 50 mM Tris-Cl pH 7.5, 100 mM NaCl, 5 mM EDTA, 1 one complete mini EDTA-free tablet (Hoffmann-La Roche Limited, Mississauga, ON) and a varying composition of detergent.

† 0.4% (v/v) NP-40
†† 2.5% (v/v) NP-40
‡ 4% (v/v) Triton X-100
‡‡ 4%Triton X-100 (v/v) and 4% (v/v) Tween-20

In-Gel Digestion and Mass Spectrometry

The optimal lysis buffer was used with the immunopurification protocol to immunopurify the FLAG tagged PAFR protein and empty vector control. Briefly, the proteins in complex with PAFR and the empty vector were immunopurified and were separated by SDS-PAGE gel electrophoresis followed by visualization by silver staining. (Figure 3-15) As well, 10% (v/v) of the purified protein complex was used for western blot analysis to test the efficiency and specificity of the immunopurification. After silver staining, gel bands were excised from the gel and digested with trypsin. The resulting peptides were then analyzed by mass spectrometry.

Seven bands each from PAFR and the control were analyzed by HPLC-ESI-MS/MS generating 90 thousand MS/MS spectra. The MS/MS spectra are annotated by Mascot, a software which performs sequence database searches against the FASTA protein sequence database using the generated MS/MS spectra (172). The software returns the most probable peptide sequence and uses them to compute the most probable full length proteins.
Mascot assigns a score to each protein match based on a probabilistic model that calculates the probability that a certain spectra produced by a peptide was produced by the actual peptide or could have just been produced by chance; a higher score represents a higher probability of a protein match (172). Prohits (133) was used to organize the protein matches into tables and remove common contaminants such as keratin, albumin and ribosomal proteins and to refine the list of protein matches to the matches which received a mascot score higher than 30, contained a unique peptide sequence match and within the a 0.01 p-value threshold. Table 3-3 shows the results of the database searching using Mascot. PAFR was found with three unique peptides, which according to literary research was the first time this protein has been identified using a

mass spectrometer. However the protein was not a top hit, and 10 proteins were found with more unique peptides than PAFR.

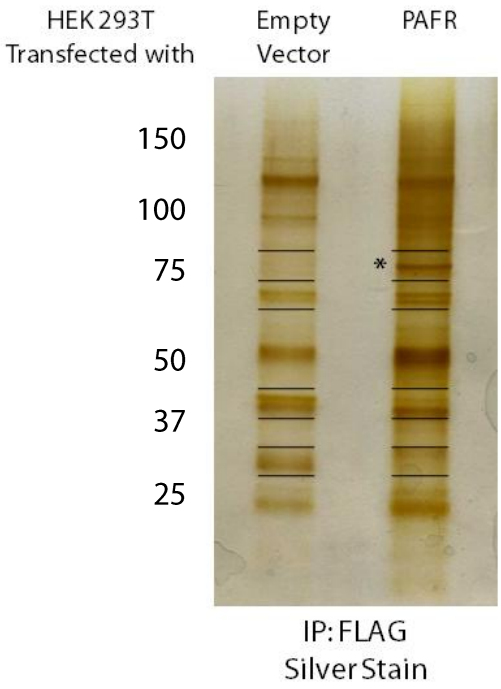
HEK 293T
Transfected with
Empty
Vector
PAFR
150
100
75
50
37
25
*
IP: FLAG
Silver Stain

Figure 3-15: Silver-stained gel obtained from the immunopurification of FLAG-tagged PAFR, the empty vector control and their interaction partners from HEK 293T cells. The gel was digested with trypsin using the in-gel digestion protocol and the resulting peptides were analyzed by mass spectrometry. The lines over top of the gel show where the cuts were made to increase the efficiency of the digestion and sequester protein of similar molecular weight together. (*) was added beside the band of the bait protein.

Table 3-3: The results of the in-gel digestion of cells transfected with the either tagged PAFR or the negative control, which is the empty vector (pCMV-Entry). Hit Gene Name: the name of the gene matched to the peptides by Mascot; Hit Protein ID: protein identifier from GI database; Hit Score: Mascot probability score associated with the protein match; Peptide Number: total number of peptide sequences matched to the protein; Unique Peptide Number: number of unique peptide sequences matched to the protein; Coverage: the percentage of amino acids matched to protein. Rows highlighted in red are bait proteins. Also shown in Appendix 3-1

PAFR

Hit Gene Name	Hit Protein ID	Hit Score	Peptide Number	Unique Peptide Number	Coverage (%)
HSPA8	5729877	699	24	13	25.9
CANX	10716563	350	13	7	12.8
PABPC1	46367787	305	10	7	13.8
HSPA1B	167466173	292	9	6	13.1
PRMT5	20070220	337	8	5	12.7
PSMD13	157502193	310	8	6	17.6
HSPA9	24234688	309	8	5	11.5
XRCC6	4503841	212	7	4	9.5
IGF2BP1	56237027	198	7	4	9.7
WDR77	13129110	182	6	3	13.5
HNRNPA1	4504445	202	5	3	15.3
SRPRB	284795266	192	5	4	24
PAFR	4506241	149	5	3	12.3
GET4	38570062	179	4	3	11.6
RPN1	4506675	168	4	3	6.6
MAP3K7	4507361	164	4	3	6.7
GAPDH	7669492	159	4	3	12.8
C1QBP	4502491	156	4	3	15.6
312922364	312922364	139	4	4	13.5
PSMA1	4506179	136	4	3	11
HIST1H1C	4885375	135	4	2	9.4
PCNA	4505641	117	4	3	16.5
PSMA7	4506189	112	4	3	14.1
NSF	156564401	84	4	2	3.6
PSMD6	7661914	119	3	3	8.5
YWHAG	21464101	110	3	1	9.7
TIMM50	48526509	109	3	2	5.9
XRCC5	10863945	107	3	2	2.7
CAPZA1	5453597	106	3	2	9.1
KCTD17	169234778	103	3	2	9.1

RNF126	37622894	101	3	2	7.1
HNRPDL	14110407	87	3	2	6.2
DNAJB1	5453690	118	2	2	9.1
YWHAQ	5803227	112	2	2	9.8
PSMD8	156631005	105	2	2	6.3
TRAFD1	5729828	91	2	1	2.1

Empty Vector

Hit Gene Name	Hit Protein ID	Hit Score	Peptide Number	Unique Peptide Number	Coverage (%)
PRMT5	20070220	665	21	12	22.6
WDR77	13129110	377	10	5	22.8
HSPA1B	167466173	233	6	4	8.4
HNRNPA1	4504445	168	4	3	13.4
KCTD5	9506651	173	4	3	20.9
HBA2	4504345	138	4	2	19
RPN1	4506675	75	2	2	4
PRPS1	4506127	68	2	2	8.8
U2AF1	5803207	58	2	1	5.4
STATH	4507261	139	2	2	54.8
DCD	16751921	68	2	1	10
GAPDH	7669492	53	1	1	4.2
PABPC4	4504715	51	1	1	1.7
SNRPA	4759156	60	1	1	3.5

Some PAFR may be lost while running the proteins through the gel and digesting them while in the gel, to answer this problem an in-solution digestion protocol was used on the proteins following an immunopurification. The peptides were analyzed by HPLC-ESI-MS/MS generating 35 thousand MS/MS spectra. The MS/MS spectra are annotated and searched against FASTA protein database by Mascot and organized and processed by Prohits (133). The results of the database searching and processing is shown in Table 3-4. PAFR was identified, but was not the number one hit and it cannot be justified that the other proteins identified are interactors and not background.

Table 3-4: The results of the in-solution digestion of cells transfected with the either tagged PAFR or the negative control, which is the empty vector (pCMV-Entry). Hit Gene Name: the name of the gene matched to the peptides by Mascot; Hit Protein ID: protein identifier from GI database; Hit Score: Mascot probability score associated with the protein match; Peptide Number: total number of peptide sequences matched to the protein; Unique Peptide Number: number of unique peptide sequences matched to the protein; Coverage: the percentage of amino acids matched to protein. Rows highlighted in red are bait proteins; rows highlighted in yellow are suspected interactors. Also shown in Appendix 3-1.

PAFR

Hit Gene Name	Hit Protein ID	Hit Score	Peptide Number	Unique Peptide Number	Coverage (%)
HIST1H1C	4885375	210	33	4	21.1
PAFR	4506241	70	15	1	6.4
HNRNPU	14141161	93	8	2	4.1
ATP1A1	21361181	113	6	2	2.8
PHB	4505773	91	6	2	9.9
SLC25A5	156071459	80	6	1	4.4
CALML5	223278387	78	5	1	15.8
LDHA	5031857	76	5	2	4.8
KIF11	13699824	50	4	1	1.3
HNRNPK	14165435	39	4	1	4.1
HSP90AB1	20149594	78	3	2	3.6
NCL	55956788	76	3	2	3
GNB2L1	5174447	60	3	1	3.8
ATP5A1	4757810	52	3	1	2.2
ENO1	4503571	41	3	1	3
RAN	5453555	38	3	1	5.1
LDHB	4557032	73	2	1	4.8
HSPA8	5729877	51	2	1	1.9
RPS27A	4506713	39	2	1	10.3
KCTD5	9506651	54	1	1	5.1
PCYT1A	31543385	45	1	1	1.9
YBX1	34098946	44	1	1	5.2
HNRNPR	5031755	42	1	1	2.1
PABPC5	18201888	42	1	1	2.4
DDX50	13129006	38	1	1	2
EIF3A	4503509	37	1	1	0.9
KPNB1	19923142	36	1	1	1.4
HNRNPH1	5031753	35	1	1	3.6
DDX5	4758138	35	1	1	2
THOC4	238776833	31	1	1	6.8

Empty Control

Hit Gene Name	Hit Protein ID	Hit Score	Peptide Number	Unique Peptide Number	Coverage (%)
DCD	16751921	47	10	1	12.7
HIST2H4A	4504301	50	5	1	9.7
HIST1H2AG	4504239	92	3	2	21.5
DSP	58530840	42	3	1	0.3
CALML5	223278387	54	1	1	15.8
HNRNPD	14110414	41	1	1	4.6
HNRNPAB	55956919	39	1	1	4.2
STAR	56243551	34	1	1	2.8
HIST1H2BC	4504257	33	1	1	7.1
VEPH1	269847546	31	1	1	0.8

In another attempt to increase the number of unique peptides found from mass spectrometry and make it a number 1 hit, a membrane isolation preparation was done coupled with immunopurification and filter-assisted sample preparation/digestion(FASP) (239). The membrane preparation protocol was taken from a paper by a lab colleague (251), and the FASP protocol was taken from a paper out of the lab of Dr. Matthias Mann (239). The membrane preparation increases the percentage of membrane proteins and membrane bound proteins in the lysate. In Dr. Hu Zhou's paper many membrane proteins not normally detected or identified were found by mass spectrometry. This proved especially valuable with regard to proteins with several transmembrane domains such as PAFR, which like other G-protein coupled receptors has 7 transmembrane domains (93). FASP allows proteins to be digested with a higher efficiency and bypass the gel which restricts the amount of membrane bound proteins to enter (251). After the digest with FASP and desalting using C18 SepBak columns, the peptides were loaded onto the mass spectrometer for analysis. The results of the Mascot database searching are shown in table 3-5. PAFR was identified but was not the number one protein found based on Mascot score or number of peptides matches. One highlight from the experiment was that the membrane isolation protocol was successful. To investigate the changes, protein matches were analyzed by Cytoscape and Biological Networks Gene Ontology tool (BiNGO) (134). BiNGO found that in the membrane isolated samples, 35.6% of proteins matches were plasma membrane proteins with a p-value of 1.7×10^{-11} and 16.2% of cytoplasmic membrane proteins with a p-value of 2.8×10^{-24}. In the samples digested using the in-gel digestion method, there were 9.7% cytoplasmic membrane proteins with a p-value of 4.4×10^{-16} and no significant amount of plasma membrane proteins found using a p-value of 0.99. The samples digested using the in-solution digestion method found 10.2% cytoplasmic membrane proteins with a p-value of 3.5×10^{-5} and no

significant amount of plasma membrane proteins found using a p-value of 0.99. A second analysis was done using Database for Annotation, Visualization and Integrated Discovery (DAVID) (90). DAVID found that the membrane isolated samples contained 37.1% plasma membrane proteins and 64.8% membrane proteins. The in-gel digested samples contained 42.5% membrane proteins and not a significant amount of plasma membrane proteins using a p-value of 0.99. The in-solution samples contained 17.7% of plasma membrane proteins and not a significant amount of membrane proteins using a p-value of 0.99.

Table 3-5: The results of the in-solution digestion of cells transfected with the either tagged PAFR or the negative control, which is the empty vector (pCMV-Entry) following a membrane isolation protocol. Hit Gene Name: the name of the gene matched to the peptides by Mascot; Hit Protein ID: protein identifier from GI database; Hit Score: Mascot probability score associated with the protein match; Peptide Number: total number of peptide sequences matched to the protein; Unique Peptide Number: number of unique peptide sequences matched to the protein; Coverage: the percentage of amino acids matched to protein. Rows highlighted in red are bait proteins; rows highlighted in yellow are suspected interactors; rows in blue are proteins known to be associated to the plasma membrane or membrane bound vesicle according to DAVID (90). Also shown in Appendix 3-1.

PTAFR

Hit Gene Name	Hit Protein ID	Hit Score	Peptide Number	Unique Peptide Number	Coverage (%)
ATP1A1	237681111	1422	139	18	24.7
ATP1A3	22748667	737	59	1	11.3
SLC3A2	61744477	778	50	12	25.2
RAB7A	34147513	630	48	10	57.5
IRS4	4504733	714	45	14	16.5
HIST2H4A	4504301	171	40	3	29.1
TFRC	189458817	813	37	15	24.1
CANX	10716563	480	35	8	15.4
MAP1B	153945728	416	35	8	4.7
BSG	38372919	190	33	3	10.9
TF	4557871	110	31	2	3.6
HSPA5	16507237	804	30	13	21.4
VDAC1	4507879	397	30	6	33.9
HSP90B1	4507677	467	28	9	12.3
LRRC59	40254924	436	28	7	29.3
ATP2B4	48255957	480	27	9	11.4
VDAC3	25188179	391	26	4	28.6
ATP2A2	4502285	621	24	10	13.1
RAB8B	7706563	194	23	2	17.4
SLC25A5	156071459	367	20	6	25.5
RAB14	19923483	331	20	6	35.3
MAP2	87578396	268	20	5	4.1
ATP2B1	48255947	334	19	2	6.6
HLAB	310114942	282	19	4	15
PTAFR	4506241	73	19	1	6.4
RPN1	4506675	474	18	8	15.7
FLOT2	94538362	491	17	7	21.5

ATP1B3	4502281	262	17	4	20.8
CYB5R3	4503327	174	16	3	14
DSG2	116534898	374	15	6	8.9
ESYT1	14149680	372	15	6	7.6
VDAC2	42476281	256	15	5	26.2
SLC1A5	223468564	128	15	2	10.2
CLTC	4758012	383	14	8	5.8
DDX21	50659095	333	14	6	10.2
RAB5C	41393545	258	14	4	25.5
RAB4A	19923260	145	14	2	15.6
SLC12A7	123701900	56	13	1	0.6
CKAP4	19920317	253	13	5	10.5
GNAI3	5729850	243	13	4	15.5
HLA-B	17986001	231	13	4	17.4
RAB2A	4506365	340	12	6	35.8
PDIA4	4758304	318	12	6	11.9
PTPRF	109633039	246	12	5	3.9
GNAI2	4504041	236	12	2	15.5
CALR	4757900	189	12	3	11.8
RAB6A	19923231	178	12	2	16.3
DDOST	20070197	314	11	6	14

Empty Control

Hit Gene Name	Hit Protein ID	Hit Score	Peptide Number	Unique Peptide Number	Coverage (%)
ATP1A1	21361181	1797	114	28	34
IRS4	4504733	907	48	17	18.6
HSPA5	16507237	780	34	13	29.5
ATP2A2	4502285	649	29	12	15.1
HSP90B1	4507677	556	26	11	15.1
ATP2B1	48255945	490	28	9	10.7
ATP2B4	48255957	488	27	4	9.9
SLC1A5	5032093	463	24	7	22
CKAP4	19920317	455	17	9	21.6
TFRC	189458817	454	19	9	14.2
MAP2	87578396	437	25	9	7.2
SLC3A2	61744477	394	18	7	14.7
RPN1	4506675	389	15	9	17.3
ATP1A3	22748667	320	21	6	10.3
DSG2	116534898	312	12	5	7.6

DDX21	50659095	309	18	8	12.4
DDOST	20070197	285	12	5	13.2
RAB5C	41393545	281	12	5	31
VDAC1	4507879	274	12	4	25.4
GNAI3	5729850	270	11	6	18.4
FLOT2	94538362	268	11	6	15.4
BSG	38372919	265	14	6	27.3
RAB7A	34147513	264	13	5	31.9
CLTC	4758012	254	10	6	4.9
RAB14	19923483	252	11	4	32.1
ESYT1	14149680	249	8	4	6.3
MAP1B	153945728	249	19	4	2.9
PDIA4	4758304	232	7	4	7.1
HSP90AB1	20149594	215	10	3	5.1
SRPRB	284795266	211	13	4	19.9
PDIA3	21361657	209	8	4	9.7
RAB2A	4506365	200	7	4	25.5
VDAC2	42476281	196	7	3	13.9
HSPA8	5729877	170	5	1	6.2
CANX	10716563	160	18	3	6.2
GANAB	38202257	157	7	4	5.9
CALR	4757900	145	6	3	8.6
HIST2H4A	4504301	137	13	3	29.1
HSD17B12	7705855	120	3	2	7.4
VAMP7	5032137	113	9	2	9.5
CYB5R3	4503327	108	4	2	8
GNAI1	33946324	105	4	1	7.6
YWHAG	21464101	90	8	1	5.7
ATP1B3	4502281	89	3	2	9
HLA-B	17986001	83	2	1	7.7
SLC25A5	156071459	82	2	1	4.4
LRRC59	40254924	71	4	1	6.8
TF	4557871	56	2	1	1.9
SLC12A7	123701900	51	4	1	0.6

After various attempts and several different techniques and protocol changes, unfortunately PAFR was not able to be purified with enough efficiency and effectiveness for further study or to be able to conclude the proteins found were associated with PAFR. PAFR expression was demonstrated through western blots several unique PAFR peptides following purification were identified, but not enough to justify further study of PAFR interactors or effects following treatment of PAFR ligands and agonists to the cells.

II. Purification and Analysis of Eh Domain Protein's Association with Low-Density Lipoprotein Receptor and Proprotein convertase subtilisin/kexin type 9

Eps15 homology domain (EHD) enables and regulates the recycling of the membrane proteins after they have been internalized (65). There are four genes that are within the EHD family, which each have different functions in the transport of proteins from the plasma membrane to different organelles of the cell such as the endocytic recycling compartment (ERC), Golgi and lysosome. Although they have different functions, the 4 homologs are closely related and have 50-60% sequence similarity (158). A recent paper suggested that Ehd function effects LDL internalization and LDLR recycling (159). Several papers have been published on the interaction of LDLR and PCSK9 and the effect PCSK9 has on LDL internalization and cholesterol levels (46, 148, 162, 247). This experiment was designed to test for changes in the interactions of the Ehd1-4, LDLR and PCSK9. Transfected cells were immunopurified using FLAG antibody coupled agarose beads, digested by trypsin and analyzed by LC-ESI-MS/MS. The immunopurification of cells transfected with EHD3 was unsuccessful and is not shown in the experimental design or the results. The experimental design is shown in figure 3-16.

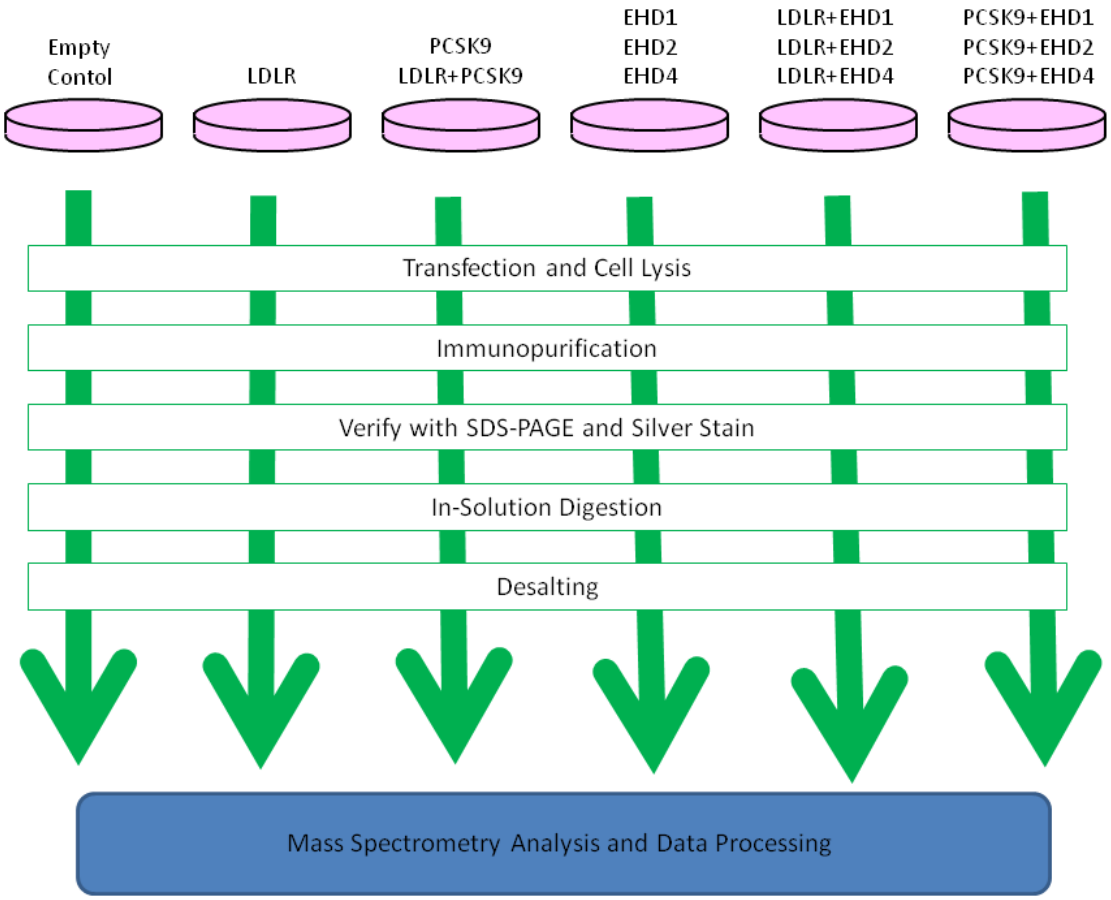
Empty
Contol
LDLR
PCSK9
LDLR+PCSK9
EHD1
EHD2
EHD4
LDLR+EHD1
LDLR+EHD2
LDLR+EHD4
PCSK9+EHD1
PCSK9+EHD2
PCSK9+EHD4
Transfection and Cell Lysis
Immunopurification
Verify with SDS-PAGE and Silver Stain
In-Solution Digestion
Desalting
Mass Spectrometry Analysis and Data Processing

Figure 3-16: Experimental protocol for immunopurification of EHD proteins, LDLR, PCSK9 and bound interactors. Immunopurifications are visually verified by SDS-PAGE electrophoresis followed by silver staining. The Immunopurified protein are digested by trypsin using an in-gel digestion protocol and analyzed by LC-MS/MS. The immunopurification of EHD3 was unsuccessful and is not shown below.

Firstly, cells were singly or doubly transfected with the plasmids containing the tagged genes. All of the EHD genes were C-terminally tagged with the DDK (FLAG) tag, PCSK9 was C-terminally tagged with the V5 tag, and LDLR was C-terminally tagged with either V5 or DDK depending on the experiment. The four EHD genes and the PCSK9 gene was sequenced by Bio Basic (Bio Basic Inc. Markham, ON) and the results are shown in supplementary results. When LDLR was transfected alone or with PCSK9 it was DDK tagged, and when LDLR was transfected with an EHD then it was V5 tagged. After the cells have been transfected and harvested they are lysed and immunopurified using either the FLAG coupled agarose beads or V5 coupled agarose beads. Before the proteins were digested by in-solution digestion, the quantity of the immunopurification was verified using a fraction of the IP for analysis by SDS-PAGE and silver stain. Unfortunately, the V5 immunopurification was unsuccessful based on the stained gels. The stained V5 gels contained very little to no protein, which may have been due to many reasons. Changes in the amount of beads, wash buffer and elution buffer were made, but the purifications were not clear enough to warrant in-solution digest. Instead of continuing with the optimization I continued with the experiments solely with the FLAG IPs. The FLAG immunopurifications looked better visually and showed changes between the different EHD's and stained for multiple bands possibly representing different interactors. The only exception was Ehd3, the immunopurifications for Ehd3 were not as effective the other three, and only Ehd1, 2 and 4 were pursued further for in-solution digestion. Some of the silver stained gels used to verify the immunopurification are shown in Figure 3-17, 3-18 and 3-19.

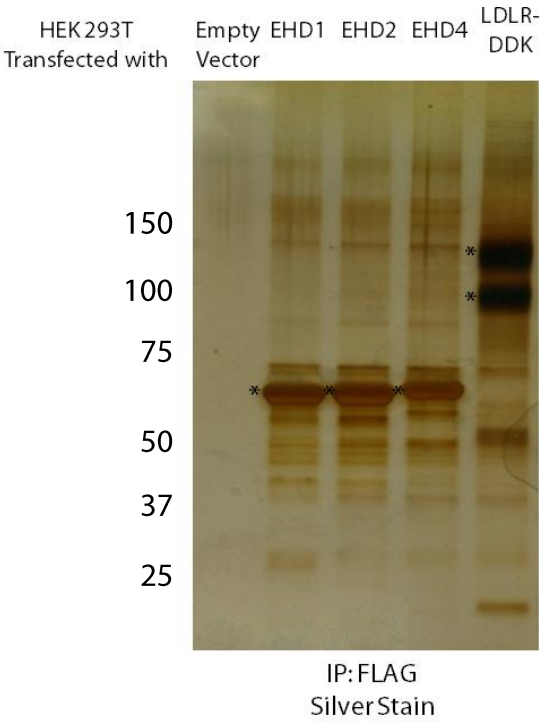
HEK 293T
Transfected with
Empty Vector
EHD1
EHD2
EHD4
LDLR-DDK
150
100
75
50
37
25
IP: FLAG
Silver Stain

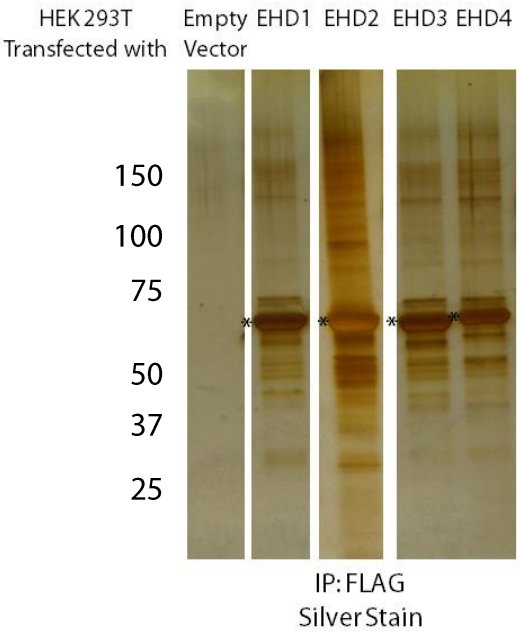
HEK 293T
Transfected with
Empty Vector
EHD1
EHD2
EHD3
EHD4
150
100
75
50
37
25
IP: FLAG
Silver Stain

Figure 3-17: Example of silver-stained gels obtained from the optimized immunopurification of the FLAG-tagged bait proteins and their interaction partners from HEK 293T cells. All cells were singly transfected with LDLR or EHD1-4, which all have the DDK (FLAG) tag or the negative control (empty vector, pCMV-Entry). These gels were not digested and were just used to visualize the efficiency of the immunopurification (*) was added beside bands of the bait protein. Expected size of bait proteins: EHD1: 61 kDa; EHD2: 61 kDa; EHD3: 61 kDa; EHD4: 61 kDa; LDLR: 93 and 120 kDa.

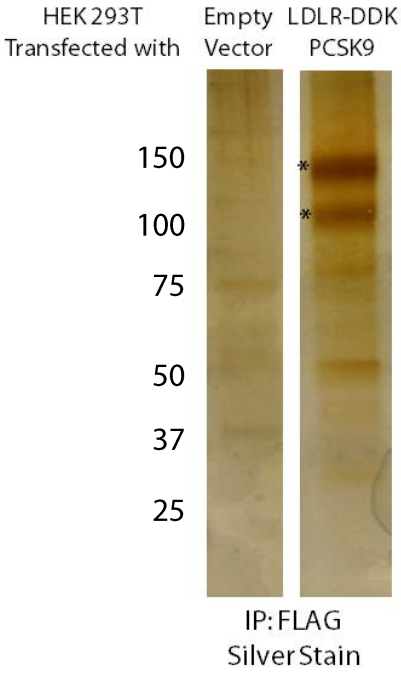
HEK 293T
Transfected with
Empty Vector
LDLR-DDK PCSK9
150
100
75
50
37
25
IP: FLAG
Silver Stain

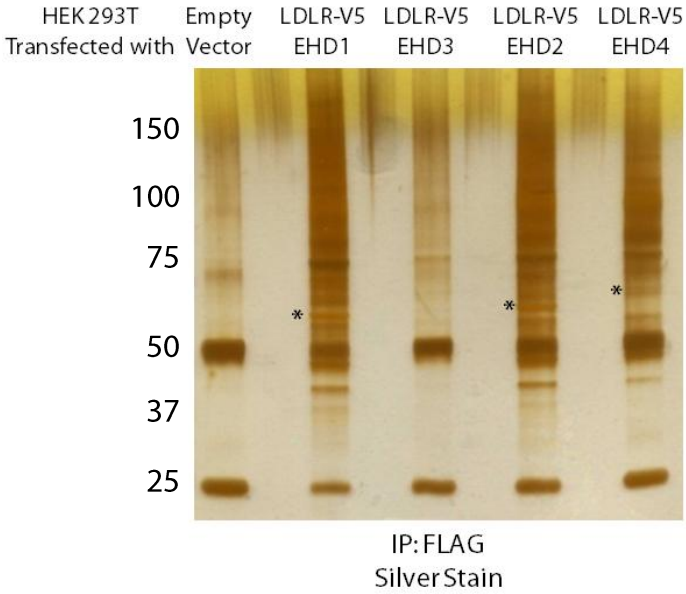
HEK 293T
Transfected with
Empty Vector
LDLR-V5 EHD1
LDLR-V5 EHD3
LDLR-V5 EHD2
LDLR-V5 EHD4
150
100
75
50
37
25
IP: FLAG
Silver Stain

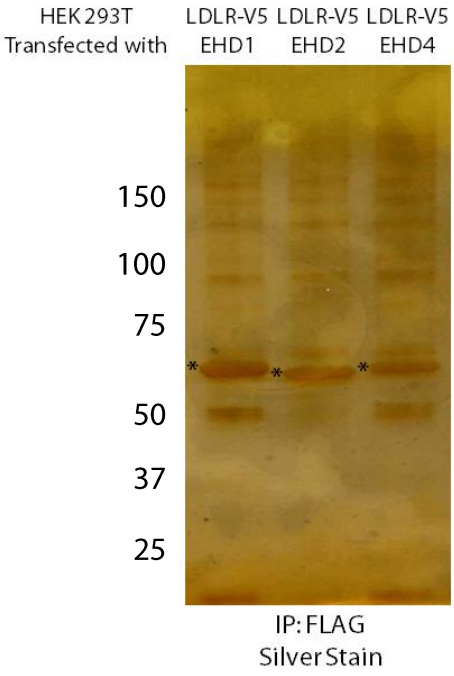
HEK 293T
Transfected with
LDLR-V5 EHD1
LDLR-V5 EHD2
LDLR-V5 EHD4
150
100
75
50
37
25
IP: FLAG
Silver Stain

Figure 3-18: Example of silver-stained gels obtained from the optimized immunopurification of the FLAG-tagged bait proteins and their interaction partners from HEK 293T cells. All cells were doubly transfected with LDLR-DDK and PCSK9-V5 or LDLR-V5 and EHD1-4. which all have the DDK (FLAG) tag or were transfected with the negative control (empty vector, pCMV-Entry). These gels were not digested and were just used to visualize the efficiency of the immunopurification (*) was added beside bands of the bait protein. Expected size of bait proteins: EHD1: 61 kDa; EHD2: 61 kDa; EHD3: 61 kDa; EHD4: 61 kDa; LDLR: 93 and 120 kDa.

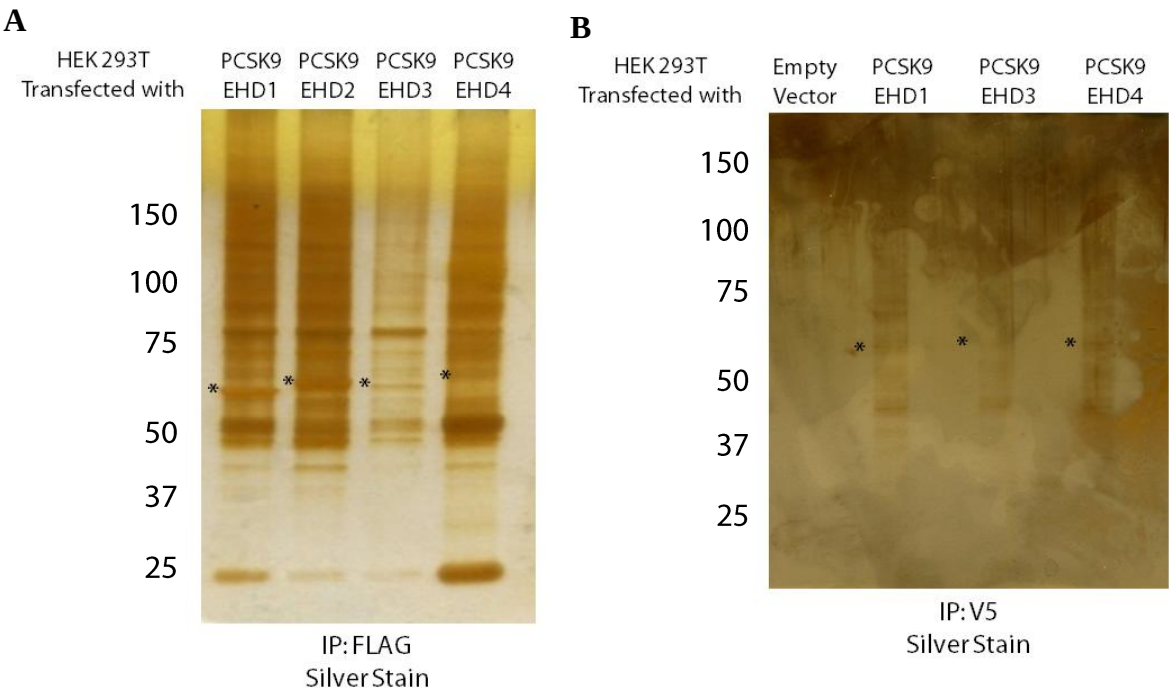
A
HEK 293T
Transfected with
PCSK9 EHD1
PCSK9 EHD2
PCSK9 EHD3
PCSK9 EHD4
150
100
75
50
37
25
IP: FLAG
Silver Stain
B
HEK 293T
Transfected with
Empty Vector
PCSK9 EHD1
PCSK9 EHD3
PCSK9 EHD4
150
100
75
50
37
25
IP: V5
Silver Stain

Figure 3-19: Example of silver-stained gels obtained from the optimized immunopurification of FLAG-tagged bait proteins or V5-tagged bait proteins and their interaction partners from HEK 293T cells. All cells were doubly transfected with PCSK9-V5 and EHD1-4, which all have the DDK (FLAG) tag or were transfected with the negative control (empty vector, pCMV-Entry). (A) This gel contains the eluted proteins from immunopurifications using FLAG coupled agarose beads. (B) This gel contains the eluted proteins from immunopurifications using V5 coupled agarose beads. These gels were not digested and were just used to visualize the efficiency of the immunopurification (*) was added beside bands of the bait protein. Expected size of bait proteins: EHD1: 61 kDa; EHD2: 61 kDa; EHD3: 61 kDa; EHD4: 61 kDa; PCSK9: 74 kDa.

The purifications which showed the best separation and most contrast from the empty vector control according to the silver stained gel were digested using the in-solution digestion protocol. This protocol allowed more samples to be digested and analyzed by the mass spectrometer in a shorter time period. These samples were run on the LTQ-Orbitrap instead of the LTQ-XL, which has a much higher mass accuracy and resolution (89). The results produced by the orbitrap have a lower false discovery rate and the researcher can be more confident with the results (89). The gradient time on the HPLC was increased along with the run time on the mass spectrometer because the in-solution digested samples contain a higher concentration and complexity of peptides compared to the in-gel digested samples. The peptides were analyzed by HPLC-ESI-MS/MS generating 600 thousand MS/MS spectra. The MS/MS spectra are annotated and searched against FASTA protein database by Mascot and organized and processed by Prohits. The results of the database searching and processing is shown in Table 3-6. No results were found for LDLR-V5 + EHD2, the silver stained gel showed dark separated bands but Mascot was not able to match any spectra to protein matches. This was most likely due to an experimental error and not an error with the sample. In most of the purifications involving EHD1, EHD2 and EHD4, other EHD proteins were purified along with the prey. For example, in the purification of EHD2, EHD1 was found as an interactor with 6 unique peptides and EHD3 was found with 2 unique peptides. Adding PCSK9 and LDLR to the EHDs showed only slight changes in the purifications. One change to note is the appearance of clathrin heavy chain in the purifications of LDLR with EHD1 and EHD4. In cells cotransfected with PCSK9 and EHD1, EHD2 or LDLR, each purification resulted in finding at least one unique peptide for PCSK9. When LDLR and EHD1 or EHD4 were cotransfected into HEK 293T cells at least 8 unique

peptide matches were matched to LDLR. Some of the above mentioned peptide matches are not shown in Table 3-6 and are presented in supplementary figures and tables.

Table 3-6: The results of the in-solution digestion of cells singly transfected with the DDK tagged EHD1-4 or LDLR, or cells doubly transfected with LDLR-V5 and DDK tagged EHD1-4 or PCSK9-V5 and DDK tagged EHD1-4 or cell transfected with the negative control (empty vector, pCMV-Entry). Hit Gene Name: the name of the gene matched to the peptides by Mascot; Hit Protein ID: protein identifier from GI database; Hit Score: Mascot probability score associated with the protein match; Peptide Number: total number of peptide sequences matched to the protein; Unique Peptide Number: number of unique peptide sequences matched to the protein; Coverage: the percentage of amino acids matched to protein. Rows highlighted in red are bait proteins; rows highlighted in yellow are suspected interactors. The top 10 results for each bait are presented. Complete results are shown in Appendix 3-2.

EHD1

Hit Gene Name	Hit Protein ID	Hit Score	Peptide Number	Unique Peptide Number	Coverage	Frequency
EHD1	30240932	870	239	13	24.9	18.18
EHD4	21264315	128	10	1	3.5	45.45
HSPA8	5729877	95	4	2	3.1	100
DCD	16751921	120	4	2	20	90.91
MAST4	148727255	36	2	1	0.7	27.27
ODZ1	110347400	42	2	1	0.3	9.09
ZNF10	21314662	38	2	1	0.9	9.09
AMY2A	4502085	39	1	1	3.1	45.45
TTF2	40807471	34	1	1	0.7	36.36
ACSL5	42794756	36	1	1	0.8	36.36

EHD2

Hit Gene Name	Hit Protein ID	Hit Score	Peptide Number	Unique Peptide Number	Coverage	Frequency
EHD2	21361462	698	121	14	25.2	18.18
EHD1	30240932	337	26	6	12.2	18.18
NCL	55956788	213	8	4	6.1	90.91
EHD4	21264315	72	7	1	3.7	45.45
HSPA8	5729877	147	6	3	4.8	100
KIF11	13699824	153	6	3	3.1	90.91
ACSL5	42794756	41	5	1	0.8	36.36
YBX1	34098946	112	4	2	10.2	72.73
DCD	16751921	125	4	2	20	90.91
HAO2	7705393	37	4	1	2.3	54.55

EHD4

Hit Gene Name	Hit Protein ID	Hit Score	Peptide Number	Unique Peptide Number	Coverage	Frequency
EHD4	21264315	1002	147	16	30.3	45.45

EHD3	7657056	202	15	1	8.2	54.55
ACSL5	42794756	41	6	1	0.8	36.36
DCD	16751921	93	4	2	20	90.91
HSPA8	5729877	75	3	2	3.7	100
EHD2	21361462	76	3	1	5.7	18.18
ATP1A1	21361181	43	2	1	1.3	90.91
PRMT5	20070220	71	2	2	4.7	81.82
KIF11	13699824	36	2	1	0.8	90.91
MAST4	148727255	34	2	1	0.7	27.27

LDLR-DDK

Hit Gene Name	Hit Protein ID	Hit Score	Peptide Number	Unique Peptide Number	Coverage	Frequency
LDLR	4504975	616	291	10	13.1	54.55
HSP90AB1	20149594	478	49	10	20	90.91
HSP90AA1	153792590	325	43	2	8.7	63.64
HSPA1B	167466173	136	13	3	6.1	90.91
ENO1	4503571	154	12	3	13.1	90.91
HSPA8	5729877	126	12	1	6	100
ENO3	301897469	103	11	1	10.1	9.09
KPNB1	19923142	131	5	3	4.8	72.73
VDAC2	42476281	69	5	2	6.8	81.82
TCP1	57863257	42	3	1	4.1	72.73

LDLR-V5 + EHD1

Hit Gene Name	Hit Protein ID	Hit Score	Peptide Number	Unique Peptide Number	Coverage	Frequency
EHD1	30240932	1304	323	19	45.3	18.18
HSP90AB1	20149594	1126	161	19	31.4	90.91
ENO1	4503571	854	153	12	35	90.91
LDLR	4504975	504	105	8	10.8	54.55
HSP90AA1	153792590	764	98	5	17	63.64
HSPD1	31542947	713	84	11	26.7	90.91
UBA1	23510338	891	84	12	17.8	45.45
HSPA8	5729877	821	77	14	23.2	100
HSPA1B	167466173	646	54	7	21.4	90.91
ATP1A1	21361181	705	42	11	14.6	90.91

LDLR-V5 + EHD4

Hit Gene Name	Hit Protein ID	Hit Score	Peptide Number	Unique Peptide Number	Coverage	Frequency
EHD4	21264315	1356	323	23	44.2	45.45

HSP90AB1	20149594	843	153	13	24.9	90.91
ENO1	4503571	639	137	8	22.4	90.91
LDLR	4504975	564	137	9	11.7	54.55
HSP90AA1	153792590	623	92	5	18.9	63.64
HSPD1	31542947	568	64	9	20.8	90.91
UBA1	23510338	557	56	9	13.1	45.45
ATP5A1	4757810	467	46	8	17	81.82
TRIM28	5032179	390	44	7	13.8	72.73
HSPA8	5729877	443	43	7	17	100

LDLR-DDK + PCSK9

Hit Gene Name	Hit Protein ID	Hit Score	Peptide Number	Unique Peptide Number	Coverage	Frequency
LDLR	4504975	637	404	11	15.8	54.55
HSP90AB1	20149594	459	110	7	11.7	90.91
HSP90AA1	153792590	302	39	1	6.3	63.64
ATP5A1	4757810	348	39	6	13.2	81.82
ATP1A1	21361181	596	38	9	12.4	90.91
ENO1	4503571	477	37	7	23.3	90.91
HSPA8	5729877	301	30	4	7.9	100
ATP5B	32189394	305	23	7	18.5	72.73
VDAC2	42476281	260	23	6	26.9	81.82
HSPA1B	167466173	224	22	2	6.1	90.91

EHD1 + PCSK9

Hit Gene Name	Hit Protein ID	Hit Score	Peptide Number	Unique Peptide Number	Coverage	Frequency
EHD1	30240932	1663	1030	25	50.9	18.18
HSP90AB1	20149594	791	138	12	26	90.91
ENO1	4503571	683	118	10	28.8	90.91
HSP90AA1	153792590	671	101	6	16.4	63.64
NCL	55956788	504	82	9	16.2	90.91
HSPA8	5729877	648	68	10	17.2	100
ATP5A1	4757810	540	62	8	17	81.82
HSPD1	31542947	574	61	8	17.8	90.91
TRIM28	5032179	536	61	9	20.7	72.73
SLC25A5	156071459	239	60	4	13.4	90.91

EHD2 + PCSK9

Hit Gene Name	Hit Protein ID	Hit Score	Peptide Number	Unique Peptide Number	Coverage	Frequency
HSP90AB1	20149594	1141	349	18	25.7	90.91

HSP90AA1	153792590	1071	311	8	23.1	63.64
EHD2	21361462	735	217	14	25	18.18
TRIM28	5032179	457	110	7	13.9	72.73
HSPA8	5729877	579	110	9	16.7	100
ATP5A1	4757810	683	94	9	18.3	81.82
ENO1	4503571	533	86	7	22.8	90.91
HSPD1	31542947	678	82	10	20.4	90.91
GNB2L1	5174447	440	75	7	24.9	72.73
HSPA5	16507237	576	66	8	19.1	90.91

EHD4 + PCSK9

Hit Gene Name	Hit Protein ID	Hit Score	Peptide Number	Unique Peptide Number	Coverage	Frequency
EHD4	21264315	594	73	11	23.1	45.45
HSP90AB1	20149594	417	36	8	14.6	90.91
HSP90AA1	153792590	327	34	2	7.1	63.64
ENO1	4503571	96	23	1	4.1	90.91
HSPA8	5729877	227	18	4	9	100
HNRNPC	117189975	153	16	2	9.2	45.45
HSPA1B	167466173	174	13	2	6.1	90.91
EHD3	7657056	236	11	2	8.6	54.55
HSPD1	31542947	217	10	5	12.2	90.91
UBA1	23510338	70	10	1	1.4	45.45

CHAPTER 4. DISCUSSION

I. The Interactome of Several Alzheimer's disease Related Genes

In an attempt to further elucidate the molecular mechanisms involved in AD, several proteins associated with AD were analyzed by protein interaction mapping. This was done by utilizing bottom-up large-scale proteomics coupled to multiple biological techniques. The main goal of the experiments was to find novel interactions of these proteins so that we have a better understanding of why they are involved in AD pathology and to provide targets for further research and studies. Additionally, with further work on a larger dataset of AD related genes, a larger more complete network of interactions can be created, which could better show how AD pathology develops and the areas of the cell most affected. The results obtained from the immunopurification, digestion and LC-MS included previously known and studied interactions as well as novel interactions. The novel interactions either fit into the functional roles of the protein or have never previously been seen and indicate a possible new role in the cell. In this type of experiment which relies heavily on the mass spectrometry data and accuracy, the interactions can only be inferred based on comparison and statistical analysis. Some interactions were validated by co-immunopurification to prove the validity of the mass spectrometry data and the data processing which followed. All of the interactions tested proved to be true based on the co-immunopurifications.

Apolipoprotein E is widely known in the scientific world for its role in AD, and has therefore been widely studied. APOE is known to bind to low-density lipoprotein receptor, other members of the LDLR family and a few other membrane bound proteins (27). It was discouraging that no LDLR was found in the experiments done, but there may be reasons for that result. The binding may have been affected by the C-terminal FLAG tag added to APOE. The LDLR binding region of APOE is in the N-terminal domain (residues 136-150) but the binding

affinity between LDLR and APOE is significantly lowered when APOE is not associated with lipid. The lipid binding region of APOE is in the C-terminal domain (residues 244-272) (81). The tag could also affect the conformation and structure of the mature protein. LDLR, like many of the previously known interactors are membrane related, and they may not have been identified because of the difficulty in purifying membrane proteins (138). Completing the immunopurifications with agarose beads and digesting the proteins by in-gel digestion results in a loss of most of the membrane proteins (251). According to Database for Annotation, Visualization and Integrated Discovery (DAVID) (90), the proteins found in all of the in-gel digestion did not contain any significant amount of plasma membrane proteins using a p-value of 0.99. While the proteins found following a membrane isolation protocol contained 37.7% proteins identified under plasma membrane using a p-value of 0.01. This is a significant difference and may represent the reason why APOE interactors were not identified.

Two of the identified proteins that were validated by co-immunopurification were voltage-dependent anion channel (VDAC) and translocase of outer mitochondrial membrane 40 homolog (TOMM40). They were matched with 13 and 3 unique peptides, respectively and had high Mascot and SAINT scores. Both are mitochondrial proteins, and involved in the movement of substances across the outer mitochondrial membrane (15). Since both these proteins are part of the mitochondrial outer membrane, there is the possibility that APOE is binding to outer membrane and purifying the entire mitochondria (246). To investigate this possibility, the protein matches found were analyzed by Cytoscape and BiNGO (134). According to BiNGO, the APOE purification had a small increase from approx. 20% to 26.3% in mitochondrion proteins compared to the purifications of the other AD-related genes. Interestingly, mitochondria proteins were found not to be prominent in the empty vector control samples. This small change in

mitochondrial proteins between ApoE and the other AD-related genes is minor and most likely does not represent the purification of the entire mitochondria. Recent research has shown that VDAC may be involved in AD pathology. In AD brains, VDAC was observed to accumulate in caveolae areas of the plasma membrane and in neurons containing plaques (182). This research tied into another study which showed that exposure to specific anti-VDAC antibodies prior to exposure with Aβ prevented neurotoxicity in two neuronal cell lines (140). An interaction between Aβ and VDAC has been suggested via GxxxG motifs present on both proteins (225). VDAC may interact with APOE in the same way; the GxxxG motif is also present on ApoE. The motif is present at amino acids 183-187 and 214-218 (http://www.ncbi.nlm.nih.gov/protein/NP_000032). Mitochondrial dysfunction has been hypothesized as a primary event in AD pathology that could cause the production of Aβ plaques, synaptic degeneration, neurofibrillary tangles and thus AD pathophysiology. Mitochondrial dysfunction has also been shown to be a commonly found pathological criterion for AD diagnosis and identification (153).

TOMM40 was also found as an interactor of APOE. As stated earlier, TOMM40 is a mitochondrial protein involved in the movement of proteins across the outer membrane (15). It is the core protein in the TOM complex. It has also been studied recently in regards to AD. Several GWAS found TOMM40 to be an at risk gene for AD just as CLU and PICALM (176, 207). In the Shen and Potkin papers, TOMM40 was found to associate with AD patients with at least a $p<10^{-6}$ significance threshold (176, 207). The number of thymine nucleotides in a region of the TOMM40 gene has also been shown to predict the age of onset of LOAD. Longer lengths of poly-Thymine repeats (~33 T residues) in APOE3 individuals results in an onset of LOAD an average of 7 years earlier than individuals with shorter repeats (~15 T residues) (192). Five other

papers have found similar results with regards to poly-T repeats (99, 130, 141, 174, 175). A relationship between the regulation of APOE genes and TOMM40 genes has also been illustrated. Depending on the cell line used, the promoter activity of TOMM40 and APOE both are affected by APOE cis regulatory elements and TOMM40 putative regulatory enhancers (16). Putting all this work on APOE, VDAC and TOMM40 into context with these purifications gives it greater meaning. APOE has been shown to possibly interact with mitochondrion during cell stress and/or mitochondrial dysfunction (30). APOE, VDAC and TOMM40 all have been shown to be related to AD onset and pathology (27, 182, 192). and TOMM40 has a direct relation to APOE (16). This proteomic work shows the possible interaction of APOE with one or both of these proteins. The results were replicated in triplicate and were validated by co-immunopurification. The interaction may represent the onset of mitochondrial dysfunction and AD or a progression of AD pathology following another cell event or stress. Future experiments may explain what role APOE and mitochondrial dysfunction play in the pathology of AD.

As with most affinity-purification mass spectrometry experiments, the results open countless directions to follow. First of all the experiment used tagged, transiently transfected APOE in HEK 293T cells. A more biologically relevant study would involve untagged, stable cell lines that were of neuronal background or in primary neuronal cultures. This was not possible in the time constraints of this project but would have been ideal. This interaction study was done using APOE3 protein and the results could differ using the APOE2 or APOE4 isoforms. Future studies could be done to compare the interaction with VDAC and TOMM40 in different APOE isoforms using quantitative proteomics such as SILAC cell lines. Functional studies could be done on the same cells, testing the opening and closing of VDAC and TOMM40 pores in the presence and absence of APOE isoforms. A change in the movement of proteins and

ions across the outer mitochondrial membrane could cause or advance the stress and dysfunction of the mitochondria and cell.

The purification and analysis of the CLU variant proteins found some known interactors and some interesting results between CLU1 and CLU2. The DNA repair complex of XRCC5, XRCC6 and PRKDC (XRCC7) were all known to have a relationship with CLU1 and were all identified by mass spectrometry (124, 242). The complex forms a DNA-dependent protein kinase which plays a critical role in resealing DNA double strand breaks by non-homologous end-joining (242). According to previous papers the interaction between CLU1 and PRKDC is indirect and is due to the interaction between CLU1 and the XRCC5 and XRCC6 dimer (242). Looking at the results of these experiments would lead to the opposite conclusion; PRKDC had more peptide matches than the other two proteins. CLU1 and CLU2 both showed a relationship to all three proteins in the complex, and in fact there were stronger results for the CLU2 purification over the CLU1. CLU2 is the cytoplasmic isoform of CLU and should not have an interaction with nuclear proteins such as the ones in this complex (123). The CLU2 isoform may be shuttled to the nucleus following the stress from the transfection or the overexpression of a gene (128, 220, 227). This data shows that the difference between the isoforms is very minimal when it pertains to the function and interactions of the protein.

A third comparison between the more common isoform of CLU, the secreted isoform, would be ideal to examine the interaction differences following secretion. The nuclear form is associated with cell death (242) and the secreted form is associated with cell protection (164), so there would be major differences if examined by quantitative proteomics. The secreted form, also known as apolipoprotein J, would be useful in relating to the results of the APOE analysis because of their similarities (164).

The significance between the interactors found and AD still needs to be elucidated. Two studies have shown that when the complex of CLU1 with XRCC5, XRCC6 and XRCC7 signals cell death (123, 242). The splicing changes that cause the formation of CLU1 instead of the other isoforms may be the first step in the apoptotic progression of neurons in AD affected individuals.

Alpha-synuclein is known to form Lewy bodies and as part of these Lewy bodies have several possible interactions. SNCA and Lewy bodies may be involved in the cause or progression of apoptosis in AD and Parkinson's disease patients (68). In this study, the very small (~15 kDa) protein/peptide resulted in very few interactors and very few background contaminants. Beta-Synuclein (SNCB) and Calmodulin-like 5 (CALML5) were both identified as possible interactors of SNCA (80, 121, 168). SNCB was expected to be found because several papers cite the interaction between these two isoforms. The binding SNCB to SNCA has been hypothesized to protect the cell by inhibiting aggregation of SNCA (80, 168). CALML5 is a suspected interaction based on other work showing an interaction between CALM1 and SNCA (121). The purification of SNCA identified very few interactions and none were related to a connection between SNCA and AD. If the stringency of the lysis and wash buffers were reduced, there would be a great chance that more possible interactors would be found. SNCA was much smaller than the other proteins studied and in order to maintain the reproducibility of the experiment the protocol was kept the same for all of the genes studied. If reproducibility was not an issue, each protein's purification could have been optimized individually to produce the greatest number of associations. If the methods change for each gene, the ability to compare between them all and speculate an interaction becomes even more difficult.

The purification of PICALM produced expected results with regards to known interactors. PICALM is involved in the initiation of clathrin-mediated endocytosis (CME) and

thus the interactors are expected to be related to clathrin and recruiting/adaptor proteins (224). Many known and not yet known, but expected interactors were found. Based on the results it shows that PICALM is involved in recruiting clathrin and adaptor proteins to the site of vesicle formation and may be involved in multiple steps of the vesicle formation process. In a recent review paper, five steps of clathrin-mediated endocytosis have been proposed, with different proteins being involved in each step (150). The results of the purification and analysis contain multiple proteins from the first three steps (nucleation, cargo selection and coat assembly) and none from the last two steps (Scission and uncoating) (150). PICALM could be one of the first proteins recruited to the site of CME and responsible for the recruiting of proteins in the following three steps. Based on previous data (9, 61, 150-152, 224) and the data found in this experiment a model of PICALM's role in CME was created and is shown in Figure 4-1.

None of the identified interactors were known to associate with AD, but clathrin-mediated endocyctosis has been associated with AD. The processing of APP into Aβ peptide is processed following internalization of the APP into endosomes. Changes in levels of PICALM could therefore affect the levels of Aβ (115) because PICALM levels correlate with endocytosis (151).

The results from the purification exemplify the abilities of mass spectrometry coupled to biological techniques such as affinity purification. Like any experiment, optimization is needed, but in the end, the results present a perspective of a protein's function, localization, and role in the cell. The results can reinforce current models and hypothesis' or present novel ideas and open new doors.

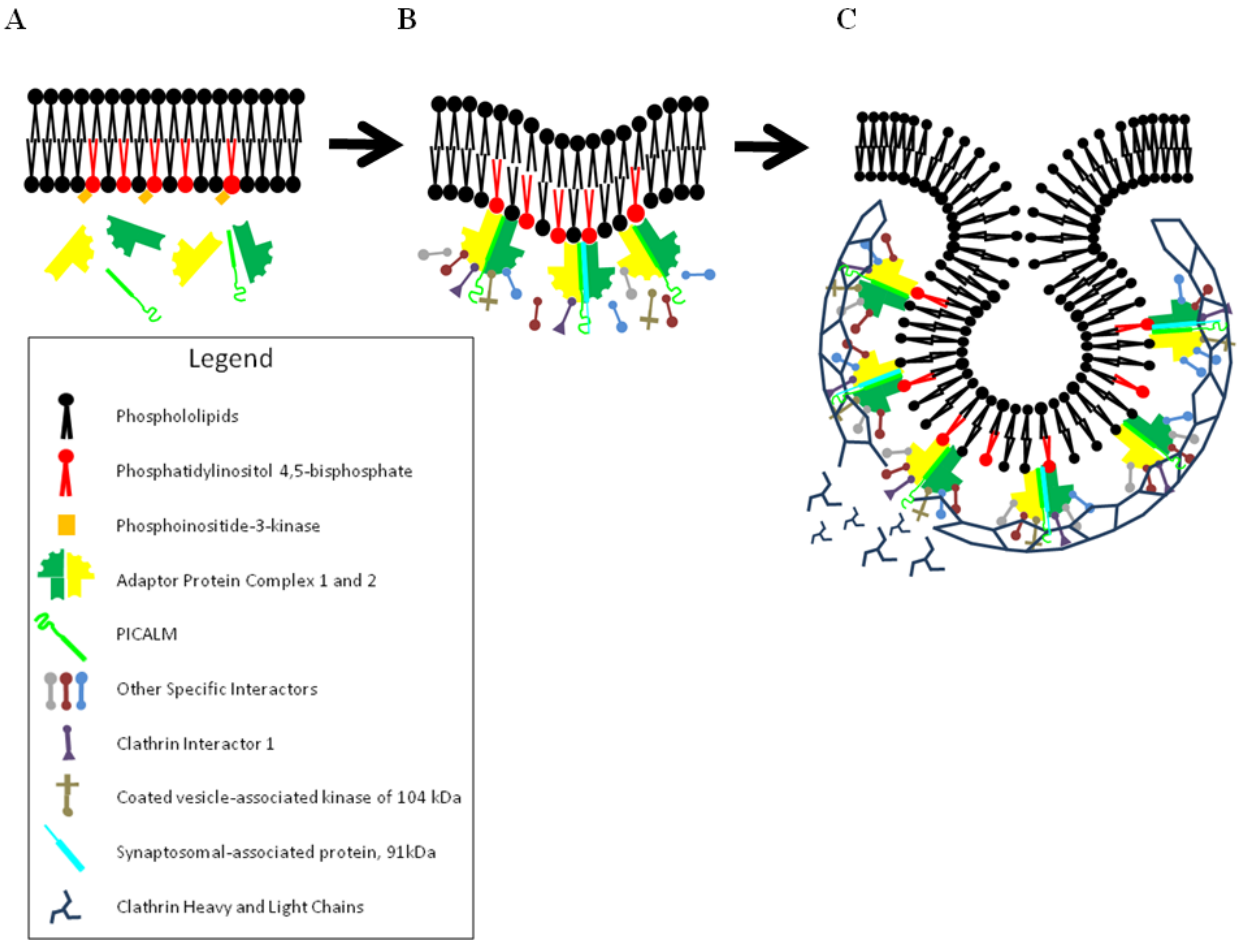
A
B
C
Legend
Phosphololipids
Phosphatidylinositol 4,5-bisphosphate
Phosphoinositide-3-kinase
Adaptor Protein Complex 1 and 2
PICALM
Other Specific Interactors
Clathrin Interactor 1
Coated vesicle-associated kinase of 104 kDa
Synaptosomal-associated protein, 91kDa
Clathrin Heavy and Light Chains

Figure 4-1: Overview of the early stages of clathrin-mediated endocytosis and PICALM's role in the process. (A) PICALM and adaptor protein complex 1 and 2 bind to phosphatidylinositol-4,5-biphosphate concentrated zones of the plasma membrane. (B) PICALM and adaptor proteins recruit other interactors and cargo specific adaptors and a clathrin-coated pit begins to form. (C) Clathrin is recruited and forms a hexangonal and pentagonal configured coat around the pit as it takes the shape of a vesicle.

II. The Purification and Analysis of the Platelet Activating Factor Receptor

The study of the platelet activating factor receptor began with high anticipation. The receptor was not extensively studied, yet it had possible important roles in the cell (93). One specific interactor was especially exciting and was thought to alter the function of PAFR greatly. Platelet activating factor (PAF) is a known ligand of PAFR and depending on the species of PAF involved the downstream effects were altered (33).

Purification of the receptor under native conditions proved to be more difficult than expected. The 7 transmembrane domains of the receptor made it difficult to show expression of the protein on a western blot and was difficult to purify (93). Progress was made over the time spent working on it. Expression of the receptor was shown by western blot and some purification of the protein was achieved. A lot of experimentation and optimization was needed to get to this point.

One interesting finding from the expression of PAFR shown by western blot is that a band would be present at ~40 kDa representing PAFR, and there would also be a band found at ~75 kDa and sometimes other bands at a heavier weight that would appear as a smear. The heavier bands may represent a dimer (or higher oligomers) or other modification. A perspective paper by Jonathan A. Javitch presented the large amount of evidence that class A G-protein coupled receptors (GPCR), such as PAFR, form dimers and higher-order oligomers (96). Some higher order bands above 75 kDa may just be the result of the aggregation of the receptor, but it appears that the band at 75 kDa represents a dimer. In a paper by Thierry Magnin et al, three GPCR proteins with a similar molecular weight to PAFR (P2Y1, OPRK, CNR2) were purified and visualized on a stained SDS-PAGE gel. Each lane contains bands at approx. 40 kDa and 75

kDa like PAFR and the researcher also believes the probable cause of the 75 kDa band to be dimerization (135). The hydrophobicity of some membrane proteins makes them susceptible to aggregation/dimerization and resistant to SDS denaturing (96, 216).

The main issue with purification of PAFR was that several proteins were found to be more prominent than PAFR in the sample according to mass spectrometry analysis. Other papers publishing the results of GPCR purifications found similar results (10, 45, 120, 135). In each paper they have had to incorporate different methods to solubilize and purify the receptor proteins. In the paper by Daulat et al. they incorporated a very similar technique to the one used in these experiments, and found comparable results (45). Affinity purification coupled to HPLC-MS was used to identify MT1 and MT2 melatonin receptor and its associated proteins. They identified the MT1 receptor with a Mascot score of 353, making it the number 7 hit and they identified the MT2 receptor with a Mascot score of 191 making it the number 13 hit (45). These are very similar scores and findings to the ones found for PAFR and in the paper they make several conclusions on the identification of MT associated proteins. They made these conclusions comparing to only one biological control while in this study many control and sample purifications were completed in conjunction with PAFR (45). By completing a large number of control and sample purifications on several different baits it increases the confidence in the associations found and in essence makes each bait a control to the others (36). If the PAFR purification were only compared to one empty vector control purification many proteins could be concluded to be associated with PAFR, when in reality they were found in other purifications and most likely represent background proteins. The other papers mentioned were also able to purify GPCRs to the same extent as PAFR, but the purpose of those papers was for the purification of the receptor and not the analysis of associated proteins (10, 120, 135). One

difference between the PAFR purification and the previously published purifications is the location of the identified peptides. All of the peptides identified for PAFR were from cytoplasmic loops and none were found from extracellular loops or the transmembrane domains (93). The other GPCR purifications identified peptides from all regions of the receptor and didn't appear to show any preference for any one region (120, 135). The bias in the peptides found may be the result of an irregular conformation of the PAFR when removed from the membrane, which may cause an issue for trypsin being able to access and cleave TM and extracellular regions during digestion.

Despite the fact that it is difficult to conclude that proteins identified are in fact associated with PAFR, some of the identified proteins are interesting and may represent some possible interactions. Guanine nucleotide binding protein (G protein), alpha 13 (GNA13) and GNAQ were both found solely in the PAFR purifications and GNAI1, GNAI2, GNAI3 were found in PAFR and control purifications but more peptides were found in the PAFR purification. GNA proteins are the alpha subunit (G_α) of G-protein heterotrimeric complex, which also includes the G_β and G_γ subunits as well (191). They are responsible for the cytoplasmic binding and hydrolyzing of GTP which affects the association of the heterotrimeric complex with the receptor and the activity of the effector proteins in the signaling pathway (165). There are 4 classes of G_α proteins each binding to different groups of receptors and effector proteins (240). According to Ingenuity Pathway Analysis software, PAFR is known to bind GNAI3 and GNAQ, two G proteins found in the purification. Based on NCBI Blast software, the most closely related protein to PAFR based on sequence is the lysophosphatidic acid (LPA) receptor. A study was done to detect which G proteins couple to the LPA receptor. G-proteins from 3 of the 4 classes were detected to couple to LPA receptor; the 3 classes detected were the only 3 identified from

the purification of PAFR (69, 188). Along with the G-proteins found, several RAB proteins were identified as well, some of them being unique to the PAFR purification. RAB proteins are also GTPases, involved in vesicle transport of membrane bound organelles and neurotransmitter release in neurons (202). No RAB proteins are known to be associated with PAFR but they are known to regulate the activity of GPCR's by membrane transport mechanisms (202). Finally, one last interesting associated protein that was found was transferrin. Transferrin is known to be a marker for the early endosome (53). GPCR's such as PAFR are known to recycle through the endosome for eventual degradation and down-regulation (52). Rab proteins are also known to be present in the early and late endosomes, and involved in shuttling proteins to the recycling endosome (155). These interactions point to the idea that PAFR is shuttled to the endosome and is being down-regulated and degraded in the cell. This could possibly be the reason why yields of PAFR from the purification were so low. Some degradation and endosomal recycling is normal for GPCR proteins but combined with the problems that were reoccurring, this may be the issue.

Improvements to the methods are possible and a more efficient purification of PAFR may still be completed. Another type of purification tag could be used such as streptavidin, TAP tag or rhodobsin (42). Other changes to the solubilization protocol and recipe to increase the solubilization of the lysates could be done. The addition of PAFR ligand, PAF 16:0 or PAF 18:0 may help reduce the amount of PAFR that is internalized to the endosome and lysosome. These types of experiments involve trial and error and optimization with no guarantee for improved results.

One success from the purification of PAFR was the implementation of a membrane isolation protocol to increase the number and ratio of membrane bound proteins in the lysate.

The percentage of plasma membrane and other membrane proteins increased considerably following the protocol. According to BiNGO (134), the in-solution and in-gel digestion samples contained no significant amount of plasma membrane proteins using the highest possible p-value, while in membrane isolation samples there was 35.6% proportion of plasma membrane using a very small p-value. There was also no decrease in the number of total proteins identified. There were approx. 300 proteins identified for each of the empty control and the PAFR samples. The paper from which this protocol is based, found over 60% plasma membrane proteins, so there is improvement still to be made (251), The reason the percentage is lower could be because of some contamination with cytoplasmic proteins or losses from the solubilization steps.

III. Purification and Analysis of Eh Domain Protein's Association with Low-Density Lipoprotein Receptor and Proprotein convertase subtilisin/kexin type 9

The purification and analysis of multiple EHD Proteins either transfected singly or cotransfected with either PCSK9 or LDLR would involve the analysis of approximately 150 samples without analyzing any replicates. In order to decrease the time needed for sample preparation and in mass spectrometry analysis, an in-solution digestion protocol was used on the purified samples. The in-solution digestion was the most efficient because the number of steps and movement between tubes/containers. The most groundbreaking result was the finding of association between different EHD isoforms and between EHD and PCSK9 and LDLR.

Previous work on studying the EHD proteins and their complexes has resulted in several known associated proteins. Between the 4 EHD isomers, the only suspected interaction was between EHD1 and EHD3, based on yeast-2-hybrid and co-immunopurification experiments (63). This was one of the few associations that was not seen. Based on the matched peptides identified it appears that there is a suspected association between EHD1 and EHD2 and EHD4, and an association between EHD4 and EHD3. Each protein match contained at least one unique peptide match, which is essential when comparing 4 very similar proteins. EHD2, EHD3, and EHD4 are 70.3%, 86.5% and 74.1% identical to EHD1, respectively (158). Each of them regulates the transport of proteins either to or from the early endosome (158). The reason that many of the EHDs associate with each other based on these results may be that some of the early endosome remains intact and bound to EHD when it is being immunopurified. Any other EHD isoforms that remain bound to the early endosome would also be purified (211).

When HEK 293 cells were cotransfected with an EHD isoform and LDLR, and the EHD isoform was purified, one of the top hits found was for LDLR. One paper has shown that LDLR

internalization may involve EHD1; EHD1 knockout mice had decreased cholesterol uptake and lipid droplet sizes (159, 181). According to the mass spectrometry results, EHD1 and EHD4 were both found to associate with LDLR equally. The number of peptides matches for LDLR was quite high and would represent a very strong interactor of EHD1 and EHD4. The results must be looked at with some skepticism because LDLR was overexpressed in the cell and the interaction may have been somewhat forced. Overexpression of LDLR may cause an increase in the recycling of LDLR to the endosome for degradation, which would also increase the amount of LDLR associated because of the strong connection between the EHD isoforms and the endosome. Another interesting finding from the LDLR-EHD contransfections was the match with clathrin heavy chain (CLTC). CLTC is needed for clathrin mediated endocytosis, the method in which LDLR is internalized (97, 150). It was not found in the EHD or LDLR purifications, only when EHD1 and EHD4 were co-transfected with LDLR. This solidifies the point that EHD1 and EHD4 are involved in the internalization of LDLR.

The co-transfection of PCSK9 with LDLR, EHD1, EHD2, and EHD4 did not present many interesting results. The proteins found to be associated with the EHD isoforms in the presence of PCSK9 were very similar to the ones found by in singly transfected cells or transfected with LDLR. The one finding that is interesting is the identification of PCSK9. PCSK9 was identified in cells contransfected with LDLR-PCSK9, EHD1-PCSK9 and EHD2-PCSK9. In each case there were only one or two unique peptides matches to PCSK9. The association between them appears to be much weaker than the association between LDLR and the EHD isoforms. Like stated earlier, the association may be partly due to overexpression of PCSK9 in the cells. The agarose beads are washed 5 times before elution takes place and the

elution is completed competitively to reduce non-specific binding and increase the confidence that the results are not caused by overexpression of another protein.

Overall the results of these experiments did differ from the AD-related genes and PAFR experiments. The proteins identified seemed to be related to translation and RNA binding. Analyzing the Mascot database search results using BiNGO (134) showed that there was an increase in the amount of translational, RNA binding, metabolic processing, and nuclear proteins in the samples for this experiment. The increase in those classifications of protein may be due the in-solution digestion method or it may be due to the EHD proteins. To determine what the cause of the increase was, the results of the several samples that were digested using the in-solution digestion protocol were compared. All the samples involving an EHD transfection were compared to the samples which were transfected with LDLR or LDLR and PCSK9, and there were no substantial differences between the classes of proteins found. All of the in-solution digestions from this project were compared to the in-solution digestions that were done on the AD-related genes, and again there were no substantial differences in the classes. It can be concluded from these results that in-solution digestion is much more effective in the digestion of RNA binding, translational and other nuclear proteins compared to in-gel digestion. The reason behind this is that RNA binding, translational and nuclear proteins are some of the most abundant proteins in the cell. The in-solution digestion samples were not fractionated outside of the HPLC separation and were run for 300 minutes per sample. The in-gel digestion samples were separated into 10-20 gel bands before the HPLC separation and were run for 75 minutes per sample. In total, an in-gel digestion sample was separated and analyzed over 750-1500 minutes while an in-solution digestion sample was done over 300 minutes. Because of this big difference

in analysis time, the high abundant peptides will be analyzed first and many low abundant peptides will be missed (6).

CHAPTER 4. CONCLUSIONS AND FUTURE DIRECTIONS

I. Conclusions

The objective of these three studies was to identify interactors of genes that are genetically or pathologically related to AD and hypercholesterolemia, with the aim of further understanding the disease and the involvement of the genes in the disease. The genes were expressed in HEK 293T cells and affinity based purification was performed to isolate the bait protein and its interactors. The success of each gene's purification varied, for example the purification of PICALM produced many known and suspected interactors while the purification of SNCA produced only one known interactor and two suspected interactions. Overall the studies demonstrated the use of immunopurification and mass spectrometry analysis as a suitable tool for elucidating interactions for further study. Four of the interactions were validated by co-immunopurification successfully to add to the confidence of the results produced. The identified interaction partners bestow a starting point for further studies, which can be used to explain changes in diseased cells and how protein-protein interactions change in different conditions.

II. Future Directions

The three projects used affinity-purification coupled to mass spectrometry, which is a common technique in the field of proteomics (231). The technique can provide a lot of information about each bait purified. The data can be used to create large network maps of cellular and disease pathways or it can be used to compare differences in the protein-protein interactions following changes to the cell or organism (120, 127). The results of this thesis fall somewhere in between. There were not enough baits used to create a large pathway maps that connect multiple baits and it was not focused enough to develop conclusions on how mutations, toxicity, over-expression, etc effect protein-protein interactions. Fortunately, the results do provide a starting point to perform larger-scale or more focused studies.

Large-scale mapping studies provide an effective way to understand the effect a disease, such as AD, has on the makeup of a cell. Several theories exist to explain the cause of AD and predict many possible therapeutic targets, but no cure (179). Numerous diseases are in the same position. Mapping of protein-protein interactions allows the causes and targets to be considered together to look for common factors and patterns (28, 105, 144). In this study 6 different genes were purified and analyzed; a small number compared to the many genes associated with AD. According to Ingenuity Pathway Analysis (184, 212), there are 671 different molecules are associated with AD, without looking at the multiple mutations and variants that are involved. The logical next step would be to continue using AP-MS to characterize more of the AD associated proteins. Continuing the project with more baits would involve a large commitment because of the time needed to prepare each bait for optimal expression and purification, and the time needed for the digestion of the purified proteins by in-gel digestion. A previous study mapped the interactions of 407 proteins implicated in more than one disease using an almost

identical process (58). The study required the collaboration of several labs and a lot of time in creating such a large database and interaction network (58).

Instead of continuing a large-scale interactome project, one or two closely related genes could be chosen for a more focused study. For example, the purification of APOE produced many novel interactions, and APOE is one of the most studied proteins in AD (107). There are three commonly studied variants of APOE and only the most prevalent variant, ε3, was looked at in this study. The experiments could be replicated with each variant, and compared. Aβ or tau proteins could be added to cells to investigate any changes in protein-protein interactions of the APOE variants. Since APOE is an excreted chaperone protein, the cell media should also be examined for any protein-protein interaction changes. Completing a focused study on one of the genes permits more conclusions to be made and theorized. Disease relevant information can be found for APOE and the experiments could be completed with other cell lines more appropriate for AD, such as PC-12 (167), and with stable transfection to avoid any effects protein overexpression may have on interactors.

The purification of PAFR still required improvement in order for conclusions to be made and future studies pursued. Other membrane purification techniques (5, 88, 136, 143, 248) could be utilized to improve the purification. If a new technique could be implemented, then the next step would be to focus on the effects of different PAFR ligands on the cell and PAFR's protein-protein interaction. Two known ligands, PC (O-16:0/2:0) and PC (O-18:0/2:0), lyso-PAF and BN 52021 (PAF antagonist) could be supplemented to the cells to examine any changes (22, 194, 196). These further studies could be performed in a more relevant cell line and using stable transfection instead of transient transfection.

The project studying the different in protein-protein interactions of the EHD proteins produced large datasets of interactors. Only few differences were seen between the EHD isoforms and when PCSK9 or LDLR were cotranfected with the EHDs. More optimization is required to perform any further studies. Firstly, more disparity in protein-protein interactions between the EHD isoforms would have to be detected. General membrane purifications could be done to enhance the amount of ER, Golgi, lysosome, endosome and plasma membrane in the lysate. Those are the areas where the EHD isoforms localize in the cell. If more variance can be detected between each isoform, different conditions can be tested, where LDLR and/or PCSK9 are cotransfected along with each EHD.

III. Bibliography

1. **Abifadel, M., M. Varret, J. -. Rabès, D. Allard, K. Ouguerram, M. Devillers, C. Cruaud, S. Benjannet, L. Wickham, D. Erlich, A. Derré, L. Villéger, M. Farnier, I. Beucler, E. Bruckert, J. Chambaz, B. Chanu, J. -. Lecerf, G. Luc, P. Moulin, J. Weissenbach, A. Prat, M. Krempf, C. Junien, N. G. Seidah, and C. Boileau.** 2003. Mutations in PCSK9 cause autosomal dominant hypercholesterolemia. Nat. Genet. **34:**154-156.

2. **Abisambra, J. F., T. Fiorelli, J. Padmanabhan, P. Neame, I. Wefes, and H. Potter.** 2010. LDLR expression and localization are altered in mouse and human cell culture models of Alzheimer's disease. PLoS ONE. **5:**.

3. **Abisambra, J. F., T. Fiorelli, J. Padmanabhan, P. Neame, I. Wefes, and H. Potter.** 2010. LDLR expression and localization are altered in mouse and human cell culture models of Alzheimer's disease. PLoS ONE. **5:**.

4. **Aebersold, R., and M. Mann.** 2003. Mass spectrometry-based proteomics. Nature. **422:**198-207.

5. **Aggarwal, S., R. Rafikov, C. M. Gross, S. Kumar, D. Pardo, and S. M. Black.** 2011. Purification and functional analysis of protein kinase G-1α using a bacterial expression system. Protein Expr. Purif. **79:**271-276.

6. **Ahmed, N., and G. E. Rice.** 2005. Strategies for revealing lower abundance proteins in two-dimensional protein maps. Journal of Chromatography B. **815:**39-50. doi: 10.1016/j.jchromb.2004.10.070.

7. **Alberts, B.** 1998. The cell as a collection of protein machines: Preparing the next generation of molecular biologists. Cell. **92:**291-294.

8. **Ankarcrona, M., F. Mangialasche, and B. Winblad.** 2010. Rethinking Alzheimer's disease therapy: Are mitochondria the key? J. Alzheimer's Dis. **20:**S579-S590.

9. **Baig, S., S. A. Joseph, H. Tayler, R. Abraham, M. J. Owen, J. Williams, P. G. Kehoe, and S. Love.** 2010. Distribution and expression of picalm in alzheimer disease. J. Neuropathol. Exp. Neurol. **69:**1071-1077.

10. **Bane, S. E., J. E. Velasquez, and A. S. Robinson.** 2007. Expression and purification of milligram levels of inactive G-protein coupled receptors in E. coli. Protein Expr. Purif. **52:**348-355.

11. **Banerjee, P., J. B. Joo, J. T. Buse, and G. Dawson.** 1995. Differential solubilization of lipids along with membrane proteins by different classes of detergents. Chem. Phys. Lipids. **77:**65-78.

12. **Bastien, Y., and B. D. Mazer.** 1994. Detection of the human platelet-activating factor receptor mRNA in human B lymphocytes by polymerase chain reaction on reverse transcripts (RT-PCR). Biochem. Biophys. Res. Commun. **202:**1373-1379.

13. **Bate, C., L. Rumbold, and A. Williams.** 2007. Cholesterol synthesis inhibitors protect against platelet-activating factor-induced neuronal damage. Journal of Neuroinflammation. **4:**.

14. **Bate, C., L. Rumbold, and A. Williams.** 2007. Cholesterol synthesis inhibitors protect against platelet-activating factor-induced neuronal damage. Journal of Neuroinflammation. **4:**.

15. **Bay, D. C., M. Hafez, M. J. Young, and D. A. Court.** 2012. Phylogenetic and coevolutionary analysis of the β-barrel protein family comprised of mitochondrial porin (VDAC) and Tom40. Biochimica Et Biophysica Acta - Biomembranes. **1818:**1502-1519.

16. **Bekris, L. M., F. Lutz, and C. -. Yu.** 2012. Functional analysis of APOE locus genetic variation implicates regional enhancers in the regulation of both TOMM40 and APOE. J. Hum. Genet. **57:**18-25.

17. **Bennett, S. A. L., J. Chen, B. A. Pappas, D. C. S. Roberts, and M. Tenniswood.** 1998. Platelet activating factor receptor expression is associated with neuronal apoptosis in an in vivo model of excitotoxicity. Cell Death Differ. **5:**867-875.

18. **Benveniste, J., P. M. Henson, and C. G. Cochrane.** 1972. Leukocyte-dependent histamine release from rabbit platelets. The role of IgE, basophils, and a platelet-activating factor. J. Exp. Med. **136:**1356-1377.

19. **Blue, M. L., D. L. Williams, S. Zucker, S. A. Khan, and C. B. Blum.** 1983. Apolipoprotein E synthesis in human kidney, adrenal gland, and liver. Proceedings of the National Academy of Sciences. **80:**283-287.

20. **Bonifacino, J. S., and R. Rojas.** 2006. Retrograde transport from endosomes to the trans-Golgi network. Nature Reviews Molecular Cell Biology. **7:**568-579.

21. **Borner, G. H. H., A. A. Rana, R. Forster, M. Harbour, J. C. Smith, and M. S. Robinson.** 2007. CVAK104 is a novel regulator of clathrin-mediated SNARE sorting. Traffic. **8:**893-903.

22. **Brewer, C., F. Bonin, P. Bullock, M. -. Nault, J. Morin, S. Imbeault, T. Y. Shen, D. J. Franks, and S. A. L. Bennett.** 2002. Platelet activating factor-induced apoptosis is inhibited by ectopic expression of the platelet activating factor G-protein coupled receptor. J. Neurochem. **82:**1502-1511.

23. **Brizzard, B. L., R. G. Chubet, and D. L. Vizard.** 1994. Immunoaffinity purification of FLAG® epitope-tagged bacterial alkaline phosphatase using a novel monoclonal antibody and peptide elution. BioTechniques. **16:**730-732+734.

24. **Brizzard, B. L., R. G. Chubet, and D. L. Vizard.** 1994. Immunoaffinity purification of FLAG® epitope-tagged bacterial alkaline phosphatase using a novel monoclonal antibody and peptide elution. BioTechniques. **16:**730-732+734.

25. **Brookmeyer, R., E. Johnson, K. Ziegler-Graham, and H. M. Arrighi.** 2007. Forecasting the global burden of Alzheimer's disease. Alzheimer's and Dementia. **3:**186-191.

26. **Bruins, A. P.** 1998. Mechanistic aspects of electrospray ionization. Journal of Chromatography A. **794:**345-357.

27. **Bu, G.** 2009. Apolipoprotein e and its receptors in Alzheimer's disease: Pathways, pathogenesis and therapy. Nature Reviews Neuroscience. **10:**333-344.

28. **Bucciantini, M., E. Giannoni, F. Chiti, F. Baroni, L. Formigli, J. Zurdo, N. Taddei, G. Ramponi, C. M. Dobson, and M. Stefani.** 2002. Inherent toxicity of aggregates implies a common mechanism for protein misfolding diseases. Nature. **416:**507-511.

29. **Caplan, S., N. Naslavsky, L. M. Hartnell, R. Lodge, R. S. Polishchuk, J. G. Donaldson, and J. S. Bonifacino.** 2002. A tubular EHD1-containing compartment involved in the recycling of major histocompatibility complex class I molecules to the plasma membrane. EMBO J. **21:**2557-2567.

30. **Chang, S., T. R. Ma, R. D. Miranda, M. E. Balestra, R. W. Mahley, and Y. Huang.** 2005. Lipid- and receptor-binding regions of apolipoprotein E4 fragments act in concert to cause mitochondrial dysfunction and neurotoxicity. Proc. Natl. Acad. Sci. U. S. A. **102:**18694-18699.

31. **Chao, W., H. Liu, D. J. Hanahan, and M. S. Olson.** 1990. Regulation of platelet-activating factor receptor and PAF receptor-mediated arachidonic acid release by protein kinase C activation in rat Kupffer cells. Arch. Biochem. Biophys. **282:**188-197.

32. **Chao, W., H. Liu, D. J. Hanahan, and M. S. Olson.** 1992. Platelet-activating factor-stimulated protein tyrosine phosphorylation and eicosanoid synthesis in rat Kupffer cells. Evidence for calcium-dependent and protein kinase c-dependent and -independent pathways. J. Biol. Chem. **267:**6725-6735.

33. **Chao, W., and M. S. Olson.** 1993. Platelet-activating factor: Receptors and signal transduction. Biochem. J. **292:**617-629.

34. **Chao, W., and M. S. Olson.** 1993. Platelet-activating factor: Receptors and signal transduction. Biochem. J. **292:**617-629.

35. **Chen, C., J. C. Magee, V. Marcheselli, M. Hardy, and N. G. Bazan.** 2001. Attenuated LTP in hippocampal dentate gyrus neurons of mice deficient in the PAF receptor. J. Neurophysiol. **85:**384-390.

36. **Chen, G. I., and A. -. Gingras.** 2007. Affinity-purification mass spectrometry (AP-MS) of serine/threonine phosphatases. Methods. **42:**298-305.

37. **Chevallet, M., V. Santoni, A. Poinas, D. Rouquié, A. Fuchs, S. Kieffer, M. Rossignol, J. Lunardi, J. Garin, and T. Rabilloud.** 1998. New zwitterionic detergents improve the analysis of membrane proteins by two-dimensional electrophoresis. Electrophoresis. **19:**1901-1909.

38. **Chiang, C. M., and R. G. Roeder.** 1993. Expression and purification of general transcription factors by FLAG epitope-tagging and peptide elution. Pept. Res. **6:**62-64.

39. **Choi, H., B. Larsen, Z. -. Lin, A. Breitkreutz, D. Mellacheruvu, D. Fermin, Z. S. Qin, M. Tyers, A. -. Gingras, and A. I. Nesvizhskii.** 2011. SAINT: Probabilistic scoring of affinity purificationg-mass spectrometry data. Nature Methods. **8:**70-73.

40. **Chrétien, M., N. G. Seidah, A. Basak, and M. Mbikay.** 2008. Proprotein convertases as therapeutic targets. Expert Opinion on Therapeutic Targets. **12:**1289-1300.

41. **Christov, N. C., D. N. Ganchev, N. D. Vassileva, N. D. Denkov, K. D. Danov, and P. A. Kralchevsky.** 2002. Capillary mechanisms in membrane emulsification: oil-in-water emulsions stabilized by Tween 20 and milk proteins. Colloids Surf. Physicochem. Eng. Aspects. **209:**83-104.

42. **Collins, M. O., and J. S. Choudhary.** 2008. Mapping multiprotein complexes by affinity purification and mass spectrometry. Curr. Opin. Biotechnol. **19:**324-330.

43. **Corder, E. H., A. M. Saunders, W. J. Strittmatter, D. E. Schmechel, P. C. Gaskell, G. W. Small, A. D. Roses, J. L. Haines, and M. A. Pericak-Vance.** 1993. Gene dose of apolipoprotein E type 4 allele and the risk of Alzheimer's disease in late onset families. Science. **261:**921-923.

44. **Corneveaux, J. J., A. J. Myers, A. N. Allen, J. J. Pruzin, M. Ramirez, A. Engel, M. A. Nalls, K. Chen, W. Lee, K. Chewning, S. E. Villa, H. B. Meechoovet, J. D. Gerber, D. Frost, H. L. Benson, S. O'Reilly, L. B. Chibnik, J. M. Shulman, A. B. Singleton, D. W. Craig, K. R. Van Keuren-Jensen, T. Dunckley, D. A. Bennett, P. L. de Jager, C. Heward, J. Hardy, E. M. Reiman, and M. J. Huentelman.** 2010. Association of CR1, CLU and PICALM with Alzheimer's disease in a cohort of clinically characterized and neuropathologically verified individuals. Hum. Mol. Genet. **19:**3295-3301.

45. **Daulat, A. M., P. Maurice, C. Froment, J. -. Guillaume, C. Broussard, B. Monsarrat, P. Delagrange, and R. Jocker.** 2007. Purification and identification of G protein-coupled receptor protein complexes under native conditions. Molecular and Cellular Proteomics. **6:**835-844.

46. **Denis, N., H. Palmer-Smith, F. Elisma, A. Busuttil, T. G. Wright, M. B. Khalil, A. Prat, N. G. Seidah, M. Chrétien, J. Mayne, and D. Figeys.** 2011. Quantitative proteomic analysis of PCSK9 gain of function in human hepatic HuH7 cells. Journal of Proteome Research. **10:**2011-2026.

47. **Dirnagl, U., C. Iadecola, and M. A. Moskowitz.** 1999. Pathobiology of ischaemic stroke: An integrated view. Trends Neurosci. **22:**391-397.

48. **Dong, L. -., S. Parkin, S. D. Trakhanov, B. Rupp, T. Simmons, K. S. Arnold, Y. M. Newhouse, T. L. Innerarity, and K. H. Weisgraber.** 1996. Novel mechanism for defective receptor binding of apolipoprotein E2 in type III hyperlipoproteinemia. Nat. Struct. Biol. **3:**718-722.

49. **Dong, L. -., and K. H. Weisgraber.** 1996. Human apolipoprotein E4 domain interaction. Arginine 61 and glutamic acid 255 interact to direct the preference for very low density lipoproteins. J. Biol. Chem. **271:**19053-19057.

50. **Dubois, B., H. H. Feldman, C. Jacova, J. L. Cummings, S. T. DeKosky, P. Barberger-Gateau, A. Delacourte, G. Frisoni, N. C. Fox, D. Galasko, S. Gauthier, H. Hampel, G. A. Jicha, K. Meguro, J. O'Brien, F. Pasquier, P. Robert, M. Rossor, S. Salloway, M. Sarazin, L. C. de Souza, Y. Stern, P. J. Visser, and P. Scheltens.** 2010. Revising the definition of Alzheimer's disease: A new lexicon. The Lancet Neurology. **9:**1118-1127.

51. **Duce, J. A., A. Tsatsanis, M. A. Cater, S. A. James, E. Robb, K. Wikhe, S. L. Leong, K. Perez, T. Johanssen, M. A. Greenough, H. -. Cho, D. Galatis, R. D. Moir, C. L. Masters, C. McLean, R. E. Tanzi, R. Cappai, K. J. Barnham, G. D. Ciccotosto, J. T. Rogers, and A. I. Bush.** 2010. Iron-Export Ferroxidase Activity of β-Amyloid Precursor Protein is Inhibited by Zinc in Alzheimer's Disease. Cell. **142:**857-867.

52. **Dupré, D. J., Z. Chen, C. Le Gouill, C. Thériault, J. -. Parent, M. Rola-Pleszczynski, and J. Stankova.** 2003. Trafficking, Ubiquitination, and Down-regulation of the Human Platelet-activating Factor Receptor. J. Biol. Chem. **278:**48228-48235.

53. **DUPREZ, V., M. SMOLJANOVIC, M. LIEB, and A. DAUTRYVARSAT.** 1994. Trafficking of Interleukin-2 and Transferrin in Endosomal Fractions of T-Lymphocytes. J. Cell. Sci. **107:**1289-1295.

54. **Düwel, M., and E. J. Ungewickell.** 2006. Clathrin-dependent association of CVAK104 with endosomes and the trans-Golgi network. Mol. Biol. Cell. **17:**4513-4525.

55. **Einhauer, A., and A. Jungbauer.** 2001. The FLAG™ peptide, a versatile fusion tag for the purification of recombinant proteins. J. Biochem. Biophys. Methods. **49:**455-465.

56. **El-Aneed, A., A. Cohen, and J. Banoub.** 2009. Mass spectrometry, review of the basics: Electrospray, MALDI, and commonly used mass analyzers. Applied Spectroscopy Reviews. **44:**210-230.

57. **Elliott, M. H., D. S. Smith, C. E. Parker, and C. Borchers.** 2009. Current trends in quantitative proteomics. Journal of Mass Spectrometry. **44:**1637-1660.

58. **Ewing, R. M., P. Chu, F. Elisma, H. Li, P. Taylor, S. Climie, L. McBroom-Cerajewski, M. D. Robinson, L. O'Connor, M. Li, R. Taylor, M. Dharsee, Y. Ho, A. Heilbut, L. Moore, S. Zhang, O. Ornatsky, Y. V. Bukhman, M. Ethier, Y. Sheng, J. Vasilescu, M. Abu-Farha, J. -. Lambert, H. S. Duewel, I. I. Stewart, B. Kuehl, K. Hogue, K. Colwill, K. Gladwish, B. Muskat, R. Kinach, S. -. Adams, M. F. Moran, G. B. Morin, T. Topaloglou, and D. Figeys.** 2007. Large-scale mapping of human protein-protein interactions by mass spectrometry. Molecular Systems Biology. **3:**.

59. **Falck, J., J. Coates, and S. P. Jackson.** 2005. Conserved modes of recruitment of ATM, ATR and DNA-PKcs to sites of DNA damage. Nature. **434:**605-611.

60. **Fenn, J. B., M. Mann, C. K. Meng, S. F. Wong, and C. M. Whitehouse.** 1989. Electrospray ionization for mass spectrometry of large biomolecules. Science. **246:**64-71.

61. **Ford, M. G. J., B. M. F. Pearse, M. K. Higgins, Y. Vallis, D. J. Owen, A. Gibson, C. R. Hopkins, P. R. Evans, and H. T. McMahon.** 2001. Simultaneous binding of PtdIns (4,5) P2 and clathrin by AP180 in the nucleation of clathrin lattices on membranes. Science. **291:**1051-1055.

62. **Ford, M. G. J., B. M. F. Pearse, M. K. Higgins, Y. Vallis, D. J. Owen, A. Gibson, C. R. Hopkins, P. R. Evans, and H. T. McMahon.** 2001. Simultaneous binding of PtdIns (4,5) P2 and clathrin by AP180 in the nucleation of clathrin lattices on membranes. Science. **291:**1051-1055.

63. **Galperin, E., S. Benjamin, D. D. Rapaport, R. Rotem-Yehudar, S. Tolchinsky, and M. Horowitz.** 2002. EHD3: A protein that resides in recycling tubular and vesicular membrane structures and interacts with EHD1. Traffic. **3:**575-589.

64. **Gent, J., and I. Braakman.** 2004. Low-density lipoprotein receptor structure and folding. Cellular and Molecular Life Sciences. **61:**2461-2470.

65. **George, M., G. G. Ying, M. A. Rainey, A. Solomon, P. T. Parikh, Q. Gao, V. Band, and H. Band.** 2007. Shared as well as distinct roles of EHD proteins revealed by biochemical and functional comparisons in mammalian cells and C. elegans. BMC Cell Biology. **8:**.

66. **Glatter, T., A. Wepf, R. Aebersold, and M. Gstaiger.** 2009. An integrated workflow for charting the human interaction proteome: Insights into the PP2A system. Molecular Systems Biology. **5:**.

67. **Go, G. -., and A. Mani.** 2012. Low-density lipoprotein receptor (LDLR) family orchestrates cholesterol homeostasis. Yale J. Biol. Med. **85:**19-28.

68. **Goedert, M.** 2001. Alpha-synuclein and neurodegenerative diseases. Nature Reviews Neuroscience. **2:**492-501.

69. **Gohla, A., R. Harhammer, and G. Schultz.** 1998. The G-protein G13 but not G12 mediates signaling from lysophosphatidic acid receptor via epidermal growth factor receptor to Rho. J. Biol. Chem. **273:**4653-4659.

70. **Gokool, S., D. Tattersall, and M. N. J. Seaman.** 2007. EHD1 interacts with retromer to stabilize SNX1 tubules and facilitate endosome-to-golgi retrieval. Traffic. **8:**1873-1886.

71. **Gopalraj, R. K., H. Zhu, J. F. Kelly, M. Mendiondo, J. F. Pulliam, D. A. Bennett, and S. Estus.** 2005. Genetic association of low density lipoprotein receptor and Alzheimer's disease. Neurobiol. Aging. **26:**1-7.

72. **Goshima, N., Y. Kawamura, A. Fukumoto, A. Miura, R. Honma, R. Satoh, A. Wakamatsu, J. -. Yamamoto, K. Kimura, T. Nishikawa, T. Andoh, Y. Iida, K. Ishikawa, E. Ito, N. Kagawa, C. Kaminaga, K. -. Kanehori, B. Kawakami, K. Kenmochi, R. Kimura, M. Kobayashi, T. Kuroita, H. Kuwayama, Y. Maruyama, K. Matsuo, K. Minami, M. Mitsubori, M. Mori, R. Morishita, A. Murase, A. Nishikawa, S. Nishikawa, T. Okamoto, N. Sakagami, Y. Sakamoto, Y. Sasaki, T. Seki, S. Sono, A. Sugiyama, T. Sumiya, T. Takayama, Y. Takayama, H. Takeda, T. Togashi, K. Yahata, H. Yamada, Y. Yanagisawa, Y. Endo, F. Imamoto, Y. Kisu, S. Tanaka, T. Isogai, J. -. Imai, S. Watanabe, and N. Nomura.** 2008. Human protein factory for converting the transcriptome into an in vitro-expressed proteome. Nature Methods. **5:**1011-1017.

73. **Grant, B. D., and J. G. Donaldson.** 2009. Pathways and mechanisms of endocytic recycling. Nature Reviews Molecular Cell Biology. **10:**597-608.

74. **Guo, Q., Z. Wang, H. Li, M. Wiese, and H. Zheng.** 2012. APP physiological and pathophysiological functions: Insights from animal models. Cell Res. **22:**78-89.

75. **Haass, C., and D. J. Selkoe.** 2007. Soluble protein oligomers in neurodegeneration: Lessons from the Alzheimer's amyloid β-peptide. Nature Reviews Molecular Cell Biology. **8:**101-112.

76. **Han, X., A. Aslanian, and J. R. Yates III.** 2008. Mass spectrometry for proteomics. Curr. Opin. Chem. Biol. **12:**483-490.

77. **Hardy, J., and D. J. Selkoe.** 2002. The amyloid hypothesis of Alzheimer's disease: Progress and problems on the road to therapeutics. Science. **297:**353-356.

78. **Harold, D., R. Abraham, P. Hollingworth, R. Sims, A. Gerrish, M. L. Hamshere, J. S. Pahwa, V. Moskvina, K. Dowzell, A. Williams, N. Jones, C. Thomas, A. Stretton, A. R. Morgan, S. Lovestone, J. Powell, P. Proitsi, M. K. Lupton, C. Brayne, D. C. Rubinsztein, M. Gill, B. Lawlor, A. Lynch, K. Morgan, K. S. Brown, P. A. Passmore, D. Craig, B. McGuinness, S. Todd, C. Holmes, D. Mann, A. D. Smith, S. Love, P. G. Kehoe, J. Hardy, S. Mead, N. Fox, M. Rossor, J. Collinge, W. Maier, F. Jessen, B. Schürmann, H. Van Den Bussche, I. Heuser, J. Kornhuber, J. Wiltfang, M. Dichgans, L. Frölich, H. Hampel, M. Hüll, D. Rujescu, A. M. Goate, J. S. K. Kauwe, C. Cruchaga, P. Nowotny, J. C. Morris, K. Mayo, K. Sleegers, K. Bettens, S. Engelborghs, P. P. De Deyn, C. Van Broeckhoven, G.**

Livingston, N. J. Bass, H. Gurling, A. McQuillin, R. Gwilliam, P. Deloukas, A. Al-Chalabi, C. E. Shaw, M. Tsolaki, A. B. Singleton, R. Guerreiro, T. W. Mühleisen, M. M. Nöthen, S. Moebus, K. -. Jöckel, N. Klopp, H. -. Wichmann, M. M. Carrasquillo, V. S. Pankratz, S. G. Younkin, P. A. Holmans, M. O'Donovan, M. J. Owen, and J. Williams. 2009. Genome-wide association study identifies variants at CLU and PICALM associated with Alzheimer's disease. Nat. Genet. **41:**1088-1093.

79. **Hart, D. A.** 1975. Studies on Nonidet P40 lysis of murine lymphoid cells. I. Use of cholera toxin and cell surface Ig to determine degree of dissociation of the plasma membrane. Journal of Immunology. **115:**871-875.

80. **Hashimoto, M., E. Rockenstein, M. Mante, M. Mallory, and E. Masliah.** 2001. beta-synuclein inhibits alpha-synuclein aggregation: A possible role as an anti-parkinsonian factor. Neuron. **32:**213-223. doi: 10.1016/S0896-6273(01)00462-7.

81. **Hatters, D. M., C. A. Peters-Libeu, and K. H. Weisgraber.** 2006. Apolipoprotein E structure: insights into function. Trends Biochem. Sci. **31:**445-454.

82. **Heiss, W. -.** 2000. Ischemic penumbra: Evidence from functional imaging in man. Journal of Cerebral Blood Flow and Metabolism. **20:**1276-1293.

83. **Hellman, N. E., E. A. Grant, and A. M. Goate.** 1998. Failure to replicate a protective effect of allele 2 of NACP/α- Synuclein polymorphism in Alzheimer's disease: An association study. Ann. Neurol. **44:**278-281.

84. **Henningsen, R., B. L. Gale, K. M. Straub, and D. C. DeNagel.** 2002. Application of zwitterionic detergents to the solubilization of integral membrane proteins for two-dimensional gel electrophoresis and mass spectrometry. Proteomics. **2:**1479-1488.

85. **Herrup, K.** 2010. Reimagining Alzheimer's disease - An age-based hypothesis. Journal of Neuroscience. **30:**16755-16762.

86. **Hjertén, S., and K. -. Johansson.** 1972. Selective solubilization with tween 20 of membrane proteins from Acholeplasma laidlawii. BBA - Biomembranes. **288:**312-325.

87. **Ho, Y., A. Gruhler, A. Heilbut, G. D. Bader, L. Moore, S. -. Adams, A. Millar, P. Taylor, K. Bennett, K. Boutilier, L. Yang, C. Wolting, I. Donaldson, S. Schandorff, J. Shewnarane, M. Vo, J. Taggart, M. Goudreault, B. Muskat, C. Alfarano, D. Dewar, Z. Lin, K. Michalickova, A. R. Willems, H. Sassi, P. A. Nielsen, K. J. Rasmussen, J. R. Andersen, L. E. Johansen, L. H. Hansen, H. Jespersen, A. Podtelejnikov, E. Nielsen, J. Crawford, V. Poulsen, B. D. Sørensen, J. Matthiesen, R. C. Hendrickson, F. Gleeson, T. Pawson, M. F. Moran, D. Durocher, M. Mann, C. W. V. Hogue, D. Figeys, and M. Tyers.** 2002. Systematic identification of protein complexes in Saccharomyces cerevisiae by mass spectrometry. Nature. **415:**180-183.

88. **Hu, J., H. Qin, F. P. Gao, and T. A. Cross.** 2011. A systematic assessment of mature MBP in membrane protein production: Overexpression, membrane targeting and purification. Protein Expr. Purif. **80:**34-40.

89. **Hu, Q., R. J. Noll, H. Li, A. Makarov, M. Hardman, and R. G. Cooks.** 2005. The Orbitrap: A new mass spectrometer. Journal of Mass Spectrometry. **40:**430-443.

90. **Huang, D. W., B. T. Sherman, and R. A. Lempicki.** 2009. Systematic and integrative analysis of large gene lists using DAVID bioinformatics resources. Nature Protocols. **4:**44-57. doi: 10.1038/nprot.2008.211.

91. **Iqbal, K., A. Del C. Alonso, S. Chen, M. O. Chohan, E. El-Akkad, C. -. Gong, S. Khatoon, B. Li, F. Liu, A. Rahman, H. Tanimukai, and I. Grundke-Iqbal.** 2005. Tau pathology in Alzheimer disease and other tauopathies. Biochimica Et Biophysica Acta - Molecular Basis of Disease. **1739:**198-210.

92. **Ishii, S., Y. Matsuda, M. Nakamura, I. Waga, K. Kume, T. Izumi, and T. Shimizu.** 1996. A murine platelet-activating factor receptor gene: Cloning, chromosomal localization and up-regulation of expression by lipopolysaccharide in peritoneal resident macrophages. Biochem. J. **314:**671-678.

93. **Ishii, S., and T. Shimizu.** 2000. Platelet-activating factor (PAF) receptor and genetically engineered PAF receptor mutant mice. Prog. Lipid Res. **39:**41-82.

94. **Ito, T., T. Chiba, R. Ozawa, M. Yoshida, M. Hattori, and Y. Sakaki.** 2001. A comprehensive two-hybrid analysis to explore the yeast protein interactome. Proc. Natl. Acad. Sci. U. S. A. **98:**4569-4574.

95. **Jankowsky, J. L., D. J. Fadale, J. Anderson, G. M. Xu, V. Gonzales, N. A. Jenkins, N. G. Copeland, M. K. Lee, L. H. Younkin, S. L. Wagner, S. G. Younkin, and D. R. Borchelt.** 2004. Mutant presenilins specifically elevate the levels of the 42 residue β-amyloid peptide in vivo: Evidence for augmentation of a 42-specific γ secretase. Hum. Mol. Genet. **13:**159-170.

96. **Javitch, J. A.** 2004. The ants go marching two by two: Oligomeric structure of G-protein-coupled receptors. Mol. Pharmacol. **66:**1077-1082.

97. **Jeon, H., and S. C. Blacklow.** 2005. Structure and physiologic function of the low-density lipoprotein receptor. Annual Review of Biochemistry. **74:**535-562.

98. **Ji, Z. -., R. Dennis Miranda, Y. M. Newhouse, K. H. Weisgraberyadong Huang, and R. W. Mahley.** 2002. Apolipoprotein E4 potentiates amyloid β peptide-induced lysosomal leakage and apoptosis in neuronal cells. J. Biol. Chem. **277:**21821-21828.

99. **Johnson, S. C., A. La Rue, B. P. Hermann, G. Xu, R. L. Koscik, E. M. Jonaitis, B. B. Bendlin, K. J. Hogan, A. D. Roses, A. M. Saunders, M. W. Lutz, S. Asthana, R. C. Green, and M. A. Sager.** 2011. The effect of TOMM40 poly-T length on gray matter volume and

cognition in middle-aged persons with APOE ε3/ε3 genotype. Alzheimer's and Dementia. **7:**456-465.

100. **Jørgensen, M. M., O. N. Jensen, H. U. Holst, J. -. Hansen, T. J. Corydon, P. Bross, L. Bolund, and N. Gregersen.** 2000. Grp78 is involved in retention of mutant low density lipoprotein receptor protein in the endoplasmic reticulum. J. Biol. Chem. **275:**33861-33868.

101. **Jović, M., N. Naslavsky, D. Rapaport, M. Horowitz, and S. Caplan.** 2007. EHD1 regulates β1 integrin endosomal transport: Effects on focal adhesion, cell spreading and migration. J. Cell. Sci. **120:**802-814.

102. **Jun, G., A. C. Naj, G. W. Beecham, L. -. Wang, J. Buros, P. J. Gallins, J. D. Buxbaum, N. Ertekin-Taner, M. D. Fallin, R. Friedland, R. Inzelberg, P. Kramer, E. Rogaeva, P. St George-Hyslop, L. B. Cantwell, B. A. Dombroski, A. J. Saykin, E. M. Reiman, D. A. Bennett, J. C. Morris, K. L. Lunetta, E. R. Martin, T. J. Montine, A. M. Goate, D. Blacker, D. W. Tsuang, D. Beekly, L. A. Cupples, H. Hakonarson, W. Kukull, T. M. Foroud, J. Haines, R. Mayeux, L. A. Farrer, M. A. Pericak-Vance, and G. D. Schellenberg.** 2010. Meta-analysis confirms CR1, CLU, and PICALM as Alzheimer disease risk loci and reveals interactions with APOE genotypes. Arch. Neurol. **67:**1473-1484.

103. **Kamboh, M. I., R. L. Minster, F. Y. Demirci, M. Ganguli, S. T. DeKosky, O. L. Lopez, and M. M. Barmada.** 2012. Association of CLU and PICALM variants with Alzheimer's disease. Neurobiol. Aging. **33:**518-521.

104. **Kato, K., G. D. Clark, N. G. Bazan, and C. F. Zorumski.** 1994. Platelet-activating factor as a potential retrograde messenger in CA1 hippocampal long-term potentiation. Nature. **367:**175-179.

105. **Kayed, R., E. Head, J. L. Thompson, T. M. McIntire, S. C. Milton, C. W. Cotman, and C. G. Glabel.** 2003. Common structure of soluble amyloid oligomers implies common mechanism of pathogenesis. Science. **300:**486-489.

106. **Keshava Prasad, T. S., R. Goel, K. Kandasamy, S. Keerthikumar, S. Kumar, S. Mathivanan, D. Telikicherla, R. Raju, B. Shafreen, A. Venugopal, L. Balakrishnan, A. Marimuthu, S. Banerjee, D. S. Somanathan, A. Sebastian, S. Rani, S. Ray, C. J. Harrys Kishore, S. Kanth, M. Ahmed, M. K. Kashyap, R. Mohmood, Y. I. Ramachandra, V. Krishna, B. A. Rahiman, S. Mohan, P. Ranganathan, S. Ramabadran, R. Chaerkady, and A. Pandey.** 2009. Human Protein Reference Database - 2009 update. Nucleic Acids Res. **37:**D767-D772.

107. **Kim, J., J. M. Basak, and D. M. Holtzman.** 2009. The Role of Apolipoprotein E in Alzheimer's Disease. Neuron. **63:**287-303.

108. **Kim, J., J. M. Castellano, H. Jiang, J. M. Basak, M. Parsadanian, V. Pham, S. M. Mason, S. M. Paul, and D. M. Holtzman.** 2009. Overexpression of Low-Density Lipoprotein

Receptor in the Brain Markedly Inhibits Amyloid Deposition and Increases Extracellular Aβ Clearance. Neuron. **64:**632-644.

109. **Kim, J., J. M. Castellano, H. Jiang, J. M. Basak, M. Parsadanian, V. Pham, S. M. Mason, S. M. Paul, and D. M. Holtzman.** 2009. Overexpression of Low-Density Lipoprotein Receptor in the Brain Markedly Inhibits Amyloid Deposition and Increases Extracellular Aβ Clearance. Neuron. **64:**632-644.

110. **Knappik, A., and A. Pluckthun.** 1994. An improved affinity tag based on the FLAG® peptide for the detection and purification of recombinant antibody fragments. BioTechniques. **17:**754-761.

111. **Korwek, K. M., J. H. Trotter, M. J. Ladu, P. M. Sullivan, and E. J. Weeber.** 2009. Apoe isoform-dependent changes in hippocampal synaptic function. Molecular Neurodegeneration. **4:**.

112. **Kowal, R. C., J. Herz, J. L. Goldstein, V. Esser, and M. S. Brown.** 1989. Low density lipoprotein receptor-related protein mediates uptake of cholesteryl esters derived from apoprotein E-enriched lipoproteins. Proc. Natl. Acad. Sci. U. S. A. **86:**5810-5814.

113. **Kozasa, T., N. Hajicek, C. R. Chow, and N. Suzuki.** 2011. Signalling mechanisms of RhoGTPase regulation by the heterotrimeric G proteins G12 and G13. J. Biochem. **150:**357-369.

114. **Krausz, C., G. Gervasi, G. Forti, and E. Baldi.** 1994. Effect of platelet-activating factor on motility and acrosome reaction of human spermatozoa. Human Reproduction. **9:**471-476.

115. **Kyriazis, G. A., Z. Wei, M. Vandermey, D. -. Jo, O. Xin, M. P. Mattson, and S. L. Chan.** 2008. Numb endocytic adapter proteins regulate the transport and processing of the amyloid precursor protein in an isoform-dependent manner: Implications for Alzheimer disease pathogenesis. J. Biol. Chem. **283:**25492-25502.

116. **Lambert, J. -., S. Heath, G. Even, D. Campion, K. Sleegers, M. Hiltunen, O. Combarros, D. Zelenika, M. J. Bullido, B. Tavernier, L. Letenneur, K. Bettens, C. Berr, F. Pasquier, N. Fiévet, P. Barberger-Gateau, S. Engelborghs, P. De Deyn, I. Mateo, A. Franck, S. Helisalmi, E. Porcellini, O. Hanon, M. M. De Pancorbo, C. Lendon, C. Dufouil, C. Jaillard, T. Leveillard, V. Alvarez, P. Bosco, M. Mancuso, F. Panza, B. Nacmias, P. Boss, P. Piccardi, G. Annoni, D. Seripa, D. Galimberti, D. Hannequin, F. Licastro, H. Soininen, K. Ritchie, H. Blanché, J. -. Dartigues, C. Tzourio, I. Gut, C. Van Broeckhoven, A. Alpérovitch, M. Lathrop, P. Amouyel, B. Arosio, E. Coto, M. D. Zompo, V. Deramecourt, J. Epelbaum, P. Forti, A. Brice, R. Ferri, E. Scarpini, G. Siciliano, V. Solfrizzi, S. Sorbi, G. Spalletta, G. Ravaglia, J. Sahel, F. Valdivieso, S. Vepsäläinen, and A. Pilotto.** 2009. Genome-wide association study identifies variants at CLU and CR1 associated with Alzheimer's disease. Nat. Genet. **41:**1094-1099.

117. **Lämsä, R., S. Helisalmi, S. -. Herukka, T. Tapiola, T. Pirttilä, S. Vepsäläinen, M. Hiltunen, and H. Soininen.** 2008. Genetic study evaluating LDLR polymorphisms and Alzheimer's disease. Neurobiol. Aging. **29:**848-855.

118. **Lämsä, R., S. Helisalmi, S. -. Herukka, T. Tapiola, T. Pirttilä, S. Vepsäläinen, M. Hiltunen, and H. Soininen.** 2008. Genetic study evaluating LDLR polymorphisms and Alzheimer's disease. Neurobiol. Aging. **29:**848-855.

119. **Lee, A. S.** 2005. The ER chaperone and signaling regulator GRP78/BiP as a monitor of endoplasmic reticulum stress. Methods. **35:**373-381.

120. **Lee, B. -., K. -. Jung, C. Son, H. Kim, N. C. VerBerkmoes, B. Arshava, F. Naider, and J. M. Becker.** 2007. Affinity purification and characterization of a G-protein coupled receptor, Saccharomyces cerevisiae Ste2p. Protein Expr. Purif. **56:**62-71.

121. **Lee, D., S. Lee, E. Lee, C. Chang, and S. Paik.** 2002. alpha-Synuclein exhibits competitive interaction between calmodulin and synthetic membranes. J. Neurochem. **82:**1007-1017. doi: 10.1046/j.1471-4159.2002.01024.x.

122. **Lee, D., J. Ha, Y. Kim, K. Bae, J. Park, W. S. Choi, H. S. Yoon, S. G. Park, B. C. Park, G. Yi, and S. Chi.** 2011. Interaction of a putative BH3 domain of clusterin with anti-apoptotic Bcl-2 family proteins as revealed by NMR spectroscopy. Biochem. Biophys. Res. Commun. **408:**541-547. doi: 10.1016/j.bbrc.2011.04.054.

123. **Leskov, K., D. Klokov, J. Li, T. Kinsella, and D. Boothman.** 2003. Synthesis and functional analyses of nuclear clusterin, a cell death protein. J. Biol. Chem. **278:**11590-11600. doi: 10.1074/jbc.M209233200.

124. **Leskov, K., D. Klokov, J. Li, T. Kinsella, and D. Boothman.** 2003. Synthesis and functional analyses of nuclear clusterin, a cell death protein. J. Biol. Chem. **278:**11590-11600. doi: 10.1074/jbc.M209233200.

125. **Leuner, K., S. Hauptmann, R. Abdel-Kader, I. Scherping, U. Keil, J. B. Strosznajder, A. Eckert, and W. E. Müller.** 2007. Mitochondrial dysfunction: The first domino in brain aging and Alzheimer's disease? Antioxidants and Redox Signaling. **9:**1659-1675.

126. **Li, H., B. Wang, Z. Wang, Q. Guo, K. Tabuchi, R. E. Hammer, T. C. Südhof, and H. Zheng.** 2010. Soluble amyloid precursor protein (APP) regulates transthyretin and Klotho gene expression without rescuing the essential function of APP. Proc. Natl. Acad. Sci. U. S. A. **107:**17362-17367.

127. **Limviphuvadh, V., S. Tanaka, S. Goto, K. Ueda, and M. Kanehisa.** 2007. The commonality of protein interaction networks determined in neurodegenerative disorders (NDDs). Bioinformatics. **23:**2129-2138. doi: 10.1093/bioinformatics/btm307.

128. **Lin, Q., S. Weis, G. Yang, Y. -. Weng, R. Helston, K. Rish, A. Smith, J. Bordner, T. Polte, F. Gaunitz, and P. A. Dennery.** 2007. Heme oxygenase-1 protein localizes to the nucleus and activates transcription factors important in oxidative stress. J. Biol. Chem. **282:**20621-20633.

129. **Lin, S. X., B. Grant, D. Hirsh, and F. R. Maxfield.** 2001. Rme-1 regulates the distribution and function of the endocytic recycling compartment in mammalian cells. Nat. Cell Biol. **3:**567-572.

130. **Linnertz, C., A. M. Saunders, M. W. Lutz, D. M. Crenshaw, I. Grossman, D. K. Burns, K. E. Whitfield, M. A. Hauser, J. J. McCarthy, M. Ulmer, R. Allingham, K. A. Welsh-Bohmer, A. D. Roses, and O. Chiba-Falek.** 2012. Characterization of the poly-t variant in the tomm40 gene in diverse populations. PLoS ONE. **7:**.

131. **Lippa, C. F., H. Fujiwara, D. M. A. Mann, B. Giasson, M. Baba, M. L. Schmidt, L. E. Nee, B. O'Connell, D. A. Pollen, P. St. George-Hyslop, B. Ghetti, D. Nochlin, T. D. Bird, N. J. Cairns, V. M. -. Lee, T. Iwatsubo, and J. Q. Trojanowski.** 1998. Lewy bodies contain altered α-synuclein in brains of many familial Alzheimer's disease patients with mutations in presenilin and amyloid precursor protein genes. Am. J. Pathol. **153:**1365-1370.

132. **Liu, B., Y. Zheng, T. -. Wang, H. -. Xu, L. Xia, J. Zhang, Y. -. Wu, G. -. Chen, and L. -. Wang.** 2012. Proteomic identification of common scf ubiquitin ligase FBXO6-interacting glycoproteins in three kinds of cells. Journal of Proteome Research. **11:**1773-1781.

133. **Liu, G., J. Zhang, B. Larsen, C. Stark, A. Breitkreutz, Z. -. Lin, B. -. Breitkreutz, Y. Ding, K. Colwill, A. Pasculescu, T. Pawson, J. L. Wrana, A. I. Nesvizhskii, B. Raught, M. Tyers, and A. -. Gingras.** 2010. ProHits: Integrated software for mass spectrometry-based interaction proteomics. Nat. Biotechnol. **28:**1015-1017.

134. **Maere, S., K. Heymans, and M. Kuiper.** 2005. BiNGO: A Cytoscape plugin to assess overrepresentation of Gene Ontology categories in Biological Networks. Bioinformatics. **21:**3448-3449.

135. **Magnin, T., C. Fiez-Vandal, N. Potier, A. Coquard, I. Leray, T. Steffan, C. Logez, F. Alkhalfioui, F. Pattus, and R. Wagner.** 2009. A novel, generic and effective method for the rapid purification of G protein-coupled receptors. Protein Expr. Purif. **64:**1-7.

136. **Magnin, T., C. Fiez-Vandal, N. Potier, A. Coquard, I. Leray, T. Steffan, C. Logez, F. Alkhalfioui, F. Pattus, and R. Wagner.** 2009. A novel, generic and effective method for the rapid purification of G protein-coupled receptors. Protein Expr. Purif. **64:**1-7.

137. **Mahley, R. W., K. H. Weisgraber, and Y. Huang.** 2009. Apolipoprotein E: structure determines function, from atherosclerosis to Alzheimer's disease to AIDS. J. Lipid Res. **50 Suppl:**S183-188.

138. **Mancia, F., and J. Love.** 2010. High-throughput expression and purification of membrane proteins. J. Struct. Biol. **172:**85-93.

139. **Manolio, T. A., F. S. Collins, N. J. Cox, D. B. Goldstein, L. A. Hindorff, D. J. Hunter, M. I. McCarthy, E. M. Ramos, L. R. Cardon, A. Chakravarti, J. H. Cho, A. E. Guttmacher, A. Kong, L. Kruglyak, E. Mardis, C. N. Rotimi, M. Slatkin, D. Valle, A. S. Whittemore, M. Boehnke, A. G. Clark, E. E. Eichler, G. Gibson, J. L. Haines, T. F. C. MacKay, S. A. McCarroll, and P. M. Visscher.** 2009. Finding the missing heritability of complex diseases. Nature. **461:**747-753.

140. **Marin, R., C. M. Ramírez, M. González, E. González-Muñoz, A. Zorzano, M. Camps, R. Alonso, and M. Díaz.** 2007. Voltage-dependent anion channel (VDAC) participates in amyloid beta-induced toxicity and interacts with plasma membrane estrogen receptor α in septal and hippocampal neurons. Mol. Membr. Biol. **24:**148-160.

141. **Maruszak, A., B. Pepłońska, K. Safranow, M. Chodakowska-Zebrowska, M. Barcikowska, and C. Zekanowski.** 2012. TOMM40 rs10524523 polymorphism's role in late-onset Alzheimer's disease and in longevity. J. Alzheimer's Dis. **28:**309-322.

142. **Marzolo, M. -., and G. Bu.** 2009. Lipoprotein receptors and cholesterol in APP trafficking and proteolytic processing, implications for Alzheimer's disease. Seminars in Cell and Developmental Biology. **20:**191-200.

143. **Mathias, R. A., Y. -. Chen, E. A. Kapp, D. W. Greening, S. Mathivanan, and R. J. Simpson.** 2011. Triton X-114 phase separation in the isolation and purification of mouse liver microsomal membrane proteins. Methods. **54:**396-406.

144. **Mathisen, P. M.** 2003. Gene discovery and validation for neurodegenerative diseases. Drug Discov. Today. **8:**39-46.

145. **Matsubara, M., H. Yamagata, K. Kamino, T. Nomura, K. Kohara, I. Kondo, and T. Miki.** 2001. Genetic association between Alzheimer disease and the alpha-synuclein gene. Dement. Geriatr. Cogn. Disord. **12:**106-109.

146. **Mattson, M. P., D. S. Gary, S. L. Chan, and W. Duan.** 2001. Perturbed endoplasmic reticulum function, synaptic apoptosis and the pathogenesis of Alzheimer's disease. Biochemical Society Symposium. **67:**151-162.

147. **Maxfield, F. R., and T. E. McGraw.** 2004. Endocytic recycling. Nature Reviews Molecular Cell Biology. **5:**121-132.

148. **Maxwell, K. N., E. A. Fisher, and J. L. Breslow.** 2005. Overexpression of PCSK9 accelerates the degradation of the LDLR in a post-endoplasmic reticulum compartment. Proc. Natl. Acad. Sci. U. S. A. **102:**2069-2074.

149. **May, P. C., M. Lampert-Etchells, S. A. Johnson, J. Poirier, J. N. Masters, and C. E. Finch.** 1990. Dynamics of gene expression for a hippocampal glycoprotein elevated in Alzheimer's disease and in response to experimental lesions in rat. Neuron. **5:**831-839.

150. **McMahon, H. T., and E. Boucrot.** 2011. Molecular mechanism and physiological functions of clathrin-mediated endocytosis. Nature Reviews Molecular Cell Biology. **12:**517-533.

151. **Miller, S. E., D. A. Sahlender, S. C. Graham, S. Höning, M. S. Robinson, A. A. Peden, and D. J. Owen.** 2011. The molecular basis for the endocytosis of small R-SNAREs by the clathrin adaptor CALM. Cell. **147:**1118-1131.

152. **Mills, I. G., G. J. K. Praefcke, Y. Vallis, B. J. Peter, L. E. Olesen, J. L. Gallop, P. J. G. Butler, P. R. Evans, and H. T. McMahon.** 2003. Epsinr: An AP1/clathrin interacting protein involved in vesicle trafficking. J. Cell Biol. **160:**213-222.

153. **Moreira, P. I., C. Carvalho, X. Zhu, M. A. Smith, and G. Perry.** 2010. Mitochondrial dysfunction is a trigger of Alzheimer's disease pathophysiology. Biochimica Et Biophysica Acta - Molecular Basis of Disease. **1802:**2-10.

154. **Mulder, M., P. J. Jansen, B. J. A. Janssen, W. D. J. Van De Berg, H. Van Der Boom, L. M. Havekes, R. E. De Kloet, F. C. S. Ramaekers, and A. Blokland.** 2004. Low-density lipoprotein receptor-knockout mice display impaired spatial memory associated with a decreased synaptic density in the hippocampus. Neurobiol. Dis. **16:**212-219.

155. **Nagabhushana, A., M. L. Chalasani, N. Jain, V. Radha, N. Rangaraj, D. Balasubramanian, and G. Swarup.** 2010. Regulation of endocytic trafficking of transferrin receptor by optineurin and its impairment by a glaucoma-associated mutant. BMC Cell Biology. **11:**.

156. **Naslavsky, N., M. Boehm, P. S. Backlund Jr., and S. Caplan.** 2004. Rabenosyn-5 and EHD1 Interact and Sequentially Regulate Protein Recycling to the Plasma Membrane. Mol. Biol. Cell. **15:**2410-2422.

157. **Naslavsky, N., and S. Caplan.** 2005. C-terminal EH-domain-containing proteins: Consensus for a role in endocytic trafficking, EH? J. Cell. Sci. **118:**4093-4101.

158. **Naslavsky, N., and S. Caplan.** 2011. EHD proteins: Key conductors of endocytic transport. Trends Cell Biol. **21:**122-131.

159. **Naslavsky, N., J. Rahajeng, D. Rapaport, M. Horowitz, and S. Caplan.** 2007. EHD1 regulates cholesterol homeostasis and lipid droplet storage. Biochem. Biophys. Res. Commun. **357:**792-799.

160. **Naslavsky, N., J. Rahajeng, M. Sharma, M. Jović, and S. Caplan.** 2006. Interactions between EHD proteins and Rab11-FIP2: A role for EHD3 in early endosomal transport. Mol. Biol. Cell. **17:**163-177.

161. **Nassoury, N., D. A. Blasiole, A. Tebon Oler, S. Benjannet, J. Hamelin, V. Poupon, P. S. McPherson, A. D. Attie, A. Prat, and N. G. Seidah.** 2007. The cellular trafficking of the secretory proprotein convertase PCSK9 and its dependence on the LDLR. Traffic. **8:**718-732.

162. **Nassoury, N., D. A. Blasiole, A. Tebon Oler, S. Benjannet, J. Hamelin, V. Poupon, P. S. McPherson, A. D. Attie, A. Prat, and N. G. Seidah.** 2007. The cellular trafficking of the secretory proprotein convertase PCSK9 and its dependence on the LDLR. Traffic. **8:**718-732.

163. **Nishida, K., and S. P. Markey.** 1996. Platelet-activating factor in brain regions after transient ischemia in gerbils. Stroke. **27:**514-519.

164. **Nuutinen, T., T. Suuronen, A. Kauppinen, and A. Salminen.** 2009. Clusterin: A forgotten player in Alzheimer's disease. Brain Res. Rev. **61:**89-104.

165. **Oldham, W. M., and H. E. Hamm.** 2008. Heterotrimeric G protein activation by G-protein-coupled receptors. Nature Reviews Molecular Cell Biology. **9:**60-71.

166. **Onuchic, A. C., C. M. L. MacHado, R. F. Saito, F. J. Rios, S. Jancar, and R. Chammas.** 2012. Expression of PAFR as part of a prosurvival response to chemotherapy: A novel target for combination therapy in melanoma. Mediators Inflamm. **2012:**.

167. **Pang, L., T. Sawada, S. J. Decker, and A. R. Saltiel.** 1995. Inhibition of MAP kinase kinase blocks the differentiation of PC-12 cells induced by nerve growth factor. J. Biol. Chem. **270:**13585-13588.

168. **Park, J., and P. Lansbury.** 2003. beta-synuclein inhibits formation of alpha-synuclein protofibrils: A possible therapeutic strategy against Parkinson's disease. Biochemistry (N. Y.). **42:**3696-3700. doi: 10.1021/bi020604a.

169. **Parrish, J. R., K. D. Gulyas, and R. L. Finley Jr.** 2006. Yeast two-hybrid contributions to interactome mapping. Curr. Opin. Biotechnol. **17:**387-393.

170. **Payami, H., D. M. Kay, C. P. Zabetian, G. D. Schellenberg, S. A. Factor, and C. C. McCulloch.** 2010. Visualizing disease associations: Graphic analysis of frequency distributions as a function of age using moving average plots (MAP) with application to Alzheimer's and Parkinson's disease. Genet. Epidemiol. **34:**92-99.

171. **Peri, S., J. D. Navarro, R. Amanchy, T. Z. Kristiansen, C. K. Jonnalagadda, V. Surendranath, V. Niranjan, B. Muthusamy, T. K. B. Gandhi, M. Gronborg, N. Ibarrola, N. Deshpande, K. Shanker, H. N. Shivashankar, B. P. Rashmi, M. A. Ramya, Z. Zhao, K. N. Chandrika, N. Padma, H. C. Harsha, A. J. Yatish, M. P. Kavitha, M. Menezes, D. R. Choudhury, S. Suresh, N. Ghosh, R. Saravana, S. Chandran, S. Krishna, M. Joy, S. K. Anand, V. Madavan, A. Joseph, G. W. Wong, W. P. Schiemann, S. N. Constantinescu, L. Huang, R. Khosravi-Far, H. Steen, M. Tewari, S. Ghaffari, G. C. Blobe, C. V. Dang, J. G. N. Garcia, J. Pevsner, O. N. Jensen, P. Roepstorff, K. S. Deshpande, A. M. Chinnaiyan, A. Hamosh, A. Chakravarti, and A. Pandey.** 2003. Development of human protein reference

database as an initial platform for approaching systems biology in humans. Genome Res. **13:**2363-2371.

172. **Perkins, D., D. Pappin, D. Creasy, and J. Cottrell.** 1999. Probability-based protein identification by searching sequence databases using mass spectrometry data. Electrophoresis. **20:**3551-3567. doi: 10.1002/(SICI)1522-2683(19991201)20:18<3551::AID-ELPS3551>3.0.CO;2-2.

173. **Pillot, T., L. Lins, J. Najib, R. Brasseur, and M. Rosseneu.** 1997. Interaction of human apoE with the fusogenic C-terminal Alzheimer's β-amyloid peptide is mediated by the lipid-binding domain of apoE. Atherosclerosis. **134:**378-379. doi: 10.1016/S0021-9150(97)89917-0.

174. **Pomara, N., D. Bruno, J. J. Nierenberg, J. J. Sidtis, F. T. Martiniuk, P. D. Mehta, H. Zetterberg, and K. Blennow.** 2011. TOMM40 poly-T variants and cerebrospinal fluid amyloid beta levels in the elderly. Neurochem. Res. **36:**1124-1128.

175. **Pomara, N., D. Bruno, J. J. Sidtis, M. W. Lutz, D. J. Greenblatt, A. M. Saunders, and A. D. Roses.** 2011. Translocase of outer mitochondrial membrane 40 homolog (TOMM40) poly-T length modulates lorazepam-related cognitive toxicity in healthy APOE ε4-negative elderly. J. Clin. Psychopharmacol. **31:**544-546.

176. **Potkin, S. G., G. Guffanti, A. Lakatos, J. A. Turner, F. Kruggel, J. H. Fallon, A. J. Saykin, A. Orro, S. Lupoli, E. Salvi, M. Weiner, and F. Macciardi.** 2009. Hippocampal atrophy as a quantitative trait in a genome-wide association study identifying novel susceptibility genes for Alzheimer's Disease. PLoS ONE. **4:**.

177. **Prescott, S. M., G. A. Zimmerman, D. M. Stafforini, and T. M. McIntyre.** 2000. Platelet-activating factor and related lipid mediators. Annual Review of Biochemistry. **69:**419-445.

178. **Puglielli, L., R. E. Tanzi, and D. M. Kovacs.** 2003. Alzheimer's disease: The cholesterol connection. Nat. Neurosci. **6:**345-351.

179. **Querfurth, H. W., and F. M. LaFerla.** 2010. Alzheimer's disease. N. Engl. J. Med. **362:**329-344.

180. **Rabilloud, T.** 1990. Mechanisms of protein silver staining in polyacrylamide gels: A 10-year synthesis. Electrophoresis. **11:**785-794.

181. **Rahajeng, J., S. S. P. Giridharan, N. Naslavsky, and S. Caplan.** 2010. Collapsin response mediator protein-2 (Crmp2) regulates trafficking by linking endocytic regulatory proteins to dynein motors. J. Biol. Chem. **285:**31918-31922.

182. **Ramírez, C. M., M. González, M. Díaz, R. Alonso, I. Ferrer, G. Santpere, B. Puig, G. Meyer, and R. Marin.** 2009. VDAC and ERα interaction in caveolae from human cortex is altered in Alzheimer's disease. Molecular and Cellular Neuroscience. **42:**172-183.

183. **Rapaport, D., W. Auerbach, N. Naslavsky, M. Pasmanik-Chor, E. Galperin, A. Fein, S. Caplan, A. L. Joyner, and M. Horowitz.** 2006. Recycling to the plasma membrane is delayed in EHD1 knockout mice. Traffic. **7:**52-60.

184. **Raponi, M., R. T. Belly, J. E. Karp, J. E. Lancet, D. Atkins, and Y. Wang.** 2004. Microarray analysis reveals genetic pathways modulated by tipifarnib in acute myeloid leukemia. BMC Cancer. **4:**.

185. **Reddy, K. B., G. Jin, M. C. Karode, J. A. K. Harmony, and P. H. Howe.** 1996. Transforming growth factor β (TGFβ)-induced nuclear localization of apolipoprotein J/clusterin in epithelial cells. Biochemistry (N. Y.). **35:**6157-6163.

186. **Richardson, R. M., B. Haribabu, H. Ali, and R. Snyderman.** 1996. Cross-desensitization among receptors for platelet activating factor and peptide chemoattractants: Evidence for independent regulatory pathways. J. Biol. Chem. **271:**28717-28724.

187. **Rigaut, G., A. Shevchenko, B. Rutz, M. Wilm, M. Mann, and B. Seraphin.** 1999. A generic protein purification method for protein complex characterization and proteome exploration. Nat. Biotechnol. **17:**1030-1032.

188. **Riobo, N. A., and D. R. Manning.** 2005. Receptors coupled to heterotrimeric G proteins of the G12 family. Trends Pharmacol. Sci. **26:**146-154.

189. **Rios, F. J. O., M. M. Koga, M. Ferracini, and S. Jancar.** 2012. Co-stimulation of PAFR and CD36 is required for oxLDL-induced human macrophages activation. PLoS ONE. **7:**.

190. **Rohner, T. C., N. Lion, and H. H. Girault.** 2004. Electrochemical and theoretical aspects of electrospray ionisation. Physical Chemistry Chemical Physics. **6:**3056-3068.

191. **Rosenbaum, D. M., S. G. F. Rasmussen, and B. K. Kobilka.** 2009. The structure and function of G-protein-coupled receptors. Nature. **459:**356-363.

192. **Roses, A. D., M. W. Lutz, H. Amrine-Madsen, A. M. Saunders, D. G. Crenshaw, S. S. Sundseth, M. J. Huentelman, K. A. Welsh-Bohmer, and E. M. Reiman.** 2010. A TOMM40 variable-length polymorphism predicts the age of late-onset Alzheimer's disease. Pharmacogenomics Journal. **10:**375-384.

193. **Rosnoblet, C., J. Vandamme, P. Völkel, and P. -. Angrand.** 2011. Analysis of the human HP1 interactome reveals novel binding partners. Biochem. Biophys. Res. Commun. **413:**206-211.

194. **Ryan, S. D., C. S. Harris, C. L. Carswell, J. E. Baenzinger, and S. A. L. Bennett.** 2008. Heterogeneity in the sn-1 carbon chain of platelet-activating factor glycerophospholipids determines pro- or anti-apoptotic signaling in primary neurons. J. Lipid Res. **49:**2250-2258.

195. **Ryan, S. D., S. N. Whitehead, L. A. Swayne, T. C. Moffat, W. Hou, M. Ethier, A. J. G. Bourgeois, J. Rashidian, A. P. Blanchard, P. E. Fraser, D. S. Park, D. Figeys, and S. A. L. Bennetta.** 2009. Amyloid-β42 signals tau hyperphosphorylation and compromises neuronal viability by disrupting alkylacylglycerophosphocholine metabolism. Proc. Natl. Acad. Sci. U. S. A. **106:**20936-20941.

196. **Ryan, S. D., C. S. Harris, F. Mo, H. Lee, S. T. Hou, N. G. Bazan, P. S. Haddad, J. T. Arnason, and S. A. L. Bennett.** Platelet activating factor-induced neuronal apoptosis is initiated independently of its G-protein coupled PAF receptor and is inhibited by the benzoate orsellinic acid. J. Neurochem. **103:**88-97.

197. **Saito, H., P. Dhanasekaran, F. Baldwin, K. H. Weisgraber, M. C. Phillips, and S. Lund-Katz.** 2003. Effects of Polymorphism on the Lipid Interaction of Human Apolipoprotein E. J. Biol. Chem. **278:**40723-40729.

198. **Sandlin, R. D., M. D. Carter, P. J. Lee, J. M. Auschwitz, S. E. Leed, J. D. Johnson, and D. W. Wright.** 2011. Use of the NP-40 detergent-mediated assay in discovery of inhibitors of β-hematin crystallization. Antimicrobial Agents Chemother. **55:**3363-3369.

199. **Schuck, S., M. Honsho, K. Ekroos, A. Shevchenko, and K. Simons.** 2003. Resistance of cell membranes to different detergents. Proc. Natl. Acad. Sci. U. S. A. **100:**5795-5800.

200. **Schulz-Schaeffer, W. J.** 2010. The synaptic pathology of α-synuclein aggregation in dementia with Lewy bodies, Parkinson's disease and Parkinson's disease dementia. Acta Neuropathol. **120:**131-143.

201. **Schwartz, J., M. Senko, and J. Syka.** 2002. A two-dimensional quadrupole ion trap mass spectrometer. Journal of the American Society for Mass Spectrometry. **13:**659-669. doi: 10.1016/S1044-0305(02)00384-7.

202. **Seachrist, J. L., and S. S. G. Ferguson.** 2003. Regulation of G protein-coupled receptor endocytosis and trafficking by Rab GTPases. Life Sci. **74:**225-235.

203. **Seguin-Py, S., G. Lucchi, S. Croizier, F. Z. Chakrama, G. Despouy, J. N. Le Grand, P. Ducoroy, W. Boireau, M. Boyer-Guittaut, M. Jouvenot, A. Fraichard, and R. Delage-Mourroux.** 2012. Identification of HSP90 as a new GABARAPL1 (GEC1)-interacting protein. Biochimie. **94:**748-758.

204. **Seidah, N. G., S. Benjannet, L. Wickham, J. Marcinkiewicz, S. B. Jasmin, S. Stifani, A. Basak, A. Prat, and M. Chretien.** 2003. The secretory proprotein convertase neural apoptosis-regulated convertase 1 (NARC-1): Liver regeneration and neuronal differentiation. Proc. Natl. Acad. Sci. U. S. A. **100:**928-933. doi: 10.1073/pnas.0335507100.

205. **Shannon, P., A. Markiel, O. Ozier, N. S. Baliga, J. T. Wang, D. Ramage, N. Amin, B. Schwikowski, and T. Ideker.** 2003. Cytoscape: A software environment for integrated models of biomolecular interaction networks. Genome Res. **13:**2498-2504. doi: 10.1101/gr.1239303.

206. **Sharma, M., N. Naslavsky, and S. Caplan.** 2008. A role for EHD4 in the regulation of early endosomal transport. Traffic. **9:**995-1018.

207. **Shen, L., S. Kim, S. L. Risacher, K. Nho, S. Swaminathan, J. D. West, T. Foroud, N. Pankratz, J. H. Moore, C. D. Sloan, M. J. Huentelman, D. W. Craig, B. M. DeChairo, S. G. Potkin, C. R. Jack, M. W. Weiner, and A. J. Saykin.** 2010. Whole genome association study of brain-wide imaging phenotypes for identifying quantitative trait loci in MCI and AD: A study of the ADNI cohort. Neuroimage. **53:**1051-1063.

208. **Shevchenko, A., H. Tomas, J. Havliš, J. V. Olsen, and M. Mann.** 2007. In-gel digestion for mass spectrometric characterization of proteins and proteomes. Nature Protocols. **1:**2856-2860.

209. **Shioi, J., A. Georgakopoulos, P. Mehta, Z. Kouchi, C. M. Litterst, L. Baki, and N. K. Robakis.** 2007. FAD mutants unable to increase neurotoxic Aβ 42 suggest that mutation effects on eurodegeneration may be independent of effects on Aβ. J. Neurochem. **101:**674-681.

210. **Shukla, S. D.** 1992. Platelet-activating factor receptor and signal transduction mechanisms. FASEB Journal. **6:**2296-2301.

211. **Sipos, G., and R. S. Fuller.** Separation of golgi and endosomal compartments, p. 351-365. *In* Anonymous Methods in Enzymologyvol. Volume 351. Academic Press.

212. **Siripurapu, V., J. Meth, N. Kobayashi, and M. Hamaguchi.** 2005. DBC2 significantly influences cell-cycle, apoptosis, cytoskeleton and membrane-trafficking pathways. J. Mol. Biol. **346:**83-89.

213. **Small, S. A., and K. Duff.** 2008. Linking Aβ and Tau in Late-Onset Alzheimer's Disease: A Dual Pathway Hypothesis. Neuron. **60:**534-542.

214. **Smith, M. A., G. Perry, P. L. Richey, L. M. Sayre, V. E. Anderson, M. F. Beal, and N. Kowall.** 1996. Oxidative damage in Alzheimer's [6]. Nature. **382:**120-121.

215. **Smith, R. D., J. A. Loo, C. G. Edmonds, C. J. Barinaga, and H. R. Udseth.** 1990. New developments in biochemical mass spectrometry: Electrospray ionization. Anal. Chem. **62:**882-899.

216. **Soulié, S., J. V. Møller, P. Falson, and M. Le Maire.** 1996. Urea reduces the aggregation of membrane proteins on sodium dodecyl sulfate-polyacrylamide gel electrophoresis. Anal. Biochem. **236:**363-364.

217. **Steen, H., and M. Mann.** 2004. The ABC's (and XYZ's) of peptide sequencing. Nature Reviews Molecular Cell Biology. **5:**699-711.

218. **Strittmatter, W. J., A. M. Saunders, M. Goedert, K. H. Weisgraber, L. M. Dong -, R. Jakes, D. Y. Huang, M. Pericak-Vance, D. Schmechel, and A. D. Roses.** 1994. Isoform-

specific interactions of apolipoprotein E with microtubule- associated protein tau: Implications for Alzheimer disease. Proc. Natl. Acad. Sci. U. S. A. **91:**11183-11186.

219. **Strittmatter, W. J., A. M. Saunders, D. Schmechel, M. Pericak-Vance, J. Enghild, G. S. Salvesen, and A. D. Roses.** 1993. Apolipoprotein E: High-avidity binding to β-amyloid and increased frequency of type 4 allele in late-onset familial Alzheimer disease. Proc. Natl. Acad. Sci. U. S. A. **90:**1977-1981.

220. **Suh, K. S., M. Mutoh, K. Nagashima, E. Fernandez-Salas, L. E. Edwards, D. D. Hayes, J. M. Crutchley, K. G. Marin, R. A. Dumont, J. M. Levy, C. Cheng, S. Garfield, and S. H. Yuspa.** 2004. The Organellular Chloride Channel Protein CLIC4/mtCLIC Translocates to the Nucleus in Response to Cellular Stress and Accelerates Apoptosis. J. Biol. Chem. **279:**4632-4641.

221. **Suh, Y. -., and F. Checler.** 2002. Amyloid precursor protein, presenilins, and α-synuclein: Molecular pathogenesis and pharmacological applications in Alzheimer's disease. Pharmacol. Rev. **54:**469-525.

222. **Surdo, P. L., M. J. Bottomley, A. Calzetta, E. C. Settembre, A. Cirillo, S. Pandit, Y. G. Ni, B. Hubbard, A. Sitlani, and A. Carfí.** 2011. Mechanistic implications for LDL receptor degradation from the PCSK9/LDLR structure at neutral pH. EMBO Rep. **12:**1300-1305.

223. **Takahashi, S., Y. Kawarabayasi, T. Nakai, J. Sakai, and T. Yamamoto.** 1992. Rabbit very low density lipoprotein receptor: A low density lipoprotein receptor-like protein with distinct ligand specificity. Proc. Natl. Acad. Sci. U. S. A. **89:**9252-9256.

224. **Tebar, F., S. K. Bohlander, and A. Sorkin.** 1999. Clathrin assembly lymphoid myeloid leukemia (CALM) protein: Localization in endocytic-coated pits, interactions with clathrin, and the impact of overexpression on clathrin-mediated traffic. Mol. Biol. Cell. **10:**2687-2702.

225. **Thinnes, F. P.** 2011. Apoptogenic interactions of plasmalemmal type-1 VDAC and Aβ peptides via GxxxG motifs induce Alzheimer's disease - A basic model of apoptosis? Wiener Medizinische Wochenschrift. **161:**274-276.

226. **Thirumangalakudi, L., A. Prakasam, R. Zhang, H. Bimonte-Nelson, K. Sambamurti, M. S. Kindy, and N. R. Bhat.** 2008. High cholesterol-induced neuroinflammation and amyloid precursor protein processing correlate with loss of working memory in mice. J. Neurochem. **106:**475-485.

227. **Tirasophon, W., A. A. Welihinda, and R. J. Kaufman.** 1998. A stress response pathway from the endoplasmic reticulum to the nucleus requires a novel bifunctional protein kinase/endoribonuclease (Ire1p) in mammalian cells. Genes and Development. **12:**1812-1824.

228. **Traub, L. M., M. A. Downs, J. L. Westrich, and D. H. Fremont.** 1999. Crystal structure of the α appendage of AP-2 reveals a recruitment platform for clathrin-coat assembly. Proc. Natl. Acad. Sci. U. S. A. **96:**8907-8912.

229. **Ungewickell, E. J., and L. Hinrichsen.** 2007. Endocytosis: clathrin-mediated membrane budding. Curr. Opin. Cell Biol. **19:**417-425.

230. **Van Biesen, T., B. E. Hawes, J. R. Raymond, L. M. Luttrell, W. J. Koch, and R. J. Lefkowitz.** 1996. Go-protein α-subunits activate mitogen-activated protein kinase via a novel protein kinase C-dependent mechanism. J. Biol. Chem. **271:**1266-1269.

231. **Völkel, P., P. Le Faou, and P. -. Angrand.** 2010. Interaction proteomics: Characterization of protein complexes using tandem affinity purification-mass spectrometry. Biochem. Soc. Trans. **38:**883-887.

232. **Volmer, D. A., and L. Sleno.** 2005. Mass analyzers: An overview of several designs and their applications, part II. Spectroscopy. **20:**90-95.

233. **Volmer, D. A., and L. Sleno.** 2005. Tutorial mass analyzers: An overview of several designs and their applications, part I. Spectroscopy. **20:**20-26.

234. **Walhout, A. J. M., G. F. Temple, M. A. Brasch, J. L. Hartley, M. A. Lorson, S. Van den Heuvel, and M. Vidal.** 2000. GATEWAY recombinational cloning: Application to the cloning of large numbers of open reading frames or ORFeomes. Methods in Enzymology. **328:**575-592.

235. **Wang, F., R. Chen, J. Zhu, D. Sun, C. Song, Y. Wu, M. Ye, L. Wang, and H. Zou.** 2010. A Fully Automated System with Online Sample Loading, Isotope Dimethyl Labeling and Multidimensional Separation for High-Throughput Quantitative Proteome Analysis. Anal. Chem. **82:**3007-3015. doi: 10.1021/ac100075y.

236. **Weisgraber, K. H.** 1990. Apolipoprotein E distribution among human plasma lipoproteins: Role of the cysteine-arginine interchange at residue 112. J. Lipid Res. **31:**1503-1511.

237. **Whitehead, S. N., W. Hou, M. Ethier, J. C. Smith, A. Bourgeois, R. Denis, S. A. L. Bennett, and D. Figeys.** 2007. Identification and quantitation of changes in the platelet activating factor family of glycerophospholipids over the course of neuronal differentiation by high-performance liquid chromatography electrospray ionization tandem mass spectrometry. Anal. Chem. **79:**8539-8548.

238. **Willnow, T. E., J. L. Goldstein, K. Orth, M. S. Brown, and J. Herz.** 1992. Low density lipoprotein receptor-related protein and gp330 bind similar ligands, including plasminogen activator-inhibitor complexes and lactoferrin, an inhibitor of chylomicron remnant clearance. J. Biol. Chem. **267:**26172-26180.

239. **Wiśniewski, J. R., A. Zougman, N. Nagaraj, and M. Mann.** 2009. Universal sample preparation method for proteome analysis. Nature Methods. **6:**359-362.

240. **Worzfeld, T., N. Wettschureck, and S. Offermanns.** 2008. G12/G13-mediated signalling in mammalian physiology and disease. Trends Pharmacol. Sci. **29:**582-589.

241. **Xia, Y., H. A. De Rohan Suva, B. L. Rosi, L. H. Yamaoka, J. B. Rimmler, M. A. Pericak-Vance, A. D. Roses, X. Chen, E. Masliah, R. Deteresa, A. Iwai, M. Sundsmo, R. G. Thomas, C. Richard Hofstetter, E. Gregory, L. A. Hansen, R. Katzman, L. J. Thai, and T. Saitoh.** 1996. Genetic studies in Alzheimer's disease with an NACP/α-synuclein polymorphism. Ann. Neurol. **40:**207-215.

242. **Yang, C. -., K. Leskov, K. Hosley-Eberlein, T. Criswell, J. J. Pink, T. J. Kinsella, and D. A. Boothman.** 2000. Nuclear clusterin/XIP8, an x-ray-induced Ku70-binding protein that signals cell death. Proc. Natl. Acad. Sci. U. S. A. **97:**5907-5912.

243. **Yang, W., J. R. Diehl, M. Yerle, J. J. Ford, R. K. Christenson, W. E. Roudebush, and W. E. Plummer.** 2003. Chromosomal location, structure, and temporal expression of the platelet-activating factor receptor (PAFr) gene in porcine endometrium and embryos relative to estrogen receptor α gene expression. Mol. Reprod. Dev. **64:**4-12.

244. **Yap, C. C. C., Z. M. Lasiecka, S. Caplan, and B. Winckler.** 2010. Alterations of EHD1/EHD4 protein levels interfere with L1/NgCAM endocytosis in neurons and disrupt axonal targeting. Journal of Neuroscience. **30:**6646-6657.

245. **Yates, J. R., C. I. Ruse, and A. Nakorchevsky.** 2009. Proteomics by mass spectrometry: Approaches, advances, and applications. Annual Review of Biomedical Engineering. **11:**49-79.

246. **Zeth, K.** 2010. Structure and evolution of mitochondrial outer membrane proteins of β-barrel topology. Biochimica Et Biophysica Acta - Bioenergetics. **1797:**1292-1299.

247. **Zhang, D. -., T. A. Lagace, R. Garuti, Z. Zhao, M. McDonald, J. D. Horton, J. C. Cohen, and H. H. Hobbs.** 2007. Binding of proprotein convertase subtilisin/kexin type 9 to epidermal growth factor-like repeat A of low density lipoprotein receptor decreases receptor recycling and increases degradation. J. Biol. Chem. **282:**18602-18612.

248. **Zhang, W., C. Zhao, S. Wang, C. Fang, Y. Xu, H. Lu, and P. Yang.** 2011. Coating cells with cationic silica-magnetite nanocomposites for rapid purification of integral plasma membrane proteins. Proteomics. **11:**3482-3490.

249. **Zhang, X., X. -. Pan, X. -. Liu, S. Wang, and L. -. Wang.** 2007. Down-regulation of platelet-activating factor receptor gene expression during focal reversible cerebral ischemia in rats. Neurochem. Res. **32:**451-456.

250. **Zhou, H., W. Hou, N. J. Denis, H. Zhou, J. Vasilescu, H. Zou, and D. Figeys.** 2009. Glycoproteomic reactor for human plasma. Journal of Proteome Research. **8:**556-566.

251. **Zhou, H., F. Wang, Y. Wang, Z. Ning, W. Hou, T. G. Wright, M. Sundaram, S. Zhong, Z. Yao, and D. Figeys.** 2011. Improved recovery and identification of membrane proteins from rat hepatic cells using a centrifugal proteomic reactor. Molecular & Cellular Proteomics : MCP. **10:**.

Appendix 3-1: The complete and full results of the digestion of cells transfected with APOE, CLU1, CLU2, LDLR, PICALM, SNCA, PAFR and cells transfected with the negative control, which is the empty vector (pCMV-Entry). Hit Gene Name: the name of the gene matched to the peptides by Mascot; Hit Protein ID: protein identifier from GI database; Peptide Number: total number of peptide sequences matched to the protein.

Hit Gene Name	Hit Protein ID	Empty	APOE	CLU1	CLU2	LDLR	PICALM	SNCA	PAFR
ABCB6	9955963	5							4
ABCC1	134142335				1				7
ABCC3	9955970	1							
ACADM	4557231			2	3	2	2		
ACADSB	4501859				2	3			
ACBD3	15826852						4		
ACP2	4557010								6
ACSL3	42794752	6	2	3					3
ACSL5	42794756	2							
ACTR2	5031571				1				
ADCY2	115387102							1	
ADPGK	31542509	2							
AFG3L2	300192933			2	4				
AGK	8922701		1						
AGPS	4501993					2			
AGRN	54873613	3							
AGTRAP	93588491								4
AHSG	156523970	17							
AIFM1	4757732			13	6	4	4		
AKAP12	21493022	11							3
AKAP8	5031579			1					
ALDH1B1	25777730			2					
ALDH3A2	4557303	4		1					1
ALDOA	4557305	2							4
AMBP	4502067		6	13	5				
AMY2A	4502085								2
ANAPC5	20127553			2					
ANK2	52426735	2							
ANP32A	5453880								8
AP1B1	260436860								2
AP1G1	71772942	1					4		
AP2A1	19913414						7		
AP2A2	27477041						5		
AP2B1	4557469						6		
AP2M1	14917109	3					7		
APH1A	117606357	1							
APOB	105990532					8			
APOD	4502163				1				
APOE	4557325	2	603	20	1				
APOL2	13562090					2			
APP	4502167	1							
ARAF	4502193				2				
ARCN1	11863154		2	1	2				
ARF1	4502201			2	1	6	4		
ARF4	4502205				3	7			
ARF5	4502209					4			3

ARFGEF2	150417986			2	4				
ARIH1	187761373						2		
ARL1	4502227				1				
ARL6IP1	24308007					5			
ARL8B	8922601	5				1			4
ASPH	14589860		1	1	2	2	1		1
ATG3	19526773						2		
ATP11C	40316839								1
ATP1A1	21361181	114	2	5	6	10	2		139
ATP1A2	4502271	9		1	2	3	1		
ATP1A3	22748667	21							59
ATP1B1	4502277	3							4
ATP1B3	4502281	3	1						17
ATP2A1	10835220	2							3
ATP2A2	4502285	29		4	6	3			24
ATP2A3	28373103				4				
ATP2B1	48255945	28			1	2			19
ATP2B4	48255957	27							27
ATP5A1	4757810	2	13	23	9	11	5		
ATP5B	32189394		8	9	6	6	9		
ATP5C1	4885079			3	2	5	1		
ATP5D	4502297		1						
ATP5F1	21361565		4			7			
ATP5G3	4502301		3						
ATP5O	4502303				3	6			
ATP6AP1	17136148	3							
ATP6V0A1	19913418	4							8
ATP6V1H	47717100				1				
ATXN10	7106299				1	2			
AZGP1	4502337	2							
B3GNT1	5802984		1						
BAAT1	304555614					3			
BAG2	4757834			11		2	5		
BASP1	30795231	29							6
BAT1	4758112				1	2			
BAX	4757838		3						
BCAP31	32171186	14	9				2		5
BRI3BP	19923665		2	2		3			
BSG	38372919	14	5		1	4			33
BTAF1	27477070			1					
BYSL	51173724		2						
C10orf58	148596959					2			2
C11orf2	8393009			2					
C11orf59	8923579	2							4
C15orf24	9910346		2						
C16orf55	23308501		2						
C19orf63	45580696		3						
C1orf35	13236559		2						
C1orf57	14150100			1	3	3			
C1QBP	4502491	3	7			5	4		
C20orf3	24308201		3						2
C22orf28	7657015						1		
C3	115298678				1				
C3orf1	59710109				2				
C4orf49	117168279				2				

C5orf32	14165278	2							
C8orf55	7706200		2						2
CABC1	34147522			2	2				
CAD	18105007			3	11		3		
CADM1	148664190		1						
CALM3	4502549								6
CALML5	223278387							1	
CALR	4757900	6							12
CALU	4502551				3				
CAND1	21361794				2				
CANX	10716563	18	41	40	36	63	7		35
CAPRIN1	42558250		4				2		
CBS	4557415			2					
CCDC47	171906582	2							2
CCDC85C	223671856					1			
CCT2	5453603	5		1		1			
CCT3	58761484		7	4	8	9	6		
CCT4	38455427			6	8	9	6		2
CCT5	24307939			2	5		4		
CCT6A	4502643	1		7	6		2		
CCT7	5453607	6		3	8	8	4		
CCT8	48762932	1		8	8	4	8		
CD276	67188443	3							2
CD63	4502679	5							
CD81	4757944	3							8
CD9	4502693	2							
CDC42	4757952	2				2			
CDC7	4502715							1	
CDK1	4502709	2	2		2	5	3		
CDK4	4502735					3			
CDKN2A	4502749						2		
CFL1	5031635					4			
CHCHD3	8923390		3						
CISD1	8923930								2
CISD2	56605994	2							
CKAP4	19920317	17							13
CKB	21536286						2		3
CKMT1A	10334859						3		
CLCC1	13194195					4			
CLDN12	6912312								2
CLDND1	11096340								2
CLINT1	7661968						11		
CLN6	8923532					1			
CLNS1A	4502891	1	4		2		3		
CLPTM1	4502897				1	2			
CLTA	4502899						3		
CLTB	4502901						4		
CLTC	4758012	10					93		14
CLTCL1	242246985	2							
CLU	42716297			57	56	4	4		
CLYBL	45545437		1				1		
CNBP	4827071			3	4	12	2		
CNNM3	40068047								4
CNNM4	94681046				2				7
CNOT1	42716275				2		2		

COMT	4502969	2							4
COPA	148536853				6		8		
COPB1	7705369			3	3	3	2		
COPE	31542319						2		
COPG	11559929				1		2		
COPG2	109134349			2		2			
COPS4	38373690						3		
COPS5	38027923						2		
COPZ1	7706337					1			
COX2	251831110		4			1			
COX4I1	4502981		3						
COX4NB	5174615		4						
COX5A	190885499		8						
COX5B	17017988		9						
COX6C	4758040		6						
COX7A2	262118227		4						
CPD	22202611	3							
CPT1B	4758050	3							3
CRTC2	32171215				1				
CSDA	224586882		11						
CSDE1	56117850						2		
CSE1L	29029559		21	11	18	44	12		
CSRP2	4503101					3			
CSTA	4885165							1	
CTNNB1	4503131	2							
CTPS	148491070			6	3		1		
CXADR	4503173	1							4
CYB5A	4503183		2						
CYB5B	83921614	2	4			2			1
CYB5R1	49574502		1						
CYB5R3	4503327	4	2			4			16
CYC1	21359867		2						
CYP51A1	4503243	4	11		2	10	2		5
DAD1	4503253	4							4
DAG1	294997282								2
DAGLB	218931251	2							
DARS	45439306			5			6		
DBN1	18426913	9					2		2
DCD	16751921	3	1		2	5	4	3	9
DCTN2	5453629	4							1
DCTPP1	13129100					1	2		
DDHD2	256017245					2			
DDOST	20070197	12	5	1	4	8	5		11
DDX1	4826686						2		
DDX19B	6005743			1					
DDX21	50659095	18							14
DDX3X	87196351			2					
DDX5	4758138		4	2			3	2	
DHCR24	13375618								4
DHCR7	119943112	5		1	5	2			2
DHRS7	7706318					2			2
DHRS7B	20149619					1			
DHX15	68509926		4	2	3		2		
DIS3	190014623			3	1				
DLEC1	90669194				2				

DNAJA1	4504511			4	6	3			
DNAJA2	5031741			4	3	2	1		
DNAJB11	7706495				2				
DNAJB12	194306640				3				
DNAJC10	24308127					3			
DNAJC13	112421122	2							
DNAJC7	221219056			3		1	3		
DPM1	4503363					3			
DPM3	19424120	2							
DPYSL2	4503377	4							9
DPYSL3	4503379								6
DRG1	4758796					3	1		
DSG1	119703744							2	
DSG2	116534898	12							15
DYNC1H1	33350932			4	18	6	4		
DYNC1I2	24307879			2	2				
EARS2	134288884			4		2			
EBP	5729810					1			
EEA1	55770888					2			
EEF1B2	4503477				2	2	1		
EEF1D	25453472	4							
EFTUD2	217272892						2		
EGLN1	13489073					4			
EHD1	30240932	9				1			
EHD3	7657056	2	2	2	2	2			
EHD4	21264315	9	2	2					
EIF3A	4503509						7		
EIF3B	33239445			1	1		4		
EIF3C	4503525						4		
EIF3F	4503519						2		
EIF3L	7705433						4		
EIF4A1	4503529	3	1	2			2		
EIF4A3	7661920						3		
EIF4B	50053795		3	2	2	4	3		
EIF6	4504771	4							
ELL2	155722987		4						
ELMO2	19718769						2		
EMD	4557553	2		7	3	3	1		2
ENO1	4503571	7	5	3	5	12	9		
ENO2	5803011	5							5
ENO3	301897469					11			
EPHA2	32967311								4
EPHX1	4503583		4			6	3		
EPRS	62241042			6	3	4	6		
ERGIC3	7706278			2					
ERLIN1	154800487		1						3
ERLIN2	6005721	10					2		4
ESYT1	14149680	8			2	4			15
ESYT2	45387945				3				2
ETFA	4503607				1		1		
ETFB	4503609				1				
EWSR1	4885225				1				
EXOC4	82546830			3	4				
FAF2	24797106	4							4
FAM134C	30023820			1		4			

FAM158A	31542298		1						
FAM162A	49355721								3
FANCI	82830440			3	4				
FARSA	4758340			5					
FASN	41872631		2	3	2		8		
FASTKD1	188497683					1			
FASTKD5	11141903			2					
FAU	4503659		2						
FDFT1	67089147					1			
FHL1	21361122					4	2		
FLG2	62122917								1
FLNA	116063573	13							
FLOT1	5031699	5							2
FLOT2	94538362	11							17
FYN	4503823	4							
G3BP1	5031703						2		
GALK1	4503895			1	5	3			
GANAB	38202257	7		6	15				11
GAPDH	7669492	14		3			4		
GARS	116805340			2		4			
GART	4503915						2		
GBAS	4503937					4			
GCN1L1	54607053		4	10	8	21	5		
GEMIN4	122939157			3	4	3			
GFPT1	205277386			2					
GNA13	24111250								8
GNAI1	33946324	4							10
GNAI2	4504041		2						12
GNAI3	5729850	11			2		1		13
GNAQ	40254462								2
GNAS	4504047	3							
GNB1	11321585		2						
GNB2L1	5174447	4		10	6	8	6		
GNB3	4504053	2							
GNB4	11055998						2		
GNE	4885285				7				
GOT2	73486658						1		
GPS1	47078238						8		
GTF3C4	156119605			1					
H1F0	4885371	5							
H1FX	5174449						2		
H3F3B	4504279	5							
HADHA	20127408		11	2	2	3			
HADHB	4504327		6				2		
HAO2	7705393	3				5			6
HAT1	4504341						1		
HAX1	13435356				3				
HBA2	4504345							3	
HBB	4504349							2	
HDGFRP2	14249158								6
HDLBP	4885409						3		
HEATR1	73695475			2	2				
HERC2	126032348				2				
HIP1R	48762942	1							
HIST1H1C	4885375	6	3				2		

HIST1H1D	4885377								1
HIST1H2AG	4504239	24	3						2
HIST1H2BC	4504257	2							
HIST2H4A	4504301	13						5	40
HK1	15991827					1			2
HK2	15553127			4	2				
HLA8	310114942								19
HLA9	310128243								17
HLA-A	24797067	2	3						1
HLA-B	17986001	2			3				13
HLA-C	52630342			2	6				
HM13	23308607	3							
HMGA1	4504433	2							
HMGB3	71143137						1		2
HMOX2	8051608								1
HNRNPA1	4504445						2		2
HNRNPA2B1	4504447	7							2
HNRNPAB	55956919		3		2		1		
HNRNPC	117189975	3							
HNRNPD	14110414	7	1				1		
HNRNPF	4826760	11		1					
HNRNPH1	5031753		2	5	6		6	3	2
HNRNPH2	316983130		2						
HNRNPK	14165435	16	4	6	9		4		
HNRNPM	14141152	3	5	5	11		4	8	
HNRNPR	5031755	6	3				2		2
HNRNPU	14141161	2	5	5	2	2	2	1	
HOOK1	7705415			2	1				
HRNR	57864582				3		3	2	
HSD17B10	4758504			2			2		
HSD17B11	142976729					1			
HSD17B12	7705855	3							11
HSP90AA1	154146191		2	18	10	43	17		
HSP90AB1	20149594	10	3	20	19	49	17		11
HSP90B1	4507677	26		3	4		3		28
HSPA1B	167466173		18	34	36	18	47	18	4
HSPA1L	124256496	3		9	4		19		
HSPA2	13676857				3				
HSPA4	38327039						16		
HSPA4L	31541941						8		
HSPA5	16507237	34	17	15	19	7	28	27	30
HSPA6	34419635						11		
HSPA8	5729877	5	28	56	57	13	41	32	9
HSPA9	24234688			7	6	7	19	9	
HSPB1	4504517			3	3	5			
HSPBP1	112363070						2		
HSPD1	31542947	5	4	16	6	14	14		6
HSPE1	4504523								2
HSPH1	42544159			3			14		
HTATSF1	21361437						5		
HUWE1	61676188				5				
HYOU1	5453832								10
IARS	94721239			6			5		
IARS2	46852147			5	4				
IDH2	28178832					2			

IDH3A	5031777				2				
IDH3G	4758582				3				
IER3IP1	7705819								4
IGBP1	4557663				4				
IGF2BP1	56237027			1					
IGF2R	119964726	24			6		13		8
IGFN1	257196151	1	2	1	2		2		
IGSF8	16445029	2							
IKBIP	24233517		2			1			
ILF2	24234747		5				3		2
ILF3	24234750		4				4		
IMMT	154354962				3				
IMPAD1	157388900						2		
IMPDH1	34328928						3		
IMPDH2	66933016						4		
INA	14249342	4							4
IPO7	5453998				5	9			2
IPO8	53759103			6	4	12			
IPO9	21361659			2	4				
IRAK1	68800243			3	7				
IRS4	4504733	48		6	6	3	4		45
ITGB1	19743813	8							5
ITIH2	70778918								2
JAGN1	190014601		4			2			
JAM3	21361905	2							
JMJD6	125988389						4		
JUP	4504811						1		
KCTD5	9506651	2	4	3	3	5	10	2	
KIAA0090	22095331	4							
KIAA1524	190194355			1		6			
KIAA1715	38176151		1						
KIF11	13699824	29	5	53	74	122	87		
KIF5B	4758648			3					
KPNA2	4504897					1	2		
KPNB1	19923142		2	6	1	13	4		2
KRTCAP2	27777661								2
KTN1	118498362	10							2
LAMP1	112380628	7				5			2
LAMP2	4504957	5		1					5
LAP3	41393561						3		
LAS1L	13654270				1				
LASP1	5453710					5			
LBR	37595750		3						
LDHA	5031857			4		4	6		
LDHB	4557032	1		4	1		6		
LDHC	4504973	1							
LDLR	4504975					291	3		2
LETM1	6912482		4			2			
LGALS3BP	5031863				2				
LMAN1	5031873		8	3		2			1
LMAN2	5803023	6	3			4	2		2
LMNB1	5031877				1				
LOC338667	169202109	1							
LOC728026	113420837	18							
LOC731751	113430845				48	29			

LPCAT1	33946291		4	3	1	3	2		2
LRP8	61744467					2			
LRPPRC	31621305				3		4		
LRRC15	288541295							2	
LRRC59	40254924	4	4			5	5		28
LRRFIP1	212276070						2		
LSM12	22748747				1				
LSR	45505163	2							
LUC7L2	116812577		4	1			4		
LYZ	4557894		2			1		2	
M6PR	4505061		1			1	3		6
MAD2L1	4505067					2			
MAGED1	52632377			5	2	2			
MAGED2	19387846			10	5				
MAP1B	153945728	19							35
MAP2	87578396	25							20
MARCKS	153070260	20		1					7
MARCKSL1	13491174	21		2		3			7
MARS	14043022			3		2			
MAST4	148727255	2							
MAT2A	5174529			1			2		
MAT2B	11034825						1		
MAZ	110347459					3			
MBP	4505123								2
MCM2	33356547						1		
MCM3	6631095			8	4	8	3		
MCM4	33469917			1					
MCM5	23510448			4		3	3		
MCM7	33469922			9	11	8	3		
MDN1	24415404				2				
METTL13	42542403				2				
MGST1	9945306								4
MGST3	4758714		1						
MLEC	7661948	1			2	3			6
MMS19	170763479			3					
MOGS	149999606	3							2
MPZL1	4506357	4							
MRI1	23943880				4				
MSH2	4557761				3				
MTCH2	7657347					1			
MTDH	223555917	15	8						7
MTHFD1	222136639			7	9	9	7		
MTR	169790923				2				
MUC6	151301154						1		
MXRA7	56549129								1
MYBBP1A	157694492						5		
NACA	5031931	2					3		2
NAMPT	5031977			5					
NAP1L1	4758756			1					
NAPA	47933379		6						
NASP	27262628								4
NCAM1	94420689	4							
NCAPD2	178056552						4		
NCAPG	21359945				2	2	1		
NCKAP1	7305303	1							

NCL	55956788	17	22	4	2	3	13		7
NCLN	51873031			4		3	1		2
NCOA5	15147335	1							
NCSTN	24638433	7							4
NDUFS1	33519475				2				
NDUFS3	4758788						2		
NDUFS7	187281616			1					
NDUFS8	4505371			1					
NEFM	157738649								2
NEK2	4505373					2			
NIPSNAP1	193211616				2				
NMD3	19923796					2			
NNT	122939153		2						
NOP14	55769587		2						
NOP2	76150623	4							
NPAT	155969714							2	
NPC1	255652944	6	1						2
NPEPPS	158937236			7	5	3			
NPM1	10835063	10	2		3	1	4		7
NPTN	6912646	4							
NRAS	4505451								2
NSDHL	8393516		3			2			4
NSF	156564401	2	11	3	3	15			
NUP188	62955803				1				
NUP205	57634534			5	9	1			
NUP210	27477134				1	2			
NUP93	208609990	2		8	7	6	1		
OAT	4557809					6	4		
OCLN	4505487	5							
OFD1	4503179	1							
OLA1	58761500						2		
OR2T27	49227791								5
OR2T35	49226830							1	
OS9	5803109				1				
OSTC	24308271								4
P4HB	20070125	4							4
PABPC1	46367787		13	7					
PABPC3	45238849				3				
PABPC4	4504715			2			3		
PABPC5	18201888				1				
PAICS	5453539						2		
PALM	93141029	2							
PANK4	8922665				6				
PARP1	156523968								1
PARP8	194018490					4			
PCBP1	222352151					2	3		
PCBP2	14141166			2		2	1		
PCNA	4505641	2		9	4	4	4		
PCYT1A	31543385						2		
PDCD2	21735592					4			
PDIA3	21361657	8			2				10
PDIA4	4758304	7							12
PDIA6	5031973	4							6
PDLIM7	11496885					2			
PEBP1	4505621	1							

PEG10	94421475							1	
PELO	31880783			1	2	1	1		
PFDN2	12408675						1		
PFDN5	22202633						2		
PFKL	48762920			1					
PFKP	11321601					4			
PGAM5	281604136					2			
PGK1	4505763	3					1		
PGRMC1	5729875	7	8	4		8	2	1	3
PGRMC2	291621647	4	4			5			
PHB	4505773	10	8		2	7	3		
PHB2	6005854	4	9	2	2	9	6		
PHF6	28557677					2			
PHGDH	23308577		2	11	13	9	5		
PI4K2A	13559514					1			2
PI4KA	4505807	1				1			
PICALM	56788366		1	4			124	10	1
PIK3C2A	157671929						10		
PKM2	33286418	3					2		
PKN2	5453974								2
PLEKHG5	38373682								1
PLIN3	255958306		9			6	2		
PLXNB2	149363636								3
PNKD	116642885			4	1				
PNN	33356174	11							
POLDIP2	7661672						1		
POLR1C	4759046				2				
POLR2B	4505941			2					
POLR2H	14589953				1		2		
POR	127139033		10	3		9			3
POTEE	134133226						6		
PPA1	11056044						2		
PPAN-P2RY11	47174861								2
PPIA	10863927	2							
PPM1B	4505995		13	8	12	6	8		
PPM1G	29826282						3		
PPP1R12A	4505317						1		
PPP2R1A	21361399					2	2		
PPP4R4	17402886			2					
PPP6C	4506029				4				
PPP6R1	151101459			1	1				
PPP6R3	13489083			1	1		1		
PRAF2	6005794	4	2			2			2
PRDX1	4505591		3	4		11			
PRDX3	5802974		1				1		
PRDX4	5453549						2		
PRDX6	4758638		2				2		
PRKCSH	48255889			3	9				6
PRKDC	13654237	3		24	7		8		
PRMT5	20070220	6	15	11	26	14	17		
PROCR	34335272	5							2
PRPF19	7657381						2		
PRPF6	40807485				1				
PRPF8	91208426						3		
PRPS1	4506127						2		

PRPSAP1	194018537				1				
PRSS21	5803197	2							
PSMA2	4506181			2					
PSMA4	4506185			2	2		3		
PSMA6	23110944			3			2		
PSMA7	4506189				2				
PSMB4	22538467						1		
PSMB5	4506201			2			2		
PSMB6	23110925				2				
PSMC1	24430151			7			5		
PSMC2	4506209			4	2	2	4		
PSMC3	21361144	1					1		
PSMC4	5729991						4		
PSMC5	24497435			2	2		2		
PSMC6	195539395				3		7		
PSMD1	25777600			4		3	3		
PSMD10	4506217						1		
PSMD11	28872725						3		
PSMD12	4506221						3		
PSMD13	157502193				5		3		
PSMD14	5031981					1			
PSMD2	25777602			7	2		8		
PSMD3	25777612			5	4	3	8		
PSMD6	7661914						4		
PSMD7	25777615				2				
PSME2	30410792		2			2			
PSME3	30410794					1			
PTAFR	4506241								19
PTDSS1	7662647								2
PTGES2	13376617			2					
PTGES3	23308579						2		
PTGFRN	41152506	5							6
PTK7	15826840	7							4
PTMS	46276863	6							9
PTPLAD1	117168248	3				2			3
PTPN1	4506289		2			3			
PTPRA	4506303								2
PTPRF	109633039								12
PVR	209413726	1							
PYCR2	21361454				1	2			
QARS	4826960				4	3	2		
QPCTL	92110027		1						
RAB10	256222019	9	10	7		10			3
RAB11A	4758984	3	2	5		5	1		2
RAB11B	190358517		8						8
RAB12	106507164								11
RAB14	19923483	11	6	6		7			20
RAB18	10880989		4	7		6			4
RAB1A	4758988	13	11	6		9			
RAB1B	13569962		12						
RAB21	7661922	2							7
RAB2A	4506365	7	4	4		4			12
RAB3A	4506367	2				2			
RAB3D	4759000					4			
RAB4A	19923260								14

RAB5A	19923262		7	4		7			
RAB5B	4506371					6			
RAB5C	41393545	12	8	8	3	10			14
RAB6A	19923231			5	3	4			12
RAB6B	96975097		7						
RAB7A	34147513	13	11	5		7	3		48
RAB8A	16933567	6				7			
RAB8B	7706563								23
RAC3	4826962	3							
RALA	33946329	9	2						4
RAN	5453555	2				4	2		2
RANBP1	4506407					2	2		
RANBP2	150418007					2			
RANGAP1	4506411					1			
RAP1A	4506413			1		3			
RAP2B	38201690								3
RAP2C	32129209								2
RARS	15149476			2	7	2			
RBBP7	4506439			1		2	3		
RBM10	20127479	2							
RBM22	8922328					2			
RBM39	4757926	1	2						2
RBMX	56699409	6					4		7
RBP4	55743122		2	4					
RCN1	4506455				1				
RCN2	4506457			3	3				
RDH11	166795268	2	4			5	4		
RDH14	10190746		4						
REEP5	115430112					4			
REEP6	19923919	1							
RETSAT	203098013					1			
RFC2	28882049				3				
RFC3	4506489			1	1	1	2		
RFC4	4506491				1				
RHOA	10835049	2							
RHOB	4757764					2			7
RIOK1	23510356		2	2	3				
RNF114	8923898				1	2			
RNF126	37622894			1	2				
RNF138	21361539				2	1			
RNF219	88759348			3	7				
RNH1	21361547			1			14		
RNPS1	6857826	7							4
ROCK1	4885583					2			
ROCK2	41872583					4			
RPN1	4506675	15	6	14	7	4	3		18
RPN2	35493916	15	3	1	1	2	1		9
RPS27A	4506713	8	8	4	1	2		1	8
RPSA	9845502				3				
RRAS	5454028					2			
RRAS2	21361416	2							6
RRBP1	110611218	10							
RRP1B	57863269		3						
RSL1D1	118498359		5				1		
RTN3	5174655		2	3					

RTN4	24431935	6	3						2
RUVBL1	4506753			4	8	4	6		
RUVBL2	5730023		4	6	7	9	3		
S100A7A	28827815						3		
S100A8	21614544		4				1		
SAAL1	116235444					1			
SACM1L	190014578			2					
SAFB2	7661936								2
SALL2	49087132					1			
SAMHD1	38016914			5	3				
SAR1A	9910542					1			
SAR1B	7705827			1					
SARNP	32129199	2							
SARS	16306548						2		
SCAMP1	116256358	2							
SCAMP2	5730031					2			4
SCAMP3	16445419	13	4		3	5	7		3
SCARB2	5031631	4	2	2		6			8
SCCPDH	55770836		3						
SCD	53759151	2							
SCFD1	33469966		5	2					
SCO1	4759068		2						
SCO2	153791313			2		2			
SCRIB	45827729	11							2
SCYL2	47604944	2		6		2	4		
SDF4	7706573				2				
SDHA	156416003		2						
SDHB	115387094		2			2	3		
SDK2	222352127								2
SEC11A	7657609	2	2	2		4			7
SEC14L4	28376621					2			
SEC16A	124378039				3		2		
SEC22B	94429050	8	4	2	2	6			8
SEC61A1	7019415	2							
SEC61B	5803165	4							
SEC62	4507525	5	3			3			
SEC63	6005872					10			
SERBP1	66346679		3	2	3	3	4		
SERPINA1	50363217	4		5	1				
SERPINH1	32454741			2	2		2		
SET	170763498								5
SF3A2	21361376						1		
SF3A3	5803167						3		
SF3B1	54112117						4		
SF3B3	54112121		1						
SF3B4	5032069	4	2						
SFXN1	23618867	1	3		2	6	2		
SFXN4	47458811			1	4				
SHPRH	27436873		2						
SHROOM3	203098098						2		
SIGMAR1	5032117	2							
SIRT1	7657575						2		
SKP1	25777713				2				
SLC12A2	4506975	3							6
SLC12A7	123701900	4							13

SLC12A9	31881740								3
SLC16A1	115583685	6				1			3
SLC19A1	34808710	3							
SLC19A2	27734719								2
SLC1A5	5032093	24	3	2	3	5	3		15
SLC25A10	20149598				2	2			
SLC25A11	259155317			3	3	2	2		
SLC25A12	21361103				3	1			
SLC25A13	7657581			4	6	3	2		
SLC25A20	4557403				2				
SLC25A3	4505775	2		3	2	4			2
SLC25A31	13775208				1				2
SLC25A5	156071459	2	7	9	10	6	3		20
SLC25A6	156071462		4	8	6				10
SLC29A1	4826716	2							
SLC2A1	166795299								2
SLC2A3	5902090								2
SLC35F2	31542943								3
SLC38A1	117168275	4							
SLC38A2	21361602	2							6
SLC3A2	61744477	18	5	3	5	7			50
SLC5A6	256985183	2							2
SLC6A15	21361693	2							7
SLC7A1	4507047	1				2			4
SLC7A5	71979932	6			1	1			5
SMC2	110347418			3	2				
SMC3	4885399			4					
SMC4	50658063			3	1				
SMPDL3B	57242798	3							2
SNAP91	7662228						1		
SNCA	4507109				2	4	4	97	
SNCB	4507111							12	
SND1	77404397	4							
SNRNP70	29568103	6							3
SNRPA1	50593002						1		
SNRPB2	4507123		2				3		
SNRPD3	4759160		2						
SNRPN	4507135				2				
SORT1	17149834	5		2		2			3
SP1	38372901					1			
SPCS2	162417971	2	8			5			7
SPCS3	11345462		4						3
SPIN1	112293285	1					1		
SPNS1	14042968	3			2				
SPTAN1	154759259	2							
SPTBN1	112382250	4							4
SPTBN2	5902122					1			
SPTLC1	5454084			1	1				
SPTLC2	4758668					3			
SQSTM1	4505571					1			
SRPR	295424842	2		1			1		
SRPRB	284795266	13	7	5	4	11	4		10
SRSF1	5902076	4	3				2		
SRSF2	47271443	4							
SRSF3	4506901								6

SRSF6	20127499	2	1						
SRSF7	72534660	3							
SRSF8	15055543	5	1						
SSB	10835067	3	3						
SSBP1	4507231	50					1		
SSR3	6005884	2	2	1	1	3			2
SSR4	5454090	5	3	4	5				5
STAT1	6274552			1	2				
STAT3	21618338					8			
STEAP3	56549145					1			
STK38	6005814		2				2		
STOM	38016907	5							8
STOML2	7305503		4		2	3			
STT3A	22749415	6			1				4
STX10	4507285					2			
STX12	28933465	2				3	7		8
STX4	20149560					3			4
STX6	5032131					1			
STX7	170932494	4	2			3	3		2
STXBP1	4507297	2							
STXBP3	118600975					3			
SUB1	217330646	3							
SUCLA2	11321583			3					
SYCP2	38373673						1		
SYNGR1	22035696	2	3	1		1			2
SYNGR2	4759202	6	2	4		3	3		
TARDBP	6678271						1		
TARS2	20070344			3		2			
TBC1D4	114688046						2		
TBCD	41350333			1		3			
TBL2	7549793	4							
TBR1	5730081			2	2				
TCEA3	41350335								6
TCOF1	57164975						5		
TCP1	57863257	4		22	17	7	5		
TECR	24475816	6							7
TELO2	225545550				2	8			
TF	4557871	2							31
TFRC	189458817	19	6	10	1	23	6		37
TGOLN2	42518068					2			
THOC4	238776833								4
THRAP3	167234419	4							
TIMM23	5454122				2				
TIMM50	48526509			6		2	4		
TM9SF2	4758874								4
TMCO1	24308133		1						
TMED1	5803040		1						
TMED10	98986464	4	3						6
TMED2	5803149		1						
TMED5	282165814	2	1						2
TMED9	39725636		2						4
TMEM109	13129092		4			6			2
TMEM111	8923857		5			1			
TMEM165	32189371			1					
TMEM192	154240704								4

TMEM205	15529966		2						2
TMEM214	134152683		5						
TMEM30A	8922720	4							
TMEM33	224589127	2	2	6	1	5	2		5
TMEM55B	154816184	2				4			2
TMEM97	109948302		2						
TMPO	4507555		2	1		2			2
TMUB1	13899257	2							
TMX1	151101292	3	5						3
TMX2	7705726		2						4
TMX3	38505222			2					
TNPO1	23510381			2		18			
TNPO2	48675813					9			
TNPO3	6912734					2			
TNRC6A	116805348			1					
TNRC6B	148491080						3		
TOMM20	7657257	2	6						
TOMM22	9910382		2						
TOMM40	5174723		3						
TOMM6	197927201		3						
TOMM70A	54607135					1			
TOR1AIP1	39753957		3						
TP53	120407068						1		
TPD52	4827038		3						
TPD52L2	40805862		3						
TPM1	63252904								2
TPM4	4507651	2							
TRAP1	155722983			1			3		
TRIM21	15208660					7	3		
TRIM23	4502197					2			
TRIM28	5032179	1		6	5	4	2		
TRO	50541946								2
TRPM3	154091314	3							
TTC27	42476022				4	1			
TTC35	7661910		3			4			
TTN	291045225					2			
TWF2	6005846		1						
TXNDC5	42794771					2			
TXNL1	4759274						2		
U2AF1	5803207		2		1		2		
UBA1	23510338					1	1		
UBA52	4507761			3	2				
UBE2R2	22212943						4		
UBL4A	7657667			4					
UBQLN2	16753207								1
UBR5	15147337		47		3				
UCK2	18699734						2		
UGGT1	9910280			1		3			
UNC45A	29725607				3	2			
UPF3A	12711676		1						
UQCRC1	46593007					2	2		
UQCRC2	50592988		5	3	5	3	1		
USP9X	145309309				2				
UTRN	110611228					1			
VAC14	39780552					3			

VAMP2	172072620								4
VAMP3	4759300	14	3						4
VAMP7	5032137	9		2		4			11
VAPA	94721252		2			4			4
VAPB	4759302	2	5			6	5		7
VARS	5454158						3		
VAT1	18379349		5		1	2	1		
VDAC1	4507879	12	157	2		1			30
VDAC2	42476281	7	93	1	1	5	1		15
VDAC3	25188179		39				3		26
VKORC1	13124770	2							
VPS52	73747799			1	1				
VTI1A	113374156					2			
WDR6	197927448	3							
WDR62	145580608				2				
WDR77	13129110	7	6	3	24	5	12		
XPO1	4507943			4	2	19			
XPO4	148886661					5			
XPO5	22748937					5			
XPO6	46049063					3			
XPO7	154448892					5			
XPOT	8051636			7	1	5			
XRCC5	10863945		10	1	3	2			
XRCC6	4503841		18	4	5				
YBX1	34098946	15	20	5	6		9		3
YES1	4885661								3
YIF1B	24308364		2			2			
YIPF6	304766239	2							
YTHDF2	116812575			2					
YWHAB	4507949	4				4			
YWHAE	5803225			2	2	5			
YWHAG	21464101	8					9		10
YWHAH	4507951	2							
YWHAQ	5803227	7	2	4		6	13		
YWHAZ	4507953	10			2	4	8		
ZC3H14	40804742					3			
ZC3H15	118150660					1			
ZC3HAV1	27477136		3						
ZFAND5	5174755					1			
ZFAND6	21359918					1			
ZMPSTE24	18379366					2			
ZNF174	4508007								1
ZNF280D	50811871								1
ZNHIT6	282165823					2			
ZRANB2	42741682						2		

Appendix 3-2: The complete and full results of the digestion of cells transfected with EHD1, EHD2, EHD4, LDLR+EHD1 (LE1), LDLR+EHD4 (LE4), LDLR+PCSK9 (LP), PCSK9+EHD1 (PE1), PCSK9+EHD2 (PE2), PCSK9+EHD4 (PE4) and cells transfected with the negative control, which is the empty vector (pCMV-Entry). Hit Gene Name: the name of the gene matched to the peptides by Mascot; Hit Protein ID: protein identifier from GI database; Peptide Number: total number of peptide sequences matched to the protein.

Hit Gene Name	Hit Protein ID	Empty	EHD1	EHD2	EHD4	LE1	LE4	LP	PE1	PE2	PE4
AARS	109148542					5	2			4	
ABCB1	42741659							1			
ABCB6	9955963	5									
ABCC3	9955970	1									
ABCE1	108773782								12	9	
ACADM	4557231								3	7	
ACLY	38569421					3			6	9	
ACSL3	42794752	6									
ACSL5	42794756	2	1	5	6						
ACTR1A	5031569									3	
ACTR2	5031571									2	
ADAMTS13	21265034									1	
ADPGK	31542509	2		2					3		1
ADSL	4557269							1			
AGRN	54873613	3									
AHSG	156523970	17									
AIFM1	4757732					6	7	1	16	39	
AIMP1	45006986								3		
AIMP2	11125770								1	1	
AKAP12	21493022	11									
ALDH18A1	21361368					3	2		10	4	
ALDH1B1	25777730					1			1	4	
ALDH3A2	4557303	4								2	
ALDOA	4557305	2									
AMY2A	4502085		1	2	2				3	3	2
ANK2	52426735	2									
AP1G1	71772942	1									
AP2M1	14917109	3									
APH1A	117606357	1									
APOB	105990532							3			
APOE	4557325	2									
APP	4502167	1									
APRT	4502171					2	1	1		3	
ARF1	4502201					8	6	9	10	17	
ARF4	4502205								3	15	
ARG1	10947139								2		
ARHGDIA	4757768					4					
ARL8B	8922601	5									
ASNS	168229248								3	2	
ATIC	20127454					9			3		
ATP1A1	21361181	114			2	42	33	38	59	50	
ATP1A2	4502271	9									
ATP1A3	22748667	21									
ATP1B1	4502277	3									
ATP1B3	4502281	3				2					

ATP2A1	10835220	2									
ATP2A2	4502285	29				6	3	7	5	5	
ATP2B1	48255945	28									
ATP2B4	48255957	27									
ATP5A1	4757810	2				37	46	39	62	94	2
ATP5B	32189394					35	37	23	54	41	4
ATP5C1	4885079			1	1						
ATP5F1	21361565									2	
ATP5H	5453559					2	1				
ATP5I	6005717					2	4	4	5	2	
ATP5L	51479156								7	2	
ATP5O	4502303					4	1	4	8	9	
ATP6AP1	17136148	3									
ATP6V0A1	19913418	4									
ATXN10	7106299								1	11	
AVEN	9966841									3	
AZGP1	4502337	2		1					1		2
BASP1	30795231	29									
BAT1	4758112					2	5		5	15	
BCAP31	32171186	14									
BSG	38372919	14				10		1	12	21	3
BUB3	4757880					1			2	4	
BZW1	41281429					1					
C11orf59	8923579	2									
C13orf40	226246554						2				
C14orf156	13654278					4	2		4	8	
C1orf57	14150100							3		3	
C1QBP	4502491	3									
C22orf28	7657015							1	1	1	
C5orf32	14165278	2									
C8orf79	153251913									1	
CAD	18105007					2			16	20	
CALR	4757900	6				14	6	9	16	28	1
CANX	10716563	18				15	17		54	24	
CASP14	6912286								2	2	2
CBS	4557415						2		3	7	
CBX3	15082258								2	4	
CCDC47	171906582	2									
CCDC56	94536771					1	1		3	2	
CCT2	5453603	5				18	13	14	10	15	
CCT3	58761484					5	4	5	3	17	
CCT4	38455427					8	16	8	10	10	
CCT5	24307939					2					
CCT6A	4502643	1						5	6	11	2
CCT7	5453607	6				11	1	14	9	10	
CCT8	48762932	1				18	6	2	7	16	
CD276	67188443	3									
CD63	4502679	5									
CD81	4757944	3									
CD9	4502693	2									
CDC42	4757952	2									
CDK1	4502709	2				6	10	4	21	8	
CDKN2A	4502749					3		1		3	
CFL1	5031635			1		4	3	1	2	2	
CISD2	56605994	2									

CKAP4	19920317	17									
CKB	21536286					8					7
CLNS1A	4502891	1				1	4	2	2		
CLPX	7242140									2	
CLTC	4758012	10				15	10				
CLTCL1	242246985	2									
CNDP2	271398239									1	
COL5A3	110735435									5	
COMT	4502969	2									
COPA	148536853							2	4	12	
COPB1	7705369								1		
COPE	31542319									2	
COPG	11559929					1				9	
COX2	251831110					3					
COX4NB	5174615					2					
COX6C	4758040					4	2		2		
COX7A2	262118227								3		
CPD	22202611	3									
CPT1B	4758050	3							3	3	
CS	38327625					2					
CSDE1	56117850									2	
CSE1L	29029559					11	4	8	9	31	
CTNNB1	4503131	2									
CTPS	148491070					4			1	6	
CTSD	4503143									3	
CXADR	4503173	1									
CYB5B	83921614	2									
CYB5R3	4503327	4									
CYP51A1	4503243	4									
DAD1	4503253	4									
DAGLB	218931251	2									
DARS	45439306					1			7	6	
DBN1	18426913	9									
DCD	16751921	3	4	4	4				4	13	4
DCTN1	13259508					2			2	2	
DCTN2	5453629	4									
DCTPP1	13129100						1				
DDB1	148529014									4	
DDOST	20070197	12				6	6	1	4	4	
DDX1	4826686								1	2	
DDX19B	6005743					8	1	1	7	10	
DDX21	50659095	18				6		5	9	2	
DDX3Y	13514809								4	2	
DDX5	4758138			3		10	5	10	11	9	
DDX50	13129006						2		5		
DHCR7	119943112	5									
DHFR	4503323					5					
DHX15	68509926									1	
DIS3	190014623								3	4	
DNAJA1	4504511					2	6	6	4	11	
DNAJA2	5031741					2		4	1	4	
DNAJC13	112421122	2									
DNAJC7	221219056					4					
DPM3	19424120	2									
DPYSL2	4503377	4									

DSG1	119703744								1		
DSG2	116534898	12								1	
DST	34577049								1		
DYNC1H1	33350932					4	4		17	13	
EEA1	55770888							1			
EEF1B2	4503477					10	10	6	6	24	
EEF1D	25453472	4				8	6	2	4	5	
EFHD2	20149675									3	
EFTUD2	217272892								1	2	
EHD1	30240932	9	239	26		323			1030		
EHD2	21361462			121	3					217	
EHD3	7657056	2		12	15		24			7	11
EHD4	21264315	9	10	7	147		323		21	7	68
EIF2AK4	65287717			1							
EIF2S1	4758256									3	
EIF2S3	4503507					1				2	
EIF3A	4503509					6	4	4	2	4	
EIF3B	33239445					12	4	4	3	4	
EIF3C	4503525					8	1			2	
EIF3F	4503519					4				1	
EIF3I	4503513						1			6	
EIF3L	7705433									9	
EIF4A1	4503529	3				16	3		35	12	1
EIF4A3	7661920					5					
EIF4G1	38201623								5	16	
EIF4G2	289577080								3	10	
EIF4G3	10092601								2		
EIF6	4504771	4					1				
ELAVL1	38201714					2					
ELL2	155722987							1	1	2	
EMD	4557553	2									
ENO1	4503571	7				153	137	37	118	86	23
ENO2	5803011	5									
EPPK1	207452735									2	
EPRS	62241042								2	4	
ERLIN2	6005721	10			2						
ESYT1	14149680	8					1			6	
ETFA	4503607					3			10	9	
ETFB	4503609					2		1	2		
FABP3	4758328				1				2	2	2
FAF2	24797106	4					2		4	4	
FARSA	4758340								1		
FARSB	124028525					6	4	2	7	12	
FASN	41872631					35	5			7	
FAU	4503659					1			1	1	
FDPS	4503685					5			4		
FHL1	21361122									3	
FKBP8	52630440								1		
FLG2	62122917								2		2
FLNA	116063573	13									
FLOT1	5031699	5									
FLOT2	94538362	11									
FURIN	4505579									1	
FYN	4503823	4									
G3BP1	5031703					4			2		

GALK1	4503895									4	
GANAB	38202257	7									
GAPDH	7669492	14				16	11	2	8	11	1
GAPVD1	51093832									7	
GART	4503915					7	5		2	4	
GBAS	4503937								1		
GCN1L1	54607053					1		10	3	4	
GLB1L	40255043			2							
GLO1	118402586					3	1				
GLS	156104878									2	
GLT25D1	31377697								1	1	
GNAI1	33946324	4									
GNAI2	4504041					4	3		1	3	
GNAI3	5729850	11									
GNAS	4504047	3									
GNB2L1	5174447	4				24	17	9	29	75	2
GNB3	4504053	2									
GNL3	45593130								3		
GRM4	4504141								2		
GTF3C1	101943240				1						
GYS1	31542868									1	
H1F0	4885371	5									
H3F3B	4504279	5					5				
HADHA	20127408					1			5	7	
HADHB	4504327									1	
HAO2	7705393	3		4					3	18	4
HAT1	4504341					4			4	1	
HDAC1	13128860					2					
HIP1R	48762942	1									
HIST1H1A	4885373			2						2	
HIST1H1C	4885375	6				22	3		25	14	
HIST1H1D	4885377							5			
HIST1H2AG	4504239	24				20	15		5	4	
HIST1H2BC	4504257	2				4	3		3	2	
HIST2H4A	4504301	13				5	7				
HLA-A	24797067	2							3		
HLA-B	17986001	2									
HM13	23308607	3								4	
HMGA1	4504433	2									
HNRNPA1	4504445									6	
HNRNPA2B1	4504447	7				30	9		23	13	
HNRNPA3	34740329					4			4	2	
HNRNPAB	55956919					8	7	5	6	6	
HNRNPC	117189975	3				22			9	4	16
HNRNPCL1	61966711						5	2			
HNRNPD	14110414	7				8	6	6	7	6	
HNRNPF	4826760	11					3		4	3	
HNRNPH1	5031753					17	7	11	6	7	
HNRNPH3	14141157								2		
HNRNPK	14165435	16				36	9	5	22	28	
HNRNPL	52632383					10		3	7	8	
HNRNPM	14141152	3		3		5	5	6	11	7	
HNRNPR	5031755	6					3		5	2	
HNRNPU	14141161	2				27	20	17	43	55	
HSD17B10	4758504					3			5		

HSD17B12	7705855	3									
HSP90AA1	154146191					98	92	39	101	311	
HSP90AB1	20149594	10		3		161	153	110	138	349	9
HSP90B1	4507677	26				30	24	5	20	34	
HSPA1B	167466173			3		54	35	22	47	58	
HSPA1L	124256496	3									
HSPA5	16507237	34				32	12	8	31	66	
HSPA6	34419635			3							
HSPA8	5729877	5	4	6	3	77	43	30	68	110	3
HSPA9	24234688					16	10	10	21	16	
HSPB1	4504517					5	1		6	5	
HSPD1	31542947	5				84	64	12	61	82	
HUWE1	61676188									2	
HYOU1	5453832					9	2		8	21	
IARS	94721239								11	2	
IDH3A	5031777					2			2		
IGF2BP1	56237027					6			7	2	
IGF2BP3	30795212								3		
IGF2R	119964726	24									
IGFN1	257196151	1									
IGSF8	16445029	2									
ILF2	24234747					9	1		1		2
ILF3	24234750					10	2	4	3		
IMMT	154354962					4	4	4			
INA	14249342	4									
IPO5	24797086					3	5	4			
IPO7	5453998						4	2	4	14	
IPO9	21361659							2			
IRS4	4504733	48				1			1		
ITGB1	19743813	8									
JAM3	21361905	2									
JUP	4504811								4		
KCNK6	4758624									1	
KCTD2	53829365									1	
KCTD5	9506651	2									
KIAA0090	22095331	4									
KIAA1279	24308113								2	6	
KIF11	13699824	29		6	2		6	15	30	32	2
KIF13A	157738621									1	
KPNA2	4504897					22	20	14	30	44	
KPNB1	19923142					32	9	7	4	9	
KTN1	118498362	10									
LAMP1	112380628	7									
LAMP2	4504957	5									
LAP3	41393561								2	8	
LARS	108773810					3	2		13	17	
LASP1	5453710							4			
LDHA	5031857					11	9	9	11	20	
LDHB	4557032	1				10	5	6	18	20	
LDHC	4504973	1									
LDLR	4504975					105	137	404			
LETM1	6912482							1	4	4	
LHPP	269847098									1	
LMAN1	5031873					1					
LMAN2	5803023	6								1	

LMNB1	5031877					4					
LOC338667	169202109	1									
LOC728026	113420837	18									
LRPPRC	31621305					7	6		15	27	
LRRC59	40254924	4									
LSR	45505163	2									
LUC7L2	116812577							1	4		
LUC7L3	19923485									2	
LYZ	4557894			2	1				2		
MAP1B	153945728	19									
MAP2	87578396	25									
MARCKS	153070260	20									
MARCKSL1	13491174	21									
MARS	14043022								5	2	
MAST4	148727255	2	2		2				2		3
MAT2A	5174529					3	4	3	4	4	
MATR3	21626466					6					1
MCM2	33356547					10				2	
MCM3	6631095								3	3	
MCM4	33469917					8		2	4	10	
MCM5	23510448								1		
MCM6	7427519					4	2			2	
MCM7	33469922						2	2	4	5	
MLEC	7661948	1									
MOGS	149999606	3									
MPZL1	4506357	4									
MST4	15011880								3	4	
MTDH	223555917	15									
MTHFD1	222136639					35	14	9	35	37	
MTHFD2	94721354								2		
N4BP2	31742492									1	
NACA	5031931	2				8			4	1	
NCAM1	94420689	4									
NCAPD2	178056552									7	
NCKAP1	7305303	1									
NCL	55956788	17		8		18	10	18	82	20	
NCLN	51873031								2		
NCOA5	15147335	1									
NCSTN	24638433	7									
NDUFAF3	41327781								1		
NDUFS1	33519475								4	4	
NDUFS2	4758786									2	
NDUFS3	4758788								3		
NIPSNAP1	193211616								2		
NMD3	19923796									3	
NNT	122939153						2		2		
NOMO2	27734709									1	
NONO	34932414					2			3	1	
NOP2	76150623	4									
NOP56	32483374					1					
NOP58	7706254								2	2	
NPC1	255652944	6									
NPEPPS	158937236					1	4	6	5	8	
NPM1	10835063	10				31	6	3	18	9	
NPTN	6912646	4									

NSF	156564401	2								2	
NUP93	208609990	2					1		4	3	
OAT	4557809								4	4	
OCLN	4505487	5									
ODZ1	110347400		2								
OFD1	4503179	1									
OSGEP	8923380									2	
P4HB	20070125	4									
PA2G4	124494254					3					
PABPC1	46367787					8	3	7	9		
PABPC5	18201888									2	
PALM	93141029	2									
PARP1	156523968					2	1		7	12	
PCBP2	14141166					5	7		11	6	
PCNA	4505641	2				9			7	3	
PCSK9	31317307							7	4	4	
PDCD6IP	22027538					1					
PDHA1	4505685					4	3	3	6	6	
PDHB	156564403					5	3		5	17	
PDIA3	21361657	8				3					
PDIA4	4758304	7									
PDIA6	5031973	4							30		
PDXDC1	190341074									1	
PEBP1	4505621	1									
PES1	7657455								2		
PFKP	11321601									4	
PGK1	4505763	3									
PGRMC1	5729875	7									
PGRMC2	291621647	4									
PHB	4505773	10				20	17	12	16	14	3
PHB2	6005854	4				5	4		3		
PHGDH	23308577					21	28	20	35	37	
PI4KA	4505807	1									
PKM2	33286418	3				20	29	21	24	23	10
PMPCB	94538354									1	
PNN	33356174	11									
POLR1C	4759046								1		
PPA1	11056044					8	7	1		1	
PPA2	29171702									2	
PPIA	10863927	2									
PPM1B	4505995						6	5	9	10	
PPM1F	7661862									1	
PPM1G	29826282					4	1			10	
PPT1	4506031					4				4	
PRAF2	6005794	4									
PRDX1	4505591					17	6	6	12	4	
PRDX3	5802974										1
PREB	7019503									1	
PRKDC	13654237	3						5	19	5	
PRMT1	151301219					4					
PRMT5	20070220	6			2	12	8	15	23	14	2
PROCR	34335272	5									
PRPF19	7657381					2				4	
PRPF8	91208426								1		
PRSS21	5803197	2									

PSMA5	23110942					3			2	1	
PSMC1	24430151						2		2	4	
PSMC2	4506209					1	2		1	3	
PSMC3	21361144	1					3			2	
PSMC5	24497435									7	
PSMD11	28872725					1					
PSMD14	5031981					1				5	
PSMD3	25777612					11	6	11	10	22	
PTCHD3	194018513			1							
PTGFRN	41152506	5									
PTGS1	18104967							2			
PTK7	15826840	7									
PTMS	46276863	6									
PTPLAD1	117168248	3									
PTPN1	4506289							1			
PUM1	13491166								4		
PVR	209413726	1									
PYCR1	24797095					2			4	2	
PYCRL	198041662									2	
PYGL	71037379								1	5	
RAB10	256222019	9									
RAB11A	4758984	3				5	5		2	2	
RAB14	19923483	11									
RAB1A	4758988	13				13	7	8	7	7	
RAB21	7661922	2									
RAB2A	4506365	7									
RAB3A	4506367	2					4				
RAB5B	4506371							2		1	
RAB5C	41393545	12									
RAB7A	34147513	13									
RAB8A	16933567	6									
RABGGTB	21359854									2	
RAC3	4826962	3									
RALA	33946329	9									
RAN	5453555	2				24	19	7	28	18	
RANBP1	4506407					3					
RANGAP1	4506411					1					
RARS	15149476					12	12	12	20	24	
RBBP7	4506439					2			2	4	
RBM10	20127479	2				1					
RBM39	4757926	1							4	3	
RBM4	93277122								1		
RBMX	56699409	6				6		5	5		
RBMXL1	21361809						4			4	
RDH11	166795268	2								3	
REEP6	19923919	1									
RFC2	28882049									7	
RHOA	10835049	2				2					
RNPS1	6857826	7									
RP1L1	117414137			2							
RPA1	4506583					2					
RPN1	4506675	15				5	7	8	7	8	
RPN2	35493916	15				9	9	5	11	21	
RPS27A	4506713	8			1	6	4		1	10	
RPSA	9845502					17	19	7	20	39	

RRAS2	21361416	2									
RRBP1	110611218	10									
RTN4	24431935	6									
RUVBL1	4506753			1		7	3		3	4	
RUVBL2	5730023						5	2	8	15	
SAE1	4885585					3			1	4	
SAMHD1	38016914								1		
SARNP	32129199	2									
SCAMP1	116256358	2						3			
SCAMP3	16445419	13				8	5	9	4	17	
SCARB2	5031631	4									
SCD	53759151	2						1			
SCRIB	45827729	11							2		
SCYL2	47604944	2									
SEC11A	7657609	2									
SEC22B	94429050	8						1			
SEC61A1	7019415	2									
SEC61B	5803165	4									
SEC62	4507525	5									
SERBP1	66346679			2					4		
SERPINA1	50363217	4									
SF3A1	5032087					2				4	
SF3A3	5803167						2		2	1	
SF3B2	55749531								2		
SF3B3	54112121					1					
SF3B4	5032069	4							1	2	
SFXN1	23618867	1				4	11	6	10	22	
SHROOM3	203098098				1				5		3
SIGMAR1	5032117	2									
SLC12A2	4506975	3						2		4	
SLC12A7	123701900	4									
SLC16A1	115583685	6								2	
SLC19A1	34808710	3									
SLC1A5	5032093	24				7	5	1	4	7	
SLC25A10	20149598								3		
SLC25A11	259155317								2	2	
SLC25A13	7657581								1		
SLC25A3	4505775	2								10	
SLC25A5	156071459	2				12	26	13	60	16	
SLC25A6	156071462						4				
SLC27A6	13325055									1	
SLC29A1	4826716	2									
SLC38A1	117168275	4									
SLC38A2	21361602	2									
SLC3A2	61744477	18				1					
SLC5A6	256985183	2									
SLC6A15	21361693	2									
SLC7A1	4507047	1									
SLC7A5	71979932	6									
SMARCE1	21264355									2	
SMC2	110347418									4	
SMPDL3B	57242798	3									
SND1	77404397	4									
SNRNP200	40217847								5	2	
SNRNP70	29568103	6									

SNRPD3	4759160					4	4	4	5	6	
SNRPE	4507129								2	6	
SNRPF	4507131									15	
SNX2	23111038					1				1	
SORT1	17149834	5									
SPCS2	162417971	2									
SPIN1	112293285	1						1			
SPNS1	14042968	3									
SPTAN1	154759259	2									
SPTBN1	112382250	4									
SQSTM1	4505571					1	1			6	
SRPR	295424842	2									
SRPRB	284795266	13							2	5	
SRSF1	5902076	4				7	3	4	4	2	
SRSF2	47271443	4		1		11	13	5	16	14	
SRSF3	4506901					1					
SRSF6	20127499	2				4	3	4	4		
SRSF7	72534660	3									
SRSF8	15055543	5					4				
SRSF9	4506903					2			1		
SSB	10835067	3									
SSBP1	4507231	50				6	7		2	1	
SSR3	6005884	2									
SSR4	5454090	5				1	2	5	8	11	
STAT1	6274552								2	2	
STOM	38016907	5									
STRAP	148727341									4	
STT3A	22749415	6									
STX12	28933465	2									
STX7	170932494	4									
STXBP1	4507297	2									
SUB1	217330646	3				4			3	3	
SUMF2	194248084								4	2	
SUPT16H	6005757								4		
SYNCRIP	228008291					7					
SYNGR1	22035696	2									
SYNGR2	4759202	6									
TAF9	7706212									1	
TALDO1	5803187					2	2				
TARDBP	6678271					1					
TARS	38202255						3		2		
TBC1D15	226342869									2	
TBL2	7549793	4									
TBR1	5730081					1			9	11	
TC2N	22748725		1								
TCOF1	57164975								1		
TCP1	57863257	4				38	9	16	26	31	
TECR	24475816	6									
TF	4557871	2									
TFRC	189458817	19				4	2	3		4	
THOC4	238776833								4	3	
THRAP3	167234419	4									
TIMM50	48526509								1		
TMED10	98986464	4									
TMED5	282165814	2									

TMEM30A	8922720	4									
TMEM33	224589127	2									
TMEM55B	154816184	2									
TMPO	4507555									3	
TMUB1	13899257	2									
TMX1	151101292	3									
TNPO1	23510381						1		3	10	
TOMM20	7657257	2		1			1		1	4	
TOMM22	9910382						2		6	12	
TPM2	42476296							9			
TPM4	4507651	2									
TRA2A	9558733					1					
TRAP1	155722983					12					
TRIM28	5032179	1				32	44	5	61	110	
TRIM33	74027249									2	
TRIP13	11321607						1		1		
TRPM3	154091314	3									
TTF2	40807471		1	1	2				1		
TYMS	4507751									2	
UBA1	23510338					84	56	19	39	38	10
UBA2	4885649						3		3	12	
UBA5	13376212									3	
UCHL5	7706753					1	4			3	
UCK2	18699734								3	5	
UNC45A	29725607					2			4	3	
UQCRC1	46593007									5	
UQCRC2	50592988								4	5	
USMG5	14249376							3	4	7	
USO1	4505541								1	8	
VAMP3	4759300	14									
VAMP7	5032137	9									
VAPB	4759302	2									
VARS	5454158					2	4	4	4	9	
VDAC1	4507879	12					2	2			
VDAC2	42476281	7				14	17	23	1		
VDAC3	25188179					2	3	2		1	
VKORC1	13124770	2									
WDR6	197927448	3									
WDR77	13129110	7				13	7	9	8	11	
XPO1	4507943					3		1	6	8	
XPO5	22748937							2		7	
XPOT	8051636							1			
YARS	4507947					6			4	11	
YBX1	34098946	15		4		3	6		13	14	
YIPF6	304766239	2									
YWHAB	4507949	4				1		2			
YWHAG	21464101	8									
YWHAH	4507951	2									
YWHAQ	5803227	7									
YWHAZ	4507953	10									
ZNF10	21314662		2								